

CHAPTER II:

***P*-STEREOGENIC LIGANDS**

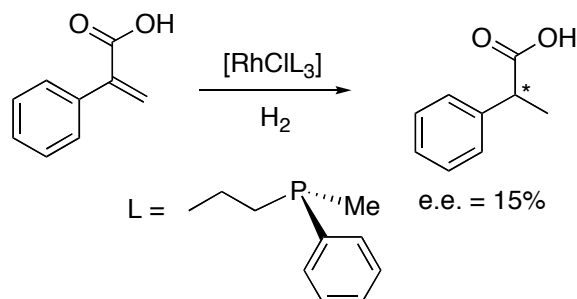


# Chapter II. *P*-stereogenic ligands

## Part I: Methods of preparation of optically pure *P*-stereogenic compounds

### 1. Introduction

Asymmetric catalysis has been and remains one of the cornerstones of chemistry, both in academia and in industry. This is not surprising and simply accounts for the fact that asymmetric catalysis opens up the possibility of obtaining a huge amount of enantiopure compounds from an achiral or racemic precursor and a tiny amount of a chiral catalyst. The early discovery, in 1966<sup>1</sup>, by the team led by Wilkinson, that certain olefins were easily hydrogenated by a soluble rhodium *bis*(triphenylphosphine) complex was followed, soon afterwards, by its asymmetric version when two years later Knowles<sup>2</sup> and Horner<sup>3</sup> independently found that substituting triphenylphosphine by chiral phosphines furnished enantioenriched products (**Equation 1**).



**Equation 1.** First use of a chiral ligand in the hydrogenation of an olefin.

Immediately before this use of chiral phosphines, Noyori<sup>4</sup> had reported the first ever asymmetrically catalyzed reaction<sup>5</sup>. He used chiral  $\phi$ -phenylethyl substituted phenylimines in copper catalyzed cyclopropanation of styrene. Although the e.e. obtained –around 6%– is insignificant for nowadays standards, it was extremely important those days, because demonstrated that chirality could be transferred from the organic ligands to the organic substrate by means of a metallic complex.

Those pioneering works spurred the search for new ligands and their application in asymmetric catalysis. As a result, since then, the field of homogeneous asymmetric catalysis has grown enormously and nowadays is a well-established area lying amongst inorganic, organic

and organometallic chemistry. Proof of that is the ever-growing number of books, journals and papers devoted to several aspects of asymmetric catalysis.

The development of asymmetric catalysis has run parallel to the evolution of optically active ligands, whose chiral information is supposed to be transferred to the substrate by means of the metallic atom in the core of the complex. Up to now, a bewildering variety of ligands (mainly bidentate) have been synthesized and tested in a wide range of reactions, and this screening still continues. These ligands have been optimized varying size, flexibility, donor atoms, bite angle and electronic properties amongst other features.

Notwithstanding, among the large number of ligands existing, phosphorus ligands and particularly phosphines, have received the maximum attention and constitute an ubiquitous class of ligands in the whole organometallic chemistry. The key of the success of phosphines as ligands is due to several factors. Among them, there are the good electron donating properties of the phosphorus atom and the possibility of optimize sterically and electronically the ligands. Finally, the magnetic properties of the  $^{31}\text{P}$  nucleus (spin of 1/2 and 100% abundance) allow the use of NMR as an easy and convenient tool to monitor the reactions and to study, *in situ*, the different species during the catalysis.

At this point, it has to be pointed out that although phosphines are the most widely used class of phosphorus ligands, other P(III) derivatives such as phosphites, phosphinites and phosphorus amidites have already met with important success in several processes and are currently being intensively studied. This THESIS, however, is devoted mainly to *P*-stereogenic phosphines and hence these other classes of compounds will not be discussed.

In order to perform asymmetric catalysis, the phosphine ligand is the source of chirality and consequently it has to be optically active (usually enantiopure). Not surprisingly, a great deal of effort has been devoted to the design and synthesis of a vast variety of enantiomerically pure phosphines.

The chirality of the phosphine can be attributed either to the organic scaffold or to the phosphorus atom itself (*P*-stereogenic or *P*-chirogenic phosphines). This THESIS is devoted to the enantiopure preparation and use of some *P*-stereogenic ligands whereas part I of this chapter aims to give an overall view of the main methods existing in the literature for the preparation of such type of ligands, focusing on those applied here.

Section 2 will briefly deal with phosphines bearing a stereogenic organic scaffold, whereas sections 3 and 4 are devoted to *P*-stereogenic ligands. There are obviously phosphines possessing *both* types of stereogenic elements and those will be discussed along with the *P*-stereogenic ones.

## 2. Phosphines bearing stereogenic backbones

In the early 70's several new phosphines were developed in order to explore their usefulness in asymmetric hydrogenation. Some of those ligands are depicted in **Figure 1**. Related to dppe, Kagan's team obtained DIOP in 1972<sup>6</sup>, while Bosnich's laboratories prepared CHIRAPHOS and PROPHOS in 1977<sup>7</sup> and 1978<sup>8</sup> respectively. The chirality of these ligands is due to the stereogenic carbon atoms in the ethylene bridge. The first phosphines including planar chirality by means of ferrocene also appeared in that decade, when Kumada and coworkers prepared BPPFA<sup>9</sup> and BPPFOH<sup>10</sup> in 1976. All these ligands, among others, were tested in Rh-catalyzed asymmetric hydrogenation of dehydroaminoacids with very good results.

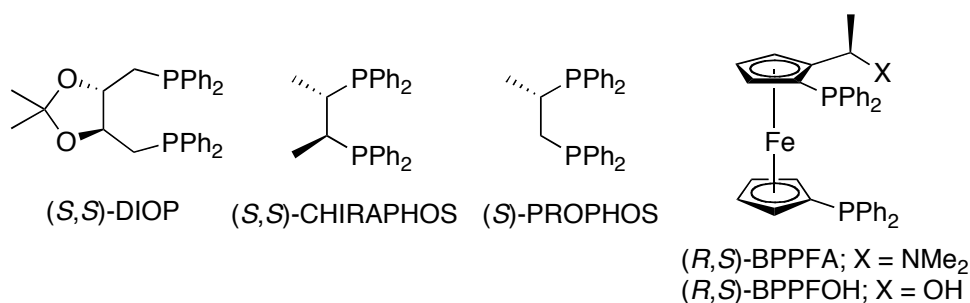


**Figure 1.** Phosphines developed during the 1970 decade.

The arrival of the 80's carried a major advance because Noyori and Takaya synthesized the phosphine BINAP<sup>11</sup> (**Figure 2**), which has been one of the most successful ligands in asymmetric catalysis. The stereogenicity of BINAP and its analogues arises from a stereogenic axis, due to the restricted rotation along the ligand backbone, a phenomenon called atropisomerism. BINAP was shown to be an extremely efficient ligand in Rh and Ru catalyzed hydrogenation. Inspired by this work, many other research groups developed, over the following years, a large number of other atropisomeric biaryl *bis*phosphine ligands, which gave excellent results in asymmetric hydrogenation. Examples of them are BICHEMP<sup>12</sup> and BICHEP<sup>13</sup>. **Figure 2** depicts these ligands.

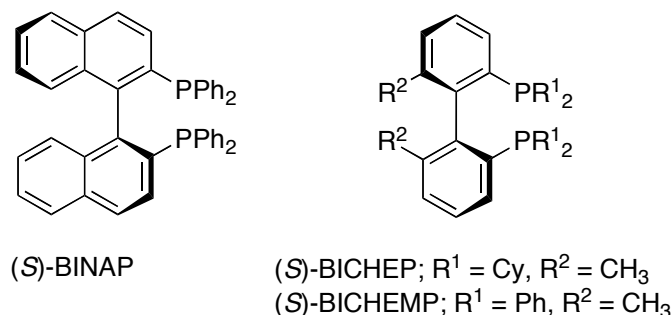


**Figure 2.** Atropisomeric chiral phosphines.

In the early 90's Burk<sup>14,15</sup> *et al.* introduced series of new ligands bearing phospholane moieties, BPE and DUPHOS, while Togni and Hayashi further developed the synthesis of phosphines based on ferrocenes and obtained Josiphos (a  $C_1$  ligand) in 1994<sup>16</sup>. These ligands are shown in **Figure 3**.

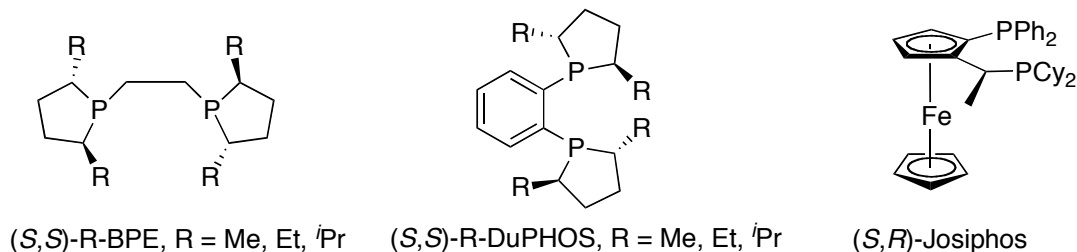


**Figure 3.** Ligands developed during the 1990 decade.

Since the middle 90's, many research groups have been introducing structural variations to all the phosphines outlined above. This systematic screening and optimization has provided loads of new ligands, many of them with improved efficiency. Moreover, new phosphines with other chiral moieties have also appeared in recent times. Just to quote a pair of examples (**Figure 4**), PHANEPHOS<sup>17</sup> takes advantage of the inherent stereogenicity of the *paracyclophane* group whereas the ligand **1**<sup>18</sup> possesses both a carbon atom and a rhenium atom as stereogenic centres.

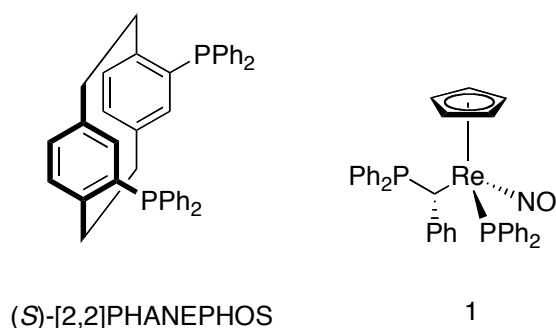


**Figure 4.** Chiral phosphines with new chiral sources.

To sum up, it is clear that the outburst of phosphorus ligands the last decades have witnessed only pursues to have a *pool* of available ligands as comprehensive as possible. This enormous synthetic work is done in order to come closer to the dream of any chemist working in asymmetric homogenous catalysis: to have the perfect ligand for a given reaction, which gives full conversion and enantioselectivity avoiding side reactions. This is the idea of *tailor-made* ligands.

### 3. Preparation of phosphines bearing stereogenic phosphorus atoms

#### 3.1. Introduction

The simple idea that a phosphorus atom surrounded by three different groups can lead to a pair of enantiomeric forms has been considered by well over 100 years and was verified experimentally, as early as in 1911, by Meisenheimer and Lichtenstadt<sup>19</sup>. *P*-stereogenic compounds can not be isolated from natural products, *i.e.*, they are not found among the natural chiral substances. Consequently, their obtention, in enantiomerically pure form, relies upon chemical synthesis. The interest in molecules containing *P*-stereogenic atoms was, originally, focused on basic studies on their stereochemistry but this interest has developed into more pragmatic fields such as asymmetric synthesis and catalysis.

In asymmetric catalysis, the interest in *P*-stereogenic ligands began after the pioneering work of the teams of Knowles<sup>2</sup> and Horner<sup>3</sup> in asymmetric hydrogenation. The first use of a *P*-stereogenic phosphine in catalysis has already been shown in section 1, **Equation 1**. Soon after this discovery, an apparently unrelated event took place: it was discovered that a fairly massive dose of L-DOPA (then a rare amino acid, **Figure 5**) was useful in treating Parkinson's disease<sup>20</sup>.

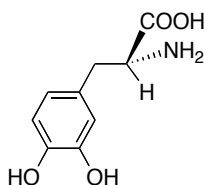
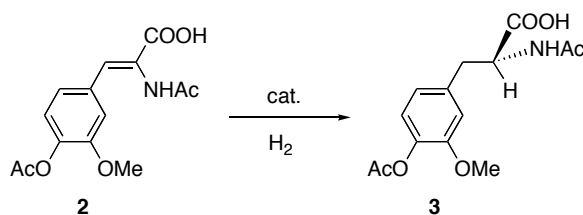


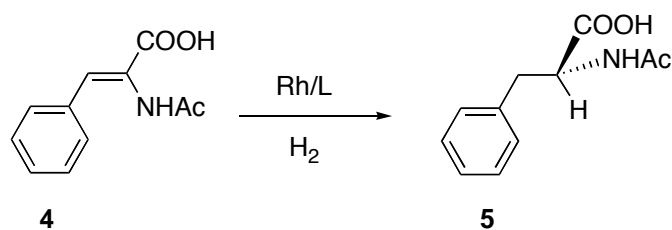
**Figure 5.** The L-DOPA amino acid.

Those days, Knowles and his team were working for Monsanto, which was interested in stereoselective synthesis of L-DOPA because its demand was increasing rapidly. One of the key steps in the synthesis of L-DOPA was the hydrogenation of the enamide **2**, as depicted in **Equation 2**.



**Equation 2.** Key step in the L-DOPA synthesis.

This process provided a golden opportunity to test the reaction using the recently developed *P*-stereogenic phosphines. A simplified model reaction (depicted in **Equation 3**), the rhodium catalyzed hydrogenation of **4**, was employed.



**Equation 3.** Asymmetric hydrogenation of a L-DOPA precursor analogue.

The reaction proceeded smoothly to full conversion. The obtained enantioselectivity for several phosphines is summarized in **Table 1**.

<i>L</i>	<i>e.e.</i> (%)
	1
	28
	28
	32
	58
( <i>S</i> )-PAMP	
	88
( <i>S</i> )-CAMP	
	96
( <i>S,S</i> )-DIPAMP	

**Table 1.** *P*-stereogenic phosphine ligands for asymmetric hydrogenation



The results from the table constituted the first time ever that enzyme-like stereoselectivity had been obtained in a man-made catalyst. The success of PAMP and DIPAMP enabled the first industrial asymmetric synthesis: the production of L-DOPA.

It seemed clear to the authors that to get good results it was necessary to have the chiral centre at the phosphorus atom, because the chiral environment was the closest to the metal, where the catalytic process took place. This assumption certainly makes sense and is easy to understand, but Kagan<sup>6</sup> demonstrated it to be false, when he obtained 88 % e.e. in hydrogenation using the DIOP ligand (**Figure 1**, § 2).

In fact, DIPAMP and DIOP are representative of two important families of chiral diphosphines. The former with *P*-stereogenic elements, while the latter with a stereogenic organic scaffold. Both are bidentate and have a  $C_2$  symmetry axis, which is thought to reduce the number of possible isomeric catalyst-substrate complexes and thus improve the stereoselectivity<sup>21</sup>. As it has been said, both type of phosphines were successfully used in asymmetric catalysis almost 30 years ago and hence it may be thought an analogous expansion of the families of *P*-stereogenic phosphines and those bearing a chiral organic scaffold. This statement has been proved to be false and *P*-stereogenic ligands have been greatly outnumbered by those with a stereogenic backbone. This paradoxical slow development of *P*-chirogenic phosphines is due to the fact that phosphines with stereogenic backbones are much easier to design and synthesize with a wide enough structural diversity. Moreover, several widespread prejudices about the low configurational stability of the phosphorus atom have also hampered the development of the use of *P*-chirogenic ligands in asymmetric catalysis. However, despite this apparent oblivion, several groups have been developing strategies towards enantioselective synthesis of *P*-stereogenic phosphines and the last decade has witnessed a revival on the chemistry of the ligands with *P*-centred chirality. This renewed interest has provided new promising approaches to the synthesis of this kind of ligands and, as a result, they are currently being applied to an increasing number of catalytic applications. In the following sections, the main methods of synthesis of molecules containing *P*-stereogenic atoms will be briefly reviewed and some of them will be used in the preparation of the ligands of this THESIS.

## 3.2. Preparation by resolution of racemates

### 3.2.1. Introduction

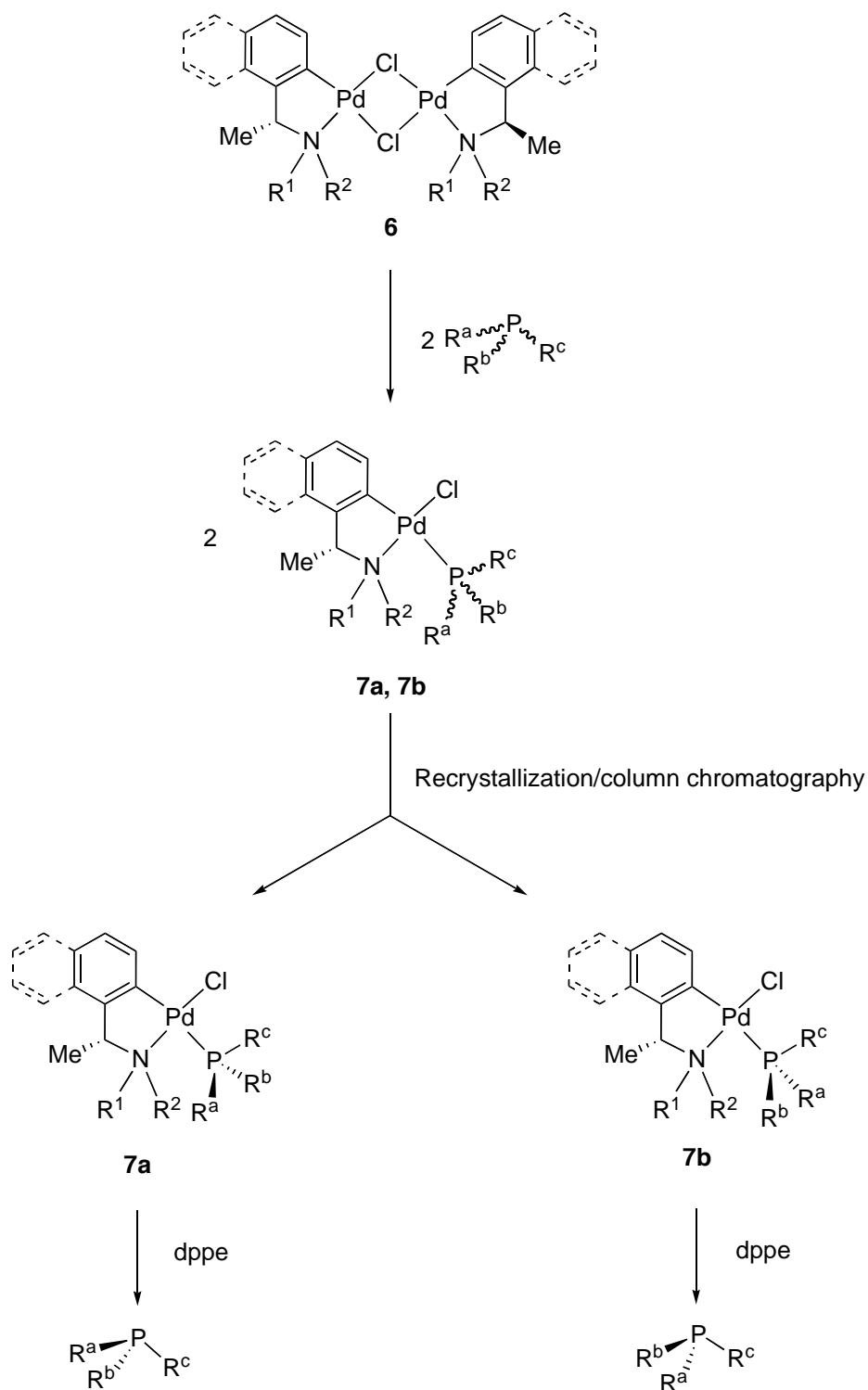
The first methodologies reported for the preparation of optically pure phosphines bearing stereogenic phosphorus atoms involved the preparation of the desired product in racemic form, followed by the resolution of this racemate by means of a chiral auxiliary. This synthetic route, generally speaking, suffers from serious drawbacks. It implies tedious recrystallizations or chromatographic separations and gives low overall yields. Moreover, its success is very dependent on the groups attached to the phosphorus atom and on the choice of the chiral auxiliary; this gives very little chance to change the structure of the groups bound to the phosphorus atom. Pietrusiewicz and Zablocka have excellently reviewed<sup>22</sup> a variety of examples of resolution of racemics in order to obtain optically pure *P*-stereogenic phosphines and derivatives.

The serious problems stated before, however, have made that nowadays this method is scarcely carried out –a very recent use of the resolution method with a tartaric acid derivative, however, has been reported by Imamoto<sup>23</sup> to prepare a very strained, *P*-stereogenic phosphine–, with the exception of the use of palladium metallacycles, which will be outlined below. At this point, however, it has to be said that *direct* resolution of racemics is accomplished by the use of preparative HPLC systems<sup>24,25</sup>. This method, although expensive, is very used mainly at industrial level –although has already been used in laboratory scale– to obtain optically pure phosphine derivatives in large quantities.

### 3.2.2. Use of chiral cyclopalladated complexes

Up to date, palladium(II) complexes containing enantiomerically pure forms of ortometallated 1-phenylethylamines and 1-naphthylethylamines<sup>26,27</sup> are considered the most efficient resolving agents, at least for certain types of phosphines<sup>28</sup>. The general procedure is depicted in **Scheme 1**. The desired phosphine, in racemic form, is made to react with the cyclometallated dimer **6**, which provides a pair of mononuclear complexes **7** in 1:1 proportion (sometimes, only half equivalent of the resolving agent is used and then, ideally, solely one enantiomer of the phosphine reacts while the other remains in solution). Complexes **7** differ only in the absolute configuration of the P atom and are thus diastereomeric, allowing, in principle, to be separated by traditional methods, such as column chromatography or recrystallization. Once separated, the phosphine is displaced from the palladium by means of dppe or another strongly coordinating agent, yielding the desired enantiomerically pure phosphine. This method has been widely used to resolve both monodentate and bidentate phosphines because the dimers **6** are straightforward to prepare and because the mononuclear

complexes **7** are usually easy to characterize and crystallize, in order to ascertain the absolute configuration of the phosphorus atom. Even when X rays are not available, a detailed 2-D NMR study of **7** generally allows the deduction of the absolute configuration of the phosphorus atom.



**Scheme 1.** Resolution of phosphines by means of chiral palladacycles.

The array of phosphines resolved by this method is quite large and they are usually obtained in high optical purity. **Table 2** summarizes the results obtained in previous work performed in Barcelona<sup>29-35</sup>.

<i>R<sup>a</sup></i>	<i>R<sup>b</sup></i>	<i>R<sup>c</sup></i>	<i>Yield of 7</i> %/%	<i>e.e. phosphines</i> %/%
Ph	Bn	H	45%/38%	>95%/52%
Ph	Me	H	63%/15%	>95%/86%
Ph	Bn	Mes	86%/40%	>95%/>95%
Ph	Bn	<sup>t</sup> Pr	54%/52%	>95%/77%
Ph	Bn	Cy	70%/66%	>95%/>95%

**Table 2.** Some resolutions of *P*-stereogenic phosphines by means of palladium metallacycles.

Some of these enantiomerically pure phosphines were used in palladium asymmetric hydrovinylation<sup>29,35</sup>.

### 3.3. Preparation by stereoselective synthesis

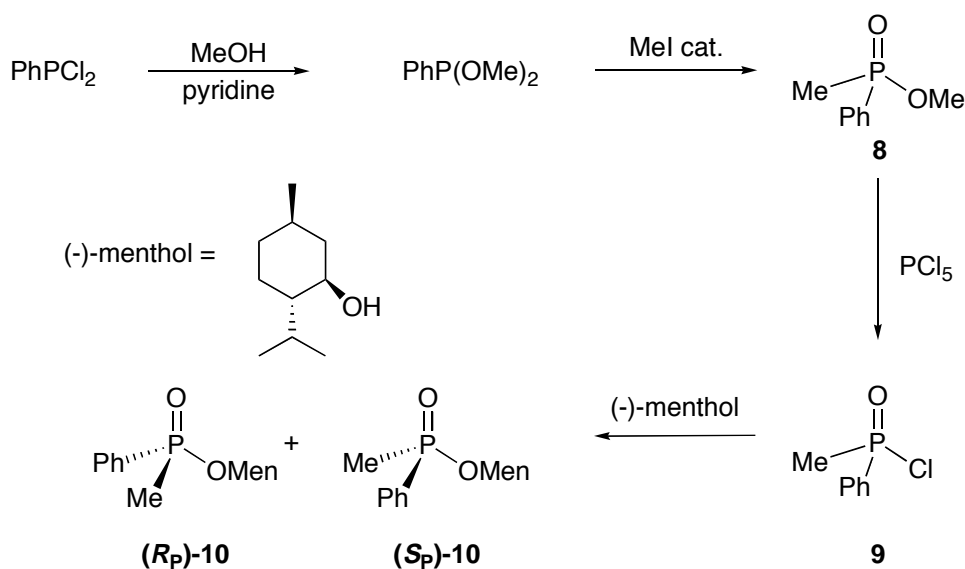
#### 3.3.1. Introduction

The lack of flexibility of the methods that implied resolutions of racemics led to the development of synthetic routes allowing the preparation of a suitable *P*-resolved precursor possessing one or more leaving groups. From this precursor, *via* stereoselective substitutions, new C-P bonds would be created to lead the desired phosphine. In the next sections, the use of menthol, ephedrine and sparteine as chiral auxiliaries to prepare such precursors will be discussed.

#### 3.3.2. Use of menthol as a chiral auxiliary

The idea outlined in the introduction of this section was first explored by Cram<sup>36</sup> and Mislow<sup>37,38</sup> in the late 60's. Using menthol as a chiral auxiliary, they were first to demonstrate that unsymmetrically substituted menthyl phosphinates (**10**, **Scheme 2**) could be separated into their diastereomeric forms by recrystallization. Starting from this work, Horner<sup>39</sup> and others<sup>40,41</sup> synthesized and separated some other pairs or menthylphosphinates.

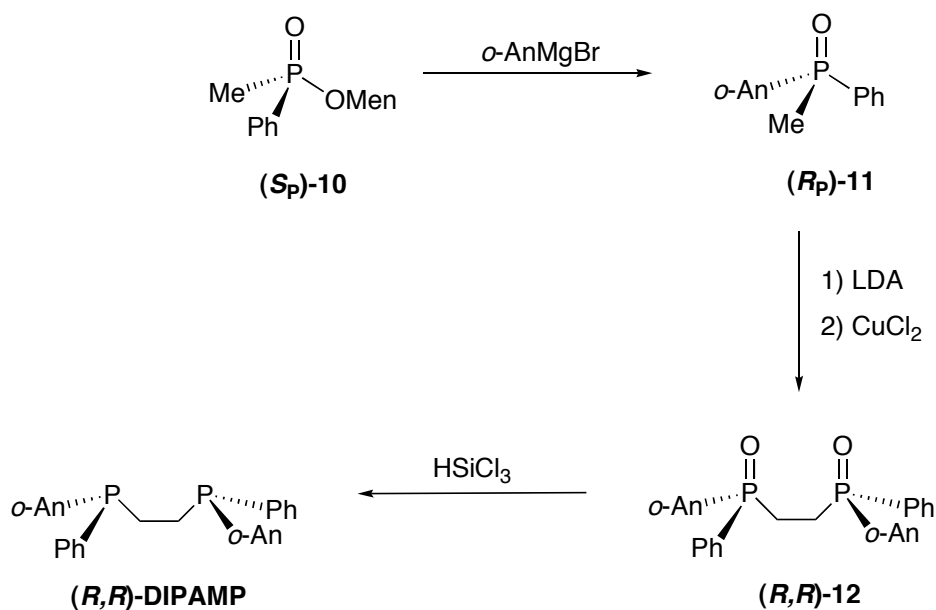
Usually, only one of the diastereomers (in **Scheme 2**, for example, the (*S<sub>P</sub>*)-**10**) was obtained in the pure form whereas the other remained in the mother liquors. Some unsuccessful attempts have also been reported.



**Scheme 2.** Synthesis of menthylphosphinates.

Once one of the menthylphosphinates had been obtained in a pure form, it was found that it could be reacted with Grignard reagents to furnish the tertiary phosphine oxides with complete inversion of configuration at the phosphorus atom.

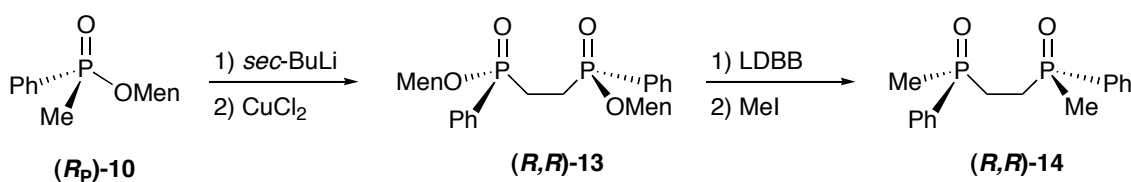
In fact Knowles used this procedure<sup>40</sup> in one of the steps of the synthesis of DIPAMP, as is shown in **Scheme 3**.



**Scheme 3.** First synthesis of DIPAMP.

The reactions of this type had to be carried out with excess of Grignard reagent and under some harsh conditions. Furthermore, the success was very sensitive to the groups attached to the phosphorus atom, oxygen and moisture. In spite of these drawbacks, the high level of stereospecificity usually attainable with this method and its flexibility attracted the attention of many groups and consequently a lot of menthylphosphinates and phosphine oxides were prepared.

At this point, Imamoto was able to replace the menthyl group at the phosphorus atom with retention of configuration<sup>42,43</sup>, by reductive stereospecific cleavage. He found that one-electron reducing agents were able to do such a transformation. Upon examining several reducing agents (alkali metals and Li-NH<sub>3</sub> among others) it was found that lithium 4,4'-di-*tert*-butyldiphenylide (LDBB) was the reagent of choice because it preserved the stereochemical integrity of the phosphorus atom. **Scheme 4** shows the use of this methodology to prepare diphosphine oxides. The diphosphide obtained upon treatment with LDBB was quenched with methyl iodide to furnish the diphosphine oxide (***R,R***-14). Several other diphosphine oxides were obtained. This method is complementary to the nucleophilic substitution of the menthyl group, in which, as it has been said, the substitution at the phosphorus atom occurs with inversion of configuration.



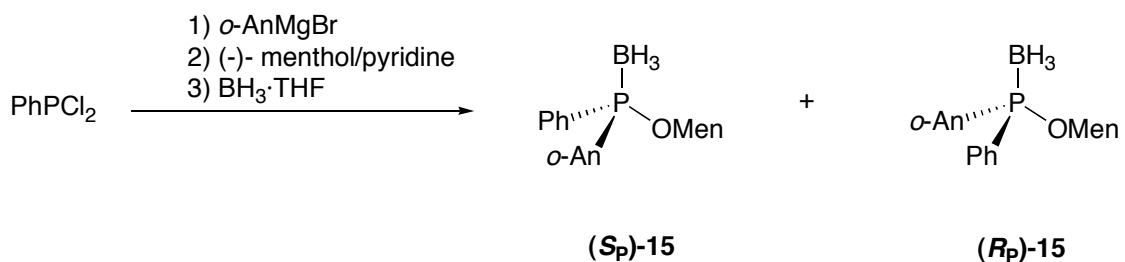
**Scheme 4.** Imamoto's strategy to synthesize diphosphine oxides.

Whatever the method employed to prepare the phosphines oxides, they have to be reduced to the desired phosphines. Such a transformation is usually carried out using silanes<sup>44,45</sup> (**Scheme 3**), sometimes mixed with amines<sup>44,46</sup>. In the literature, there are methodologies that proceed with retention of configuration<sup>44,46</sup> at the phosphorus atom and others that provide inverted phosphines<sup>44,46</sup>. Nonetheless, these methods are not completely selective and some loss of optical purity is almost always observed<sup>47</sup>. Sometimes even racemization takes place<sup>48</sup>; depending on the specific reducing agent used, the reaction time and the groups attached to the phosphorus atom. These drawbacks have been overcome with the use of phosphine-boranes<sup>49-53</sup> instead of phosphine oxides, as it will be described in the next paragraphs.

In a seminal paper, in 1990, Imamoto<sup>49</sup> went one step further in the menthol methodology by using phosphine-boranes instead of phosphine oxides. This was the first example of the use of phosphine-boranes as versatile intermediates in the synthesis of *P*-stereogenic phosphines. Phosphine-boranes were discovered to be much more suitable intermediates than oxides. They are crystalline, chemically and configurationally stable even under severe conditions (oxidant, acid or basic media). Those features enable working with phosphine-boranes without inert atmosphere and using classic methods like crystallizations and column chromatography to purify the intermediates. Moreover, the use of phosphine-boranes

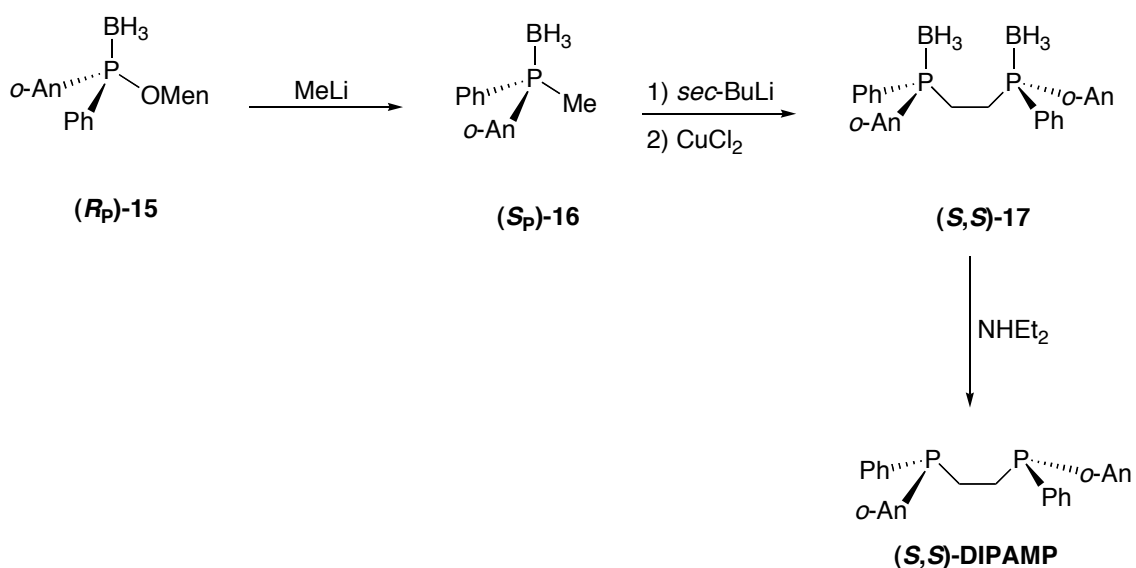
avoids the handling of the malodorous, air-sensitive and sometimes corrosive free phosphines until they are needed. The removal of the boranato group (§ 3.3.4.6) is easily achieved by stirring the phosphine-borane in a large excess of amines<sup>49</sup>, such as diethylamine, morpholine or DABCO. This step has been found to proceed with full retention of configuration at the phosphorus atoms, in contrast to the aforementioned stereochemical problems associated with reduction of oxides.

The strategy of Imamoto began with the synthesis of the phosphinite-boranes<sup>49</sup> as it is shown in **Equation 4**.



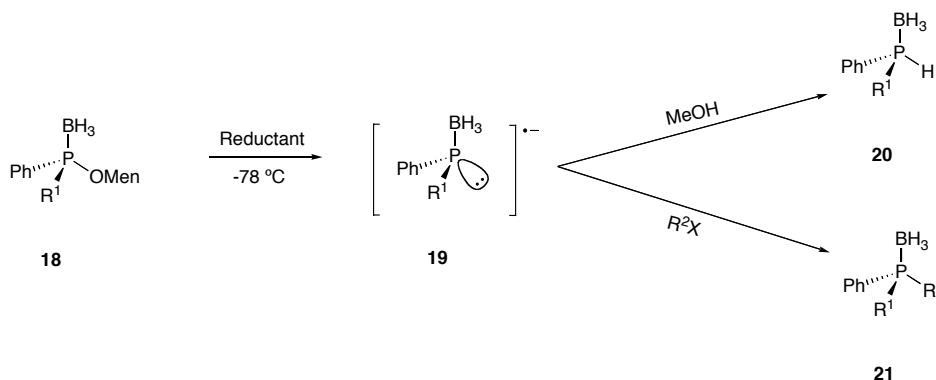
**Equation 4.** Synthesis of menthylphosphinite-boranes.

The diastereomeric phosphinite-boranes **15** were separated by means of chromatography and *R<sub>P</sub>*-**15** was then converted to (*S,S*)-DIPAMP as depicted in **Scheme 5**.



**Scheme 5.** Synthesis of (*S,S*)-DIPAMP using phosphine-boranes methodology.

Imamoto, in an analogous way as he did with menthylphosphinates (**Scheme 4**), also succeeded in removing the menthyl group reductively<sup>42</sup>, at low temperature, with total preservation of phosphorus configurational integrity (**Scheme 6**). The anionic tricoordinated phosphorus species **19** were subsequently allowed to react with methanol or alkyl halides, still at low temperature, to afford optically active secondary (**20**) or tertiary (**21**) phosphine-boranes, both in high optical purity, with an e.e. value above 90 % in most cases.



**Scheme 6.** Reductive cleavage of menthyl group in menthylphosphinite-boranes.

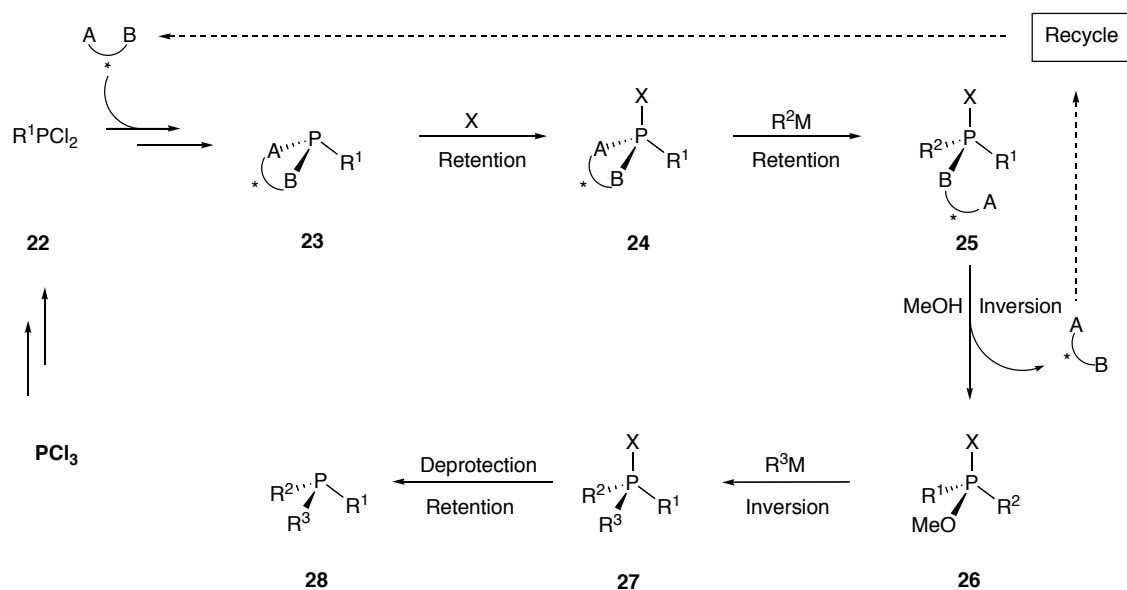
The reductants explored were LDBB, Li-NH<sub>3</sub> and lithium naphthalenide. The reaction was complete in 5 minutes. Upon raising the temperature, it was found that the anionic species **19** quickly racemized, presumably *via* pyramidal inversion.

### 3.3.3. Use of heterobifunctional chiral auxiliaries

In the previous section, it has become clear that nucleophilic substitution of an alkoxy group, either in a phosphinate or in a phosphinite-borane usually proceeds with high stereoselectivity, with inversion of configuration at the phosphorus atom. This fact led to expectations that two sequential substitutions could also provide a means for stereoselective synthesis of phosphine derivatives. For such an approach, a conveniently resolved *P*-stereogenic precursor, possessing two potentially different leaving groups, at least in their leaving abilities, was a prerequisite. This idea crystallized in the work of several laboratories<sup>54-56</sup> and it was soon recognized that the most successful results were obtained when two leaving groups were both part of the same molecule, *i.e.* when a heterobifunctional chiral auxiliary was used, with the formation of cyclic derivatives (phospholidines).



The general strategy is depicted in **Scheme 7**.



**Scheme 7.** Preparation of *P*-stereogenic phosphines using a chiral bifunctional auxiliary.

Starting from  $\text{PCl}_3$ , –which can be *formally* regarded as the starting point for the preparation of P(III) compounds, by three stepwise nucleophilic substitutions– dichlorophosphines **22** can be obtained *via* Grignard or organolithium reagents (when the compound **22** is not commercially available). The diastereoisomerically pure (with the phosphorus atom resolved) cyclic phospholidine **23** is then prepared by using the suitable chiral auxiliary  $\text{A}-\text{B}$ . Afterwards this compound is conveniently protected with the protecting group  $\text{X}$ . Compound **24** is, indeed, the starting *resolved P-stereogenic precursor*, possessing two leaving groups potentially different as defined in the preceding paragraph. The use of the protective group,  $\text{X}$ , was found to be necessary to stabilize the configuration of the phosphorus atom during the synthesis and has the additional advantage of protecting the phosphine from oxidation. Starting from **24**, two nucleophilic attacks and a methanolysis step furnish the protected phosphine **27**, which is stereospecifically deprotected to furnish the desired phosphine **28**. The reaction steps were highly regio- and stereoselective and an e.e. greater than 90% for **28** was generally observed.

Three groups successfully followed this scheme. The exact conditions they used are summarized in **Table 3**.

<i>Author</i>	<i>A</i>	<i>B</i>	<i>X</i>	<i>M</i>	<i>Deprotection</i>
Jugé <sup>54</sup>	O	N	BH <sub>3</sub>	Li	NHEt <sub>2</sub>
Corey <sup>56</sup>	S	O	S, BH <sub>3</sub>	Li	Si <sub>2</sub> Cl <sub>6</sub>
Brown <sup>55</sup>	O	N	O	MgBr	φ <sup>a</sup>

<sup>a</sup>: Deprotection was not carried out.

**Table 3.** Stereoselective synthesis of *P*-stereogenic phosphines *via* cyclic chiral auxiliaries.

The protected, diastereomerically pure cyclic derivatives **24** were prepared from (–)-ephedrine, **29** (Brown<sup>55</sup>, Jugé<sup>54</sup>), or from the camphor derivative, **30** (Corey<sup>56</sup>). These chiral auxiliaries are shown in **Figure 6**. The choice between boranato, sulphide and oxide is *formally* a choice between P(III) (boranato) or P(V) (oxide or sulphide).

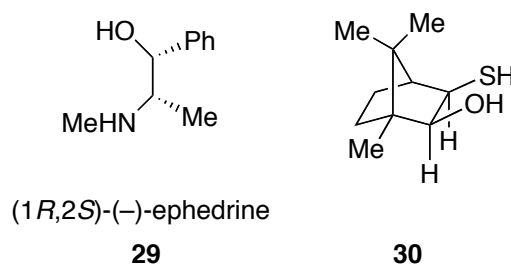


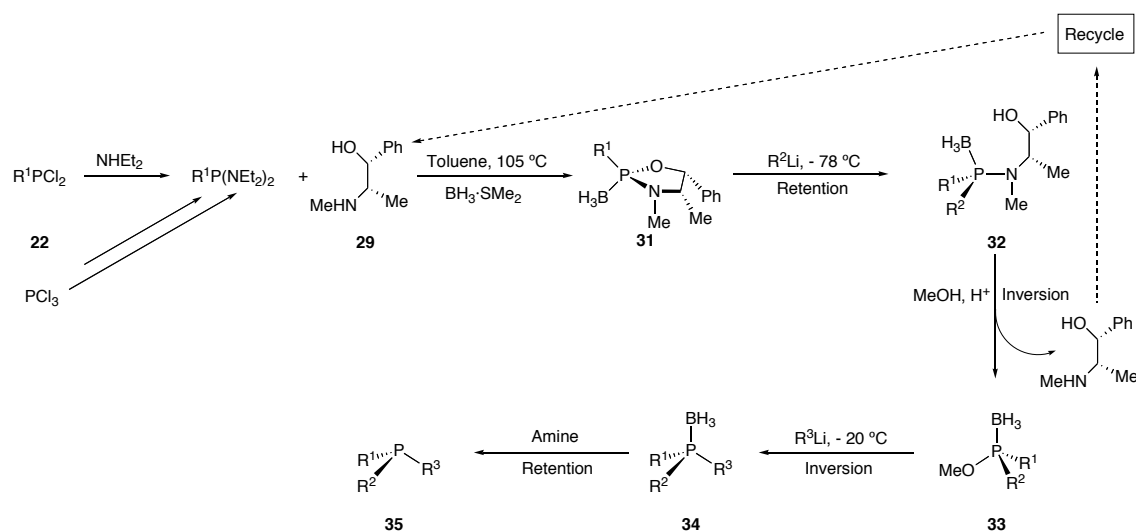
**Figure 6.** Chiral auxiliaries used to prepare the *P*-resolved precursors **24**.

Examining the literature related to each of the three methodologies depicted in **Table 3**, one can find that the most successful method, in terms of versatility, stereoselectivity, simplicity and availability of the chiral auxiliary is the approach of Jugé<sup>54</sup>. Furthermore, Jugé's method is the most widely used<sup>57-69</sup> of the presented methods and, in fact, it is also the one applied in this THESIS to prepare the ligands. For these reasons, the next sections will deal with this method in detail.

### 3.3.4. Use of ephedrine as a chiral auxiliary

#### 3.3.4.1. Introduction

Jugé developed a powerful method for the preparation of *P*-stereogenic phosphines<sup>54</sup>, depicted in **Scheme 8**, based on the use of ephedrine as a chiral auxiliary. In the original method, R<sup>1</sup> was Ph, but some variations have been made<sup>57,69</sup> and, in principle, it is applicable to other substituents. In the following discussion, however, it will be assumed that R<sup>1</sup> is phenyl. The coming sections will deal with each one of the steps of the procedure.

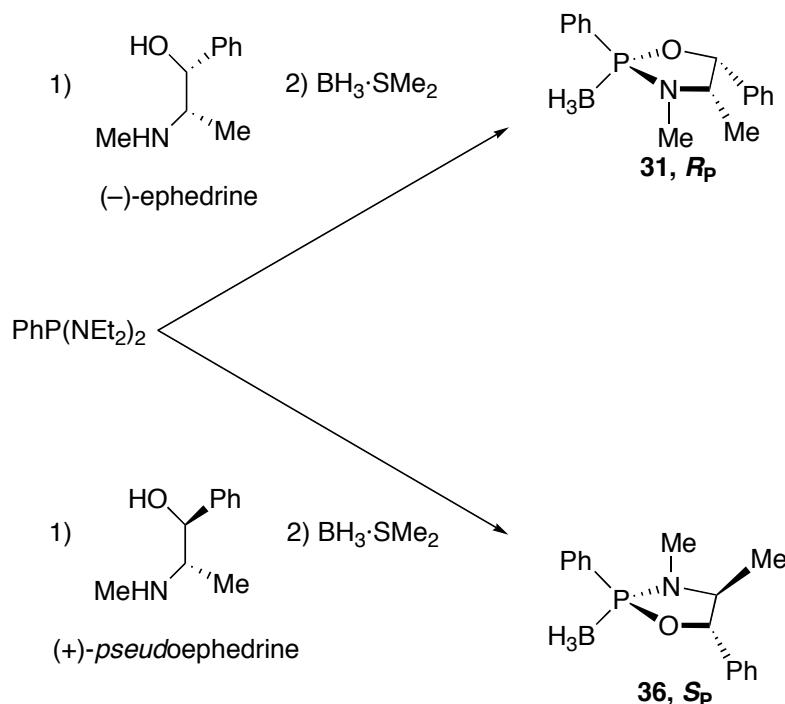


**Scheme 8.** The method developed by Jugé for the synthesis of *P*-stereogenic phosphines.

#### 3.3.4.2. Stereoselective cyclization of ephedrine

The key intermediate is the oxazaphospholidine-borane **31**, prepared by a one-pot reaction from *bis*(diethylamino)phenylphosphine, and (–)-ephedrine, at  $105\text{ }^\circ\text{C}$ , followed by protection with  $\text{BH}_3$ . The cyclization of the ephedrine takes place stereoselectively<sup>54,62</sup>, with preferential formation of the  $R_p$  diastereomer, in 90% d.e. The absolute configuration at the phosphorus atom has been determined by chemical correlation and NMR analysis<sup>70</sup> and corroborated by single crystal diffraction of **31**<sup>71,72</sup>. The high stereoselectivity in the formation of **31** can be explained by steric reasons because the phenyl group is in the opposite position respect to the substituents of the (–)-ephedrine<sup>60</sup>. In order to gain further insight into this question,

Hansen prepared<sup>60</sup> the compound **36**, which is analogous to **31** but using (+)-(1*S*,2*S*)-pseudoephedrine (**Scheme 9**).



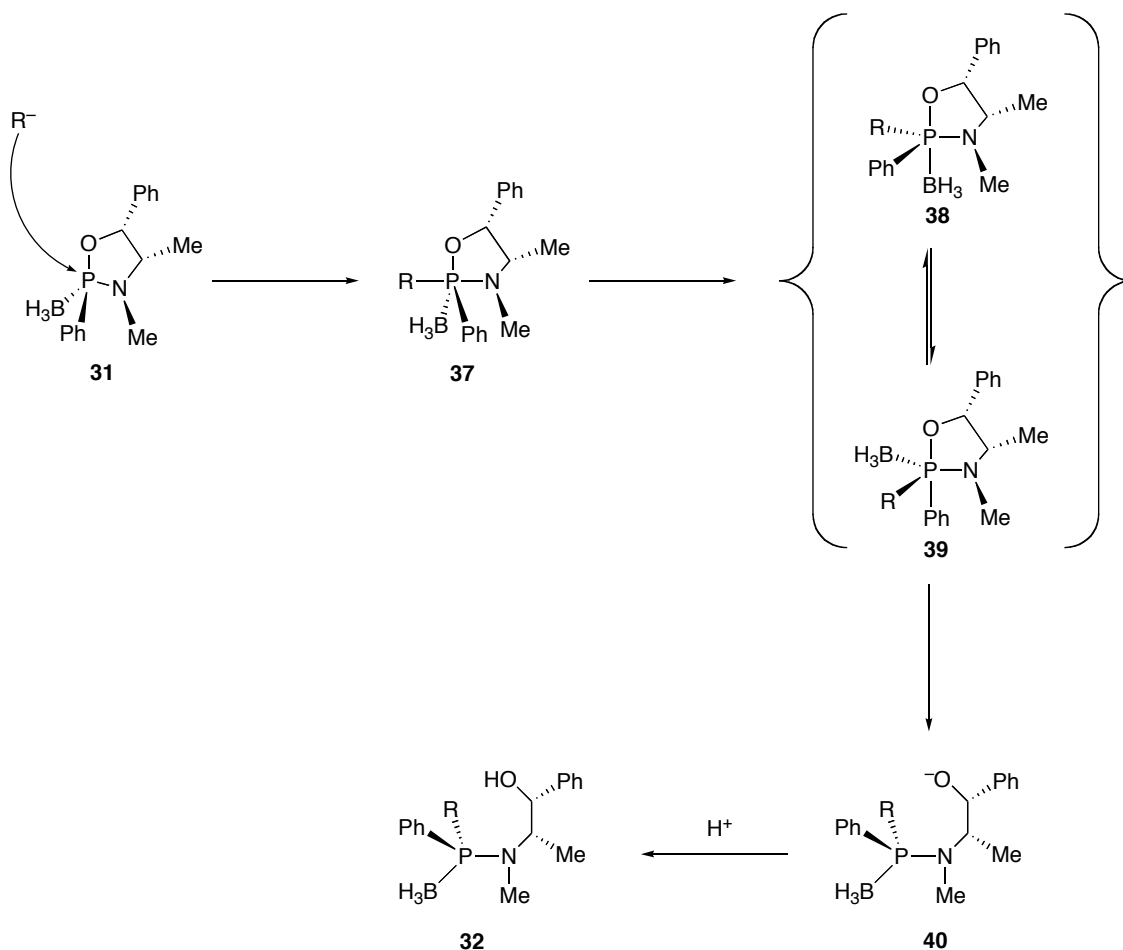
**Scheme 9.** The different oxazaphospholidine-boranes prepared by Hansen.

He found that the absolute configuration of the phosphorus atom was opposite than in **31**. Hence he concluded that the configuration at the Ph substituted C(1) in the ephedrine controlled the absolute configuration at the phosphorus atom, in such a way that the preferred isomer is the one in which the Ph in the C(1) and the one in the phosphorus atom are in a *trans* fashion.

### 3.3.4.3. Selective ring opening of oxazaphospholidine-boranes

As already depicted in paragraph 3.3.4.1, **Scheme 8**, alkyl and aryl lithium reagents cleanly opened the oxazaphospholidine-borane **31**, at  $-78^\circ\text{C}$  in THF, to give the corresponding aminophosphine-boranes **32**. Jugé discovered that this step is totally regioselective<sup>62</sup> by breaking the P-O bond whereas the P-N bond remains intact. The stereoselectivity of the reaction was also studied by the X-ray analysis<sup>60,62</sup> of some phosphamide-boranes **32**. It was discovered that the reaction occurs with retention of configuration at the phosphorus atom and with a d.e. greater than 85%. This fact is in sharp contrast with other acyclic chiral phosphorus derivatives, whose P-C forming reactions with organometallic compounds occur with inversion of configuration at the phosphorus atom. Grignard reagents are also able to react with **31**, but they require higher temperatures and important losses of stereoselectivity are observed, so organolithium reagents are the nucleophilic reagents of choice.

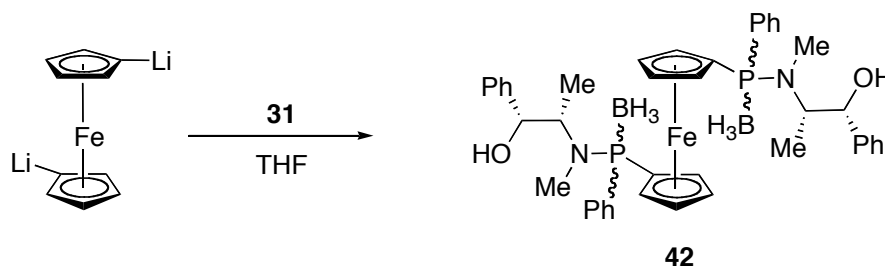
To account for the observed retention of configuration, the mechanism depicted in **Scheme 10** was proposed<sup>62</sup>.



**Scheme 10.** Proposed mechanism for the nucleophilic alkylation of oxazaphospholidine-borane **31**.

The crystal structure of the starting complex **31** shows a distorted oxazaphospholidine ring, where the methyl substituent of the nitrogen is on the back side of the O leaving group. Consequently, it was deduced that the stereochemistry of the P-C bond formation is under kinetic control and the nucleophilic attack of R<sup>-</sup> occurs on the less hindered side of the P-O bond, which is opposite to the nitrogen atom, with the formation of the pentacoordinate intermediate **37**. This compound stereopermutes into another one (**38** or **39**), having the substituents on the phosphorus atom in a staggered position with respect to the N-methyl group. The presence of the oxygen group in the apical position of the intermediate permits the cleavage of the P-O bond and the formation of the compound **40** with retention of configuration. Brown arrived to a similar conclusion studying the reaction between an oxazaphospholidine oxide and Grignard reagents<sup>55</sup>. This mechanism agrees with the knowledge of stereochemistry of substitution reactions at the phosphorus atom with other cyclic compounds<sup>73,74</sup>.

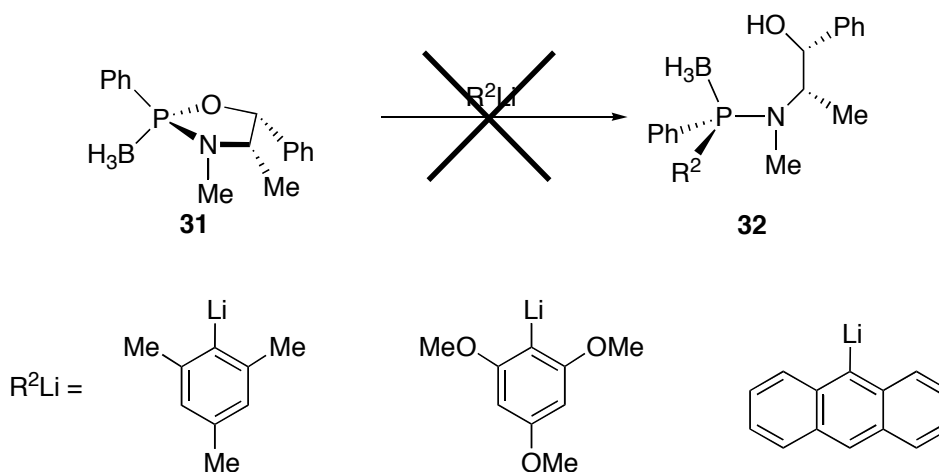
As it has been said, a variety of alkyl- and aryllithium reagents, with diverse electronic and steric properties, are able to react smoothly with **31**, but some limitations have been found. The first of them arose in the preparation of *P*-stereogenic analogues of dppf (**Equation 5**).



**Equation 5.** Introduction of a ferrocene moiety to **31**.

It was discovered that 1,1'-dilithioferrocene did react with **31**, though a poor yield and stereoselectivity were found for this reaction<sup>59,65</sup>. Jugé<sup>65</sup> only reported the overall yield of the bisaminophosphine-boranes **42**, whereas van Leeuwen<sup>59</sup> estimated the diastereomeric ratio  $R_P,R_P$ :*pseudomeso* of **42** to be 65:35. These rather disappointing results were explained by the steric hindrance of the ferrocene, which requires higher temperatures for the reaction to proceed, implying a serious decrease in stereoselectivity. At this point, it has to be said that using other approaches, ferrocene has been successfully introduced (in terms of yield and stereoselectivity) by several groups, as it will be commented in paragraph **3.3.4.5**.

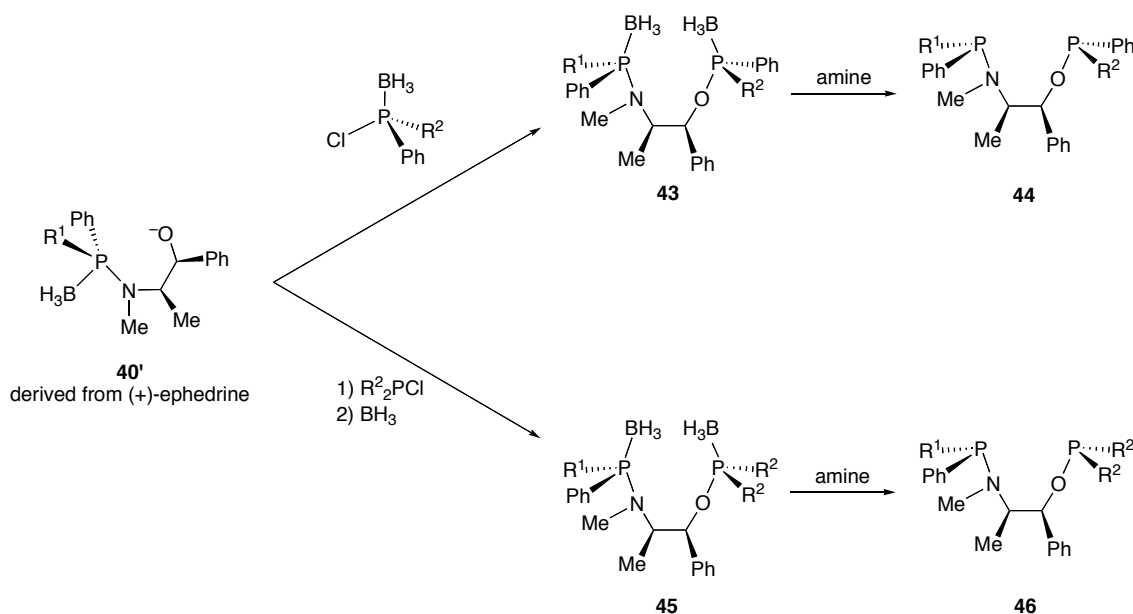
Another limitation of this first nucleophilic step was pointed out more recently in Mezzetti's laboratories<sup>57</sup>, when trying to prepare phosphines bearing highly symmetric, bulky substituents. In this study it was found that *o,o'*-disubstituted aryllithium compounds did not react with **31**, as shown in **Equation 6**.



**Equation 6.** Unsuccessful attempt to introduce *o,o'*-disubstituted aryls at the phosphorus atom.

This result contrasts strikingly with the facile introduction of an *o*-substituted aryl group (*o*-anisyl, 1-naphthyl, etc), reported by other groups<sup>59,64</sup>, and restricts the applicability of the oxazaphospholidine approach.

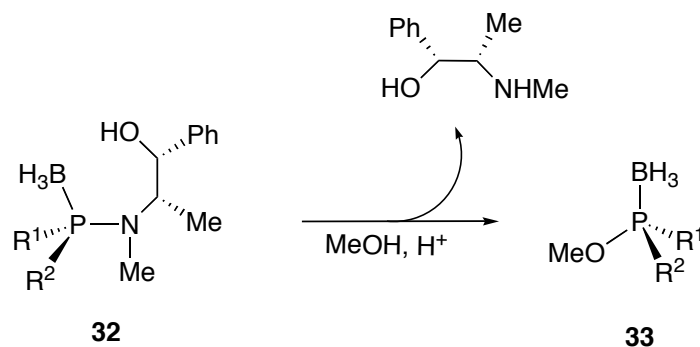
Vogt<sup>66</sup> and Jugé<sup>63</sup> used the synthon **40** (**Scheme 10**) in the synthesis of new aminophosphine-phosphinite ligands (AMPP). These kinds of compounds contain either one (**46**) or two (**44**) stereogenic phosphorus atoms, as shown in **Scheme 11**.



These AMPP ligands were coordinated to rhodium and successfully used in catalytic hydrogenation<sup>63</sup> and hydroformylation<sup>66</sup>.

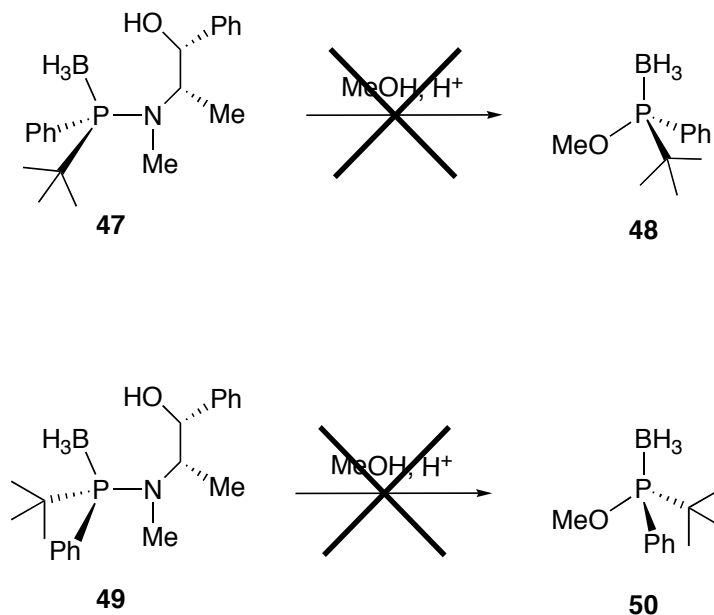
#### 3.3.4.4. Stereoselective methanolysis of aminophosphine-boranes

Following the general method depicted in paragraph 3.3.4.1, **Scheme 8**, the next step in the synthesis is the acidic methanolysis of **32** to produce the phosphinite-boranes **33** as schematized in **Equation 7**.



Reaction conditions are straightforward: the aminophosphine-boranes **32** are dissolved in methanol and one equivalent of sulphuric acid is added at 0 °C or at room temperature. One equivalent of (–)-ephedrine is released and can be recycled.

Generally speaking, this step usually works without problem, affording **33** in high yield and stereoselectivity, with inversion of configuration at the phosphorus atom, because it is considered a S<sub>N</sub>2 process. An exception to the straightforwardness of the reaction was found by Rippert<sup>60</sup>, who observed that the introduction of a *tert*-butyl group precludes the methanolysis step (**Equation 8**).



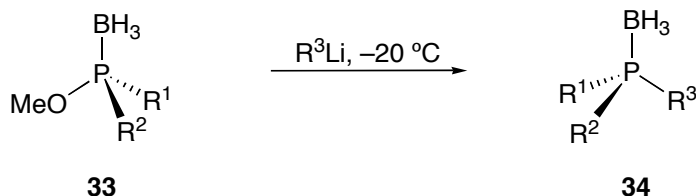
**Equation 8.** Unsuccessful attempt to synthesize phosphinite-boranes bearing a *tert*-butyl group.

Neither **47** (derived from (–)-ephedrine) nor **49** (derived from (+)-*pseudo*ephedrine) react with methanol, even at reflux. The steric hindrance and the basicity of the *tert*-butyl group probably account for this lack of reactivity.



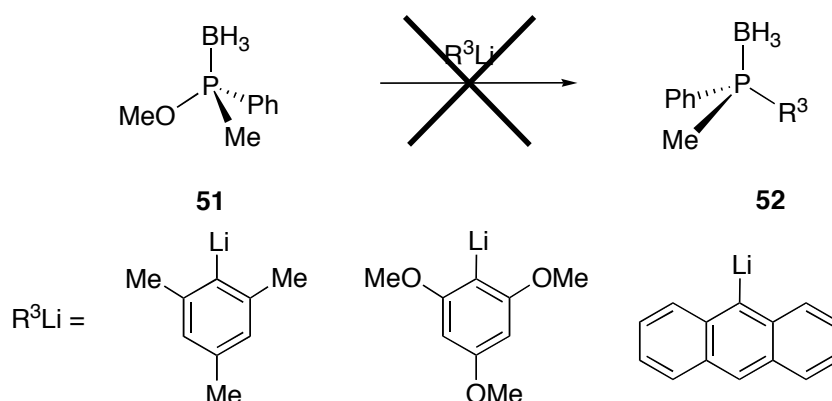
### 3.3.4.5. Stereoselective nucleophilic attack on phosphinite-boranes

The phosphinite-boranes **33** react with organolithium reagents, at low temperature, to afford the tertiary phosphine-boranes **34**, with clean inversion of configuration at the phosphorus atom, as depicted in **Equation 9**.



**Equation 9.** Reaction of phosphinite-boranes **33** with organolithium reagents.

The reaction has been proved to be quite general, both aryl and alkyl lithium derivatives give the desired reaction. An exception to this assertion, however, was found by Mezzetti's group<sup>57</sup>, as shown in **Equation 10**.



**Equation 10.** *o,o'*-disubstituted aryllithium reagents do not react with **51**.

Parallel to what is shown in **Equation 6** (§ 3.3.4.3), it was found that *o,o'*-disubstituted aryllithium reagents do not react either with the phosphinite **51**. Mezzetti's group pursued in their interest of obtaining *P*-stereogenic phosphines with *o,o'*-disubstituted groups by synthesizing the oxazaphospholidine **31** (§ 3.3.4.1) with R<sup>1</sup> = mesityl and continuing with the scheme depicted in **Scheme 8**. Although they met with some success, the strategy was abandoned because of the low yields when opening the compound **31** and in the subsequent methanolysis step<sup>57</sup>.

At this point, thus, it seems clear that the Jugé's method does not allow the introduction of *o,o'*-disubstituted aryl groups, which restricts the applicability of this method in the synthesis of highly crowded phosphines.

Introducing a ferrocene, which, as it has been stated before, was a troublesome issue, met with more success when ferrocenyllithium (or 1,1'-dilithioferrocene) was introduced in this second nucleophilic substitution (**Equation 9**). Although some loss of optical purity was observed, chromatographic techniques allowed the preparation of the desired enantiomerically pure phosphine-boranes. By this token, mono and bidentate ferrocenyl phosphines, some of them shown in **Figure 7**, were successfully prepared and used in some asymmetrically catalyzed reactions<sup>59,67-69,75-77</sup>.

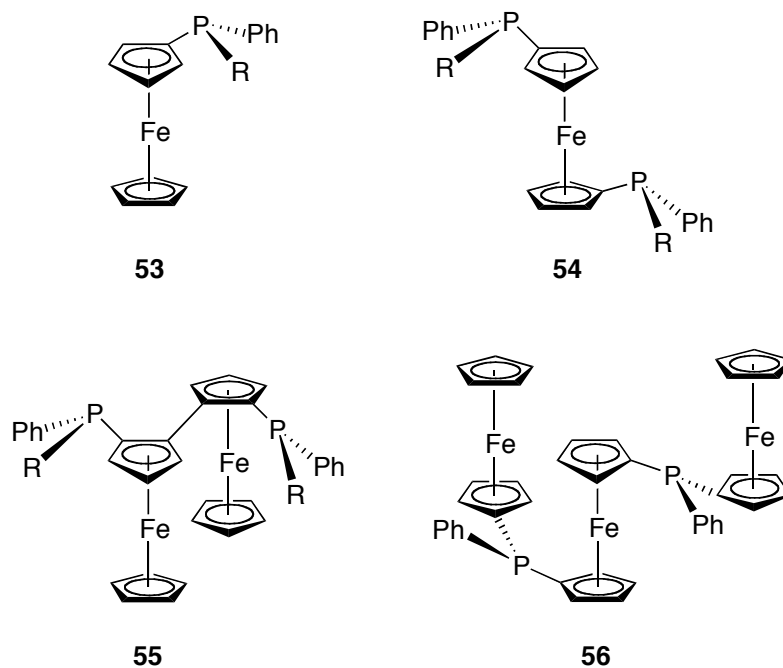
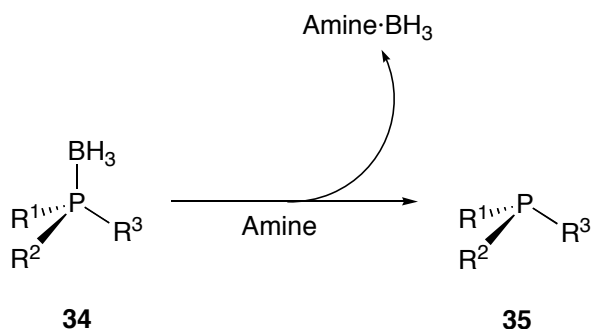


**Figure 7.** *P*-stereogenic phosphines containing ferrocene.

In phosphines **53**, R is an aryl or alkyl group, whereas in phosphines **55**, R is an aryl group.

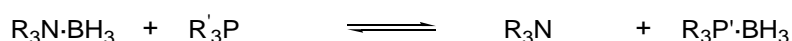
### 3.3.4.6. Deboronation of phosphine-boranes

Turning back to **Scheme 8** (§ 3.3.4.1), the last step in the method is the deboronation of the phosphine-boranes **34** to furnish the desired free phosphines **35** (**Equation 11**). This deboronation is usually done by using secondary amines, such as diethylamine or morpholine. The first examples were reported by Imamoto<sup>49</sup>, and since then, this procedure has become routine.



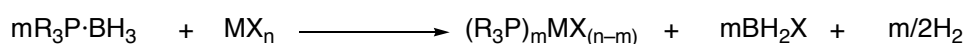
**Equation 11.** Deboronation of phosphine-boranes using amines.

Although in general,  $R_3P \cdot BH_3$  adducts are more stable than the corresponding  $R_3N \cdot BH_3$ , the equilibrium shown in **Equation 12** enables the  $BH_3$  group to migrate to amines<sup>51</sup>. Hence, the free phosphine can be released by treatment of the phosphine-borane with a large excess of strong amines<sup>51,52</sup>. When secondary amines are not sufficiently effective, it has been found that cyclic, highly reactive amines such as DABCO or pyrrolidine are useful<sup>52,78</sup>.



**Equation 12.** Equilibrium between phosphine-boranes and free amines

The reaction proceeds *via* dissociation mechanism. In contrast to the reduction of the phosphine oxides, the removal of the  $BH_3$  group does not jeopardize the configurational integrity of the stereogenic phosphorus atom. The removal of the borane group has even been performed in a one-pot reaction, followed by complexation to a catalytically active metal to avoid the handling of the free phosphine<sup>78,79</sup>. With this idea, in a recent paper, Juge<sup>80</sup> took advantage of the reducing properties of the borane group and prepared, in one-pot reaction, phosphine complexes of Pd(0) and Rh(I) from Pd(II) and Rh(III) salts and *P*-chirogenic phosphine-boranes, in a general reaction described in **Equation 13**. The complexes were directly tested in catalyzed reactions.



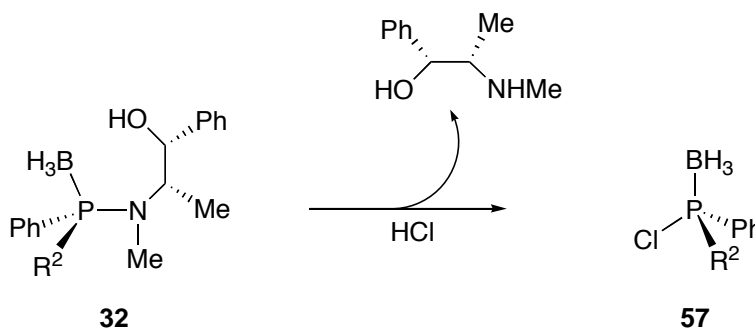
**Equation 13.** Direct coordination of phosphines with concomitant reduction of the metal.

In electron rich phosphine-boranes, the P-B bond is rather inert and therefore these compounds react sluggishly with amines. Livinghouse developed a procedure suitable to deprotect this kind of compounds<sup>81</sup>. He found that phosphine-boranes could be cleanly deprotected using certain acids such as methansulfonic or tetrafluoroboric followed by neutralization with NaHCO<sub>3</sub> or K<sub>2</sub>CO<sub>3</sub>. The most efficient reagent, in terms of rate and yield was HBF<sub>4</sub>·OMe<sub>2</sub>. This method, complementary to the classic one with amines, has been successfully used by Imamoto in the preparation of a large family of *P*-stereogenic diphosphines (§ 3.3.5.3, 3.3.5.4 and 3.3.5.5). The decomplexation has been demonstrated to preserve completely the stereochemical integrity of the stereogenic phosphorus atom, with total retention of configuration.

During this section, the method developed by Jugé has been explained in detail. As it has been described, albeit some limitations, it allows the preparation of *P*-stereogenic phosphines in multigram scale with wide flexibility when choosing the groups attached to the phosphorus atom. Moreover, the intermediates (the phosphine-boranes) are stable at air, which greatly facilitates the synthetic and purification steps. Not surprisingly, though, this methodology has been used by many groups for the last 15 years and has contributed importantly to the renewed interest that *P*-chirogenic ligands have been and are currently living.

### 3.3.4.7. *P*-chirogenic chlorophosphine-boranes

Moulin and Jugé have recently developed<sup>61,63,82,83</sup> (**Equation 14**) a strategy for the preparation of enantiomerically pure chlorophosphine-boranes **57**. This strategy was developed by analogy to the methanolysis step, when other acids apart from sulphuric were tested.



**Equation 14.** Stereoselective synthesis of chlorophosphine-boranes.

The preparation of the chlorophosphine-boranes is *formally* similar to the methanolysis step (§ 3.3.4.4), but with the difference that chlorophosphine-boranes **57** are much more reactive towards nucleophiles than the corresponding phosphinite-boranes **33**.

As the chlorophosphine-boranes are highly reactive, usual hydrochloric acid solutions in water can not be used and so dry sources of HCl are necessary. Toluenic solutions of HCl, obtained by bubbling pure HCl through toluene, were originally used, after titration, by Jugé.

Recently, however, Mezzetti<sup>57</sup> and others have successfully used commercial solutions of HCl in diethyl ether as a more practical reagent.

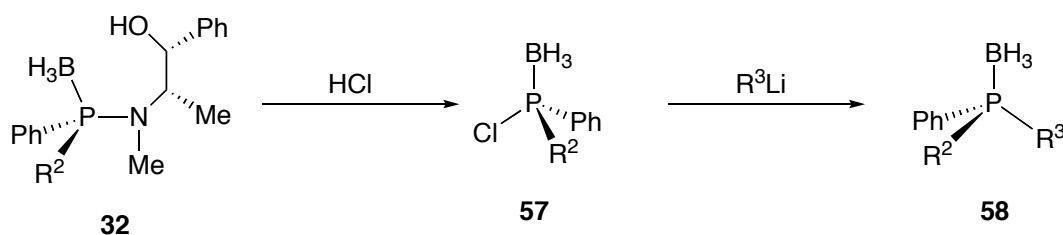
In spite of the formal similarity between the methanolysis step to produce the phosphinite-boranes **33** and the acidolysis step to produce the chlorophosphine-boranes **57**, several differences must be considered.

Firstly, the stability of the compounds **33** and **57** is very different. Whereas the phosphinite-boranes **33** are completely stable compounds which can be recrystallized, chromatographed and stored with no special care, the chlorophosphine-boranes **57** are much more sensitive to atmospheric conditions and have to be handled with care. Several attempts to purify this kind of compounds, by column chromatography, have met with decomposition and/or racemization.

Secondly, stereoselectivity in their formation deserves special attention. Generally speaking, the excellent stereoselectivity attained in the preparation of phosphinite-boranes **33** is not achieved in the chlorophosphine-boranes, although high values of enantiomeric excesses are found, and analogously to the preparation of **33**, with inversion of configuration at the phosphorus atom.

Those reasons account for the very few applications of chiral chlorophosphine-boranes in the literature. Nevertheless, they are useful synthons when they are used *in situ*, without isolating them. At this point, it is interesting to state that without the protection of the borane group, Jugé showed<sup>82</sup> –by means of calculation– that the asymmetrically substituted chlorophosphines, R<sup>1</sup>R<sup>2</sup>PCl, are extremely prone to racemization when traces of HCl (almost impossible to avoid in experimental conditions) are present, precluding their synthetic utility.

Returning to the stereoselectivity of the formation of chlorophosphine-boranes **57**, it depends on the groups attached to the phosphorus atom, the molar excess of HCl, the concentration of reagents and the reaction time. Jugé investigated systematically<sup>83</sup> these factors and was able to draw some general conclusions. Due to the sensitivity of this kind of compounds, the chlorophosphine-boranes were quenched with alkyllithium compounds to perform the analysis of yield and selectivity (**Scheme 12**). It was assumed that this step was quantitative and with full inversion of configuration at the phosphorus atom.



**Scheme 12.** Preparation of *P*-stereogenic phosphine-boranes from chlorophosphine-boranes.

<i>Entry</i>	<i>R</i> <sup>2</sup>	<i>Eq. HCl</i>	<i>[HCl]/mM</i>	<i>R</i> <sup>3</sup>	<i>Yield of 58 (%)</i>	<i>e.e. (%)</i>
1	Methyl	2.1	20	<i>o</i> -anisyl	80	90
2	<i>o</i> -anisyl	2.1	180	Me	90	98
3	<i>o</i> -tolyl	6.0	60	Me	61	98
4	1-naphthyl	2.1	20	Me	50	0
5	2-naphthyl	3	130	Me	46	85
6	2-biphenyl	6	20	Me	41	99
7	Cyclohexyl	6	60	Me	46	80
8	<i>tert</i> -butyl	6	60	—	—	—

**Table 4.** Optimized conditions for the synthesis of chlorophosphine-boranes **57**.

**Table 4** shows the best conditions (in terms of stereoselectivity) for each substituent  $R^2$  at the phosphorus atom.

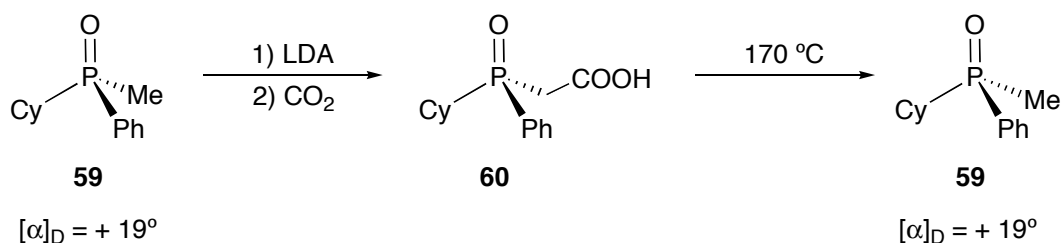
Firstly, it should be noted that the more the steric hindrance the slower the acidolysis reaction proceeds. Thus, at a given time, the chemical yields of the chlorophosphine-boranes **57** decreases as the  $R^2$  group in **32** becomes bulkier (entries 1-7). In fact, when  $R^2 = \textit{tert}$ -butyl the reaction does not occur (entry 7), analogously to what happens with the methanolysis (§ 3.3.4.4). Secondly, it has been confirmed that by increasing the reaction time, although the conversion is usually higher, the enantiomeric purity of the chlorophosphine-borane decreases.

As it has been depicted in **Scheme 12**, chlorophosphine-boranes react instantaneously with organolithium reagents to furnish phosphine-boranes with inversion of configuration at the phosphorus atom. This fact makes compounds **57** attractive synthons when the phosphinite-boranes **33** are not reactive enough. Furthermore, the chlorophosphines **57** also react with other milder nucleophiles such as alkoxides or thiolates, opening up the possibility of an easy synthesis of a large number of *P*-stereogenic compounds<sup>83</sup>.

### 3.3.5. Stereoselective deprotonation of enantiotopic methyl groups

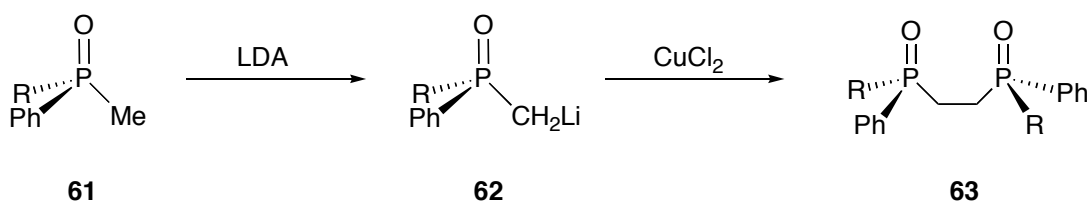
#### 3.3.5.1. Introduction

The starting point of this section is certainly the observation, published in 1968 by Mislow and coworkers<sup>38</sup>, that deprotonation of the P-Me group in phosphine oxides occurs with total preservation of configurational integrity of the neighbouring stereogenic phosphorus centre (**Scheme 13**). The  $\phi$ -carbanion derived from **59** can react with electrophiles to give  $\phi$ -functionalized phosphines.



**Scheme 13.** First example of deprotonation of a P-Me group of a *P*-stereogenic compound.

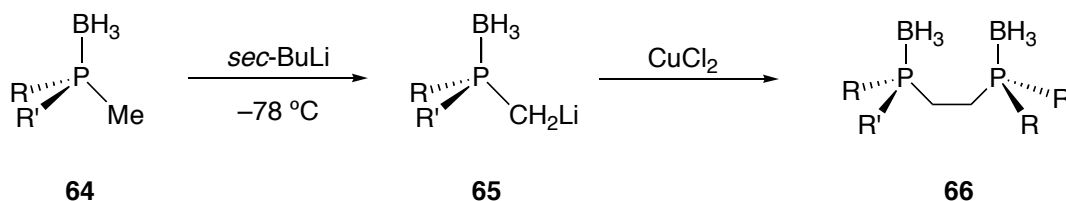
One important application of this relative *acidity* of methyl protons came in 1973, when Mislow discovered that methylphosphine oxides can be oxidatively coupled with Cu *via* their  $\phi$ -carbanions to yield directly the corresponding resolved symmetrical, *P*-stereogenic 1,2-diphosphinoethane oxides<sup>84</sup>, **63** (**Scheme 14**).



**Scheme 14.** Copper promoted oxidative coupling of phosphinomethylide oxides.

This step was used by the Monsanto group (**Scheme 3** and **Scheme 4**, § 3.3.2) in their preparation of DIPAMP<sup>40</sup> and it was later adapted by other groups to synthesize several  $C_2$  symmetrical diphosphines.

It was found that in analogy to the oxides, phosphine-boranes bearing a methyl, it is readily deprotonated by strong bases<sup>49,85</sup>. This relative acidity is attributed to the electron-withdrawing effect of the P-B bond, which activates adjacent C-H bonds<sup>51</sup>. In phosphine-boranes, deprotonations are usually carried out using organolithium reagents, particularly *sec*-butyllithium and *n*-butyllithium. The highly nucleophilic carbanions **65** obtained react with electrophiles to give the  $\phi$ -functionalized products and can also be oxidatively coupled by copper (**Scheme 15**).



**Scheme 15.** Copper promoted oxidative coupling of phosphinomethylide-boranes.

The deprotonation of methylphosphine-boranes would allow the synthesis of a high variety of optically pure *P*-stereogenic compounds, provided that *an enantiomerically pure P-stereogenic methylphosphine-borane was available*. The latter assertion was true until a new approach was disclosed by Evans in 1995<sup>86</sup>, whose features will be discussed in the following paragraphs.

Examining the previous discussion in this chapter, one can see that menthol and ephedrine have been successfully used (with very different approaches, however) as chiral auxiliaries to prepare enantiomerically pure *P*-stereogenic phosphines. In the next section the use of another chiral auxiliary, sparteine, is discussed. The molecular structure of sparteine is shown in **Figure 8**.

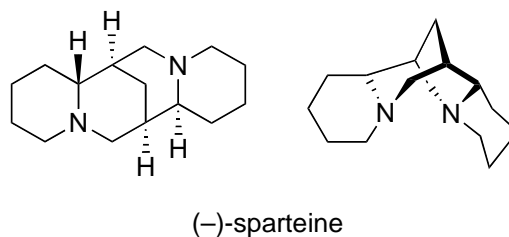


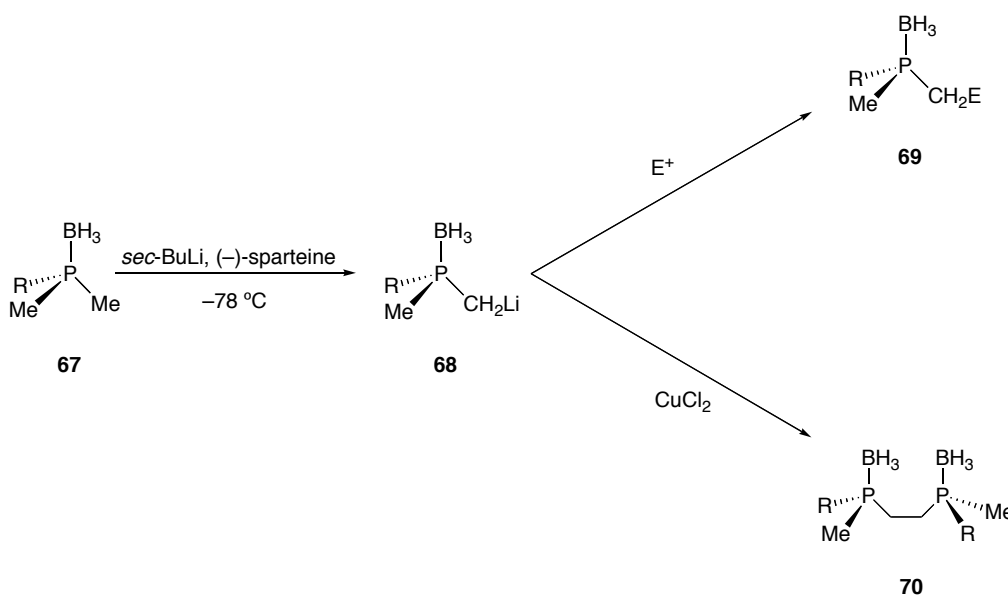
**Figure 8.** Two views of the structure of (-)-sparteine.

The usual representation of (-)-ephedrine is the one at left, although the representation at right is more similar to the real structure of this amine in solution, when complexes the lithium atom.



### 3.3.5.2. Use of sparteine as a chiral auxiliary

The approach of Evans<sup>86</sup> is schematized in **Scheme 16**. It is based in enantioselective deprotonation of aryldimethylphosphine-boranes, using *sec*-BuLi and (–)-sparteine as a chiral auxiliary. Sparteine effectively complexes the lithium atom<sup>87,88</sup> while the deprotonation takes place and, in this chiral environment, *sec*-BuLi is able to differentiate between the two enantiotopic methyl groups, deprotonating selectively one of them, to generate a single *P*-stereogenic,  $\phi$ -carbanion **68**, which is made reacted with an electrophile to yield **69** or coupled with Cu(II) to produce the corresponding diphosphine-borane with a 1,2-ethanediyl bridge, **70**.



**Scheme 16.** Stereoselective deprotonation of an enantiotopic methyl group.

By this method, a small family of diphosphine-boranes was prepared with good diastereomeric and enantiomeric excesses. The results are gathered in **Table 5**.

<i>R</i>	( <i>S,S</i> ): <i>meso</i>	Yield (%)	<i>e.e.</i> (%)
Phenyl	79:21	54	98
<i>o</i> -anisyl	85:15	65	99
<i>o</i> -tolyl	90:10	56	99
1-naphthyl	89:11	51	96

**Table 5.** Diphosphine-boranes obtained by Evans using enantioselective deprotonation.

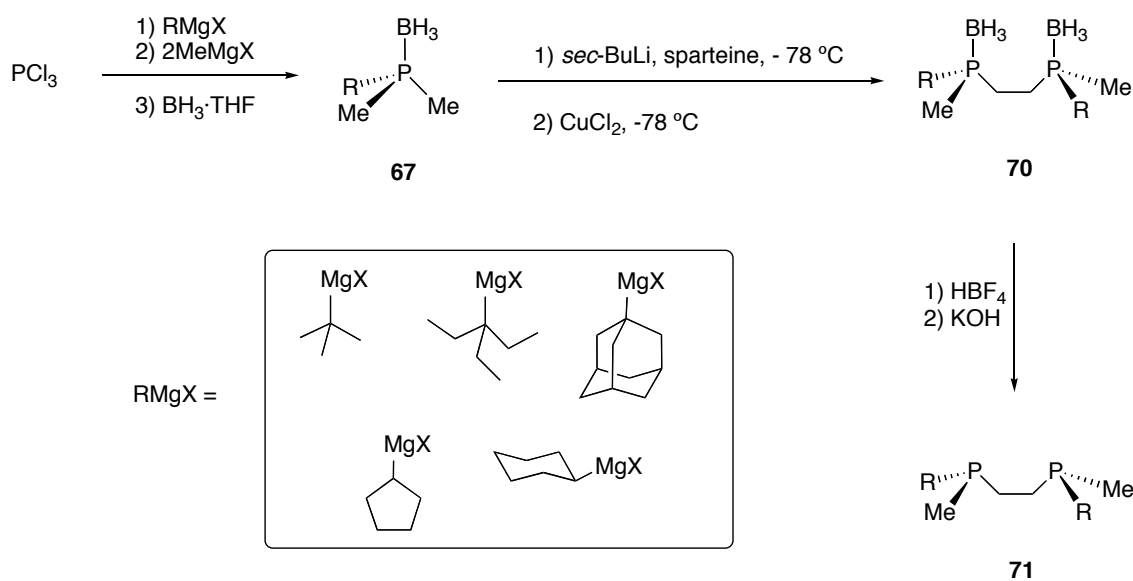
For the diphosphine-boranes, the absolute configuration at the phosphorus atom was established to be (*S,S*) for *R* = *o*-anisyl, by preparing — stereoselectively and with retention—

the corresponding oxide, which was already known. For the other ligands, the (*S,S*) configuration was assigned by analogy.

The scope of enantioselective deprotonation of dimethylphosphine-boranes has been greatly expanded by continued work of Imamoto's laboratories, as it will be described in the following sections.

### 3.3.5.3. Synthesis of symmetric BisP\* diphosphines

In Evan's work, one of the groups attached to each of phosphorus atoms was an aryl group. In 1998 Imamoto's team published<sup>89,90</sup> the approach depicted in **Scheme 17**, which allows the synthesis of *C*<sub>2</sub>-type diphosphines bearing only alkyl groups at the phosphorus atoms. In fact, each phosphorus atom bears one bulky group and the smallest alkyl group, namely the methyl group. This family of diphosphines was called BisP\*. Electronically they are electron-rich phosphines, which were complexed to rhodium and used in the catalytic asymmetric hydrogenation of several substrates, with high degree of activity and enantioselectivity. Furthermore, they were used in detailed studies of the mechanism of enantioselection.



**Scheme 17.** Imamoto's approach to the synthesis of *C*<sub>2</sub>, *P*-chirogenic diphosphines.

It is noteworthy that this strategy starts from simple materials to yield diphosphine-boranes **70** in one-pot reaction. Noticeably, the usual deboronation reaction with amines did not work properly with these electron-rich phosphines and the aforementioned method developed by Livinghouse<sup>81</sup> had to be applied.

Regarding the diastereo- and enantioselectivity of the formation of the diphosphine-boranes **70**, they were good, although not excellent, as it is depicted in **Table 6**.

<i>R</i>	( <i>S,S</i> ): <i>meso</i>	Yield (%)	<i>e.e.</i> (%)
<i>t</i> Bu	87:13	35	99
Et <sub>3</sub> C-	95:5	69	99
1-ad	95:5	33	— <sup>a</sup>
<i>c</i> -C <sub>5</sub> H <sub>9</sub>	71:29	46	75
Cy	— <sup>a</sup>	55	— <sup>a</sup>

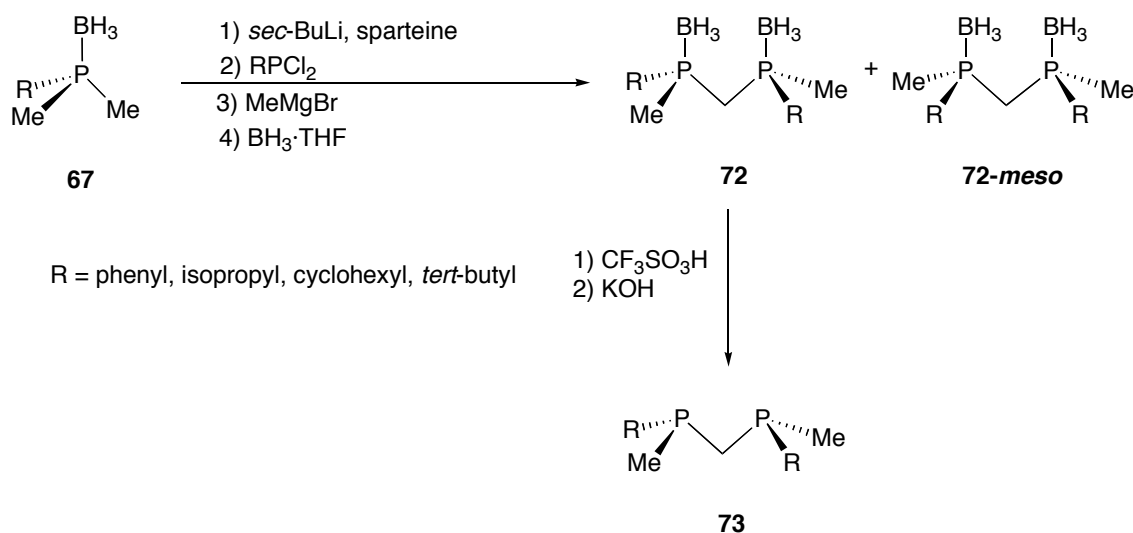
<sup>a</sup>: Not determined.

**Table 6.** Diphosphine-boranes obtained by Imamoto's team.

The pure diphosphines **70** were separated from the *meso* diphosphines by means of recrystallization. The absolute configurations at the phosphorus atoms were determined using single crystal X-ray analyses.

### 3.3.5.4. Synthesis of MiniPhos diphosphines

Starting from the work of the preceding section, Imamoto's team succeeded in the synthesis of analogues of **71** but with the shortest alkyl bridge, namely the methylene bridge<sup>91</sup>. This work is summarized in **Scheme 18**.



**Scheme 18.** Synthesis of methylene bridged, *P*-stereogenic diphosphines.

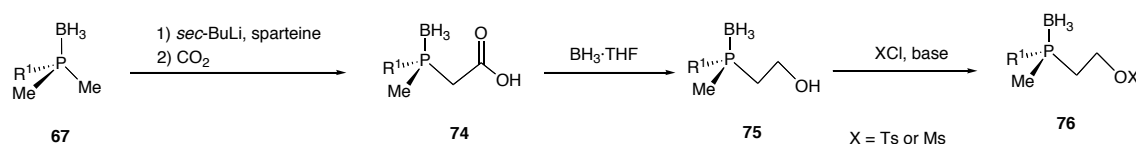
A mixture *ca.* 1:1 of the desired phosphine-boranes **72** and the *meso* isomer was obtained. This mixture was easily separated by recrystallization from methanol or ethanol and the desired phosphine-boranes **72** were obtained in optically pure form and deprotected to furnish the pure diphosphines **73**, which were called MiniPhos. X-ray structure determination was used to ascertain the absolute configuration at the phosphorus atom.

The MiniPhos ligands were obtained as enantiomerically pure products, although with modest overall yields (< 30%). Those ligands were used in some representative catalytic asymmetric reactions (hydrogenation, hydrosilylation and Michael addition) and were found to exhibit, in some cases, excellent to almost perfect levels of enantioselectivity, despite being quite simple and small in comparison with previously reported chiral diphosphines.

### 3.3.5.5. Synthesis of unsymmetric BisP\* diphosphines

At this point, Imamoto's team, having seen the good results of BisP\* ligands, envisaged the synthesis of analogue phosphines but bereft of the  $C_2$  symmetry axis, that is, with different substituents on each phosphorus atom<sup>92,93</sup>. To tackle this endeavour, two precursors were prepared.

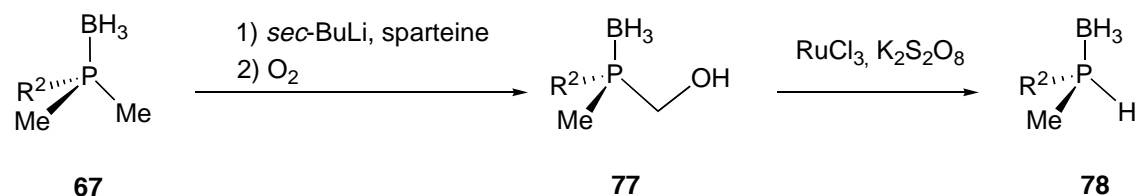
The first of them were the phosphine-boranes **76**, bearing a good leaving group (mesylate or tosylate) on the  $\phi$  position<sup>92,93</sup>. The synthesis of such a product is depicted in **Scheme 19**.



**Scheme 19.** Synthesis of precursors **76** bearing a mesyl or tosyl group.

The dimethylphosphine-boranes **67** were enantioselectively deprotonated with *sec*-BuLi in the presence of (–)-sparteine, and then bubbled with  $CO_2$  to afford the phosphinoacetic-borane acids **74**. Reduction of these carboxylic acids by borane-THF complex afforded, in quantitative yield, the phosphinoethanol-boranes **75**, which were tosylated or mesylated to afford the desired compounds **76**.

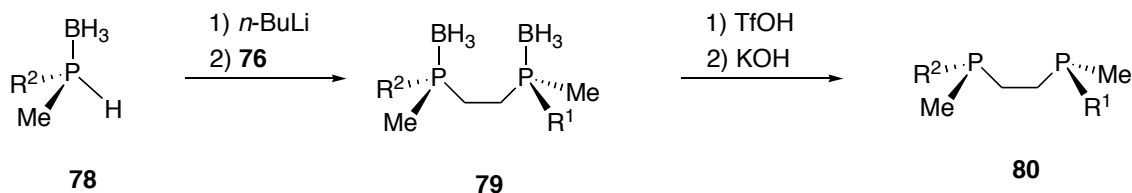
The second type of precursors needed were enantiomerically pure, secondary phosphine-boranes **78**<sup>94</sup>. These were prepared using the method of **Scheme 20**.



**Scheme 20.** Preparation of enantiomerically pure, secondary phosphine-boranes.

The first step was the preparation of the primary alcohols **77**, by oxidation, with molecular oxygen, of the organolithium compounds derived from **67**. These alcohols were oxidatively degraded –taking advantage of a known procedure– to yield the secondary phosphine-boranes **78**.

With the products **76** and **78** in hand, Imamoto *et al.* prepared<sup>92,93</sup> (Scheme 21) the desired unsymmetrical BisP\*·BH<sub>3</sub> (this was the name coined for the ligands **80**). Deprotection furnished the free diphosphines. At this point, it has to be reminded that R<sup>1</sup> and R<sup>2</sup> are bulky alkyl groups, such as adamantyl or *tert*-butyl.

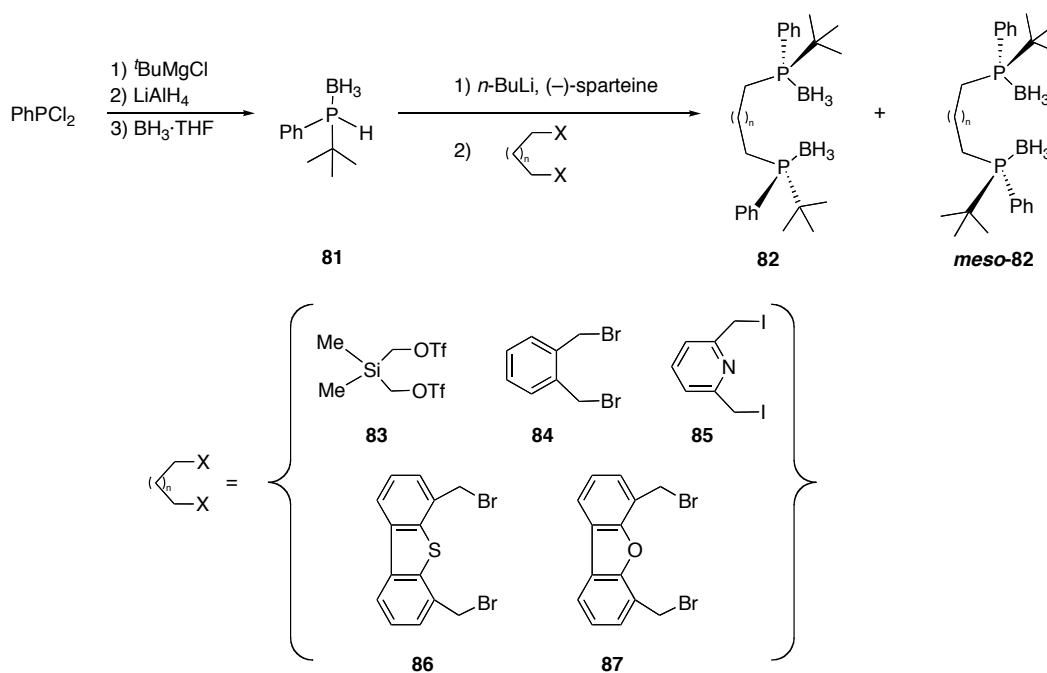


Scheme 21. Preparation of unsymmetrical BisP\* ligands.

This kind of ligands were used in asymmetric, rhodium catalyzed hydrogenation of several substrates. The results obtained were very promising, with high activities and enantioselectivities, which were better, in some cases, than those obtained with C<sub>2</sub> counterparts.

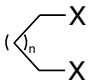
### 3.3.6. Dynamic resolution of P-chirogenic phosphides

At this point, it is interesting to note that enantioselective deprotonation with sparteine has also been used with racemic secondary phosphine-boranes. This method, discovered by Livinghouse<sup>95</sup> and shown in Scheme 22, was applied with success to prepare several diphosphine-boranes bearing a *tert*-butyl and a phenyl group at the phosphorus atoms and different backbones between them.



Scheme 22. Preparation of diphosphine-boranes by means of deprotonation of secondary phosphines.

The racemic substrate selected was *tert*-butylphenylphosphine-borane, **81**, which was readily prepared from  $\text{PhPCl}_2$  and *tert*-butylmagnesium chloride, with a final reduction with  $\text{LiAlH}_4$ . This compound was subjected to deprotonation using *n*-BuLi in presence of (–)-sparteine, at  $-78\text{ }^\circ\text{C}$ . It was found that lithiated **81** could be dynamically resolved in good enantioselectivity. This enantioselectivity was temperature and time dependent. After a systematic variation of these two parameters, it was deduced that the optimum conditions for equilibration to proceed were 1h at room temperature. Afterwards, the suspension was cooled again at  $-78\text{ }^\circ\text{C}$  and was left to react with the dihalide or *bis*(triflate), to furnish **82**. The phosphine-boranes prepared by this method are listed in **Table 7**.

	<b>82:meso 82</b>	<b>Yield (%)</b>	<b>e.e. (%)</b>
<b>83</b>	15.0:1	67	— <sup>a</sup>
<b>84</b>	21.7:1	68	>99
<b>85</b>	11.3:1	71	>99
<b>86</b>	18.4:1	76	>99
<b>87</b>	11.8:1	75	>99

<sup>a</sup>: No resolution of the enantiomers could be obtained by HPLC.

**Table 7.** Bisalkylations involving dynamically resolved *tert*-butylphenylphosphine-borane.

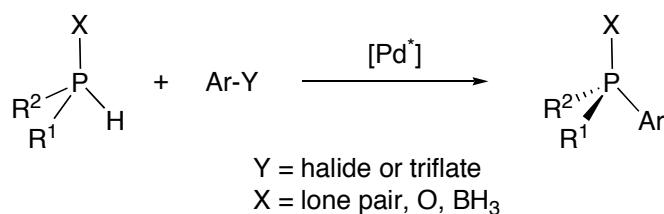
## 3.4. Preparation by asymmetric catalysis

### 3.4.1. Introduction

A scrutiny of the principal available methods to prepare enantiomerically pure *P*-stereogenic phosphines, described in this chapter, reveals that either resolution of racemics or either asymmetric synthesis need a stoichiometric amount of a chiral auxiliary, such as menthol, ephedrine or sparteine. These are quite expensive products when they are needed in multigram or kilogram quantities. Hence, an approach that would need a *catalytic* amount of a chiral product would be highly desirable. This endeavour, in principle, can be carried out by transition metal, chiral catalysts. In the recent years, some reports in the literature suggest that this is a feasible approach.

Glueck's group has been publishing seminal papers<sup>96-99</sup> developing the aforementioned idea. Initial work on hydrophosphination<sup>96</sup> (addition of a secondary phosphine, to an olefin double bond, to produce a stereogenic carbon and/or a stereogenic phosphorus atom), catalyzed by a chiral platinum complex achieved modest success (in terms of activity and enantioselective), but demonstrated that the reaction was catalytic.

More recently, palladium catalyzed asymmetric phosphination has met with very promising results. Pd-catalyzed asymmetric phosphination is a cross-coupling of a secondary, racemic phosphine (or derivative) with an aryl halide or triflate; to prepare a tertiary, *P*-chirogenic phosphine with control of the stereochemistry at the phosphorus atom, as shown in **Equation 15**. In principle, the use of chiral palladium catalyst could lead to enantioenriched products starting from racemic, secondary phosphines or derivatives.



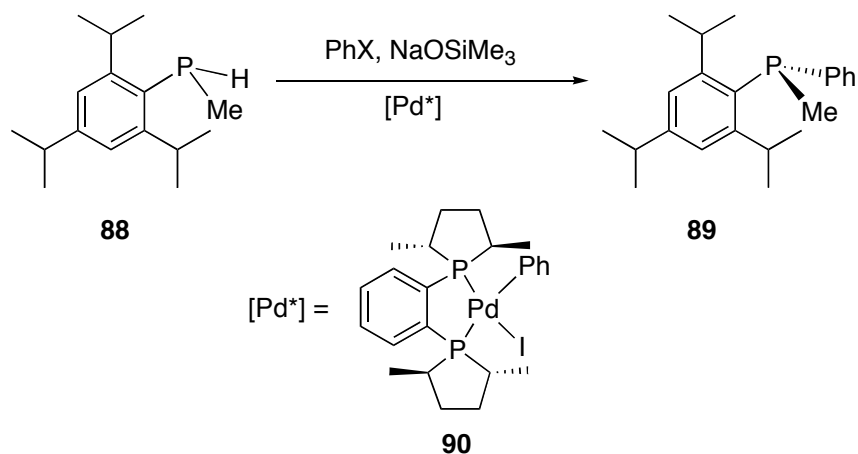
**Equation 15.** Pd-catalyzed phosphination.

*P*-chirogenic, secondary phosphine oxides undergo palladium-catalyzed coupling with aryl or vinyl halides or triflates with retention of configuration at the phosphorus atom<sup>100</sup>. With phosphine-boranes, however, Imamoto observed<sup>101</sup> that coupling enantiopure P(BH<sub>3</sub>)HMePh with *o*-iodoanisole led the PAMP-BH<sub>3</sub> with retention or inversion of configuration at the phosphorus atom depending on base, solvent and temperature.

More recently, Livinghouse showed<sup>102</sup> that adding Cu(I) to similar reaction mixtures gave tertiary phosphine-boranes in high stereoselectivity with retention of configuration at the phosphorus atom.

### 3.4.2. Synthesis of *P*-stereogenic phosphines

With the aim of preparing enantioenriched products from racemic secondary phosphines, one of the reactions studied in Glueck's laboratories<sup>97</sup> is shown in **Equation 16**. Racemic **88**, containing the bulky group 2,4,6-*tris*(isopropyl)phenyl (denoted commonly as *Is*), is coupled to a phenyl group to furnish the enantioenriched phosphine **89**, in a reaction catalyzed by the palladium complex **90**.



**Equation 16.** Pd-catalyzed asymmetric phosphination.

At this point it has to be reminded that the introduction of 2,6 substituted groups is cumbersome (§ 3.3.4.3 and 3.3.4.5). Furthermore, product **89** is a precursor of bidentate phosphines, by coupling with Cu(II).

The catalyst was the DUPHOS palladium complex **90**. The reaction was easily monitored with  $^{31}\text{P}$  NMR spectroscopy. The conditions used and the results obtained are listed in **Table 8**.

<i>Entry</i>	<i>X</i>	<i>Solvent</i>	<i>T</i> (°C)	<i>Yield</i> (%)	<i>e.e.</i> (%)
1	I	THF	21	69 <sup>b</sup>	66
2	I	MeCN	21	60 <sup>b</sup>	58
3	I	Toluene	21	71 <sup>b</sup>	73
4	I	Toluene	4	84 <sup>c</sup>	78
5	Br	Toluene	50	60 <sup>c</sup>	42
6	OTf	Toluene	50	53 <sup>c</sup>	38
7	I	Toluene	21	70 <sup>c</sup>	50
8	I	Toluene	21	90 <sup>d</sup>	70
9	I	Toluene	21	88 <sup>d</sup>	73

<sup>a</sup> Base = NaOSiMe<sub>3</sub> (1 M in THF); catalyst = **90** (5% for all entries except entries 1-2 (7%) and entry 9 (2.5%); 2 equivalents of PhX except in entry 4 (1 equivalent) and entries 8-9 (1.05 equivalents)).

<sup>b</sup> By  $^1\text{H}$  NMR integration after column chromatography.

<sup>c</sup> Isolated yield after column chromatography.

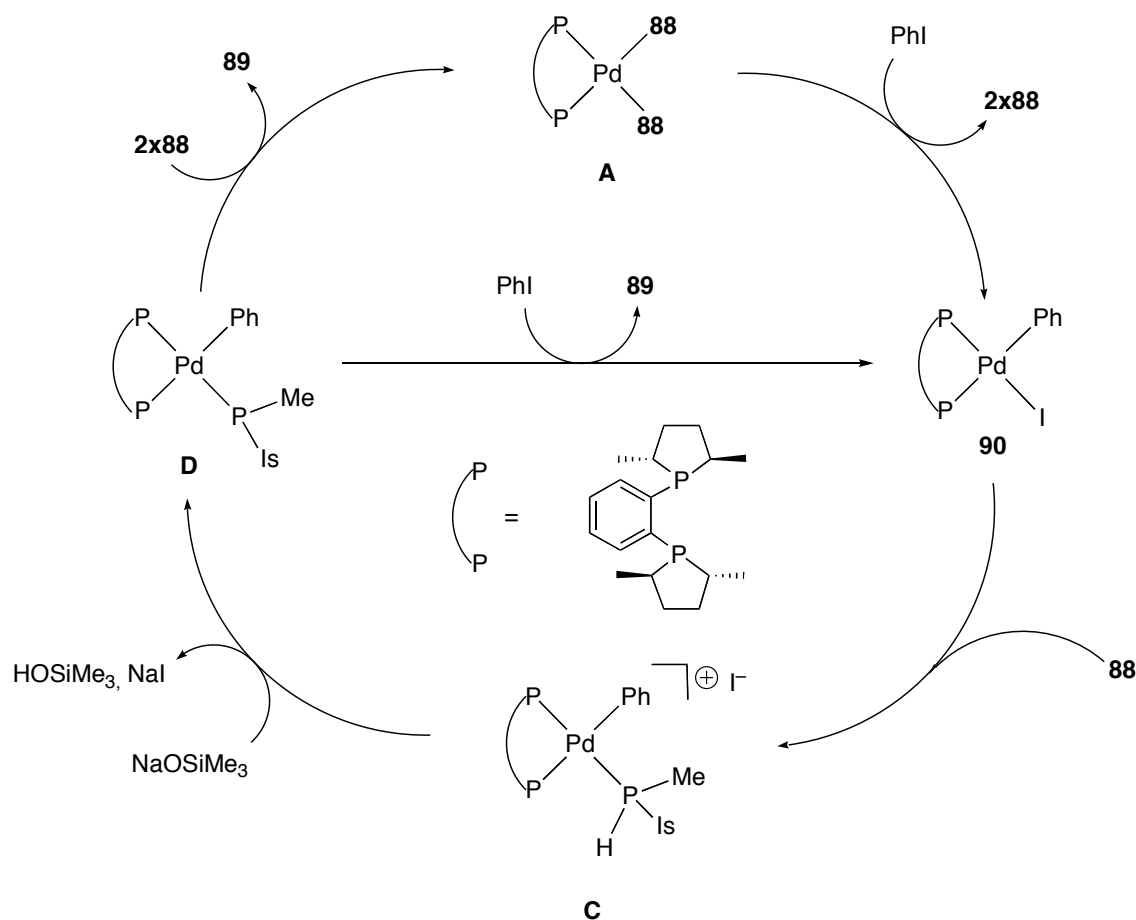
<sup>d</sup> Isolated yields after washing with petroleum ether/THF.

**Table 8.** Pd-catalyzed asymmetric synthesis of **89** from **88**<sup>a</sup>.

With 5% mol of **90**, a typical reaction was complete in about 1 h. Toluene was the preferred solvent (entries 1-3), with increase and reduction of the e.e. at lower and at higher temperatures (entries 4 and 5 respectively). Phenyl bromide and triflate could also be used, albeit e.e.'s were lower (entries 5 and 6).



Some mechanistic studies were performed, which allowed the deduction of a possible catalytic cycle, shown in **Scheme 23**. At low temperature,  $^{31}\text{P}\{^1\text{H}\}$  NMR study of the individual steps in this mechanism provided some insight into the origin of the stereoselectivity.



**Scheme 23.** Catalytic cycle proposed for Pd-catalyzed asymmetric phosphination.

Treatment of the catalyst **90** with the phosphine **88** displaced the iodide to form the cationic complex **C** as a nearly 1:1 mixture of diastereomers. This complex is deprotonated by NaOSiMe<sub>3</sub> to give the phosphido complex **D**. Neither the catalyst **90** nor the phosphine **88** react with NaOSiMe<sub>3</sub> and thus the formation of **D** appears to proceed by this two step process.

The phosphido complex **D** exist as a 40:1 mixture of diastereomers, which presumably interconvert through inversion at the phosphorus atom, as it has been early reported for a similar type of complexes. Reductive elimination of the tertiary phosphine **89** was observed to occur at temperatures above  $-20\text{ }^{\circ}\text{C}$ . Oxidative addition of PhI occurs smoothly to regenerate the catalyst **90**. Complex **A** was also detected, meaning that **D** can also react with two equivalents of the phosphine **88** to generate **A**, which is known to react readily with PhI to form the catalyst **90**. Thus, both routes are operative.

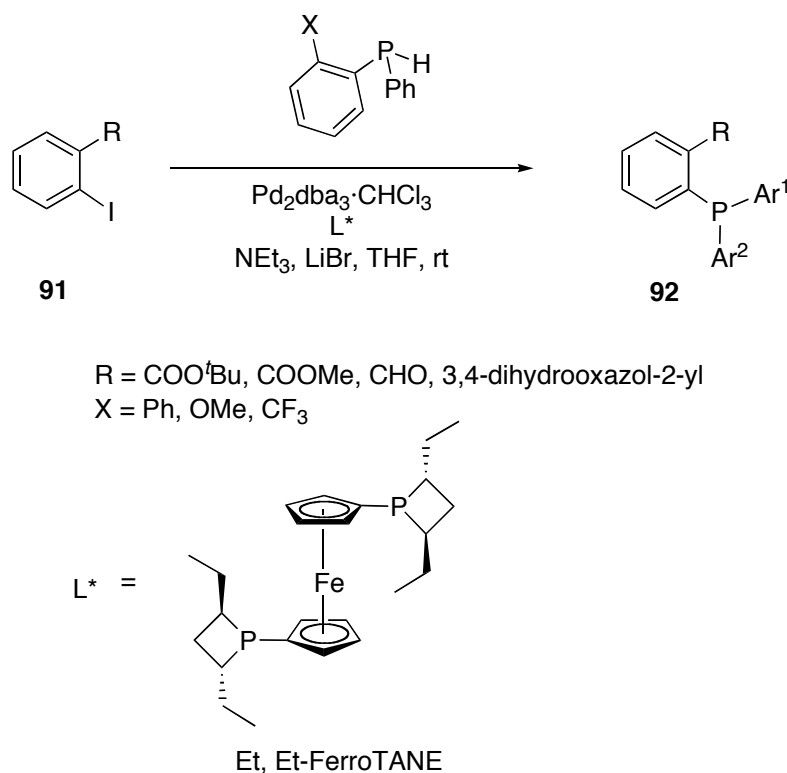
Regarding the origin of enantioselectivity, two possible extreme routes are conceivable. If the two diastereomers of **D** undergo reductive elimination at similar rates, faster than the inversion at the phosphorus atom, the e.e. of the product **89** would reflect their thermodynamic

ratio. Alternatively, if interconversion of the two diastereomers of **D** by inversion at the phosphorus atom is faster than reductive elimination, their relative rates of reductive elimination could control the e.e.

To assess this question, the relative rates of inversion at the phosphorus atom and reductive elimination in complex **D** were evaluated. Deprotonating a 1:1.4 diastereomeric mixture of complex **C**, produced a 1:6 enantiomeric mixture of the final phosphine **89**. This fact implies that inversion at the phosphorus atom in complex **D** is equal or faster than reductive elimination because otherwise the initial ratio of diastereomers of **C** would have been carried through the product. The mechanism of enantioselection, hence, can be described as a dynamic resolution.

Helmchen's group has further developed<sup>103</sup> the C-P cross-coupling reactions catalyzed by palladium. Previous work of this group had enabled the synthesis of some *P*-chirogenic phosphinoxazoline (PHOX) ligands, bearing both carbon and phosphorus as stereogenic elements. Their stereoselective preparation was accomplished *via* substrate controlled diastereoselection, because the oxazoline moiety was enantiopure. By this method, however, only the major diastereomers were reasonably accessible and it was not applicable when the oxazoline group was not chiral.

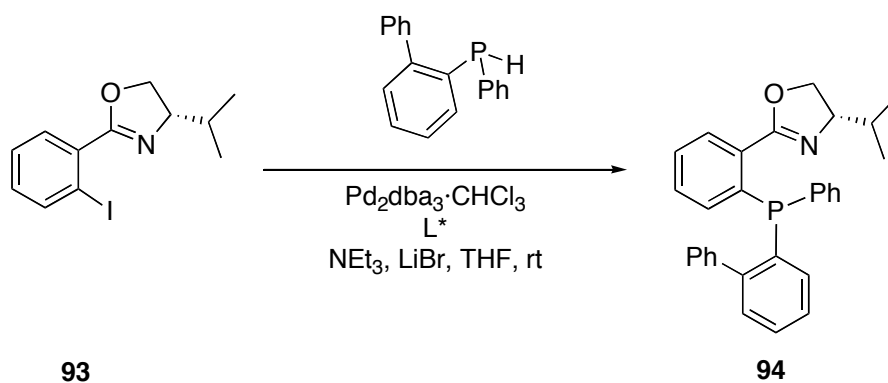
For those reasons, Pd catalyzed cross-coupling was explored with substrates of the type **91**. The substrates and conditions used are shown in **Equation 17**.



**Equation 17.** Pd-catalyzed, cross-coupling reaction.

The effect of the base, the additive (LiBr or Bu<sub>4</sub>NBr) and the R and X groups on the enantioselectivity were investigated. Good yields and enantioselectivities (up to 93%) were found. The absolute configuration of some of the phosphines was determined by crystal structure analysis of **92** or the sulphide derivative.

Further work of the same group (**Equation 18**)<sup>103</sup> was directed to the investigation of the double asymmetric induction controlled by the catalyst and the preformed stereogenic centre in **93**.



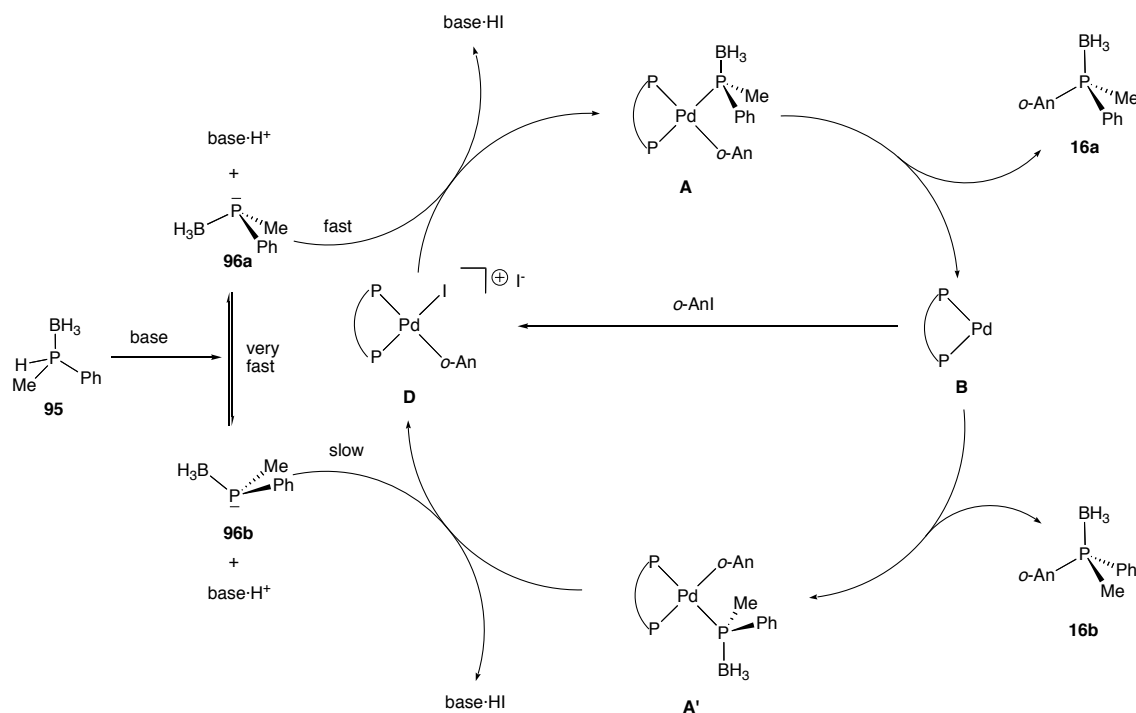
**Equation 18.** Double asymmetric induction in the synthesis of *P*-stereogenic phosphines.

By changing the absolute configuration of the Et,Et-FerroTANE ligand it was observed that the absolute configuration of the resulting phosphine **94** was inverted and so it was clearly demonstrated that catalyst control dominates over substrate control.

### 3.4.3. Synthesis of *P*-stereogenic phosphine-boranes

Further work of the Glueck's group<sup>99</sup>, very recently, has focused the interest in the catalytic, asymmetric synthesis of phosphine-boranes. The first efforts, obviously, are devoted to the stereoselective synthesis of PAMP·BH<sub>3</sub>.

The proposed catalytic cycle for such a reaction is shown in **Scheme 24**.



**Scheme 24.** Proposed mechanism for asymmetric phosphination with phosphine-boranes.

Both Imamoto<sup>104</sup> and Livinghouse<sup>95</sup> have reported that a loss of P stereochemistry is possible during the formation of PAMP-BH<sub>3</sub> (**16**) from enantiopure **95**, presumably because the anion **96** can racemize before the Pd-P bond formation. If this racemization occurs more quickly than Pd-P bond formation with a chiral Pd catalyst, and if one enantiomer of the anion reacts more quickly than the other with **D**, as depicted in **Scheme 24**, a dynamic, kinetic resolution might afford enantioenriched PAMP-BH<sub>3</sub> (**16**) *via* the mechanism shown.

Exploiting this idea, Glueck's group screened<sup>99</sup> a range of commonly used chiral diphosphines (CHIRAPHOS, DUPHOS, Tol-BINAP and <sup>t</sup>Bu-Josiphos) to evaluate their activity and stereoselectivity. It was found that the palladium complex **D** with <sup>t</sup>Bu-Josiphos was a robust catalyst, although the reaction was slow and the stereoselectivity was low (< 10% e.e.). Studies of the stoichiometric steps of the cycle led to separation, isolation and determination of the absolute configurations of the Pd phosphido-borane complexes (**A** and **A'**). Moreover, detailed mechanistic information on this useful class of Pd-mediated reactions was gathered. This enabled the first *direct* corroboration of long-held assumptions about the stereochemistry of the reductive elimination (with retention of configuration), suggesting that the reactions of M-P and M-C bonds are similar in terms of stereochemistry.

This method, does not have—at the moment—, direct synthetic application. Nevertheless, it was demonstrated that *P*-stereogenic phosphine-boranes can be successfully prepared *via* Pd-catalyzed asymmetric phosphination. It is reasonable to think that in the near future further work in this area will lead to synthetically useful methodologies to prepare *P*-chirogenic phosphines.

## 4. Conclusion

Part I of this chapter has summarized the main available methods for the synthesis of *P*-stereogenic phosphines and some of their derivatives. The development of methods in their full array ranging from classical resolutions to enantiodifferentiating asymmetric catalysis continues at fast pace and much further progress can be expected in the near future.

Up to now, quite a large number of *P*-chirogenic ligands, with different structural types and different functionalities have been obtained and constitute a promising *pool* to test in asymmetric catalysis. Asymmetric processes based on the chirality transfer from phosphine ligands to the desired organic product have been developed with almost perfect stereoselectivity. Following these successful insights, it is reasonable to think that phosphorus atom stereogeneity, alone or in conjunction with other type of stereogenic elements can still lead to useful ligands in asymmetrically catalyzed reactions. From the literature, it seems clear that the time has come for the *P*-chirogenic ligands to merge the stream and to bring the *P*-stereogeneity factor into play again.

## Part II: Synthesis and characterization of *P*-stereogenic compounds

### 5. Introduction

The topic of this THESIS is the preparation and use in catalysis of a small group of chiral phosphines containing stereogenic phosphorus atoms.

Previous work of the group<sup>105,106</sup> has dealt with phosphine ligands applied to nickel-catalyzed ethylene dimerization and oligomerization, either with neutral complexes of the type  $[\text{NiBr}(\text{Mes})\text{P}_2]$ , or with cationic ones of the type  $[\text{Ni}(\text{Mes})(\text{CH}_3\text{CN})\text{P}_2][\text{BF}_4]$ ; where P is a simple achiral phosphine such as  $\text{PEt}_3$ ,  $\text{PMe}_2\text{Ph}$ ,  $\text{PPh}_3$  or  $\text{PBN}_3$  among others.

Following this work, these cationic nickel complexes and their palladium analogues were then used in catalytic heterodimerization of styrene with ethylene, namely in the hydrovinylation reaction<sup>107</sup>.

In order to study the asymmetric version of the hydrovinylation, phosphines bearing stereogenic backbones, such as **97** (derived from myrtanol) and **98** (derived from limonene), depicted in **Figure 9**, were prepared.

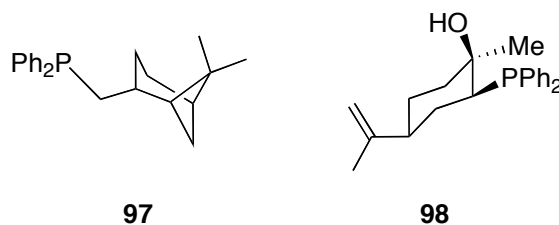


**Figure 9.** Chiral phosphines used in hydrovinylation.

*P*-stereogenicity was introduced later and ligands **99**<sup>30</sup>, **100**<sup>29</sup>, **101**<sup>31</sup> and **102**<sup>35</sup>, shown in **Figure 10**, were prepared in racemic form and then resolved by means of chiral palladium metallacycles (Part I, § 3.2.2).

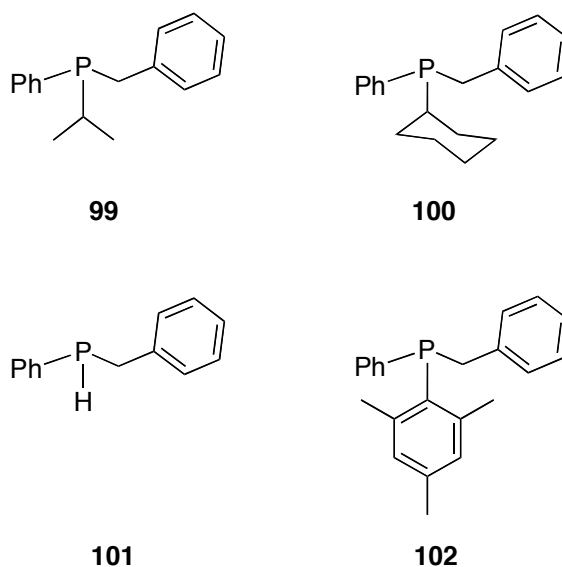


**Figure 10.** *P*-stereogenic ligands resolved by means of palladium metallacycles.

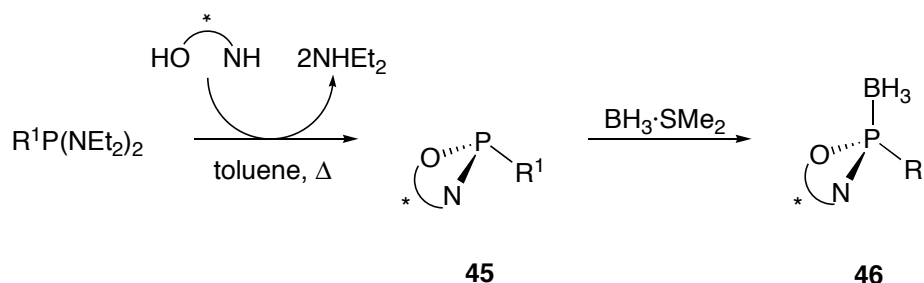
The phosphines **99-102** were obtained in high optical purity and were successfully used in hydrovinylation.

A scrutiny of the methods available to prepare *P*-stereogenic phosphines, detailed in Part I, revealed that one of the most successful methods up to date has been the one developed by Jugé (Part I, § 3.3.4), based on the use of ephedrine as a chiral auxiliary. Consequently, this approach was used for the preparation of the ligands of this THESIS.

## 6. *P*-chirogenic oxazaphospholidine-boranes. Preparation and characterization

### 6.1. Introduction

This section deals with the stereoselective preparation of chiral oxazaphospholidine-boranes **24**, as was schematized in Part I (§ 3.3.3, **Scheme 7**). These compounds are the key *P*-resolved intermediates used to prepare the *P*-stereogenic phosphines. They are prepared from the suitable enantiomerically pure aminoalcohol and the desired *bis*(diethylamino)phosphine, with subsequent protection with borane, as is shown in **Scheme 25**.



**Scheme 25.** Preparation of *P*-resolved oxazaphospholidine-boranes.

In this section, thus, the reasons for the choice of  $R^1$  and the aminoalcohol are explained in detail along with the results obtained with each system, in terms of yield and stereoselectivity.

### 6.2. Synthesis of *bis*(diethylamino)phosphines

Whatever the chosen aminoalcohol is, its cyclization around the phosphorus atom to yield **23** requires to have the suitable *bis*(diethylamino)phosphine, whose synthesis and characterization is described in this section. These compounds carry the first group that will remain attached to the phosphorus atom until the final step. The *bis*(diethylamino)phosphines prepared are shown in **Figure 11**.



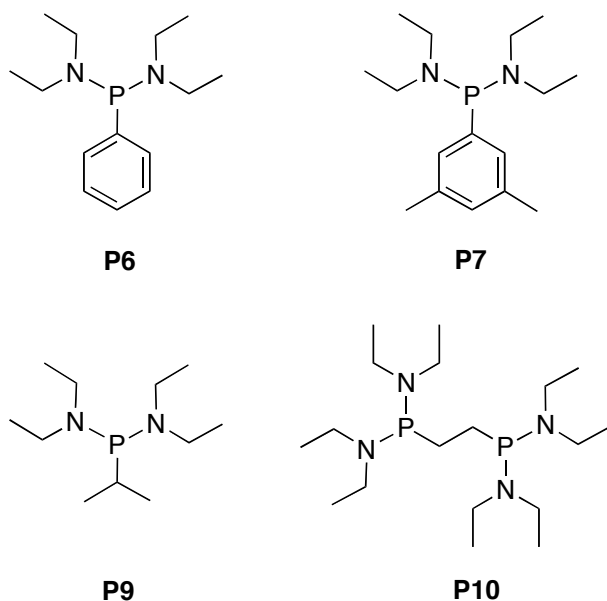


**Figure 11.** Prepared *bis*(diethylamino)phosphines.

In the vast majority of literature reports, the only precursor used to prepare *P*-stereogenic phosphines was **P6** and consequently one the groups attached to the phosphorus atom is a phenyl group. Exceptions to this assertion were provided by van Leeuwen's<sup>69</sup> and Mezzetti's<sup>57</sup> laboratories, where the precursors **103-105** (**Figure 12**) were prepared.

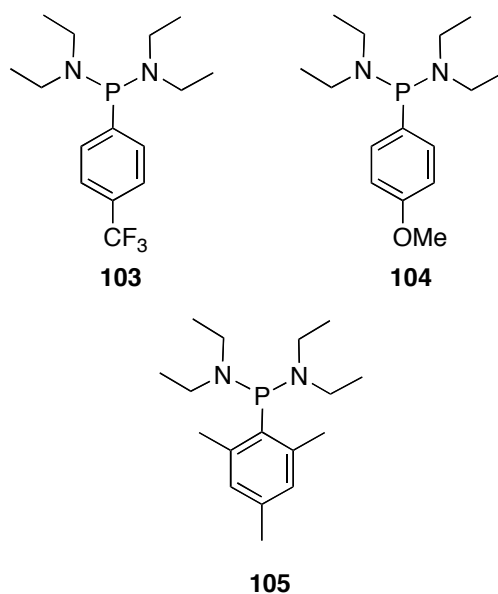


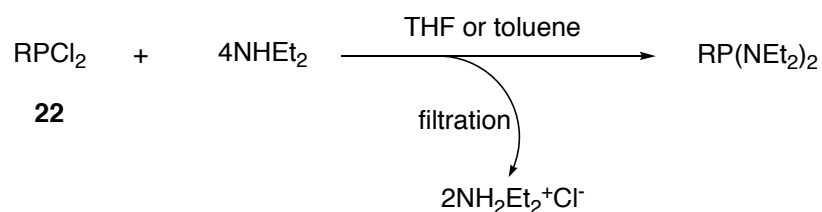
**Figure 12.** *Bis*(diethylamino)phosphines used in literature to prepare *P*-chirogenic phosphines.

Van Leeuwen's<sup>69</sup> group prepared ferrocenyldiphosphines from precursors **103** and **104**, to investigate the electronic effects in hydroformylation, whereas Mezzetti's<sup>57</sup> interest into obtaining bulky, highly symmetric phosphines made necessary the preparation of **105**. The *bis*(diethylamino)phosphines **103** and **104** were successfully used to prepare *P*-chirogenic phosphines using the Jugé approach, but when using **105** it was found that the reactions,

when took place, were sluggish and low-yielding, precluding the synthetic utility of **105** with this method.

Consequently, it was decided to prepare the precursors **P6**<sup>108</sup>, **P7**, **P9** and **P10**<sup>109</sup>. These set of *bis*(diethylamino)phosphines are potential precursors for mono and bidentate phosphines, with different steric and electronic properties of the first organic group that will be attached to the phosphorus atom in the final phosphine.

Among the existing methods to prepare such compounds, the most usual way is depicted in **Equation 19**, provided that the dichlorophosphines **22** are available<sup>108</sup>.

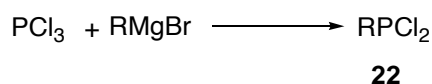


**Equation 19.** Preparation of *bis*(diethylamino)phosphines.

The reaction between dichlorophosphine, **22**, and an excess of diethylamine affords the desired *bis*(diethylamino)phosphine while the two equivalents of HCl released are neutralized with the excess of amine to form the ammonium salt, which is easily filtered out.

Products **P6**, **P9** and **P10** have been obtained in good yields by this method as colorless liquids after distillation of the crude product obtained after filtration of the ammonium salts. The reaction was done in THF at reflux for **P6** and in toluene at room temperature for **P9** and **P10**, because it was found that extensive decomposition and oxidation took place when doing the reaction in THF. The final products were pure as judged by their <sup>31</sup>P{<sup>1</sup>H}, <sup>1</sup>H and <sup>13</sup>C{<sup>1</sup>H} NMR spectra.

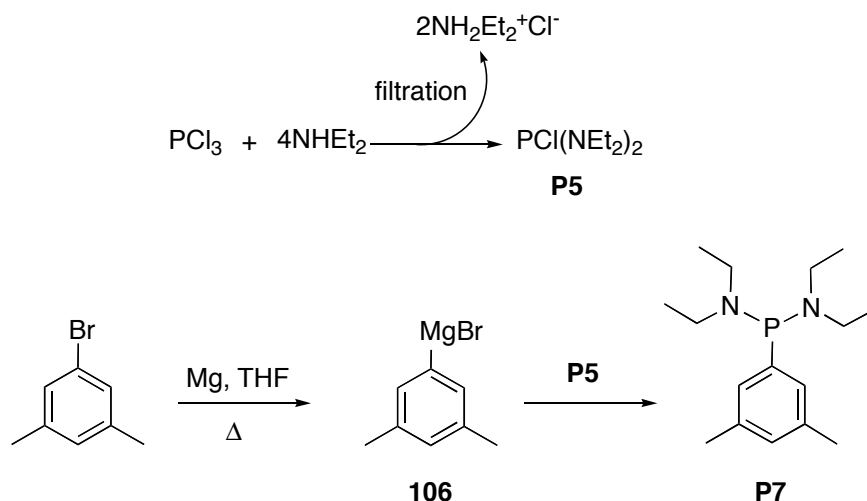
To prepare the product **P7**, an alternative route was applied because 3,5-(dimethylphenyl)dichlorophosphine is not a commercial product. The classical route for the synthesis of this kind of precursors, **22**, is the reaction between one equivalent of the appropriate Grignard reagent and phosphorus trichloride, as shown in **Equation 20**. From the precursor **22**, the synthesis shown in **Equation 19** would be resumed.



**Equation 20.** Synthesis of dichlorophosphines.

Although this route appears to be convenient by its shortness, a literature survey shows<sup>110</sup> that it is not easy to match the exact stoichiometry between the Grignard reagent and phosphorus trichloride. Consequently, disubstituted and trisubstituted products are usually formed in variable amounts to give complex mixtures very difficult to separate. Even if the

compound **22** was the major product, impurities of  $R_2PCl$  would also react with diethylamine in the next step (Equation 19) and then with the aminoalcohol in the synthesis of the oxazaphospholidine-borane. For these reasons, a more roundabout but convenient path was chosen<sup>110</sup> for the preparation of compound **P7**, also applied to prepare the compound **105**. The strategy is depicted in Scheme 26.



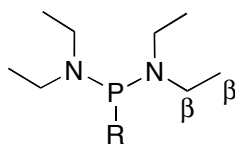
**Scheme 26.** Preparation of **P7** by two-step synthesis.

The strategy encompasses two steps: the first one is the preparation of the compound **P5**<sup>109,111,112</sup>, which is then subjected to nucleophilic attack with the Grignard reagent **106** to afford the desired product **P7**. In this step the P-N bonds remain intact.

In the preparation of **P5** it was observed that an exact relation between phosphorus trichloride and diethylamine was crucial in order to succeed. Although stoichiometrically a 1:4 ratio between  $PCl_3$  and  $NH_2Et_2$  is needed, it was found that the best conditions were a 1:3.6 ratio.  $^{31}P\{^1H\}$  NMR showed that excess of diethylamine produced some quantity of  $P(NEt_2)_3$  whereas shortage of it produced some  $PCl_2(NEt_2)$ . When the proportion was exactly 1:3.6, however, only the desired product **P5** was observed. The solvent of choice was dry hexane, from which the product was isolated after filtration of the ammonium salts and evaporation of the solvent. Compound **P5** is an air-sensitive, fuming and malodorous liquid, which was used without purification for the next step.

The reaction of **P5** with the Grignard reagent **106** worked smoothly in THF at  $-20\text{ }^\circ\text{C}$  and **P7** was obtained pure and in good yield after vacuum distillation.

The characterization of *bis*(diethylamino)phosphines was made by multinuclear NMR. **Table 9** lists some of the data of these compounds, whereas atop of this table figures the employed nomenclature. Examining **Table 9** it can be seen that the resonances of protons and carbons of the ethyl group did not change significantly among the different compounds.



<i>Compound</i>	<i>Yield</i> %	<sup>31</sup> P NMR <sup>a</sup> ϕ(ppm)	<sup>1</sup> H NMR <sup>b</sup> ϕ(ppm)	<sup>13</sup> C NMR <sup>a,b</sup> ϕ(ppm)
<b>P5</b>	64	147.6	3.10-3.18	42.1
			( <i>m</i> , H <sub>ϕ</sub> )	( <i>d</i> , C <sub>ϕ</sub> , 17.8)
			1.11	13.8
			( <i>t</i> , H <sub>ϕ</sub> , 7.1)	( <i>d</i> , C <sub>ϕ</sub> , 4.6)
<b>P6</b>	74	98.7	3.05-3.15	42.8
			( <i>m</i> , H <sub>ϕ</sub> )	( <i>d</i> , C <sub>ϕ</sub> , 16.4)
			1.11	14.7
			( <i>t</i> , H <sub>ϕ</sub> , 7.1)	( <i>d</i> , C <sub>ϕ</sub> , 3.2)
<b>P7</b>	86	97.9	3.07-3.19	41.8
			( <i>m</i> , H <sub>ϕ</sub> )	( <i>d</i> , C <sub>ϕ</sub> , 16.4)
			1.15	13.6
			( <i>t</i> , H <sub>ϕ</sub> , 3.2)	( <i>d</i> , C <sub>ϕ</sub> , 3.2)
<b>P9</b>	— <sup>c</sup>	101.5	2.87-3.10	42.5
			( <i>m</i> , H <sub>ϕ</sub> )	( <i>d</i> , C <sub>ϕ</sub> , 14.1)
			0.85-1.30 <sup>d</sup>	14.5
			( <i>m</i> , H <sub>ϕ</sub> )	( <i>d</i> , C <sub>ϕ</sub> , 3.2)
<b>P10</b>	82	90.3	2.94	41.5
			( <i>m</i> , H <sub>ϕ</sub> )	( <i>d</i> , C <sub>ϕ</sub> , 16.0)
			0.97	13.9
			( <i>t</i> , H <sub>ϕ</sub> , 7.0)	( <i>s</i> , C <sub>ϕ</sub> )

<sup>a</sup>: Proton decoupled.

<sup>b</sup>: Multiplicities and coupling constants (in Hertz) given in brackets. Acquisition conditions given in experimental part (Chapter VII), section 3.1.2.

<sup>c</sup>: Quantitative yield based on <sup>31</sup>P{<sup>1</sup>H} NMR.

<sup>d</sup>: Signals overlapped with the ones from the methyl substituents of the isopropyl group.

**Table 9.** Data of *bis*(diethylamino)phosphines.

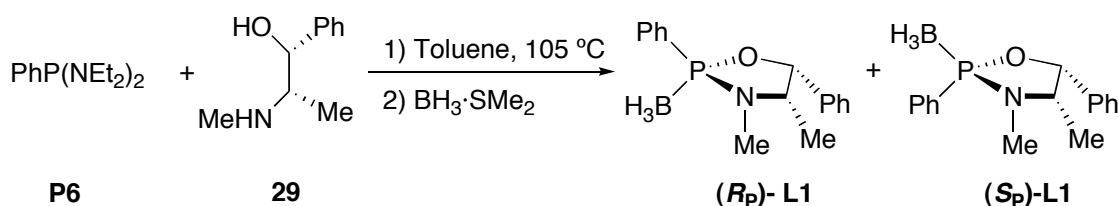
The  $^{31}\text{P}\{^1\text{H}\}$  NMR chemical shift strongly depends on the groups attached to the phosphorus atom, so it is not surprising that in compounds **P6**, **P7**, **P9** and **P10** it does not change noticeably, whereas in compound **P5**, which is a chlorophosphine, appears at a much lower field.

With these *bis*(diethylamine)phosphines in hand, the preparation of the enantiomerically pure oxazaphospholidine-boranes could be resumed.

### 6.3. Obtention of oxazaphospholidine-boranes

#### 6.3.1. Preparation of (*R<sub>p</sub>*)-L1

The initial efforts were directed towards the synthesis of **L1**, reproducing the experimental conditions of Jugé<sup>54</sup>. These conditions consist on heating a mixture of **P6** and (–)-ephedrine (**29**) in toluene overnight, to produce the reaction described in **Equation 21**. The absolute configuration at the phosphorus atom of the major isomer, as described in Part I (§ 3.3.4.2), was unequivocally determined by single X ray diffraction by Jugé<sup>71</sup>.



**Equation 21.** Obtention of **L1** under Jugé's conditions.

In the first experiments (*R<sub>p</sub>*)-**L1** was prepared, albeit with a disappointing 40% yield compared to Jugé, who managed to obtain (*R<sub>p</sub>*)-**L1** in 80% yield. The  $^{31}\text{P}\{^1\text{H}\}$  NMR spectrum showed complete conversion (no peak of **P6** was observed at  $\delta = 98.7$  ppm in the spectrum), but an important quantity of *P*-oxides and oligomers appeared in the region between  $\delta = 20$  ppm and  $\delta = 60$  ppm, apart from the desired product at  $\delta = 141.5$  ppm. An observation published by Jugé in 1997<sup>65</sup> was the key to improve the yield. The cyclization of ephedrine releases two equivalents of diethylamine, which has to be removed in order to draw the reaction to completion. The synthesis was repeated but under a slow flow of deoxygenated dry nitrogen passing through the system, to take away the diethylamine formed. With this modification, the pure product was obtained in 70% yield in the best case, after precipitation with methanol. It was a white and crystalline solid. This yield could not be further improved.

Apart from optimizing the reaction conditions, the interest was also in the stereoselectivity of the formation of **L1**. It has been shown in Part I (§ 3.3.4.2) that (*R<sub>p</sub>*)-**L1** is formed predominantly, with 92 % of d.e. It was possible to observe *directly* this high diastereoselection by means of  $^{31}\text{P}\{^1\text{H}\}$  NMR. An aliquot of the reaction mixture was taken before adding the borane, whose  $^{31}\text{P}\{^1\text{H}\}$  NMR spectrum is shown in **Figure 13**.

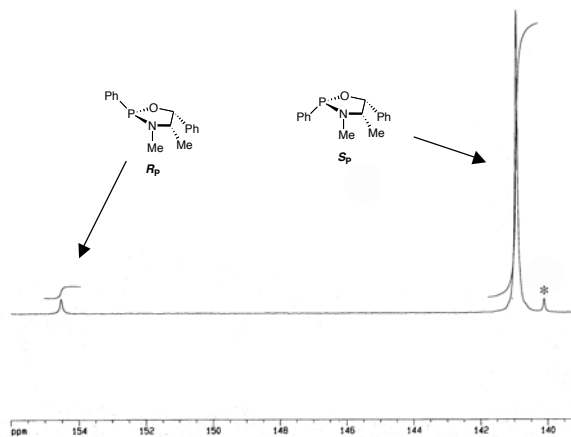
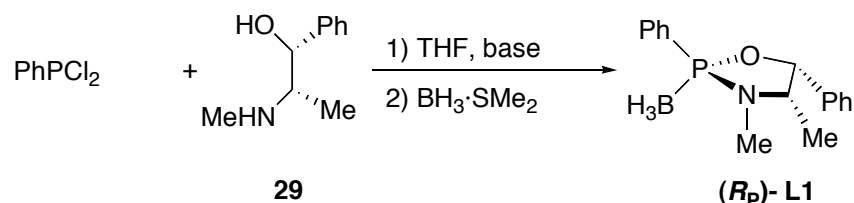


**Figure 13.**  $^{31}\text{P}\{^1\text{H}\}$  NMR spectrum (250 MHz, 298 K) showing the diastereoselective cyclization of (-)-ephedrine. \*: TMP.

In this spectrum the peaks of the two diastereomers are clearly discernable at  $\delta = 140.9$  ppm and at  $\delta = 154.5$  ppm. These two peaks could be recognised following the work of Richter<sup>70</sup>, who prepared and characterized both diastereomers. Upon integration, it was found a d.e. of 92%, in concordance with previous literature. When adding  $\text{BH}_3\cdot\text{SMe}_2$ , the products **L1** were formed quantitatively, and again with distinct  $^{31}\text{P}\{^1\text{H}\}$  NMR shift, but precipitation with methanol afforded only the major product, (*R<sub>p</sub>*)-**L1**, from which, after complete characterization, the synthesis of the *P*-stereogenic phosphines was resumed.

In order to study in some detail this cyclization step of (-)-ephedrine around the phosphorus atom, it was found interesting to test whether milder reaction conditions could be also appropriate. With this purpose, some experiments were carried out in dichloromethane at 50 °C and at 65 °C (reflux) while checking the conversion by  $^{31}\text{P}\{^1\text{H}\}$  NMR spectroscopy. In both cases, the desired product was formed, and probably with better diastereoselection (the peak of the minor diastereomer was not intense enough to perform the integration of the  $^{31}\text{P}\{^1\text{H}\}$  NMR spectrum). However, two drawbacks hampered the synthetic utility of this modification. Firstly, the reaction time required to achieve complete conversion was of 72 hours. Secondly,  $^{31}\text{P}\{^1\text{H}\}$  NMR showed the formation of a large quantity of *P*-oxides and oligomers. Nevertheless, pure **L1** could be successfully precipitated with methanol, albeit in a yield of only 20%. In conclusion, although possible, performing the reaction in dichloromethane at lower temperature does not improve the overall results.

Another set of trials was made with the idea of obtaining (**R<sub>p</sub>**)-**L1** by *direct* condensation between dichlorophenylphosphine and (–)-ephedrine, with no need to obtain **P6**. This strategy is shown in **Equation 22**.



**Equation 22.** Direct preparation of **L1** from dichlorophenylphosphine.

If possible, this approach would be interesting, as it would allow the synthesis of (**R<sub>p</sub>**)-**L1** starting from commercial products.

The employed bases were anhydrous sodium carbonate, anhydrous potassium carbonate, anhydrous cesium carbonate, pyridine and triethylamine, with different conditions of dilution and temperature. Reactions were monitored by  $^{31}\text{P}\{^1\text{H}\}$  NMR spectroscopy.

With sodium and potassium carbonates, at room temperature, slow conversions were achieved and no peaks of the products **L1** were detected. After filtration, only a great number of peaks at the region between  $\phi = 20$  ppm and  $\phi = 40$  ppm were observed, attributable to oxidation and oligomerization. Probably, the low solubility of  $\text{Na}_2\text{CO}_3$  and  $\text{K}_2\text{CO}_3$  in THF could account for the slowness of the reaction. Performing the reaction at higher temperature (until 80 °C, at reflux of THF), using  $\text{Cs}_2\text{CO}_3$  (much more soluble in THF than  $\text{Na}_2\text{CO}_3$  or  $\text{K}_2\text{CO}_3$ ) or amines (pyridine and triethylamine) consumed the starting  $\text{PhPCl}_2$  more quickly, but did not yield the expected products, but the complex mixture of oxidation/oligomerization outlined above. These results are in accordance with previous literature. Interestingly, however, it has been reported the successful *direct* preparation of the *tert*-butyl (–)-ephedrine oxazaphospholidine from  $t\text{-BuPCl}_2$ , with triethylamine as a base<sup>70</sup>.

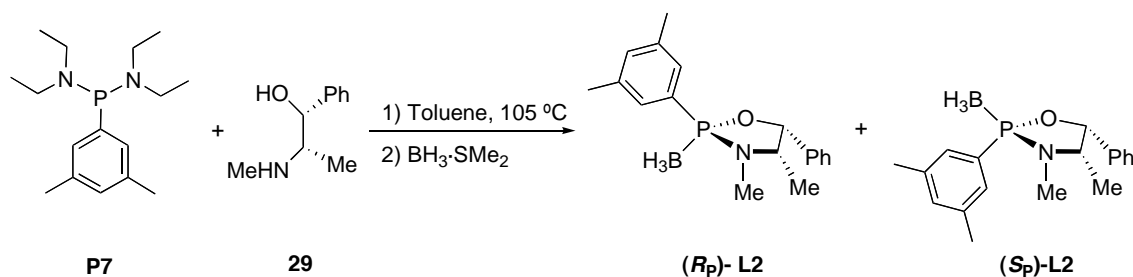
Very recently, however, a direct preparation of (**S<sub>p</sub>**)-**L1** from  $\text{PhPCl}_2$  and (+)-ephedrine has appeared<sup>67</sup>. The reaction is performed in THF and with diisopropylethylamine as a base. The yield is of 38%. The combined yield of preparation of **P6** and then **L1** is about 52%. For this reason, the classic procedure of Jugé was followed to prepare **L1**.

### 6.3.2. Preparation of (**R<sub>p</sub>**)-**L2**

The initial thought was the preparation of analogues of **L1** but with more crowded substituents, such as mesityl. However, Mezzetti's group<sup>57</sup> experience (§ 6.2) with the precursor **105** (**Figure 12**), made us change the plans and use a less hindered precursor. In consequence, 1-bromo-3,5-dimethylbenzene (which is commercially available) was used to prepare **P7** and

from this precursor the synthesis of (*R<sub>p</sub>*)-**L2** was undertaken. This compound is analogue to (*R<sub>p</sub>*)-**L1** but bearing the *meta* positions of the phenyl group attached to phosphorus methylated.

The synthesis was carried out under the usual conditions. The reaction is shown in Equation 23.



Equation 23. Synthesis of the oxazaphospholidine-borane **L2**.

As before,  $^{31}\text{P}\{^1\text{H}\}$  NMR spectroscopy was found to be an ideal tool to monitor the progress of the reaction. It was assumed that the methyl groups at the *meta* positions would not affect seriously the stereoselectivity of the reaction, and so the structures of the diastereomers of **L2** were assigned similarly to those of **L1** (§ 6.3.1).

After 24 hours of reaction, before adding the borane, no peaks of the starting *bis*(diethylamino)phosphine **P7** were perceived in the  $^{31}\text{P}\{^1\text{H}\}$  NMR spectrum. Two peaks at  $\phi = 142.3$  ppm (major) and at  $\phi = 156.3$  ppm (minor) appeared, which were assigned to the (*R<sub>p</sub>*)-**L2** and (*S<sub>p</sub>*)-**L2** diastereomers respectively, in parallel to the peaks of **L1** commented in section 6.3.1. Along with these peaks, however, a number of other peaks at the region between  $\phi = 20$  ppm and  $\phi = 40$  ppm also appeared, being attributed again to *P*-oxides and oligomers. The proportion of those peaks in relation to the ones of **L2** was greater than in the preparation of **L1**. This fact can be explained by the greater basicity of **L2** with respect to **L1** due to the more electron rich phenyl group in the former.

The diastereoselectivity, as predictably, was found to be very close to that encountered in the preparation of **L1**. The integration of the two diastereomers of **L2** gives a ratio (*R<sub>p</sub>*)-**L2**:(*S<sub>p</sub>*)-**L2** of 98:2, *i.e.*, a 96% of d.e. It means that introducing the *meta* methyl groups in the phenyl group produces a slightly better diastereoselection in the cyclization of ephedrine.

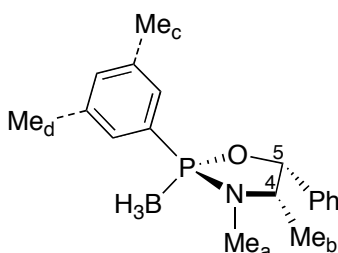
Anyway, the oxazaphospholidine was protected with borane, and the final product precipitated in methanol. Analogously to (*R<sub>p</sub>*)-**L1**, (*R<sub>p</sub>*)-**L2** was obtained as a white and crystalline solid. The yield, however, was only 34%. This fact is in concordance with the major quantity of oxides and oligomers observed.



### 6.3.3. Characterization of (*R<sub>p</sub>*)-L1 and (*R<sub>p</sub>*)-L2

Compound (*R<sub>p</sub>*)-L1 has been known since 1990<sup>54</sup> and has been fully characterized, including its X ray structure<sup>71</sup>. By analogy, it was possible to do the same for compound (*R<sub>p</sub>*)-L2. The full data for both compounds can be found in the experimental part, here only the most relevant NMR data is discussed.

The most distinctive NMR data is listed in **Table 10**. A comparison between the data shows a very close similarity between the two compounds.



Compound	<sup>11</sup> B NMR <sup>a, b</sup>	<sup>31</sup> P NMR <sup>a, b</sup>	<sup>1</sup> H NMR <sup>b</sup>	<sup>13</sup> C NMR <sup>a, b</sup>
	ϕ(ppm)	ϕ(ppm)	ϕ(ppm)	ϕ(ppm)
<i>(R<sub>p</sub></i> )-L1			3.66 ( <i>m</i> , H <sub>4</sub> )	59.1 ( <i>d</i> , C <sub>4</sub> , 1.7)
			5.58 ( <i>dd</i> , H <sub>5</sub> , 6.0, 3.0)	84.2 ( <i>d</i> , C <sub>5</sub> , 7.8)
	-41.1 ( <i>d</i> , 78)	134.5 ( <i>q</i> , 71)	2.66 ( <i>d</i> , Me <sub>a</sub> , 11.0)	29.5 ( <i>d</i> , Me <sub>a</sub> , 8.1)
			0.81 ( <i>d</i> , Me <sub>b</sub> , 6.5)	13.6 ( <i>d</i> , Me <sub>b</sub> , 3.5)
			3.67 ( <i>m</i> , H <sub>4</sub> )	59.1 ( <i>d</i> , C <sub>4</sub> , 1.6)
			5.59 ( <i>dd</i> , H <sub>5</sub> , 6.0, 3.0)	84.1 ( <i>d</i> , C <sub>5</sub> , 7.5)
<i>(R<sub>p</sub></i> )-L2	-40.8 ( <i>d</i> , 78.4)	135.1 ( <i>q</i> , 71)	2.68 ( <i>d</i> , Me <sub>a</sub> , 10.9)	29.5 ( <i>d</i> , Me <sub>a</sub> , 8.1)
			0.82 ( <i>d</i> , Me <sub>b</sub> , 6.5)	13.5 ( <i>d</i> , Me <sub>b</sub> , 3.4)
			2.38 ( <i>d</i> , Me <sub>c, d</sub> , 6.5)	21.4 ( <i>s</i> , Me <sub>c, d</sub> )

<sup>a</sup>: Proton decoupled.  
<sup>b</sup>: Multiplicities and coupling constants (in Hertz) given in brackets. Acquisition conditions given in experimental part (Chapter VII), section 3.2.

**Table 10.** NMR data from compounds (*R<sub>p</sub>*)-L1 and (*R<sub>p</sub>*)-L2.

In compound (*R<sub>p</sub>*)-**L2**, Me<sub>c</sub> and Me<sub>d</sub> are not distinguishable neither in <sup>1</sup>H NMR nor in <sup>13</sup>C{<sup>1</sup>H} NMR spectra, in spite of being diastereotopic and hence potentially discernible in NMR. These fact probably means that the 3,5-dimethylphenyl group rotates freely in solution.

**Figure 14** shows the <sup>1</sup>H NMR spectrum of **L2**, whereas **Figure 15** shows its <sup>13</sup>C{<sup>1</sup>H} NMR spectrum.

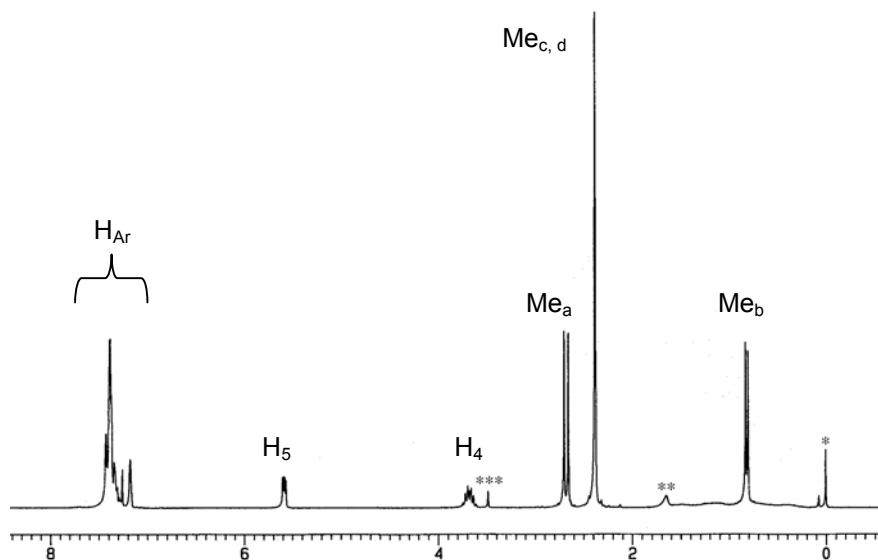


**Figure 14.** <sup>1</sup>H NMR spectrum (250 MHz, CDCl<sub>3</sub>, 298 K) of (*R<sub>p</sub>*)-**L2**. \*: TMS, \*\*: H<sub>2</sub>O, \*\*\*: CH<sub>3</sub>OH.

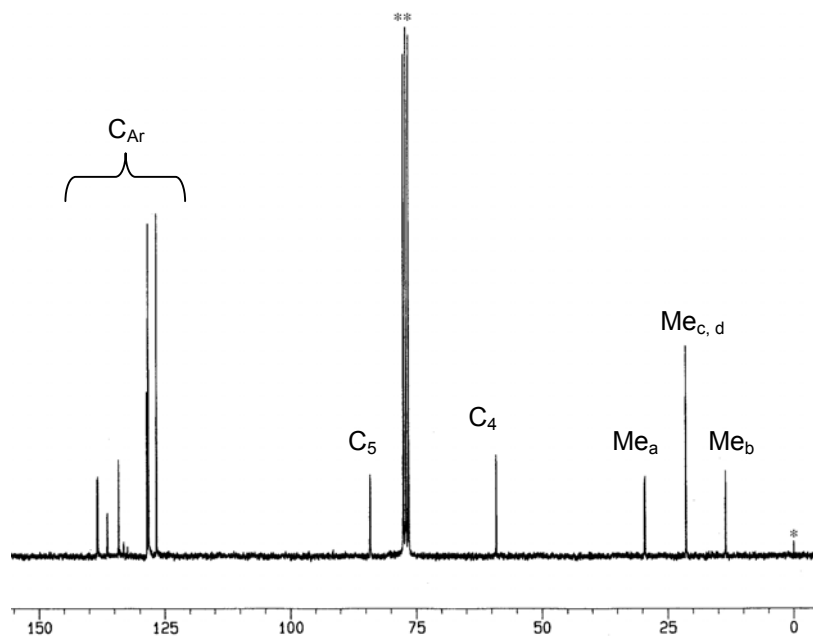
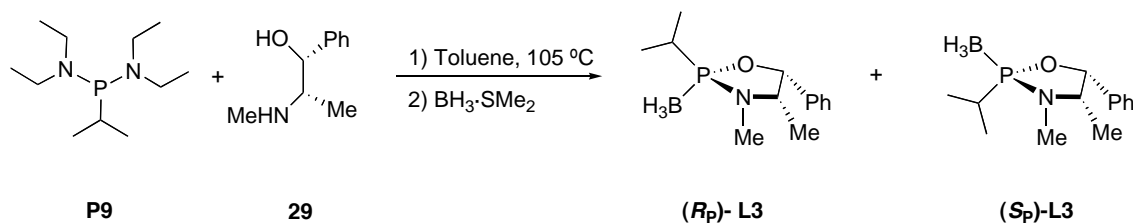


**Figure 15.** <sup>13</sup>C{<sup>1</sup>H} NMR spectrum (62.9 MHz, CDCl<sub>3</sub>, 298 K) of (*R<sub>p</sub>*)-**L2**. \*: TMS, \*\*: CDCl<sub>3</sub>.

### 6.3.4. Preparation of L3

After successful preparations of (*R<sub>p</sub>*)-L1 and (*R<sub>p</sub>*)-L2, the possibility of introducing an alkyl substituent instead of an aryl one in the oxazaphospholidine-boranes was envisaged. Consequently, **P9** was subjected to the usual conditions in order to prepare the oxazaphospholidine with (–)-ephedrine (**Equation 24**). As it was done in section 6.3.2, (**Equation 23**) the absolute configuration of the diastereomers shown is done by analogy.



**Equation 24.** Preparation of L3.

After 14 hours of reaction, before the addition of  $\text{BH}_3$ , the  $^{31}\text{P}\{^1\text{H}\}$  NMR spectrum of the solution was recorded. This spectrum is reproduced in **Figure 16**. It shows no peak of the starting *bis*(diethylamino)phosphine **P9** but the two peaks of the expected cyclic diastereomeric oxazaphospholidines, at  $\delta = 168.2$  ppm (major) and  $\delta = 181.0$  ppm (minor).

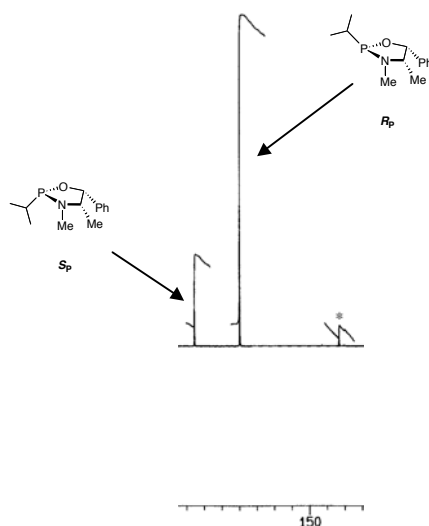


**Figure 16.**  $^{31}\text{P}\{^1\text{H}\}$  NMR spectrum (101.1 MHz, 298 K) showing the different diastereomers of the precursors of L3. \*: TMP.

The integration of these peaks revealed a 1:4 ratio, meaning a 60% of d.e. Addition of  $\text{BH}_3\cdot\text{SMe}_2$  protected the oxazaphospholidines to yield the pair of diastereomers (*R<sub>p</sub>*)-L3 and (*R<sub>p</sub>*)-L3, whose  $^{31}\text{P}\{^1\text{H}\}$  NMR spectrum is shown in **Figure 17**. As it is described

in the experimental part (chapter VII, § 3.2),  $^1\text{H}$  NMR spectrum also shows the presence of two diastereomers in 1:4 ratio.

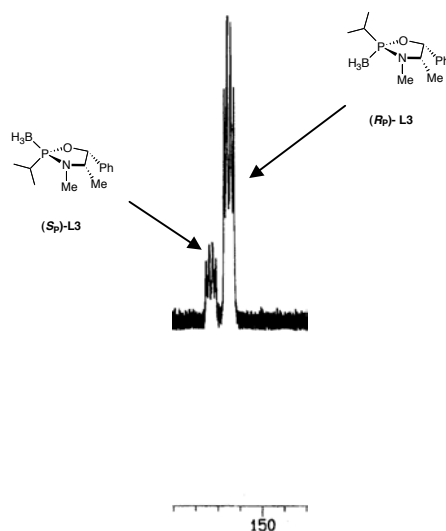


**Figure 17.**  $^{31}\text{P}\{^1\text{H}\}$  NMR spectrum (101.1 MHz, 298 K) showing the different diastereomers of **L3**.

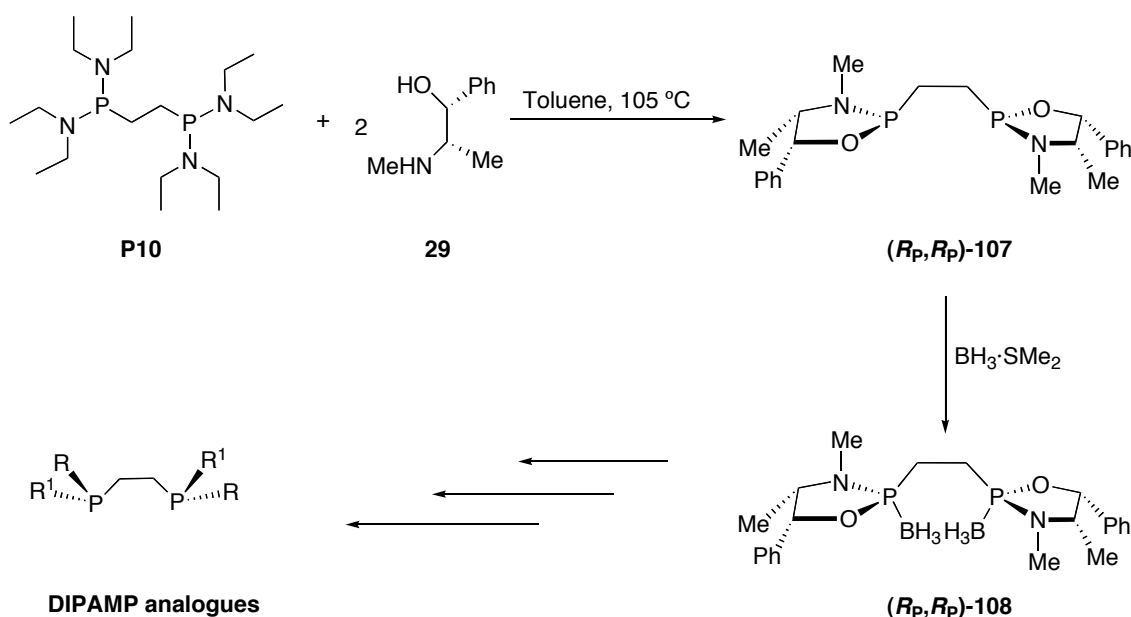
The low diastereoselectivity in the formation of **L3** can be attributed to the smaller bulkiness of the isopropyl group compared to the phenyl group.

In parallel of the work described in section 6.3.1, **L3** was tried to be obtained by direct cyclization of ephedrine on  $^i\text{PrPCl}_2$ , at room temperature, to simplify the method and to improve the stereoselectivity. Again, however,  $^{31}\text{P}\{^1\text{H}\}$  NMR showed no signs of the desired products and only starting dichlorophosphine and/or oxidation and oligomerization peaks could be detected.

Attempts to separate the two diastereomers of **L3**, by crystallization and column chromatography, were unsuccessful. This fact and the relatively low stereoselectivity in the formation of **L3** made us abandon the synthesis of *P*-stereogenic ligands starting from **L3**. At this stage, it should be noted that the isopropyl group has been successfully introduced later in the synthesis, as it will be discussed in sections 9.2, 9.3, 9.5 and 9.6.

### 6.3.5. Attempted obtention of a bis(oxazaphospholidine)-diborane

Starting from precursor **P10** (§ 6.2) the preparation of the *bis*(oxazaphospholidine)-diborane **108**, with an ethylene bridge, precursor of *P*-stereogenic diphosphines of the family of DIPAMP (Scheme 27) was attempted. Other diastereomeric products (with different absolute configurations in one or the two phosphorus atoms) similar to **107** and **108** can also be formed, but are not represented for the sake of simplicity.



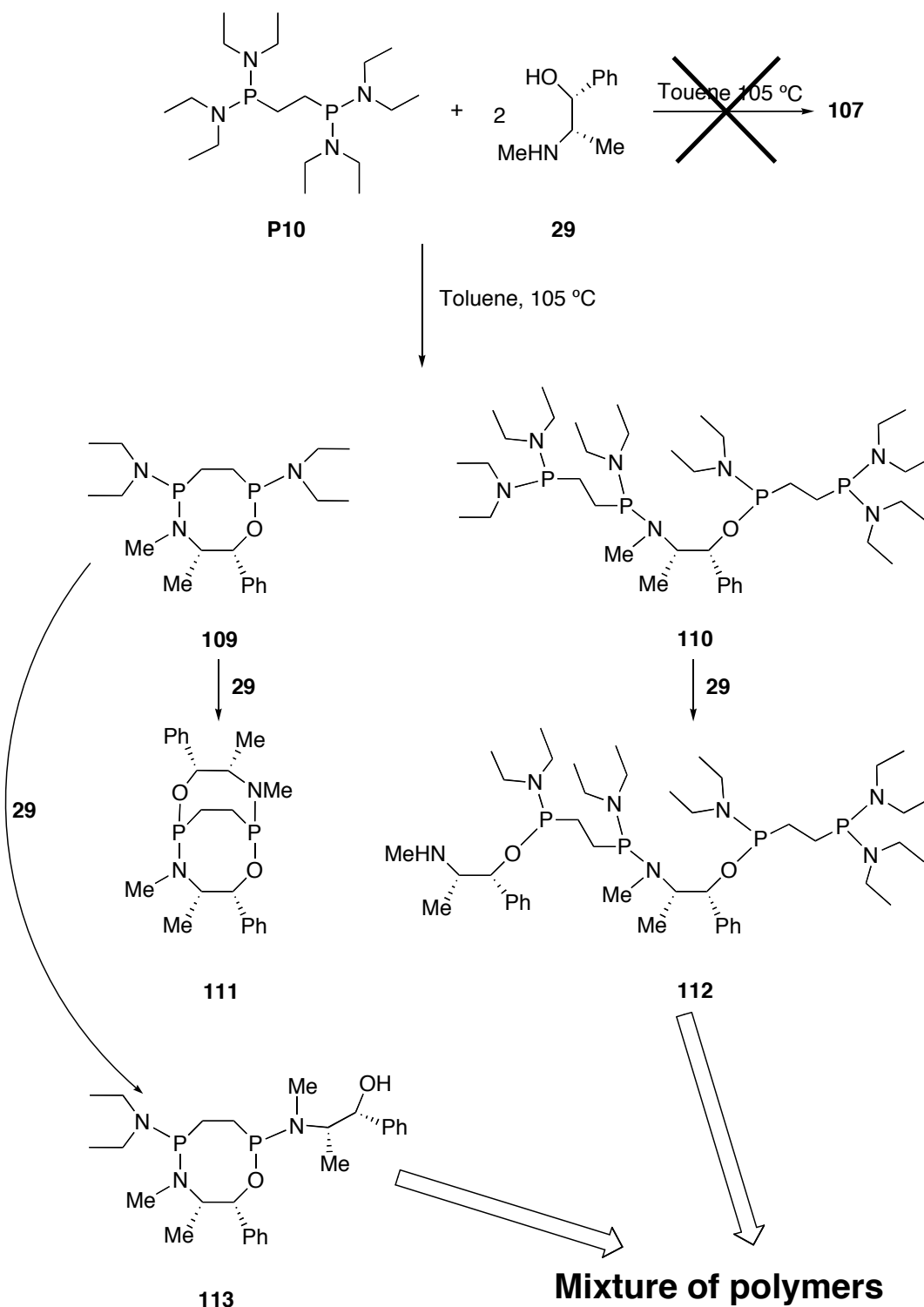
Scheme 27. Attempted synthesis of the compound **108**.

Upon reacting overnight two equivalents of (–)-ephedrine and one of the *bis*(diethylaminophosphine) **P10** in toluene at 105 °C, a sticky white product was found at the bottom of the *schlenk* tube. The  $^{31}\text{P}\{^1\text{H}\}$  NMR spectrum of the solution consisted in a number of peaks gathered narrowly between  $\delta = 38.8$  ppm and  $\delta = 41.3$  ppm. The solid, however, could not be dissolved in the common organic solvents and no NMR data could be obtained.

$\text{BH}_3 \cdot \text{SMe}_2$  was added to the solution and the mixture was stirred vigorously overnight. The solid dispersed into the liquid, with the concomitant formation of a white precipitate. This final solid was filtered and washed with ether. It could not be dissolved in common organic solvents and consequently no NMR data was acquired. The IR spectrum in KBr showed C-H and B-H stretching bands.

The results described in the lines above probably account for the formation of complex mixtures of oligomeric and polymeric species. Probably the lighter oligomers are soluble in toluene whereas the polymeric species are not. The bifunctional character of both **P10** and

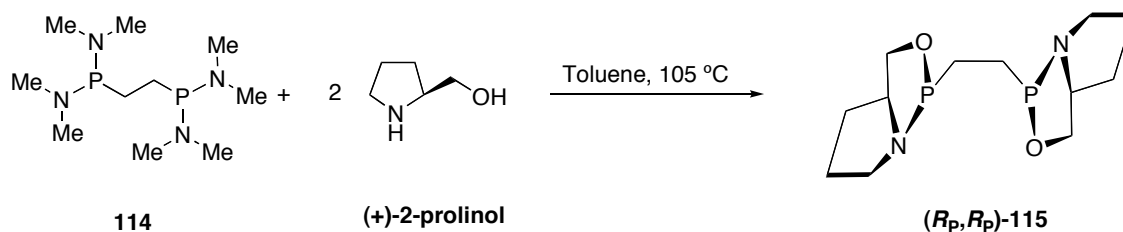
(-)-ephedrine (**29**) most likely contribute to the formation of those polymeric species. **Scheme 28** shows —without considering stereochemistry around the phosphorus atom— some of the simplest possibilities of cocondensation between **P10** and **29**. Either cyclic (**109**, **111**, **113**) or linear (**110**, **112**) species are feasible, from which an endless number of other oligomeric and polymeric products can be conceived.



**Scheme 28.** Some of the simplest cocondensations between **P10** and **29**.

All the modifications (temperature, time and concentration of the reagents) afforded the same white solid. Because of these disappointing results, the strategy was abandoned and it was decided to prepare diphosphines by other methods that will be developed later (§ 10).

It has to be noted, however, that a compound similar to **107** (Scheme 27) has been successfully synthesized<sup>70</sup> in 50% yield and with a d.e. greater than 95% using (*S*)-(+)-2-pyrrolidinemethanol (2-prolinol), as it is rendered in Equation 25.



**Equation 25.** Use of (+)-2-prolinol as a chiral auxiliary to prepare the *bis*(oxazaphospholidine) **115**.

The higher rigidity of prolinol compared to that of ephedrine almost certainly accounts for the very different reactivity of these two chiral auxiliaries.

### 6.3.6. Preparation and characterization of (*S<sub>P</sub>*)-L4

Every extension of the *basic* method of Jugé (Part I, § 3.3.4), developed in sections 6.3.1, 6.3.2 and 6.3.5, points towards further variation of the phosphorus atoms substituents. As a last parameter to modify, it was found interesting to change the aminoalcohol used to resolve the phosphorus atom; to broaden the range of chiral auxiliaries used to prepare *P*-chirogenic phosphine derivatives (Part I, § 3.3.3) and to compare with ephedrine. When searching a different chiral auxiliary, amongst the vast number of heterobifunctional, optically pure reagents existing, it was decided to be restricted by the following guidelines:

- Limit the search to *cis*-1,2-aminoalcohols so as to compare more directly with ephedrine.
- Search for a molecule with a rigid structure, to compare with the more flexible ephedrine.
- Search only for commercially available products.
- Exclude of the structure of the molecule functions not compatible with organolithium reagents (such as carbonyl or ciano groups) in order to be able to use the standard protocol for the synthesis of phosphines.

After a scrutiny of reagents meeting the requirements outlined above, it was found that (1*R*,2*S*)-*cis*-1-amino-2-indanol (**116**, **Figure 18**) could be a promising candidate, because of the rigidity of its bicyclic structure. It is commercially available in various diastereomeric forms but the most common of them is **116**, which was selected to be used as a chiral auxiliary.

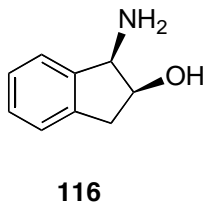
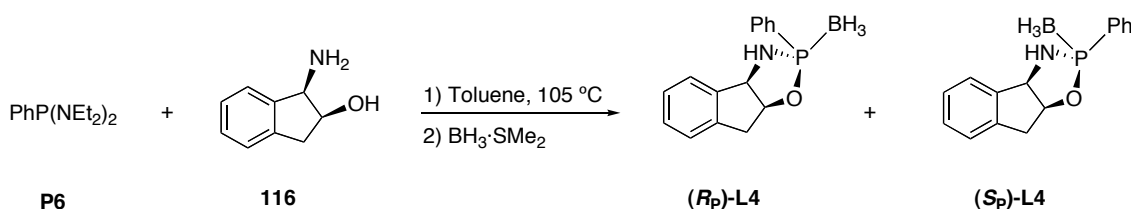


**Figure 18.** (1*R*,2*S*)-*cis*-1-amino-2-indanol.

The reaction was successfully accomplished under usual conditions, as it is rendered in **Equation 26**, to furnish the oxazaphospholidine-borane **L4**.



After 9 hours of reaction, before the addition of  $\text{BH}_3\cdot\text{SMe}_2$ , the  $^{31}\text{P}\{^1\text{H}\}$  NMR spectrum of the reaction mixture showed no peaks of the starting **P6** and two peaks at  $\phi = 138.5$  ppm and  $\phi = 143.1$  ppm, ascribed to the two possible diastereomers formed. Part of this spectrum is shown in **Figure 19**. The absolute configurations at the phosphorus atoms were assigned as it is described later in this section.

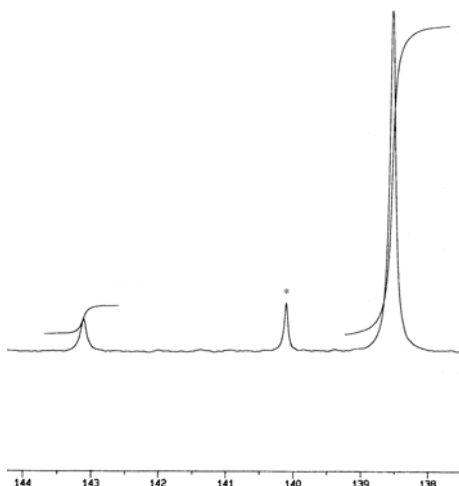


**Figure 19.**  $^{31}\text{P}\{^1\text{H}\}$ NMR spectrum (250 MHz, 298 K) of the formation of **L4**, before the addition of  $\text{BH}_3\cdot\text{SMe}_2$ . \*: TMP.



The integration of those two peaks gave a d.e. of 84 %, slightly worse than the one obtained with (-)-ephedrine (§ 6.3.1).

Addition of  $\text{BH}_3 \cdot \text{SMe}_2$ , evaporation of toluene and precipitation with methanol furnished a white and crystalline solid in a 50% yield. Analogously to the preparation of **L1** and **L2**, this solid was diastereomerically pure, as was evidenced by its  $^{31}\text{P}\{^1\text{H}\}$ ,  $^{13}\text{C}\{^1\text{H}\}$  and  $^1\text{H}$  NMR spectra.

Product **L4** had not been reported, and a complete characterization of it was undertaken. Elemental analysis and mass spectrometry confirmed the molecular identity of **L4**. Infrared spectroscopy showed typical stretching bands of the N-H,  $\text{C}_{\text{Ar}}\text{-H}$ ,  $\text{C}_{\text{Alk}}\text{-H}$  and B-H bonds.

The numbering scheme followed to list the multinuclear NMR data is shown in **Figure 20**.

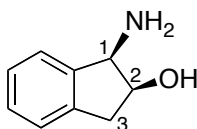


**Figure 20.** Numbering scheme of the indanol moiety used in **Figure 21** and **Table 11**.

**Figure 21** shows the  $^1\text{H}$  NMR spectrum of **L4**.

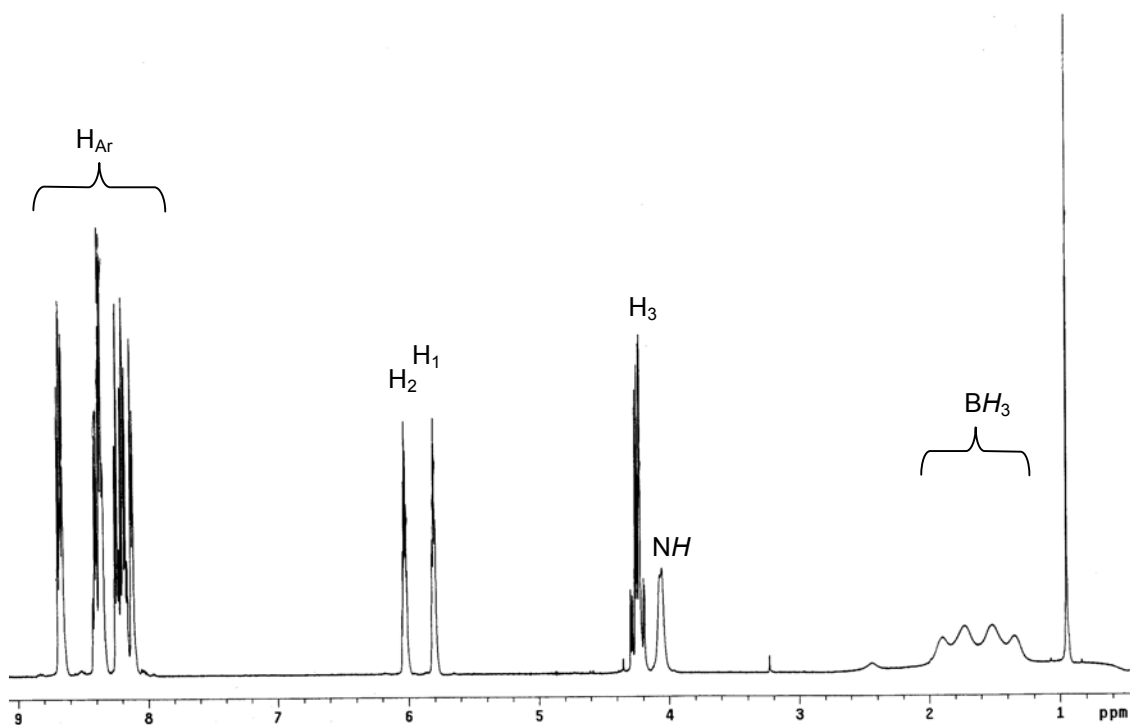
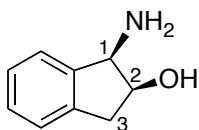


**Figure 21.**  $^1\text{H}$  RMN spectrum (500 MHz,  $\text{CDCl}_3$ , 298 K) of **L4**.

The most characteristic parts of  $^1\text{H}$  and  $^{13}\text{C}\{^1\text{H}\}$  NMR spectra are the resonances of the positions 1, 2 and 3 of the cyclopentane ring. They are easily assigned by comparison to indanol (**116**). **Table 11** lists NMR data for the two compounds.



Compound	$^{11}\text{B}$ NMR <sup>a, b</sup>	$^{31}\text{P}$ NMR <sup>a, b</sup>	$^1\text{H}$ NMR <sup>b</sup>	$^{13}\text{C}$ NMR <sup>a, b</sup>
	$\phi(\text{ppm})$	$\phi(\text{ppm})$	$\phi(\text{ppm})$	$\phi(\text{ppm})$
<b>116</b>	—	—	2.45 (s, NH)	—
	—	—	2.89-3.13 (m, H <sub>3</sub> )	39.4 (s, C <sub>3</sub> )
	—	—	4.28 (d, H <sub>1</sub> , 5.3)	58.6 (s, C <sub>1</sub> )
	—	—	4.36-4.41 (m, H <sub>2</sub> )	72.8 (s, C <sub>2</sub> )
<b>L4</b>	—40.0 (d, 68.3)	140.1 (q, 70)	4.06 (d, NH, 8.0)	—
	—	—	4.18-4.30 (m, H <sub>3</sub> )	38.7 (d, C <sub>3</sub> , 4.3)
	—	—	5.75-5.82 (m, H <sub>1</sub> )	64.8 (d, C <sub>1</sub> , 2.8)
	—	—	6.01-6.04 (m, H <sub>2</sub> )	84.8 (d, C <sub>2</sub> , 8.4)

<sup>a</sup>: Proton decoupled.  
<sup>b</sup>: Multiplicities and coupling constants (in Hertz) given in brackets. Acquisition conditions given in experimental part (Chapter VII).

**Table 11.** NMR data for compounds **116** and **L4**.

From the table, some conclusions can be drawn. A strong displacement of the shifts of the protons (1.2 ppm-1.6 ppm) and of the carbons (6 ppm-12 ppm) to lower fields is found when going from **116** to **L4**. An exception is the carbon C<sub>3</sub>, which remains almost unaffected.

To complete the characterization of **L4**, the absolute configuration at the phosphorus atom had to be determined. Crystals of **L4** were slowly grown in different mixtures but, unfortunately, no single crystals of enough quality were obtained to solve the structure by X-ray analysis. Hence, other methods were employed.

Firstly, the optimized structures and the heat of formation of the two diastereomers of the precursor of **L4** (without  $\text{BH}_3$ , when the cyclization of the indanol takes place) were calculated using a semiempirical PM3 method. **Figure 22** shows these structures.

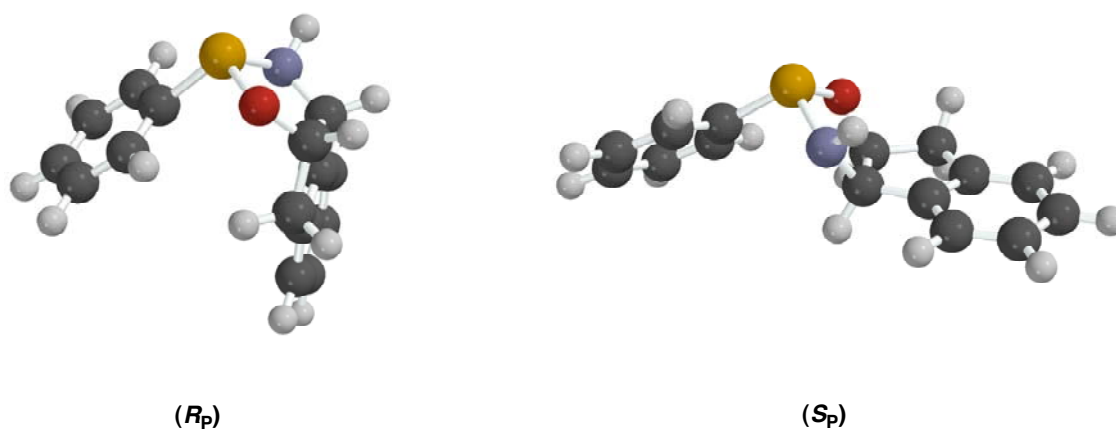


**Figure 22.** Optimized structures for the diastereomeric forms of the precursors of **L4**.

From a quick look at **Figure 22**, it is clear that the  $R_p$  diastereomer is much more strained than the  $S_p$ . The outcome from the calculus of the energies of formation reproduces this qualitative observation:  $\phi H_f(R_p) = -55.39 \text{ KJmol}^{-1}$ ,  $\phi H_f(S_p) = -65.09 \text{ KJmol}^{-1}$ . This result, hence, predicts the  $S_p$  isomer to be more stable than the  $R_p$  and consequently, the obtained product should ( $S_p$ )-**L4**.

In order to assess this prediction, a 2D  $^1\text{H}$ - $^1\text{H}$  NOESY experiment was performed to **L4**. The numbering scheme used is shown in **Figure 23**.

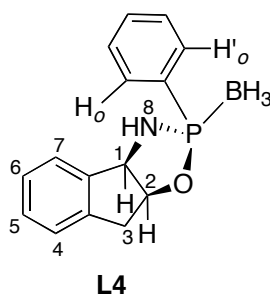


**Figure 23.** Numbering scheme to analyse the NOE contacts in **L4**.

The NOE contacts found are listed in **Table 12**.

<i>NOE contacts in L4<sup>a</sup></i>		
1↔2	2↔3 <sup>c</sup>	
1↔3 <sup>b,c</sup>	<b>2↔o</b>	
1↔7		3 <sup>c</sup> ↔4
1↔8		
<b>1↔o</b>		

<sup>a</sup>: 500 MHz, CDCl<sub>3</sub>, 298 K. The contacts between aromatic protons are not listed.  
<sup>b</sup>: Very weak.  
<sup>c</sup>: The two diastereotopic protons in 3 appeared as a unresolved multiplet and it has not been determined which of them has the NOE contacts shown in this table.

**Table 12.** NOE contacts found in compound **L4**.

The analysis of these contacts and the optimized structures shown in **Figure 22** allow the deduction of the absolute configuration at the phosphorus atom. The contacts not highlighted in **Table 12** do not define any stereochemistry around the phosphorus atom and would be predictable whichever this absolute configuration was. Notwithstanding, it can be seen in **Figure 22** that the contacts between the protons in 1 and 2 and the *ortho* protons –which are not discernible in the spectrum, albeit they are diastereotopic– of the phenyl group at the phosphorus atom (in bold in **Table 12**), are only possible in the *S<sub>P</sub>* isomer as it is shown schematically in **Figure 24**.

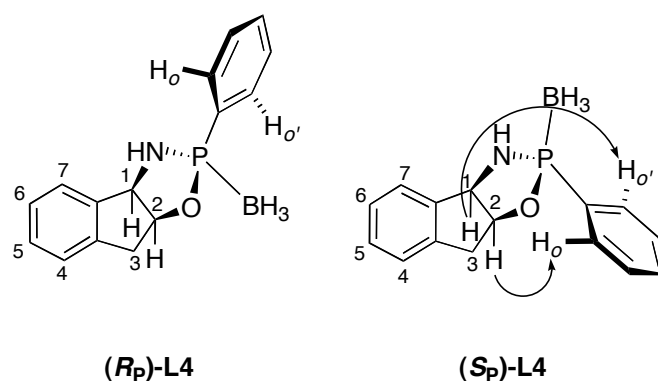


**Figure 24.** Key <sup>1</sup>H-<sup>1</sup>H NOE contacts found in **L4**, which define the stereochemistry around the phosphorus atom.

In conclusion, (*S<sub>P</sub>*)-**L4**, a new, *P*-resolved oxazaphospholidine-borane has been prepared and its absolute configuration has been deduced by means of calculation and NMR.

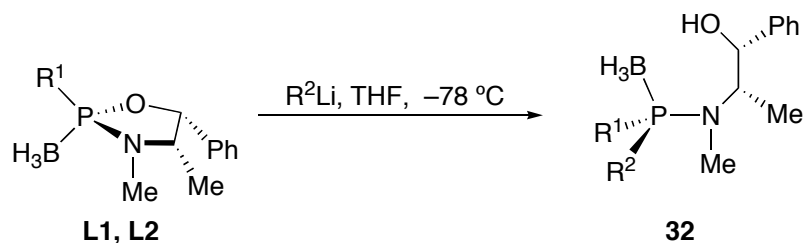
In terms of yield and stereoselectivity, however, (*S<sub>P</sub>*)-**L4** appears to be inferior to **L1**. Moreover, (1*R*,2*S*)-*cis*-1-amino-2-indanol is rather expensive compared to (–)-ephedrine. For these reasons, (*S<sub>P</sub>*)-**L4** was not further used for synthetic purposes.

## 7. *P*-chirogenic aminophosphine-boranes.

### Preparation and characterization

#### 7.1. Introduction

With the pure oxazaphospholidine-boranes ( $R_P$ )-**L1** and ( $R_P$ )-**L2** in hand, it was possible to continue towards the preparation of *P*-stereogenic phosphines. The first step is the regio and stereoselective ring opening of **31** by organolithium reagents, as it is depicted in **Equation 27**, to furnish the aminophosphines **32**.



**Equation 27.** Regio and stereoselective ring opening on oxazaphospholidine-boranes.

At this point, the selection of the groups to be attached to the phosphorus atom had to be made. The interest was the preparation of small families of encumbered *P*-stereogenic phosphines with similar electronic properties but with increasing steric bulkiness. Examining the scheme of Jugé, in principle it is possible to introduce the groups at the phosphorus atom either in this step of opening of the oxazaphospholidine-boranes or later in the synthesis, after the methanolysis; both steps *via* organolithium reagents. It was decided to explore both possibilities with the organolithium reagents shown in **Figure 25**. Those organolithium reagents were chosen (among much others which would have met the requirements of this paragraph) because they were commercial or relatively easy to prepare.

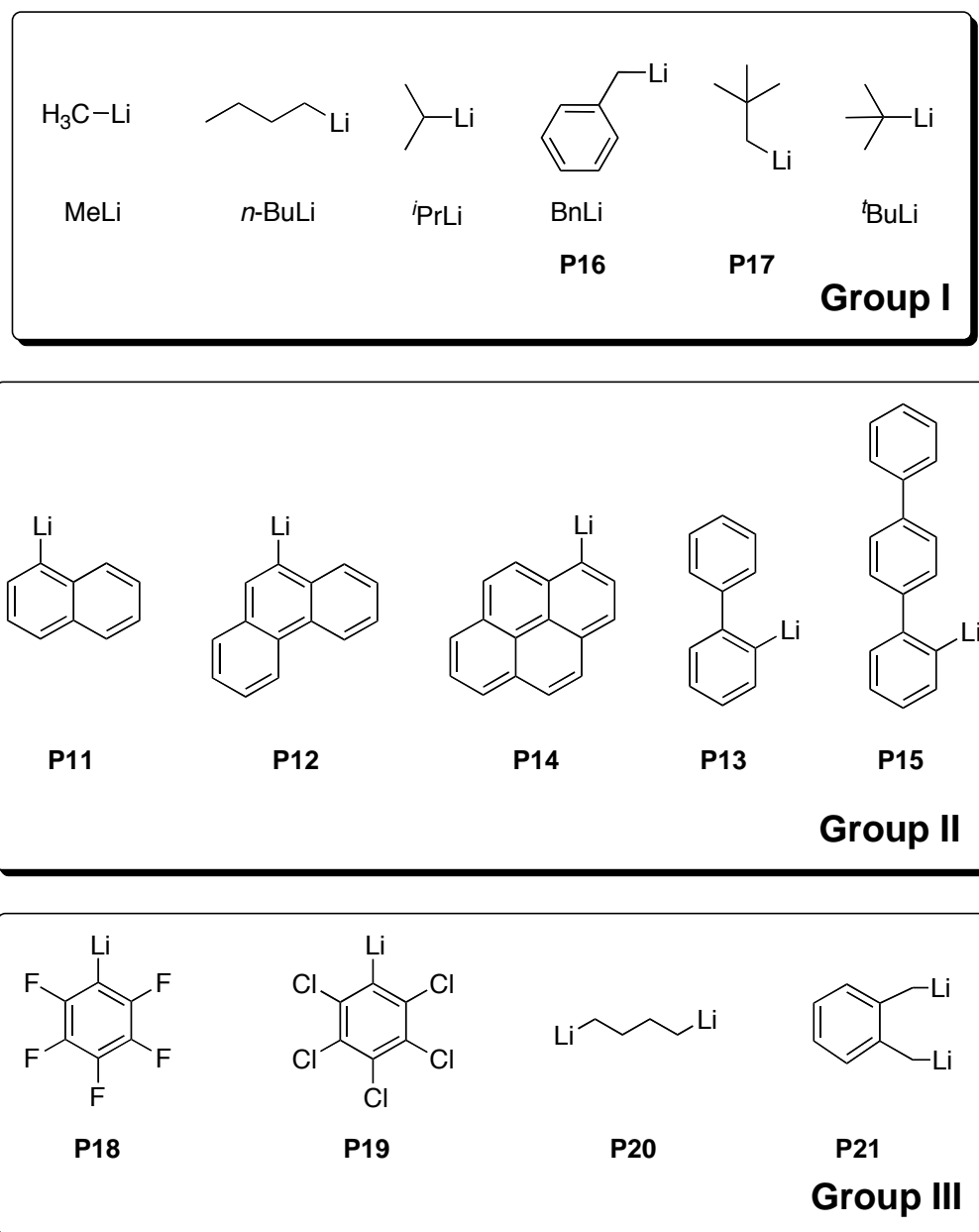


**Figure 25.** Organolithium reagents used to prepare the *P*-stereogenic phosphine-boranes.

If succeeded, hence, the final phosphines would have a phenyl substituent (starting from **L1**) or a 3,5-dimethylphenyl substituent (starting from **L2**) and the other two groups would be among the ones listed in **Figure 25**. In this figure, the organolithium reagents are divided in three groups. Group I are organolithium compounds with alkyl groups, with similar electronic properties but with different steric bulkiness, going from methyl to *tert*-butyl. Group II organolithium reagents, in some sense, follows the same objective: they are fully aromatic but with increasing size. **P11**, **P12** and **P14** are polycyclic aromatic compounds whereas **P13** and **P15** were chosen to explore if having a long linear group in *ortho* position would lead to interesting features of the final ligands. Finally, group III organolithium reagents were selected for other reasons. **P18** and **P19** would allow the synthesis of *P*-stereogenic

phosphines bearing a perhalogenated group, whose special electronic characteristics are of interest. Finally, **P20** and **P21** would eventually furnish *P*-stereogenic diphosphines.

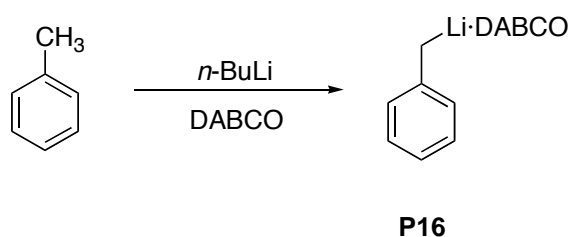
## 7.2. Preparation of organolithium reagents

All the organolithium compounds are flammable and pyrophoric and consequently inert atmospheres and dry, deoxygenated solvents are mandatory. Extreme care has been taken when handling <sup>t</sup>PrLi and <sup>t</sup>BuLi solutions, because they are extremely pyrophoric and burn easily in contact with air.

Solutions of MeLi, *n*-BuLi, <sup>t</sup>PrLi and <sup>t</sup>BuLi are commercially available in ether (MeLi) and in a mixture of alkanes (the rest). They were used without further purification. The other organolithium reagents were prepared and, due to their sensitivity, used immediately in the synthesis, except solid benzyl-lithium, **P16**, which can be stored for months under strictly inert atmosphere.

### 7.2.1. Preparation of **P16**

Before trying to prepare benzyl lithium, **P16**, a literature survey<sup>113-115</sup> revealed that reaction of benzyl halides with lithium metal or with alkyl lithium compounds give, at best, a very poor yield of **P16**. It has been found, however, that metallation of toluene is a particularly attractive and simple method (**Equation 28**)<sup>116,117</sup>.

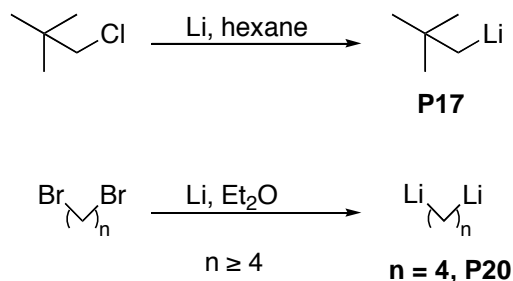


**Equation 28.** Preparation of **P16** by DABCO-assisted metallation of toluene.

This reaction occurs to a very small extent by treating toluene with *n*-butyllithium, but it is almost quantitative in presence of TMEDA or DABCO. *n*-Butyllithium was added to a toluenic solution of DABCO. Upon stirring the solution at 80 °C for one hour, the adduct between benzyl lithium and DABCO separated as bright-yellow needles. Solid **P16**, once filtrated and dried under nitrogen, is stable under nitrogen atmosphere, but it is hydrolyzed in seconds in contact with air.

## 7.2.2. Preparation of **P17** and **P20**

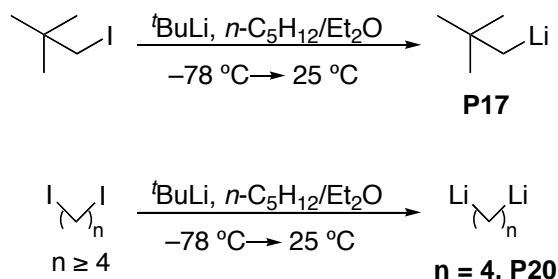
The classic procedure to prepare such compounds has been the lithiation of the corresponding alkyl halides with Li metal or Li-Na alloys (**Scheme 29**).



**Scheme 29.** Traditional preparation of organolithium compounds **P17** and **P20**.

In a classic investigation, 60 years ago, West and Rochow established<sup>118</sup> that dilithio derivatives can be prepared from  $\phi, \phi$ -dibromoalkanes and lithium metal in ether only if four or more methylene groups separated the two functions. Using the same method to prepare neopentyllithium, **P17**, Schrock reported<sup>119</sup> that is necessary to reflux neopentyl chloride and lithium in hexane during a whole week to obtain **P17** in 80% yield.

In 1990, Bailey<sup>120</sup> and Negishi<sup>121</sup> independently developed an easier way to prepare such kind of compounds based on iodine-lithium interchange with <sup>t</sup>BuLi. This strategy is shown in **Scheme 30**.



**Scheme 30.** Preparation of organolithium compounds by I-Li exchange.

This strategy provides a clean, high-yielding and convenient method for preparing primary alkyl lithium compounds. Experimental conditions, detailed in chapter **VII** (§ **3.1.3**), involved the lithiation at  $-78^\circ\text{C}$  with 2.1-2.2 equivalents of <sup>t</sup>BuLi per atom of I. Only few minutes were necessary to achieve complete conversion. Upon warming to rt, it was found that the excess of <sup>t</sup>BuLi remaining in solution was easily consumed by rapid proton abstraction from diethyl ether, leaving a clean solution of the less reactive, primary alkyl lithium compound **P17** or **P20**. This solution was cooled again and used for the desired reaction.



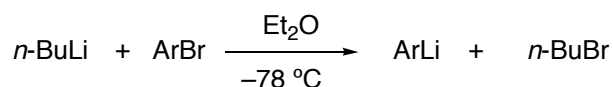
### 7.2.3. Preparation of **P11-P15** and **P18-P19**

This family of organolithium reagents has been prepared by lithium-halogen exchange, a reaction discovered more than 60 years ago by the groups of Wittig<sup>122</sup> and Gilman<sup>123</sup>. The general equilibrium depicted in **Equation 29**, lies towards the side giving the organolithium compound whose organic group is better able to accommodate the carbanionic character. This method, hence, is specially suited for the preparation of aryllithium reagents from the corresponding aryl halides and an alkyllithium compound.



**Equation 29.** General reaction of Li-halogen exchange.

This method has been successfully applied to prepare the organolithium reagents **P11-P15** and **P18-P19**, **Equation 30**.



**Equation 30.** Preparation of **P11-P15** and **P18-P19**.

The aryl bromide (or chloride in the synthesis of **P19**) was dissolved in diethyl ether (THF in **P14** and **P15**, due to the poor solubility of the halides in Et<sub>2</sub>O) and cooled to -78 °C in a dry ice/acetone bath. The reaction was performed with a commercial solution of *n*-BuLi 1.6 M in hexanes, 2h at -78 °C. Warming to -20 °C ensured the complete lithiation of the aryl halide. A creamy suspension, containing the desired organolithium reagent, was ready to be used.

All the aryl halides necessary were commercial, except 1-bromopyrene (**P1**) and 2-bromo-*p*-terphenyl (**P3**) (**Figure 26**), which had to be prepared.

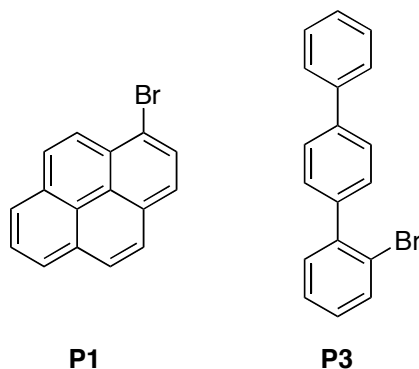
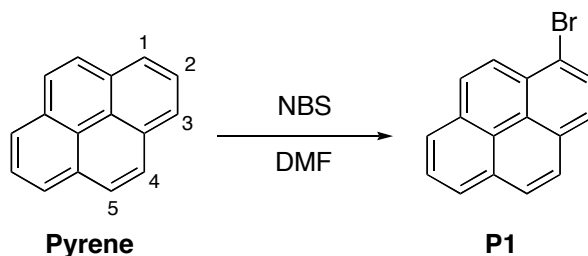


**Figure 26.** Aryl bromides prepared.

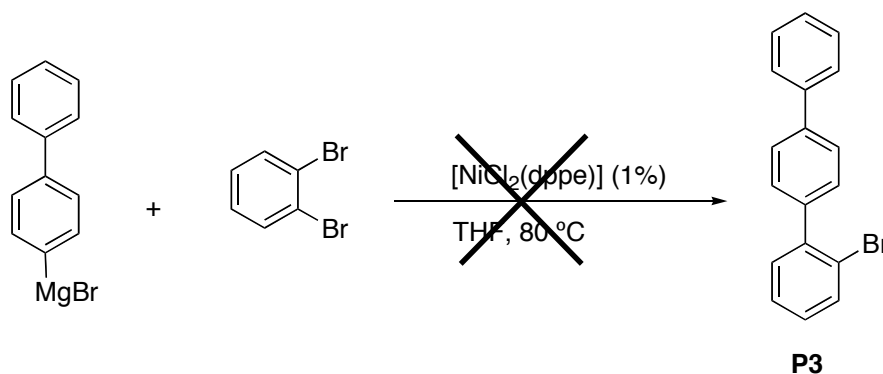
1-bromopyrene, **P1**, was readily prepared<sup>124</sup> by the reported radicalary bromination of pyrene, which is available commercially. **Equation 31** renders this synthesis.



**Equation 31.** Preparation of 1-bromopyrene.

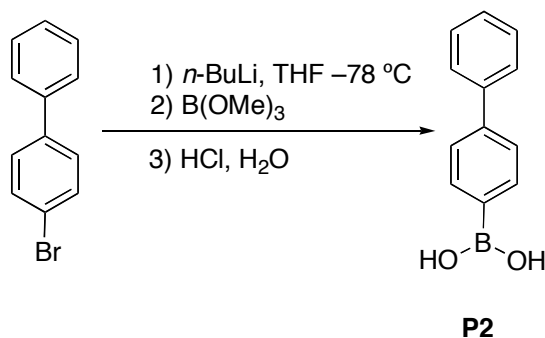
It is noteworthy that NBS regioselectively brominates only the 1 position of pyrene and nor bromination in other positions neither dibromination takes place. After extractive workup, the product **P1** is obtained in 86% yield as a brown solid.

Preliminary attempts to obtain 2-bromo-*p*-terphenyl, **P3**, by nickel catalyzed cross-coupling reaction between 4-biphenylmagnesium bromide and *o*-dibromobenzene were unsuccessful and only biphenyl could be recovered from the reaction mixture (**Equation 32**).



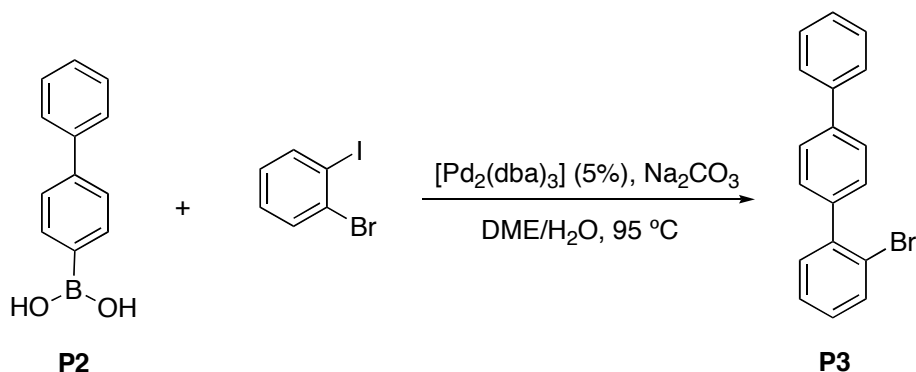
**Equation 32.** Unsuccessful preparation of **P3** via Ni(II) catalyzed cross-coupling.

**P3**, was finally prepared in a two-step reaction. In the first step, the *p*-biphenylboronic acid, **P2**, was synthesized in 73% yield<sup>125</sup>, using the standard protocol shown in **Equation 33**.



**Equation 33.** Preparation of **P2**.

The boronic acid **P2** was then subjected to Suzuki coupling, catalyzed by Pd(0), with *o*-bromiodobenzene, to furnish the desired product **P3** (Equation 34) in 51% yield<sup>125</sup>.

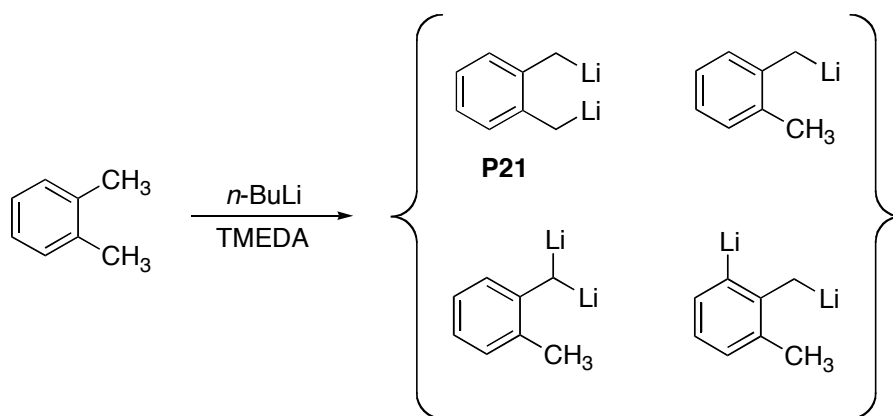


Equation 34. Preparation, *via* Suzuki coupling, of **P3**.

Attempts to perform this coupling with *o*-dibromobenzene did afford a mixture of **P3** and the product of double coupling, as determined by GC-MS. With *o*-bromiodobenzene, however, the reaction was highly specific towards the iodo coupling site to furnish **P3**. Mass spectrometry of **P3** showed the expected double molecular peak, produced by the characteristic isotopic distribution (49% <sup>79</sup>Br and 51% <sup>81</sup>Br) of bromine.

#### 7.2.4. Preparation of **P21**

Similarly to **P16**,  $\phi, \phi'$ -dilithio-*o*-xylene, **P21**, can not be prepared from  $\phi, \phi'$ -dibromo-*o*-xylene. In contrast to that case, however, metallation of *o*-xylene does not yield pure **P21** either, but a complicate mixture of products has been reported<sup>126</sup>, some of them are illustrated in Scheme 31.

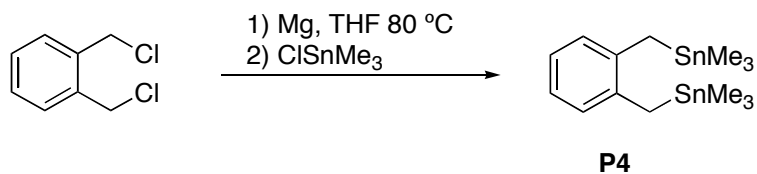


Scheme 31. Metallation of *o*-xylene with *n*-butyllithium.

This approach produces **P21** in 50% yield in the best case. Provided that the other organolithium reagents would interfere in the reactions, it is not synthetically useful.

To prepare **P21**, a recent protocol developed by Eisch<sup>127</sup> was used, based on tin-lithium exchange in organotin compounds.

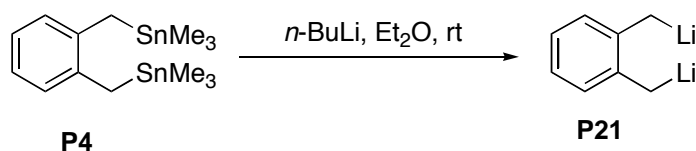
The strategy comprises two steps. Firstly, the diorganotin compound **P4** was prepared as shown in **Equation 35**.



**Equation 35.** Preparation of precursor **P4**.

The product **P4** was obtained by Mg-Sn transmetalation, as a colorless viscous oil, with a 46% yield.

From this precursor, the desired organolithium compound **P21** was obtained easily with *n*-butyllithium at room temperature, as it is depicted in **Equation 36**.

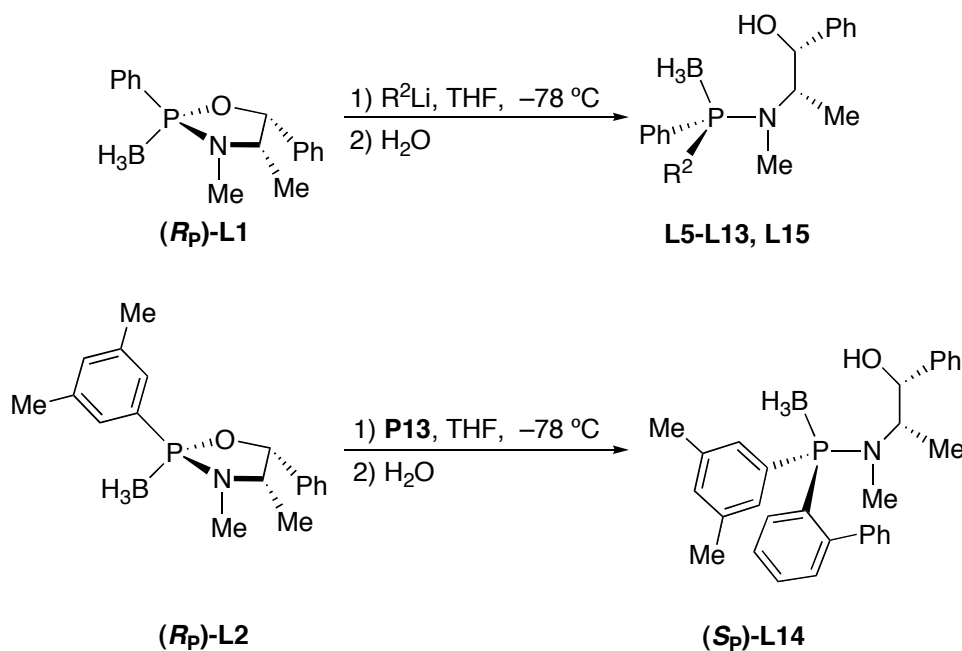


**Equation 36.** Preparation of **P21** from **P4**.

The product **P21** appeared as an air-sensitive, bright yellow solid.

### 7.3. Preparation and characterization of aminophosphine-boranes

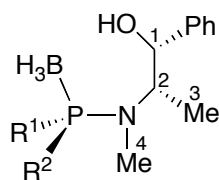
Once having optimized the organolithium compounds synthetic methods and with the oxazaphospholidine-boranes ( $S_p$ )-**L1** and ( $S_p$ )-**L2** already prepared, the corresponding aminophosphine-boranes **L5-L15** (Scheme 32) were obtained.



Scheme 32. Preparation of aminophosphine-boranes.

It has been described in Part I, section 3.3.4.3 that the reaction occurs with clean retention of configuration at the phosphorus atom. Products **L5-L15** were obtained in good yield as white or yellowish solids, foams or oils, after extractive workup. The reaction was very clean and only one single peak was detected in the  $^{31}\text{P}\{^1\text{H}\}$  NMR spectrum.  $^1\text{H}$  NMR spectrum revealed that the only impurities were remaining THF and some hydrocarbons derived from the preparation of the organolithium reagents. These impurities were separated later in the synthesis. This fact made purification procedures unnecessary. At this point, it has to be said that ( $R_p$ )-**L6**, with an *n*-butyl group was prepared only for comparison purposes, *i.e.* to check whether this compound was formed when preparing compounds ( $S_p$ )-**L10**-( $S_p$ )-**L15** with aryllithium reagents obtained with *n*-butyllithium.

The characterization of aminophosphine-boranes was made by multinuclear NMR spectroscopy. The spectroscopic data obtained agreed with the compounds that had been reported before<sup>54,57-60,67</sup>. Table 13 lists some data for the aminophosphine-boranes bearing an alkyl group at the phosphorus atom, **L5-L9**, whereas Table 14 does the same for the remaining aminophosphines, which bear two aryl groups on the phosphorus atom.



L5-L15

Compound	Yield (%)	$^{31}\text{P}$ NMR (ppm) <sup>a, b</sup>	$^1\text{H}$ NMR (ppm) <sup>b</sup>			
			$^{13}\text{C}$ NMR (ppm) <sup>a, b</sup>			
			1	2	3	4
<b>(R<sub>p</sub>)-L5</b> R <sup>1</sup> = Ph, R <sup>2</sup> = Me	92	65.8 ( <i>d</i> , 79)	4.76 ( <i>d</i> , 7.1)	4.05 ( <i>m</i> )	1.54 ( <i>d</i> , 9.0)	2.50 ( <i>d</i> , 8.6)
			77.8 ( <i>d</i> , 6.3)	58.0 ( <i>d</i> , 8.2)	14.1 ( <i>s</i> )	29.0 ( <i>s</i> )
<b>(R<sub>p</sub>)-L6</b> R <sup>1</sup> = Ph, R <sup>2</sup> = <i>n</i> -Bu	75	65.6 ( <i>d</i> , 84)	4.85 ( <i>d</i> , 7.1)	3.96-4.11 ( <i>m</i> )	1.18 ( <i>d</i> , 6.8)	2.56 ( <i>d</i> , 7.8)
			— <sup>c</sup>	— <sup>c</sup>	— <sup>c</sup>	— <sup>c</sup>
<b>(R<sub>p</sub>)-L7</b> R <sup>1</sup> = Ph, R <sup>2</sup> = <i>i</i> Pr	59	76.5 ( <i>d</i> , 85)	4.79 ( <i>d</i> , 4.8)	4.15 ( <i>m</i> )	— <sup>d</sup>	— <sup>d</sup>
			78.9 ( <i>d</i> , 2.2)	58.8 ( <i>d</i> , 8.1)	16.6 ( <i>s</i> )	29.6 ( <i>d</i> , 3.1)
<b>(R<sub>p</sub>)-L8</b> R <sup>1</sup> = Ph, R <sup>2</sup> = <i>t</i> Bu	77	86.4 ( <i>d</i> , 85)	5.20 ( <i>d</i> , 3.4)	4.15 ( <i>m</i> )	1.16 ( <i>d</i> , 7.0)	2.88 ( <i>d</i> , 6.4)
			79.8 ( <i>s</i> )	58.4 ( <i>d</i> , 9.1)	10.6 ( <i>d</i> , 4.1)	33.7 ( <i>d</i> , 4.6)
<b>(R<sub>p</sub>)-L9</b> R <sup>1</sup> = Ph, R <sup>2</sup> = Bn	50	72.8 ( <i>d</i> , 88)	4.80 ( <i>d</i> , 5.6)	3.80-4.10 ( <i>m</i> )	0.63 ( <i>d</i> , 6.8)	2.59 ( <i>d</i> , 7.3)
			— <sup>c</sup>	— <sup>c</sup>	— <sup>c</sup>	— <sup>c</sup>

<sup>a</sup>: Proton decoupled.  
<sup>b</sup>: Multiplicities and coupling constants (in Hertz) given in brackets. Acquisition conditions given in experimental part (Chapter VII, § 3.3).  
<sup>c</sup>: Not measured.  
<sup>d</sup>: Peaks overlapped with alkyl impurities.

**Table 13.** Selected NMR data of the aminophosphine-boranes with R<sup>2</sup> = alkyl group.

Compound	Yield (%)	$^{31}\text{P}$ NMR (ppm) <sup>a, b</sup>	$^1\text{H}$ NMR (ppm) <sup>b</sup>			
			$^{13}\text{C}$ NMR (ppm) <sup>a, b</sup>			
			1	2	3	4
<b>(S<sub>p</sub>)-L10</b> R <sup>1</sup> = Ph, R <sup>2</sup> = 1-naphthyl	82	72.7 ( <i>d</i> , 59)	5.02 ( <i>t</i> , 3.4)	4.52 ( <i>m</i> )	1.32 ( <i>d</i> , 6.9)	2.65 ( <i>d</i> , 7.4)
			79.2 ( <i>d</i> , 3.0)	58.1 ( <i>d</i> , 10.0)	11.6 ( <i>d</i> , 4.0)	31.5 ( <i>d</i> , 3.1)
<b>(S<sub>p</sub>)-L11</b> R <sup>1</sup> = Ph, R <sup>2</sup> = 2-biphenyl	70	71.9 ( <i>d</i> , 69)	4.86 ( <i>d</i> , 1.7)	3.92-3.97 ( <i>m</i> )	0.69 ( <i>d</i> , 6.9)	2.56 ( <i>d</i> , 7.2)
			78.8 ( <i>s</i> )	58.5 ( <i>d</i> , 10.0)	9.9 ( <i>d</i> , 6.4)	31.7 ( <i>s</i> )
<b>(S<sub>p</sub>)-L12</b> R <sup>1</sup> = Ph, R <sup>2</sup> = 9-phenanthryl	83	71.8 ( <i>d</i> , 64)	5.09 ( <i>d</i> , 3.7)	4.50-4.65 ( <i>m</i> )	1.39 ( <i>d</i> , 6.8)	2.74 ( <i>d</i> , 7.5)
			79.2 ( <i>d</i> , 2.5)	58.2 ( <i>d</i> , 10.4)	11.6 ( <i>d</i> , 4.3)	31.6 ( <i>d</i> , 3.5)
<b>(S<sub>p</sub>)-L13</b> R <sup>1</sup> = Ph, R <sup>2</sup> = 9-pyrenyl	85	71.5 ( <i>broad</i> )	5.10 ( <i>d</i> , 3.3)	4.60-4.66 ( <i>m</i> )	1.41 ( <i>d</i> , 6.8)	2.70 ( <i>d</i> , 7.5)
			79.2 ( <i>d</i> , 2.6)	58.3 ( <i>d</i> , 10.4)	11.8 ( <i>d</i> , 4.2)	31.6 ( <i>d</i> , 3.5)
<b>(S<sub>p</sub>)-L14</b> R <sup>1</sup> = 3,5-dimethylphenyl, R <sup>2</sup> = 2-biphenyl	85	71.7 ( <i>q</i> , 67)	4.87 ( <i>broad</i> )	3.94-4.01 ( <i>m</i> )	0.75 ( <i>d</i> , 6.9)	2.57 ( <i>d</i> , 7.2)
			79.2 ( <i>s</i> )	58.4 ( <i>d</i> , 10.1)	10.5 ( <i>d</i> , 6.4)	32.2 ( <i>d</i> , 3.9)
<b>(S<sub>p</sub>)-L15</b> R <sup>1</sup> = Ph, R <sup>2</sup> = 2- <i>p</i> -terphenyl	82	71.4 ( <i>broad</i> )	4.84 ( <i>broad</i> )	4.02 ( <i>m</i> )	0.69 ( <i>d</i> , 6.8)	2.59 ( <i>d</i> , 10.0)
			79.1 ( <i>s</i> )	58.6 ( <i>d</i> , 10.3)	10.4 ( <i>d</i> , 6.5)	32.1 ( <i>d</i> , 4.2)

<sup>a</sup>: Proton decoupled.  
<sup>b</sup>: Multiplicities and coupling constants (in Hertz) given in brackets. Acquisition conditions given in experimental part (Chapter VII § 3.3).

**Table 14.** Selected NMR data of the aminophosphine-boranes with R<sup>2</sup> = aryl group.

An overview of the tables reveals slight modification of the shifts and the coupling constants in both  $^1\text{H}$  and  $^{13}\text{C}\{^1\text{H}\}$  NMR spectra.  $^{31}\text{P}\{^1\text{H}\}$  shifts show to be very dependent on the steric crowding around the phosphorus atom. While the shift value remains almost unchanged around  $\phi = 72$  ppm, when R<sup>2</sup> is an aryl group (**Table 14**), it displaces gradually to lower fields upon increasing the crowding of the alkyl group (**Table 13**) when R<sup>2</sup> goes from methyl to *tert*-butyl.

As an example to illustrate **Table 14**, the  $^1\text{H}$  NMR spectrum of ( $S_P$ )-**L10** is reproduced in **Figure 27**

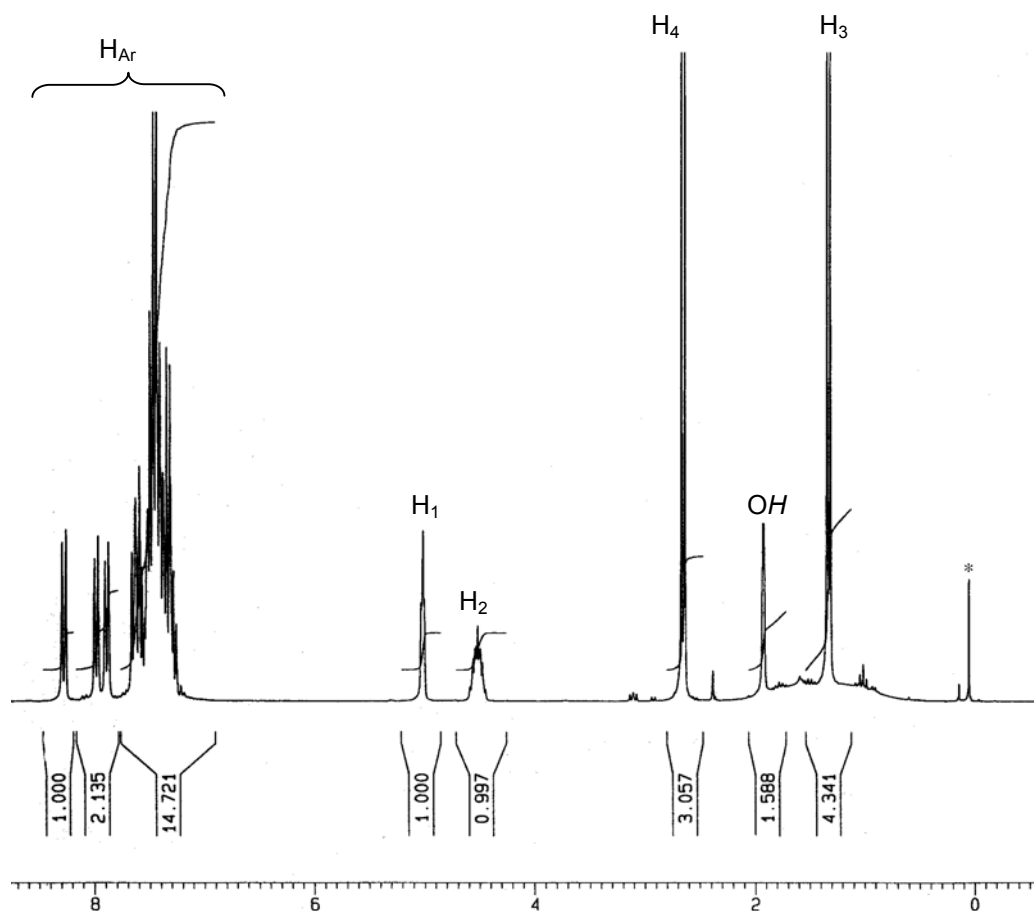


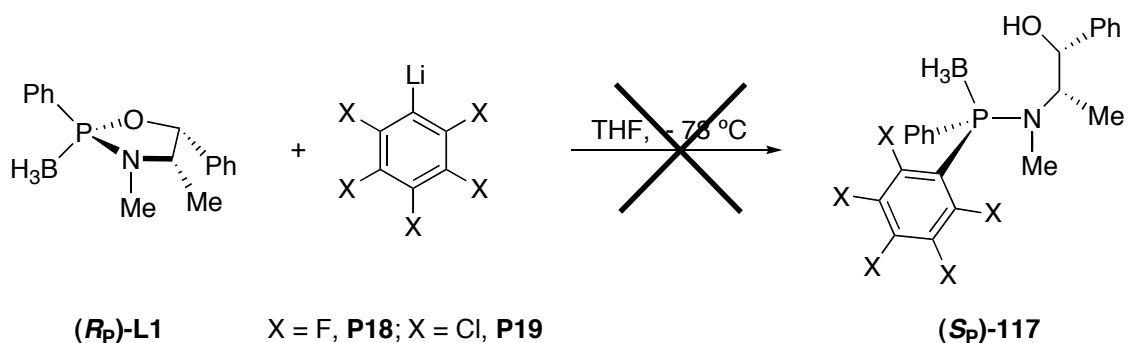
**Figure 27.**  $^1\text{H}$  NMR spectrum (250 MHz,  $\text{CDCl}_3$ , 298 K) of the amino-borane ( $S_P$ )-**L10**. \*: TMS.

All the aminophosphine-boranes prepared had already been reported, except **L7**, **L9**, **L14** and **L15**. For the compounds reported, the diastereomeric ratio was found to be superior to 97:3 towards the expected diastereomer. This ratio can be estimated by  $^1\text{H}$  NMR and/or  $^{31}\text{P}\{^1\text{H}\}$  NMR. For all the aminophosphine-boranes prepared in this THESIS, the analysis of that spectra showed only one diastereomer, so a d.e. greater than 95% can be estimated, in agreement with the reported compounds.



## 7.4. Unsuccessful essays

In Part I (§ 3.3.4.3) it has been pointed out that some *o,o'*-disubstituted aryllithium compounds (mesityllithium, 9-anthryllithium, etc) do not react with (*S<sub>p</sub>*)-**L1**. All this organolithium reagents had a carbon atom or an oxygen atom in both *ortho* positions. Organolithium compounds **P18** and **P19**, with halogens in the *ortho* positions were tested in the reaction, to check if at least **P18**, with small fluorine atoms would lead to the desired perfluorinated aminophosphine-borane (*S<sub>p</sub>*)-**117** (Equation 37).



**Equation 37.** Attempt to obtain perhalogenated aminophosphine-boranes **117**.

The reaction was carried out under the usual conditions, but after stirring 14 hours,  $^{31}\text{P}\{^1\text{H}\}$  NMR spectrum showed only the signals of the starting product (*R<sub>p</sub>*)-**L1** for either **P18** and **P19** organolithium reagents.

These results support Mezzetti's suggestion<sup>57</sup> that 2,6 substituted aryllithium reagents are not able to react with (*R<sub>p</sub>*)-**L1**, probably due to their bulkiness.

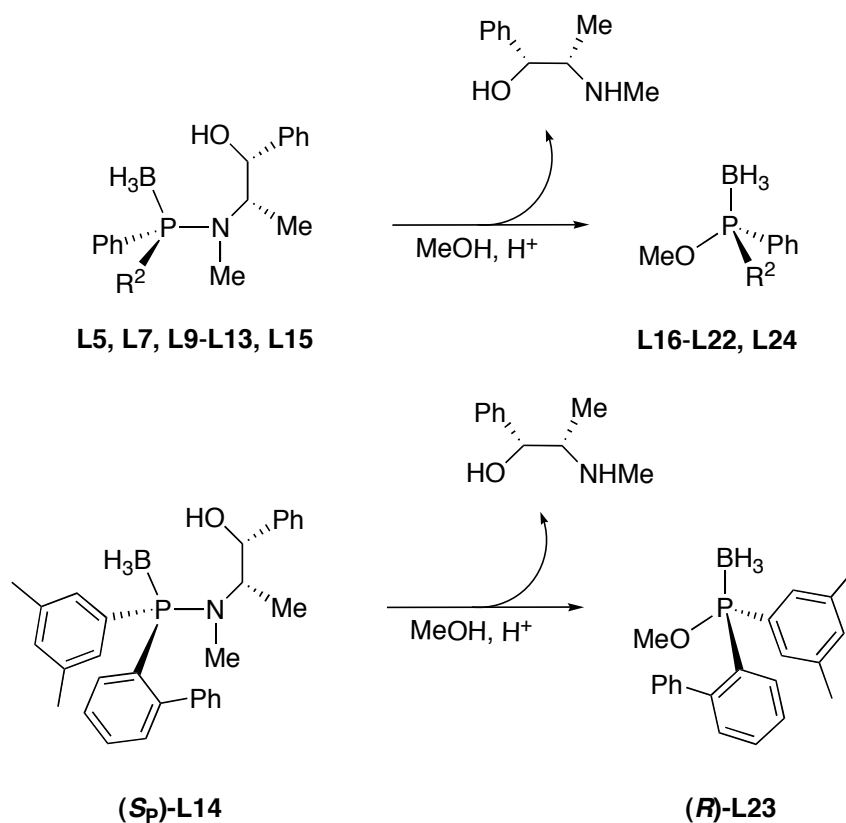
## 8. *P*-chirogenic phosphinite-boranes.

### Preparation and characterization

#### 8.1. Introduction

Following the general scheme of Jugé (Part I, § 3.3.4.1), the methanolysis of the aminophosphine-boranes **L5** and **L7-L15**, prepared in section 7, was undertaken.

The reaction conditions are straightforward: the phosphamide-borane is dissolved in dry, deoxygenated methanol, at 0 °C and one equivalent of sulphuric acid is then added. The reaction is summarized in **Scheme 33**.

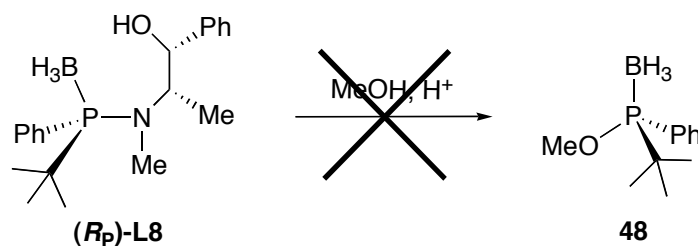


**Scheme 33.** Preparation of the phosphinite-boranes **L16-L23**.

## 8.2. Phosphinite-boranes: synthesis and characterization

Several aspects of the methanolysis reaction, presented in the introduction, deserve special attention. Firstly, there are differences in the reaction time. The usual conditions were stirring in methanol for 12 hours. After this time,  $^{31}\text{P}\{^1\text{H}\}$  NMR spectrum of the methanolic mixtures showed no sign of the starting aminophosphine-borane peaks for any case, except for **(R<sub>p</sub>)-L9**, **(R<sub>p</sub>)-L7** and **(R<sub>p</sub>)-L8**. Each of these aminophosphine-boranes carried a phenyl group and benzyl, an isopropyl and a *tert*-butyl group respectively. It was found that for achieving total conversion were necessary 48 hours for **(R<sub>p</sub>)-L9** and 7 days for **(R<sub>p</sub>)-L7**. **(R<sub>p</sub>)-L8** showed no sign of reaction neither after 15 days of stirring at rt nor at reflux of methanol for 4 hours.

These facts agree with previous literature, which state that secondary and tertiary alkyl-substituted aminophosphine-boranes are notoriously difficult to convert to phosphinite-boranes and usually require heating to obtain the desired product, often in low yield<sup>67</sup>. This difficulty turns into impossibility in the case of **(R<sub>p</sub>)-L8**, with a *t*Bu substituent at the phosphorus atom, as is shown in **Equation 38**.



**Equation 38.** Inertness of **(R<sub>p</sub>)-L8** to methanolysis.

It has been claimed that under these circumstances the P atom is inert to further substitution reactions (*neopentyl rule*)<sup>60</sup>. The *t*Bu group combines high basicity and steric crowding making methanolysis impossible.

Another aspect to be pointed out is the exact work-up of the reactions. After evaporation of the solvent, (–)-ephedrine hydrogensulphate was precipitated in ethyl acetate and was filtered out. From the ethyl acetate, the desired compounds were obtained as outlined below.

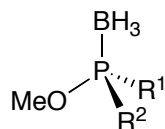
Compounds **(S)-L16**-**(S)-L18**, bearing a phenyl group and an alkyl group at the phosphorus atom (methyl, isopropyl and benzyl respectively), were obtained as colourless liquids or pale yellow oils after evaporation of ethyl acetate. The  $^{31}\text{P}\{^1\text{H}\}$  NMR spectra showed practically pure products, with a minor amount of an unknown impurity at  $\phi_{\text{P}} \approx 90$ -100 ppm.  $^1\text{H}$  NMR spectra showed the same purity, with some undesired, but weak peaks in the aliphatic

region (below  $\phi = 2$  ppm) that could correspond to impurities from previous synthetic steps, presumably coming from the organolithium compounds.

Compounds **(R)-L19**–**(R)-L22**, bearing a phenyl group and an aromatic fragment at the phosphorus atom (1-naphthyl, 2-biphenyl, 9-phenanthryl and 1-pyrenyl respectively) were obtained by a slightly modified procedure. After separation of (–)-ephedrine hydrogensulphate and evaporation of ethyl acetate, the desired compounds were solubilized in ether and then recrystallized from dichloromethane/ethanol. Eventually the products were obtained as white, crystalline solids except **(R)-L22**, which was yellow due to the conjugation in the pyrenyl group. The gummy product insoluble in ether showed, by  $^1\text{H}$  NMR analysis, that it was mainly the coupling product of *n*-butyllithium and the aryl bromide used to prepare the aminophosphine-boranes. For example, in the preparation of **(R)-L19**, it was determined to be 1-butylnaphthalene, for comparison with literature data<sup>128</sup>. The method of ether solubilization and recrystallization was found to effectively remove these compounds and yield pure products.

Finally, compounds **(R)-L23** (with a 3,5-dimethylphenyl group) and **(R)-L24** (with a 2-*p*-terphenyl group) were obtained with another slightly modified procedure. Provided the similarity of both compounds with **(R)-L20** the precipitation in dichloromethane/ethanol and other mixtures was attempted. In spite of numerous efforts, it was not possible to isolate neither **(R)-L23** nor **(R)-L24** in a solid form, but as yellowish, sticky substances. These substances were repeatedly washed with pentane until the  $^{31}\text{P}\{^1\text{H}\}$  and  $^1\text{H}$  NMR spectra showed that the chemical purity was high enough for synthetic purposes.

The obtained phosphinite-boranes were characterized by the usual techniques: multinuclear NMR, IR, elemental analysis,  $[\phi]_{\text{D}}$  and HPLC. **Table 15** lists a summary of the characterization for these compounds.



Compound	Yield (%)	$^{11}\text{B NMR}$	$^{31}\text{P NMR}$	$^1\text{H NMR}$	$^{13}\text{C NMR}$	$[\phi]_D$
		$\phi(\text{ppm})^{a, b}$	$\phi(\text{ppm})^{a, b}$	$\phi(\text{ppm})^b$ <i>P-OCH<sub>3</sub></i>	$\phi(\text{ppm})^{a, b}$ <i>P-OCH<sub>3</sub></i>	$[\phi]_D^f$
<b>(S)-L16</b> R <sup>1</sup> = Ph, R <sup>2</sup> = Me	92	— <sup>c</sup>	112.6 ( <i>q</i> , 69)	3.56 ( <i>d</i> , 12.0)	53.6 ( <i>d</i> , 29.9)	— <sup>c</sup> — <sup>e</sup>
<b>(S)-L17</b> R <sup>1</sup> = Ph, R <sup>2</sup> = <sup><i>i</i></sup> Pr	56	— <sup>c</sup>	109.6 ( <i>d</i> , 79)	3.62 ( <i>d</i> , 11.5)	— <sup>c</sup>	— <sup>c</sup> — <sup>f</sup>
<b>(S)-L18</b> R <sup>1</sup> = Ph, R <sup>2</sup> = Bn	74	— <sup>c</sup>	112.4 ( <i>d</i> , 79)	3.57 ( <i>d</i> , 11.6)	54.7 ( <i>d</i> , 3.0)	— <sup>c</sup> — <sup>f</sup>
<b>(R)-L19</b> R <sup>1</sup> = Ph, R <sup>2</sup> = 1-naphthyl	60	−39.3 ( <i>d</i> , 78.0)	112.4 ( <i>d</i> , 79)	3.78 ( <i>d</i> , 12.2)	54.1 ( <i>d</i> , 12.5)	−15.8° −14.9°
<b>(R)-L20</b> R <sup>1</sup> = Ph, R <sup>2</sup> = 2-biphenyl	82	−39.4 ( <i>d</i> , 66.0)	112.4 ( <i>d</i> , 75)	3.57 ( <i>d</i> , 12.0)	54.0 ( <i>d</i> , 2.2)	−19.4° −17.4°
<b>(R)-L21</b> R <sup>1</sup> = Ph, R <sup>2</sup> = 9-phenanthryl	42	−38.6 ( <i>d</i> , 60.9)	111.5 ( <i>d</i> , 75)	3.85 ( <i>d</i> , 12.0)	54.1 ( <i>d</i> , 2.4)	+70.1° +78.1°
<b>(R)-L22</b> R <sup>1</sup> = Ph, R <sup>2</sup> = 1-pyrenyl	42	−38.3 ( <i>d</i> , 62.0)	111.6 ( <i>d</i> , 72)	3.87 ( <i>d</i> , 12.3)	54.1 ( <i>d</i> , 2.6)	−69.4° — <sup>f</sup>
<b>(R)-L23</b> R <sup>1</sup> = 3,5-diMePh, R <sup>2</sup> = 2-biphenyl	76	— <sup>c</sup>	109.1 ( <i>d</i> , 75)	3.56 ( <i>d</i> , 12.0)	53.9 ( <i>s</i> )	— <sup>c</sup> — <sup>f</sup>
<b>(R)-L24</b> R <sup>1</sup> = Ph, R <sup>2</sup> = 2- <i>p</i> -terphenyl	58	— <sup>c</sup>	110.6 ( <i>d</i> , 78)	3.61 ( <i>d</i> , 12.0)	— <sup>c</sup>	— <sup>c</sup> — <sup>f</sup>

<sup>a</sup>: Proton decoupled.

<sup>b</sup>: Multiplicities and coupling constants (in Hertz) given in brackets. Acquisition conditions given in experimental part (Chapter VII, § 3.4).

<sup>c</sup>: Not determined.

<sup>d</sup>: Literature value.

<sup>e</sup>: Value not reported.

<sup>f</sup>: Compound not reported.

**Table 15.** Relevant data for the phosphinite-boranes prepared in this THESIS.

As can be inferred from the table, phosphinite-boranes are obtained in moderate to good yields. Their  $^{11}\text{B}\{^1\text{H}\}$  and  $^{31}\text{P}\{^1\text{H}\}$  NMR spectra show very little variation: around  $\phi = -40$  ppm and  $\phi = 110$  ppm respectively. In the  $^{13}\text{C}\{^1\text{H}\}$  and  $^1\text{H}$  NMR spectra the shift of the methyl substituent of the methoxy group is very characteristic. In the  $^1\text{H}$  NMR spectrum, it appears as a sharp doublet, around  $\phi = 3.7$  ppm, with a large coupling constant ( $> 10$  Hz) with the phosphorus atom.

**Figure 28** displays the  $^1\text{H}$  NMR spectrum of (*R*)-**L20** as an example.

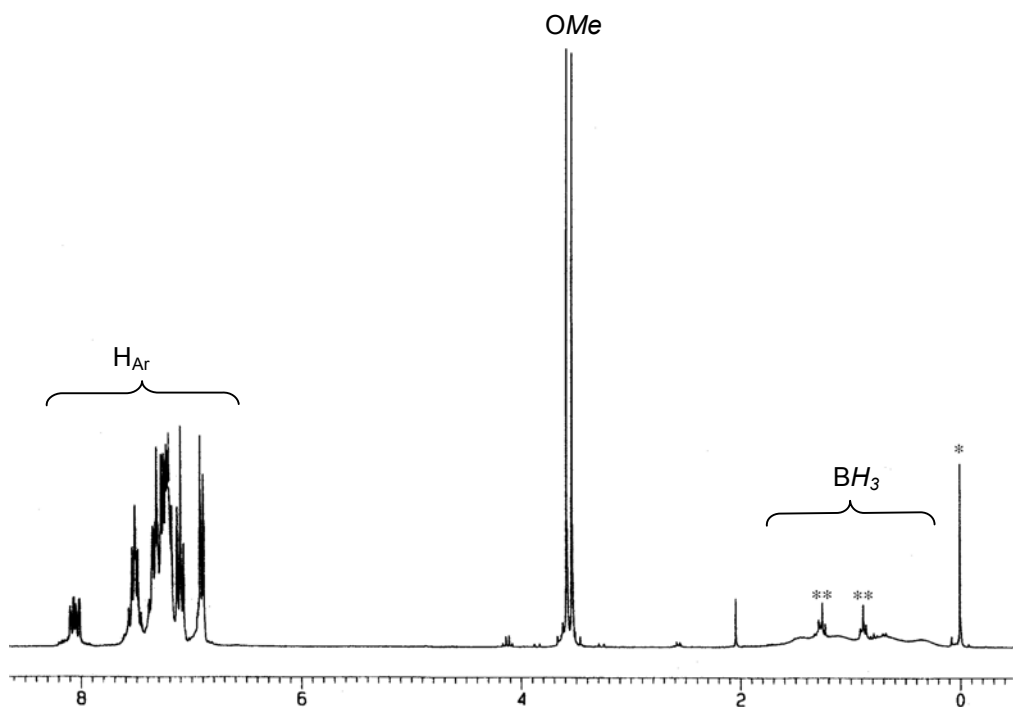


**Figure 28.**  $^1\text{H}$  NMR (250 MHz,  $\text{CDCl}_3$ , 298 K) spectrum of (*R*)-**L20**. \*: TMS, \*\*: *n*-pentane.

In the  $^{13}\text{C}\{^1\text{H}\}$  NMR spectrum it also appears as a doublet very close to  $\phi = 54.0$  ppm. In this case, however, the coupling constant is more variable.

The specific rotation and the infrared spectrum of compounds (*R*)-**L19**-(*R*)-**L22** were also measured. The IR spectra showed typical C-H and B-H stretching bands, whereas the optical rotation values were consistent with the published ones as is listed in the table.

In order to check the optical purity of the compounds, HPLC analysis on a chiral column was performed in products (*R*)-**L19**-(*R*)-**L22**. In all cases, the chromatograms showed only one peak and hence accounted for an enantiomeric purity greater than 95% e.e., as it has been reported previously for some of these compounds.

Compounds (*S*)-**L16**-(*S*)-**L18** were not further used for synthetic purposes (§ 9.1) and because they were not obtained as totally pure products its HPLC chromatograms, apart from the peak of the main product, showed many weak peaks, making difficult to assign which of them could correspond to the minor enantiomer. For this reason, its enantiomeric purity was not determined, although it is supposed to be high. For the same reasons, compounds (*R*)-**L23** and (*R*)-**L24** were not analyzed by HPLC, although their enantiomeric purity should be similar to their counterpart (*R*)-**L20**.

### 8.3. X-ray crystalline structure of (*R*)-L22

Phosphinite-boranes (*R*)-L19-(*R*)-L21, bearing a phenyl group, an aryl group and the methoxy moiety had already been prepared and characterized in the literature<sup>54,58,59,67</sup>.

In contrast, the phosphinite borane (*R*)-L22, which bears a 1-pyrenyl group, had not been reported previously, to the best of our knowledge. In order to complete the characterization of the phosphinite-boranes, its crystalline structure was determined.

Yellow crystals were grown from CH<sub>2</sub>Cl<sub>2</sub>/hexane, at 4 °C. The molecular structure of (*R*)-L22 is shown in **Figure 29**. The crystal contains discrete (*R*)-L22 molecules with normal nonbonded interactions. The expected *R* absolute configuration at the phosphorus atom is confirmed by this X-ray structure.

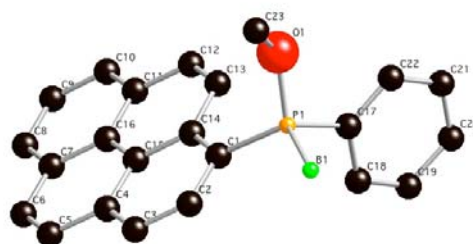


**Figure 29.** Molecular structure of (*R*)-L22. Arbitrary numbering of the atoms. Hydrogen atoms have been omitted for clarity.

The geometry of the *P* atom is approximately tetrahedral, with normal P-B, P-C and P-O distances. Selected bond distances and angles of this structure are reported in **Table 16**, following the numbering of **Figure 29**.

<i>Bond</i>	<i>Length</i> (Å) <sup>a</sup>	<i>Angle</i>	<i>Value</i> (°) <sup>a</sup>
P-B	1.899(2)	C(1)-P-O	107.87(8)
P-O	1.6005(14)	C(1)-P-C(17)	108.11(8)
P-C(1)	1.8081(19)	C(1)-P-B	113.04(10)
P-C(17)	1.7934(19)	C(17)-P-O	101.41(8)
C(23)-O	1.443(2)	C(17)-B-P	110.06(10)
		B-P-O	115.54(10)

<sup>a</sup>: Standard deviations in parentheses.

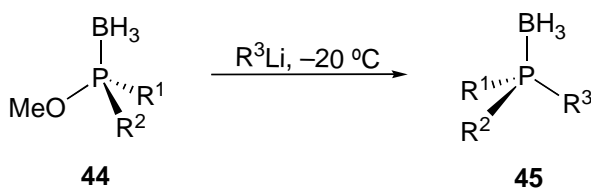
**Table 16.** Selected bond lengths and angles in (*R*)-L22.

## 9. *P*-chirogenic monophosphine-boranes.

### Preparation and characterization

#### 9.1. Introduction

The *P*-stereogenic phosphinite-boranes, described in section 8, are the precursors of the *P*-stereogenic phosphine-boranes, by nucleophilic substitution of the methoxy group by the desired organolithium reagent, as illustrated in **Equation 39**.



**Equation 39.** Stereoselective, nucleophilic attack on phosphinite-boranes **33**.

With the phosphinite-boranes **33** in hand and the organolithium compounds available or ready to be prepared, it was necessary to decide which phosphines would be attempted to prepare be prepared.

After previous experience of the group with phosphines, it was found interesting the preparation of some bulky, *P*-stereogenic monophosphines to be used, firstly, in Pd-catalyzed hydrovinylation and afterwards in some other catalytic processes. Following this idea, it was planned to prepare a family of similar ligands but increasing, *gradually*, their steric crowding around the phosphorus atom. Among the phosphinite-boranes described in section 8, those having a phenyl group (or a 3,5-dimethylphenyl group) and a bulky aryl group at the phosphorus atom (1-naphthyl, 9-phenanthryl, 1-pyrenyl and 2-biphenyl) were selected. In order to increase, gradually, the steric hindrance of the ligand, it was envisaged the installation of simple alkyl groups at the phosphorus atom with increasing bulkiness. Consequently, a sequence of methyl, isopropyl and *tert*-butyl groups was thought to be suitable to this endeavour.



For these reasons, the array of phosphine-boranes depicted in **Figure 30** was bound to be prepared.

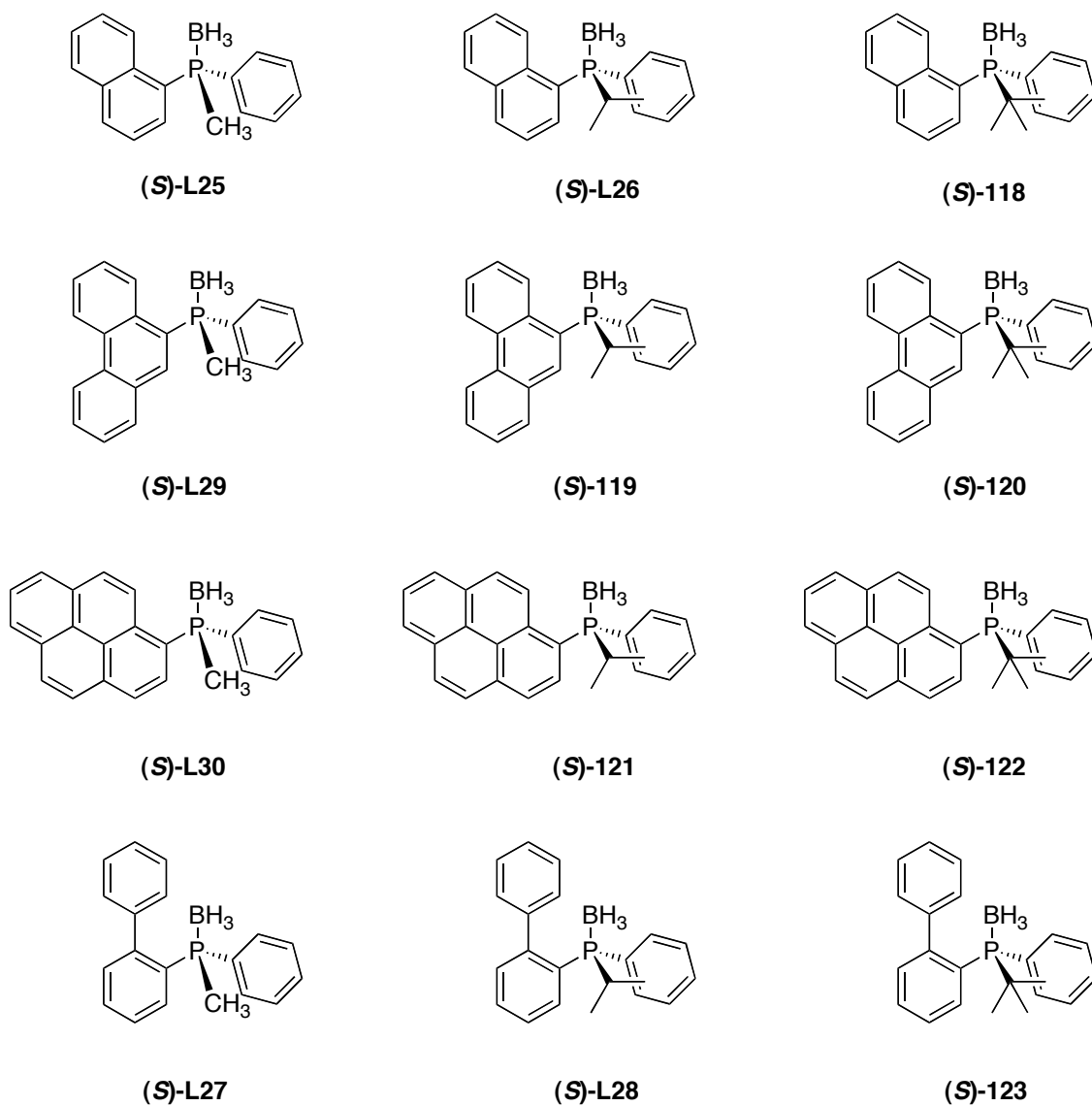


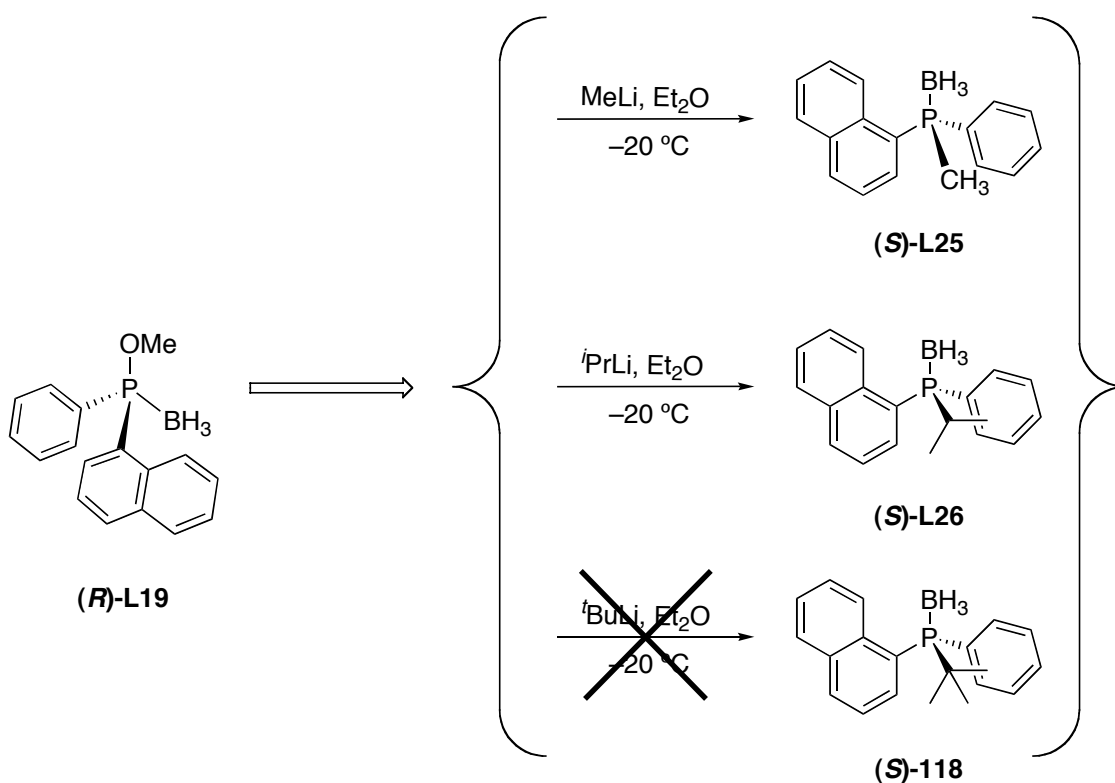
**Figure 30.** *P*-chirogenic monophosphines planned to be prepared in this THESIS.

With the experience gained in the preparation of these compounds, some additional phosphine-boranes with a 3,5-dimethylphenyl and with a 2-*p*-terphenyl group (starting from **(R)-L23** and **(R)-L24**, respectively) would also be prepared.

## 9.2. Phosphine-boranes bearing a 1-naphthyl group

### 9.2.1. Synthesis of (S)-L25 and (S)-L26

The first efforts were devoted to the synthesis of phosphine-boranes bearing a 1-naphthyl group. Following what it has been stated in the above introduction, the reactions presented in **Scheme 34** were attempted.



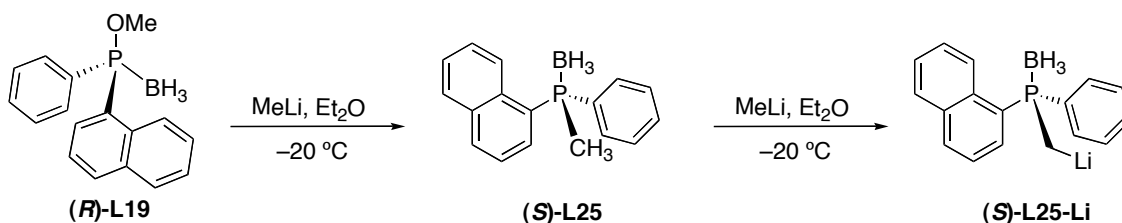
**Scheme 34.** Preparation of phosphine-boranes bearing a 1-naphthyl group.

A literature survey revealed that the phosphine-borane (S)-L25 had already been prepared by Jugé<sup>54</sup> (who also prepared the free phosphine) and more recently by Mezzetti<sup>58</sup>, who reported its detailed characterization, including the X-ray crystalline structure. The free phosphine derived from (S)-118 was prepared in racemic form by Trippett<sup>129</sup>. Phosphine-borane (S)-L26 and its derived free phosphine have been, to the best of our knowledge, not reported.

The choice of solvent was made by screening the literature for this kind of reactions. Both THF<sup>54</sup> and Et<sub>2</sub>O<sup>130</sup> have been successfully used. In THF the phosphinite-boranes, such as (R)-L19 are considerably more soluble than in Et<sub>2</sub>O, especially at low temperature. THF, however, is significantly more readily cleaved by alkyllithium compounds<sup>116</sup>. Moreover, THF is much less easily dried and more hygroscopic than diethylether. For these reasons, Et<sub>2</sub>O was selected as a solvent of choice.

The phosphinite-borane (**R**)-**L19** was dissolved in Et<sub>2</sub>O and cooled to -20 °C. An excess of solution of the suitable organolithium reagent was added by syringe. Colour changed from colorless to brownish or dark brown. After stirring overnight and extractive work-up, phosphine-boranes (**S**)-**L25** and (**S**)-**L26** were obtained as white, crystalline solids after recrystallization in dichloromethane/ethanol. The yields were 63% and 61%, respectively. In contrast, the phosphine (**S**)-**118**, was not obtained, as will be explained in section 9.2.2.

The reactions were monitored by <sup>31</sup>P{<sup>1</sup>H} NMR spectroscopy, which showed the disappearance of the peak of (**R**)-**L19** ( $\delta = 112.4$  ppm) and the appearance of the peak of (**S**)-**L25** ( $\delta = 11.5$  ppm) or (**S**)-**L26** ( $\delta = 25.6$  ppm). The preparation of (**S**)-**L25**, also illustrated that an excess of methyllithium was necessary, because part of it was consumed concomitantly in the deprotonation of the formed (**S**)-**L25** to yield (**S**)-**L25-Li** ( $\delta = 15.0$  ppm). This reaction is rendered in **Scheme 35**. Apart from this product, which is converted to the desired phosphine (**S**)-**L25** by the normal aqueous work-up, the reaction went smoothly, with no other side products detected.



**Scheme 35.** Deprotonation of (**S**)-**L25** by methyllithium.

The conversion towards the final phosphines (**S**)-**L25** and (**S**)-**L26** was total, although the velocities of the reactions were remarkably different. Methyllithium reacted quickly with (**R**)-**L19** (30 minutes after the addition, the reaction was complete) whereas isopropyllithium was much slower and took several hours. This difference is explained by the higher steric hindrance of isopropyl group compared to methyl group.

The phosphine-boranes (**S**)-**L25** and (**S**)-**L26** were fully characterized, as will be described in section 9.7.

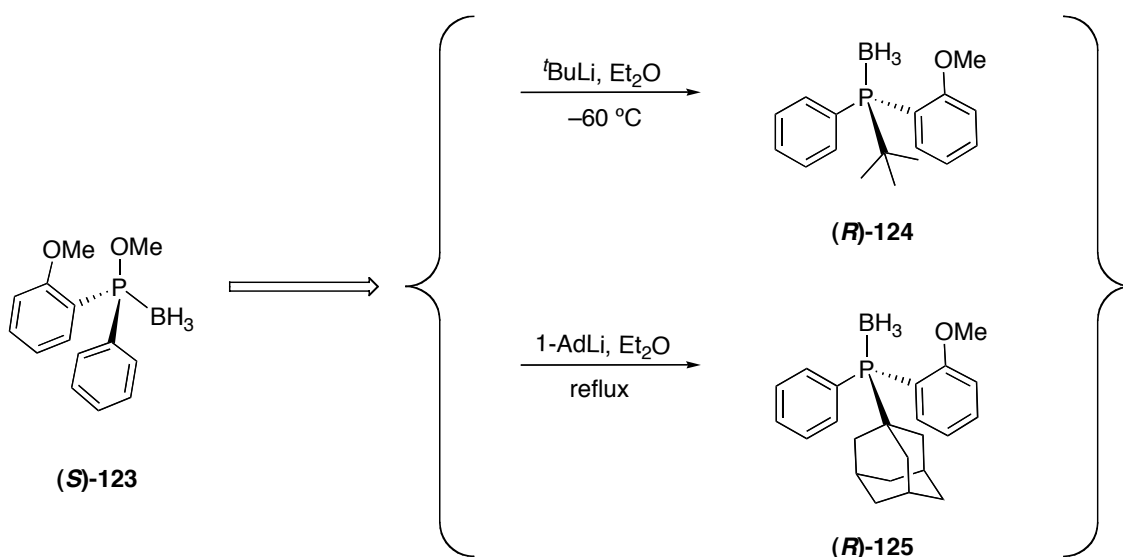
In sections 9.2.3.2, 9.3.2, 9.5.2 and 10.3, the use of the carbanions derived from deprotonation of methylphosphine-boranes, such as (**S**)-**L25-Li**, will be developed.

### 9.2.2. Unsuccessful attempts to introduce a <sup>t</sup>Bu group

The success achieved in the synthesis of either (*S*)-**L25** or (*S*)-**L26** contrasts with the unsuccessful preparation of (*S*)-**118**. Addition of <sup>t</sup>BuLi to the phosphinite-borane (*R*)-**L19** afforded many unidentified products, which gave peaks between  $\delta = -50$  ppm and  $\delta = 40$  ppm in the <sup>31</sup>P{<sup>1</sup>H} NMR spectrum. Some of the peaks were broad, indicating that the phosphorus atom was bonded to boron, whereas other peaks were sharp, indicating that deboration had occurred. In fact, during work-up, the characteristic free phosphine smell was detected. It is plausible to think that one of this peaks could correspond to the desired phosphine-borane (expected at  $\delta \approx 35$  ppm), but given the complexity of the spectrum indicating a large number of products, the separation of them was considered non practicable and was not attempted.

All experiments performed changing the experimental conditions of temperature ( $-78$  °C to  $+20$  °C) or solvent (Et<sub>2</sub>O, THF, hexane), failed and <sup>31</sup>P{<sup>1</sup>H} NMR spectra showing the signal of the starting material (*R*)-**L19** and/or several more signals were invariably obtained. The results probably account for the high steric hindrance of the *tert*-butyl group that precludes the expected nucleophilic substitution in (*R*)-**L19**. Instead of this nucleophilic substitution, *tert*-butyllithium, which is a very powerful base and lithiating agent, probably attacks the borane group and the phenyl or naphthyl groups at the phosphorus atom, giving several products.

The impossibility to substitute the methoxy group by a <sup>t</sup>Bu, encountered here, is in sharp contrast with the results of Brown and Laing<sup>130</sup>, who successfully managed to carry the reactions depicted in **Scheme 36**.



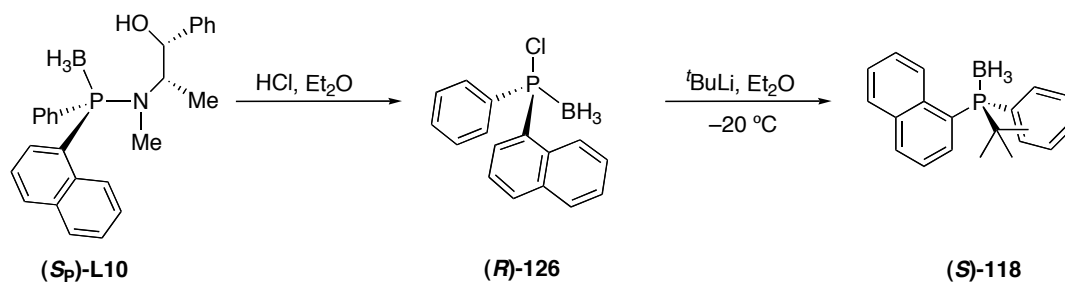
**Scheme 36.** Synthesis of bulky *P*-stereogenic phosphines from (*S*)-**123**.

The *tert*-butyl group and the even bulkier 1-adamantyl group could be attached to the phosphorus atom (compounds (*R*)-**124** and (*R*)-**L125**, respectively). This fact demonstrates that

(*R*)-**L19** behaves in a different way compared to (*S*)-**123**. The reason of this difference is probably the bulkier 1-naphthyl substituent in (*R*)-**L19** compared to the *o*-anisyl substituent in (*S*)-**123** although other factors, such as different electronic properties of the two groups and chelating capacity of the *o*-anisyl group may play their role.

In order to introduce the <sup>t</sup>Bu group, other attempts were carried out, which will be described in the paragraphs below.

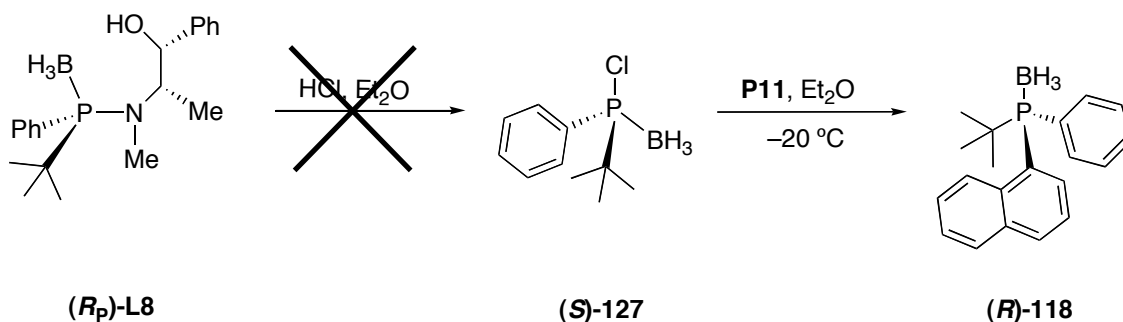
An alternative was to start from a more reactive precursor than the phosphinite borane (*R*)-**L19** to prepare the desired phosphine-borane (*S*)-**118**. Following a publication of Jugé on configurational stability of chlorophosphines, the synthetic scheme of **Scheme 37** was devised<sup>82</sup>.



**Scheme 37.** Alternative route to prepare (*S*)-**118**.

This reaction has been explained in detail in Part I, section 3.3.4.7. The key precursor (*R*)-**126** is prepared from the aminophosphine-borane (*S<sub>p</sub>*)-**L10** with HCl. Chlorophosphine-boranes are much more reactive towards nucleophiles than the corresponding phosphinite-boranes and hence it was found interesting to test whether (*R*)-**126** would be able to react with *tert*-BuLi to give the desired (*S*)-**118**. Shortly before the reaction was going to be attempted, another paper of Jugé making a study of the stereoselectivity in the formation of several chlorophosphine-boranes appeared<sup>83</sup>. Among them, precisely (*S*)-**126** was found to be obtained in racemic form, for rather unexplained reasons. As the interest was focused on the obtention of enantiopure phosphines, the reaction of **Scheme 37** was eventually not attempted.

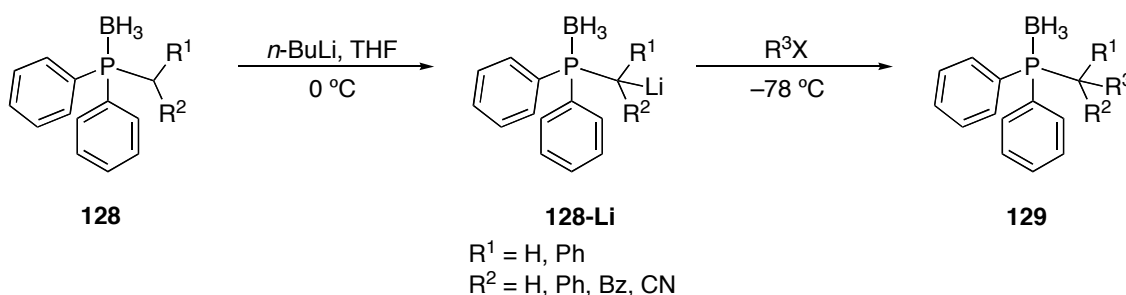
Another attempt was made in the same direction than in **Scheme 37**, but with reverse order, as shown in **Scheme 38**. Again, however, the attempt was not successful because the aminophosphine borane (*R<sub>p</sub>*)-**L8** did not suffer the acidolysis to yield (*S*)-**127**.



**Scheme 38.** Preparation of (*R*)-**118** by the intermediate (*S*)-**123**.

(*R<sub>p</sub>*)-**L8**, hence, shows the same inertness towards HCl in diethylether than it showed towards H<sub>2</sub>SO<sub>4</sub> in methanol (§ 8.2). Soon after this unsuccessful experiment, Jugé arrived to the same conclusion<sup>83</sup>. It has to be noted that if the reaction had worked, the enantiomer *R* at the phosphorus atom would have been expected, because the order of introduction of the substituents is reverse than in **Scheme 37**.

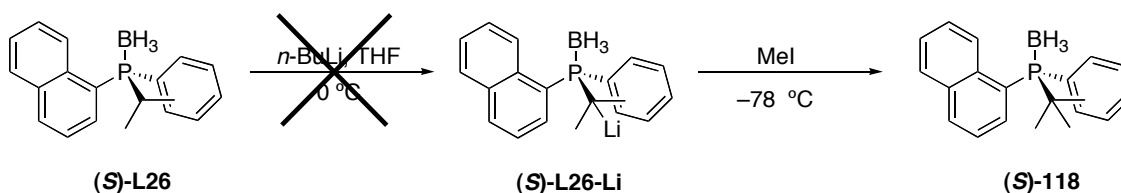
It seems clear, hence, that (*R*)-**L19** (**Scheme 34**) does not allow the nucleophilic attack of <sup>t</sup>BuLi at the phosphorus atom. Consequently, a different precursor that would not imply attack at the *P* atom would be highly desirable. From this reflection, a last strategy was built. Le Corre *et al.* had reported<sup>131</sup>, in 1993, that not only methylphosphine-boranes could be deprotonated but also some  $\phi$ -alkylated and  $\phi, \phi'$ -dialkylated phosphine-boranes suffered such deprotonations. This work is rendered in **Scheme 39**.



**Scheme 39.** Functionalization of  $\phi$ -alkylated methylphosphine-boranes.

The anions **128-Li** were made to react with several electrophiles to yield the final phosphine-boranes **129**.

This method could be applied to prepare the desired phosphine (*S*)-**118** from the previously prepared phosphine borane (*S*)-**L26**, as depicted in **Scheme 40**. Again, unfortunately, this scheme failed because the deprotonation of (*S*)-**L26** did not occur.

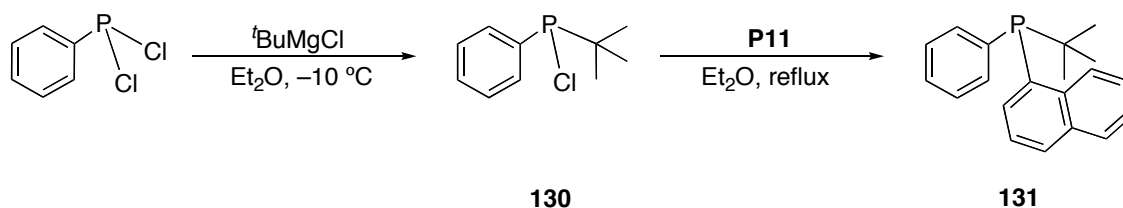


**Scheme 40.** Attempted synthesis of (*S*)-**118** via the  $\phi$ -carbanion derived from (*S*)-**L26**.

It is probable that even the strong base *n*-BuLi is not able to effectively abstract the proton at the  $\phi$  position in (*S*)-**L26**. In fact, the phosphine-boranes **128** in **Scheme 39** have a more acidic proton, because they do not have two electron donating groups as the two methyl groups in (*S*)-**L26**.

It seems clear, therefore, that the method of Jugé does not allow the synthesis of (*S*)-**118**.

As a concluding remark, it has to be said that the free phosphine derived from (*S*)-**118**, **131**, was prepared, in racemic form, more than 30 years ago<sup>129</sup> by simple stepwise nucleophilic substitutions on PhPCl<sub>2</sub>, as it is illustrated in **Scheme 41**.



**Scheme 41.** Preparation of the racemic phosphine **127**.

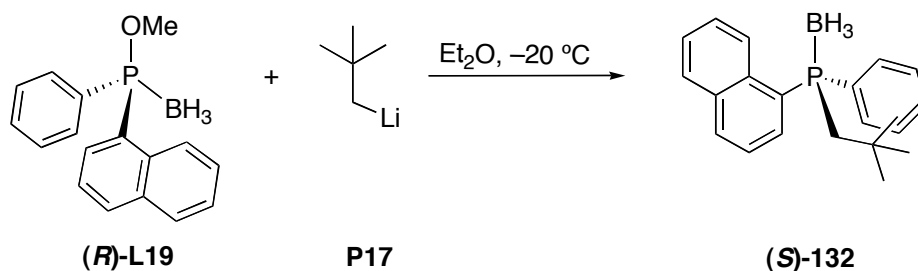
This fact means that the phosphine **131** is completely stable, although its borane adduct can not be prepared from the precursors (*R*)-**L19** or (*R<sub>p</sub>*)-**L8**.

After all the unsuccessful efforts described in this section, the synthesis of (*S*)-**118** was finally abandoned.

### 9.2.3. Introduction of $\phi, \phi, \phi$ -trisubstituted groups

#### 9.2.3.1. Introduction of the neopentyl group

Given the impossibility of introducing a <sup>t</sup>Bu group in (*R*)-**L19**, the next attempt was the introduction of a neopentyl (2,2-dimethylpropyl) group, which would have a methylene spacer between the phosphorus atom and the <sup>t</sup>Bu moiety. **Equation 40** illustrates such a reaction.



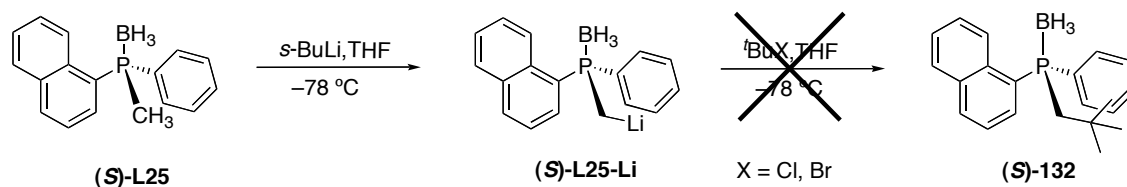
**Equation 40.** Attempted synthesis of (*S*)-**132**.

Neopentyllithium, **P17**, was prepared as detailed in section 7.2.2. The reaction was carried out under usual conditions –in Et<sub>2</sub>O at –20 °C– and was monitored by <sup>31</sup>P{<sup>1</sup>H} NMR spectroscopy. Stoichiometric ratio between (*R*)-**L19** and **P17** resulted in no conversion at all. Excess of organolithium reagent (up to 3 equivalents) were added and the <sup>31</sup>P{<sup>1</sup>H} NMR spectrum recorded again. In this case, no starting (*R*)-**L19** was detected, but several peaks between  $\phi = 10$  ppm and  $\phi = 30$  ppm appeared, some of them with the characteristic broadness and shape of phosphine-borane adducts. The major one, at  $\phi = 18.6$  ppm ( $J_{\text{BP}} = 64.8$  Hz) could

correspond to the desired phosphine because its shift is between (*S*)-**L25** (bearing a methyl group) and (*S*)-**L26** (bearing an isopropyl group). After extractive work-up and extraction, precipitation with pentane afforded a white solid, which was characterized.

The  $^{31}\text{P}\{^1\text{H}\}$  NMR spectrum looked satisfactory, with the single peak at  $\delta = 18.6$  ppm. The  $^1\text{H}$  NMR spectrum, however, was much more complicated than it would be expected for (*S*)-**L26**. Apart from the aromatic part, there was a complex pattern of signals between  $\delta = 2.1$  ppm and  $\delta = 2.6$  ppm and another set between  $\delta = 1.2$  ppm and  $\delta = 1.5$  ppm. Moreover, a sharp singlet at  $\delta = 0.85$  ppm was also present. The integration was approximately 2:4:9 respectively. The singlet could certainly account for the 9 H atoms of the neopentyl group, but neither the integration nor the pattern of the other signals fit with the structure of (*S*)-**L26**. Attempts to purify the white solid were made, but the same  $^1\text{H}$  spectrum was found. It was finally not possible to discern whether a pure product different to (*S*)-**L26** was obtained or whether (*S*)-**L26** was obtained but impurified with some unknown substance. For this reason and given the low yield obtained (< 20%, if the white solid was pure (*S*)-**L26**), the strategy was abandoned. At this point, it seems clear that with the precursor (*R*)-**L19** the bulkier group that can be attached to the phosphorus atom without problem has, approximately, the size of isopropyl.

Pursuing in the interest to obtain (*S*)-**L26**, another different approach was conceived, based on the deprotonation of (*S*)-**L25** and quenching of the anion (*S*)-**L25-Li** with *tert*-butyl halide to obtain the desired neopentylphosphine-borane (*S*)-**L26**, as shown in **Scheme 42**.



**Scheme 42.** Attempt to prepare (*S*)-**L26** starting from (*S*)-**L25**.

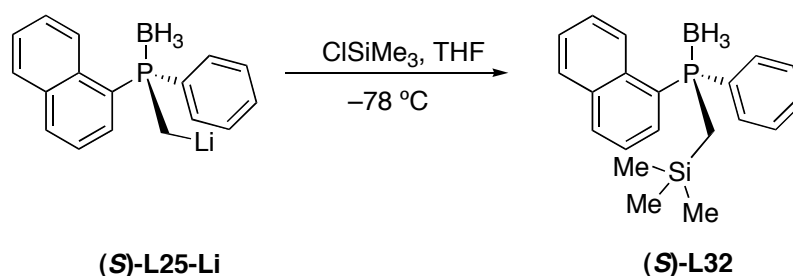
Deprotonation of the methyl group occurred smoothly (section 9.2.3.2), but the anion (*S*)-**L25-Li**, when made react with the *tert*-butyl halide, only furnished unchanged (*S*)-**L25**. This result is presumably due to the fact that  $\text{t-BuX}$  is a tertiary halide and the anion (*S*)-**L25-Li**, in spite of being highly nucleophilic, is also very basic and hence an elimination reaction occurs, yielding isobutene and restoring the initial phosphine-borane (*S*)-**L25**.

After these unsuccessful attempts, the idea of introducing a neopentyl group was discarded. The following section, however, describes the successful introduction of a Si-analogue of the neopentyl group.



### 9.2.3.2. $\phi$ -silylation of (*S*)-L25

The  $\phi$ -carbanion (*S*)-L25-Li, should be highly nucleophilic, although it did not show this character in the reaction of **Scheme 42**, because  $\text{}^t\text{BuX}$  is a bad substrate to perform nucleophilic substitutions. Going one step further,  $\text{}^t\text{BuX}$  was changed by its silicon analogue, chlorotrimethylsilane, because this compound is not prone to elimination as  $\text{}^t\text{BuX}$  is. With this change, the reaction went smoothly to the desired  $\phi$ -trimethylsilyl functionalized phosphine, (*S*)-L32, as illustrated in **Equation 41**.

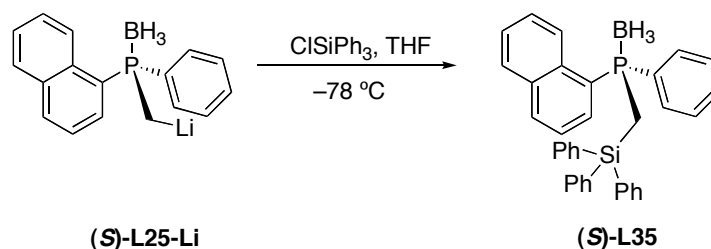


**Equation 41.** Preparation of (*S*)-L32.

In some essays, along with (*S*)-L32, the  $^{31}\text{P}\{^1\text{H}\}$  NMR spectrum showed a signal of the starting methylphosphine-borane (*S*)-L25. This was, however, not a serious problem, because addition of more *sec*-BuLi and then more  $\text{ClSiMe}_3$  displaced the reaction towards the formation of (*S*)-L32. No other products were detected.

These results contrast strikingly with the unsuccessful synthesis of (*S*)-132 by the same procedure and points out the differences existing between the C-Cl and the Si-Cl bonds. The product (*S*)-L32 was obtained as a white solid in a 45% of yield after recrystallization. It was fully characterized, including its crystalline structure, as it will be described in sections 9.7.2.3 and 9.7.4.1.

The straightforwardness in the obtention of (*S*)-L32 prompted us to try the same reaction but with another bulkier chlorosilane. A screening of the commercially available chlorosilanes provided an interesting candidate:  $\text{ClSiPh}_3$ . The reaction was carried out under the same conditions and, as **Equation 42** illustrates, the desired bulky phosphine-borane (*S*)-L35 was obtained as an amorphous white powder.



**Equation 42.** Preparation of (*S*)-L35.

Once more, the  $^{31}\text{P}\{^1\text{H}\}$  NMR spectrum showed only the signal of (*S*)-**L35**. Full characterization of this compound is developed in section 9.7. The yield –19% after recrystallization– was very low, but it could probably be optimized.

### 9.3. Phosphine-boranes bearing a 9-phenanthryl group

#### 9.3.1. Synthesis of (*S*)-**L29**

Following the array of phosphine-boranes to be prepared, listed in **Figure 30**, the synthesis of the phosphine-boranes carrying a 9-phenanthryl group was undertaken.

9-phenanthryl group is very similar to 1-naphthyl, with another fused benzene ring in positions 3-4. The structures and the IUPAC numbering of these two compounds are shown in **Figure 31**.

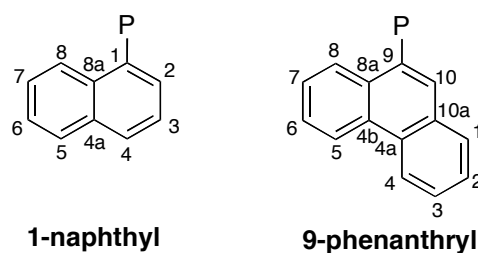
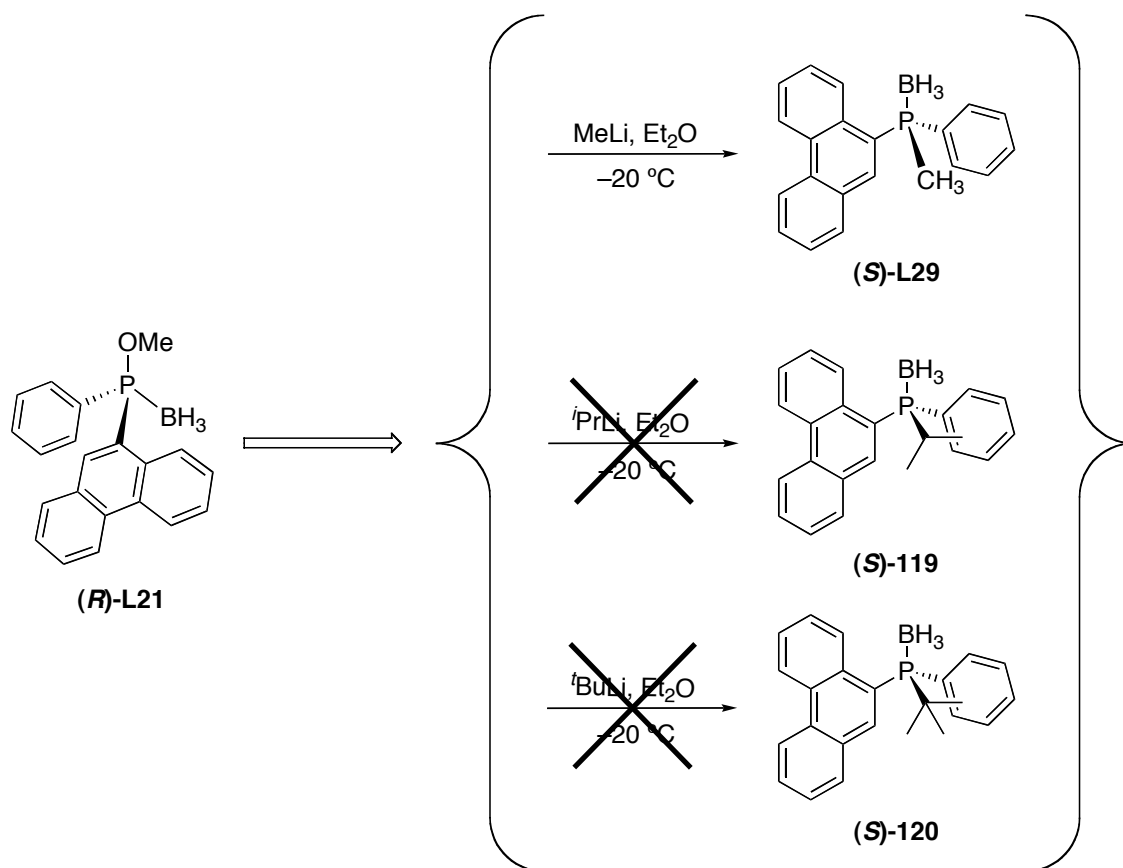


**Figure 31.** Molecular structures and numbering for 1-naphthyl and 9-phenanthryl groups.

Starting from the phosphinite-borane (*R*)-**L21**, the synthesis of the phosphine-boranes (*S*)-**L29**, (*S*)-**119** and (*S*)-**120** was undertaken (**Scheme 43**).



**Scheme 43.** Preparation of phosphine-boranes bearing a 9-phenanthryl group.

A literature inspection revealed that, to the best of our knowledge, only the free phosphine derived from **(S)-L29** has already been reported, albeit in racemic form<sup>132</sup>.

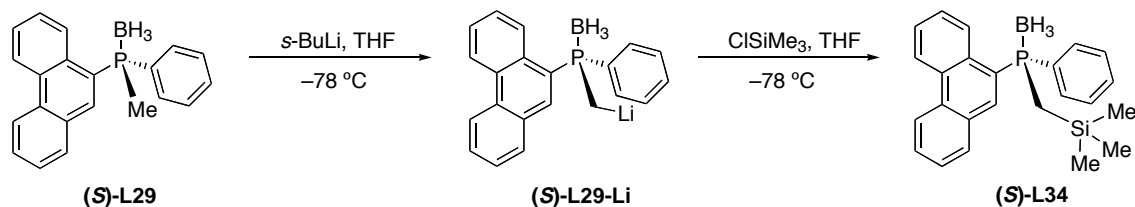
The reactions were carried out under the usual conditions, with a slight excess of organolithium reagent, in Et<sub>2</sub>O at  $-20\text{ }^\circ\text{C}$ . The control of the reaction was done, as usual, by  $^{31}\text{P}\{^1\text{H}\}$  NMR spectroscopy. The phosphine-borane **(S)-L29** was prepared in 45% yield after recrystallization, as a white and amorphous solid, which was fully characterized, including its crystalline structure. Its characterization will be developed in section 9.7.

Although it seemed that the phosphine-borane **(S)-119** had also been prepared, the white solid obtained was, in fact, another unexpected but identified product, which will be described in section 9.3.3.

Regarding the preparation of **(S)-120**, the  $^{31}\text{P}\{^1\text{H}\}$  NMR spectrum showed a wealth of peaks between  $\phi = 0\text{ ppm}$  and  $\phi = 40\text{ ppm}$ , in parallel to the preparation of its naphthyl derivative, **(S)-118** (§ 9.2.2). This result was expected, given the similarity between 1-naphthyl and 9-phenanthryl groups. Having not succeeded in the preparation of **(S)-118**, the synthesis of **(S)-120** was not further pursued.

### 9.3.2. $\phi$ -silylation of (S)-L29

In parallel to the silylation of (S)-L25, developed in section 9.2.3.2, the same reaction was attempted with (S)-L29 with chlorotrimethylsilane, as it is rendered in **Scheme 44**.



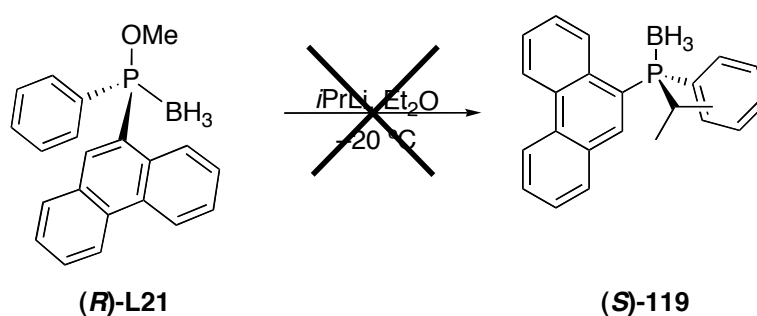
**Scheme 44.**  $\phi$ -silylation of (S)-L29 to furnish (S)-L34.

The reaction was clean towards the formation of the desired phosphine-borane (S)-L34, which was obtained, after recrystallization, in a 50% yield (unoptimized). Section 9.7.2.3 describes the characterization of this compound, including its crystalline structure (§ 9.7.4.2).

### 9.3.3. Unsuccessful preparation of (S)-119. Unexpected obtention of rac-L31

#### 9.3.3.1. Introduction

As it has been stated in section 9.3.1, the reaction between (R)-L21 and isopropyllithium does not furnish the expected phosphine-borane (S)-119 (**Equation 43**) but another unexpected product.



**Equation 43.** Unsuccessful synthesis of (S)-119.

The reaction of (R)-L21 with 1.1 equivalents of isopropyllithium in ether at  $-20\text{ }^\circ\text{C}$ , yielded, after 12 hours of stirring at room temperature, a dark brown solution. The  $^3\text{1P}\{^1\text{H}\}$  NMR spectrum of this solution was very clean: it showed a mixture of the starting product

(at approximately  $\phi = 111$  ppm) and a new product, at  $\phi = 10$  ppm. The ratio between them was, approximately, 1:1. It was considered that the peak at  $\phi = 10$  ppm should be the expected phosphine-borane (*S*)-**119** (although it was expected to observe a  $\phi \approx 25$  ppm, similarly to (*S*)-**L26**) and therefore the solution was cooled again and more isopropylolithium was added, until total conversion was achieved. Quenching the solution with water, rather unexpectedly, changed the shift to  $\phi = 26.6$  ppm. Eventually, following the usual work-up procedure described in the experimental section (chapter VII, § 3.5) a white solid was obtained, whose full characterization was undertaken.

$^{31}\text{P}\{^1\text{H}\}$  and  $^{11}\text{B}\{^1\text{H}\}$  NMR spectra were consistent with the expected structure of (*S*)-**119** –by comparison with (*S*)-**L26** (§ 9.7)– but the  $^1\text{H}$  NMR spectrum showed the presence of more peaks than those required for (*S*)-**119**. In principle, it was thought in some kind of impurity bereft of phosphorus, but recrystallizations furnished a product with an identical spectrum.

### 9.3.3.2. Characterization of *rac*-**L31**

Scrutiny of the  $^1\text{H}$  NMR spectrum of the product, –the aliphatic part of it shown in **Figure 32**–, suggested the presence of two isopropyl moieties, as it was deduced from the coupling schemes and integration, the latter shown in lower part of the figure.

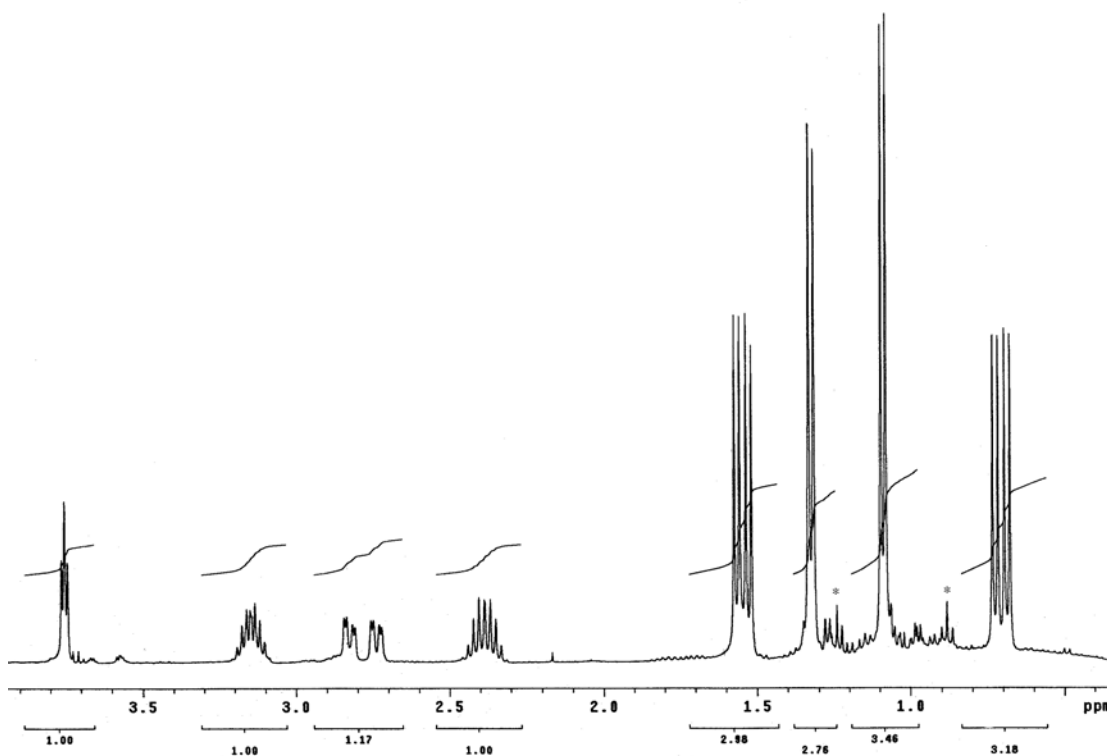


**Figure 32.** Aliphatic part of the  $^1\text{H}$  NMR spectrum (500 MHz,  $\text{CDCl}_3$ , 298 K) of the product resulting from (*R*)-**L21** and isopropylolithium. \*: pentane.

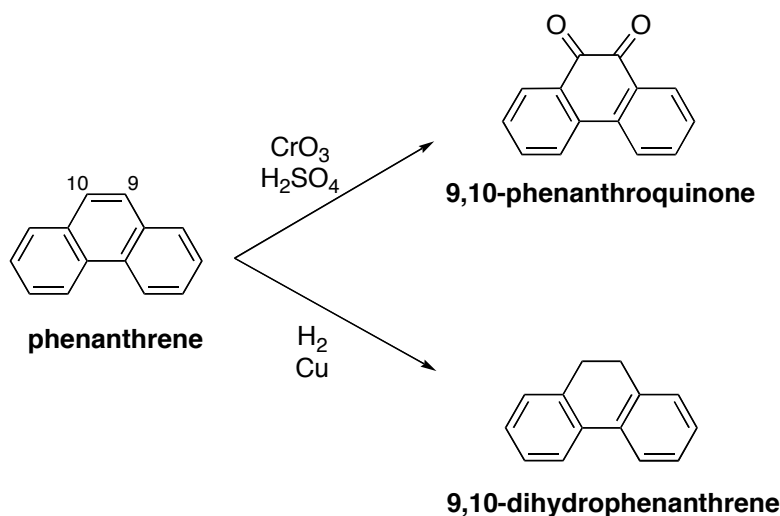
Comparing with (*S*)-**L26**, one of the isopropyl groups should be attached to the phosphorus atom –as it was expected for (*S*)-**119**– because of the doublet of doublets observed pattern. This isopropyl would account for the signals at  $\phi = 0.68\text{--}0.73$  ppm,  $\phi = 1.52\text{--}1.57$  and for one of the multiplets (due to the *CH*) at  $\phi = 2.40$  ppm or  $\phi = 2.75$  ppm. The second isopropyl appeared not to be bonded to the phosphorus atom, because the two methyl groups appeared as doublets at  $\phi = 1.09$  ppm and  $\phi = 1.32$  ppm. The *CH* would correspond to the other multiplet. Where this second isopropyl group was bonded to was no known, but it was conjectured that it might be at the phenanthryl fragment.

Two more sets of signals, with an integration of 1H each, remained unassigned. They constituted a complex pattern (presumably a *ddd*) at  $\phi = 2.75$  ppm and a triplet at  $\phi = 3.75$  ppm.

In order to gain further insight into the structure,  $^{13}\text{C}\{^1\text{H}\}$  DEPT NMR spectrum was recorded. It showed the presence, in the aliphatic region, of four primary and four tertiary carbons. The four  $\text{CH}_3$  were anticipated from the two isopropyls previously deduced, but only two *CH* were expected. These two additional *CH* were the key to assign the structure of the compound.

The two supplementary aliphatic *CH* carbons should come from the 9-phenanthryl or phenyl group after some kind of partial dearomatization reaction, promoted by isopropyllithium. No such reaction had been encountered in the preparation of (*S*)-**L26** with phenyl and 1-naphthyl groups, hence, it was foreseen that the singularity could reside in the particular chemical properties of the phenanthryl group.

It is known, from general organic chemistry<sup>133</sup>, that in phenanthrene the 9-10 bond is much more reactive than the other bonds. **Scheme 45** gives a pair of examples of that regioselective reactivity, both in an oxidation and in a reduction, respectively.



**Scheme 45.** High reactivity of the 9 and 10 positions in phenanthrene.

From that reactivity and the NMR evidences described above, the structure shown in **Figure 33** was proposed, with no regard to stereochemistry, which will be discussed later in this section. The compound, following the usual nomenclature, was labelled as **L31**.

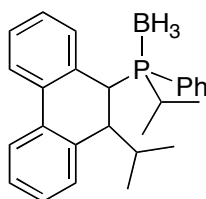


**Figure 33.** Proposed structure for **L31**.

According to the proposed structure, isopropyllithium had provoked the dearomatization (reduction) of the 9-10 bond in phenanthrene, yielding a dialkylphosphine with a 9,10-dihydrophenanthrene substituent at the phosphorus atom. Moreover, the formation of **L31** required one additional H atom. This H atom could come, presumably, from the final quenching with water.

This structure certainly fits with the  $^1\text{H}$ ,  $^{13}\text{C}\{^1\text{H}\}$  and  $^{13}\text{C}\{^1\text{H}\}$ -DEPT NMR data, but more conclusive evidences were needed. With this goal in mind, three different 2D-NMR experiments were performed.  $^1\text{H}$ - $^{13}\text{C}$  HSQC allowed the matching between the C and their respective H;  $^1\text{H}$ - $^1\text{H}$  COSY experiment allowed the deduction of the coupling scheme and finally  $^1\text{H}$ - $^1\text{H}$  NOESY spectrum confirmed the expected structure indicating H-H proximity through space.

These three experiments confirmed the molecular structure of **L31** and allowed the assignation of the resonances in the aliphatic region for both  $^1\text{H}$  and  $^{13}\text{C}\{^1\text{H}\}$  NMR spectra. **Figure 34** shows the numbering scheme used to indicate the different H and C atoms.

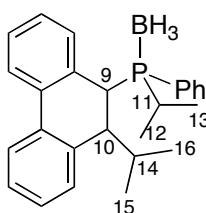


**Figure 34.** Numbering scheme for **L31**.

**Figure 35**, **Figure 36** and **Figure 37** show, respectively,  $^1\text{H}$ - $^{13}\text{C}$  HSQC,  $^1\text{H}$ - $^1\text{H}$  COSY and  $^1\text{H}$ - $^1\text{H}$  NOESY NMR spectra in the aliphatic region of **L31**.

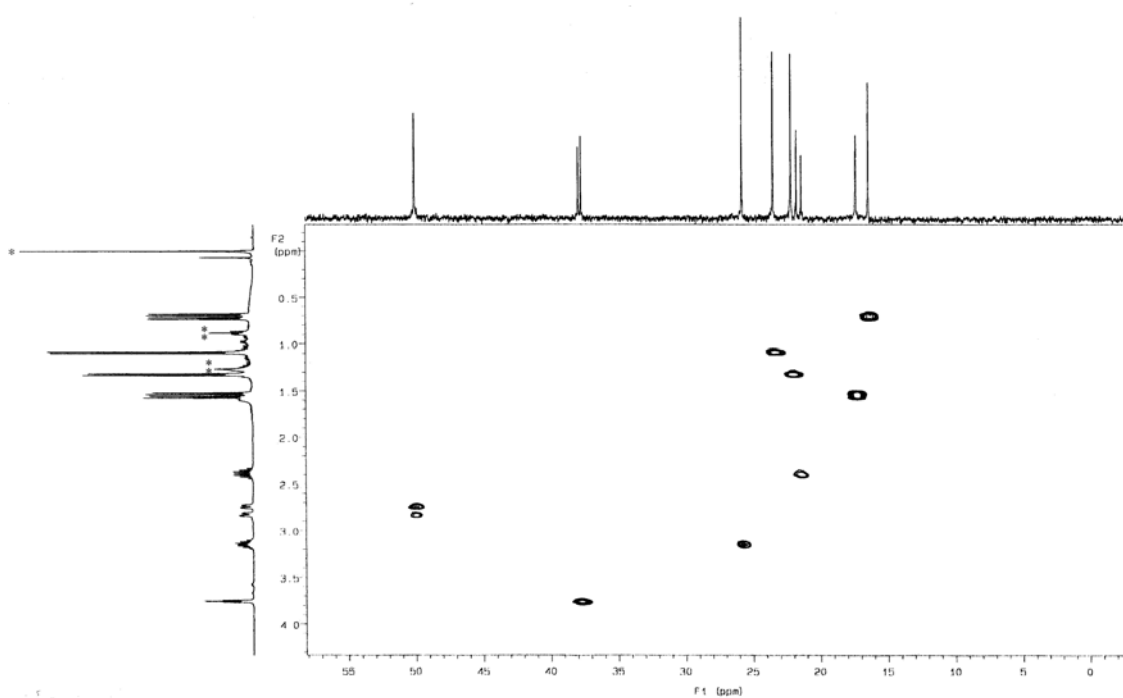


**Figure 35.**  $^1\text{H}$ - $^{13}\text{C}$  HSQC spectrum (400MHz,  $\text{CDCl}_3$ , 298K) of the aliphatic region in **L31**. \*: TMS, \*\*: *n*-pentane.

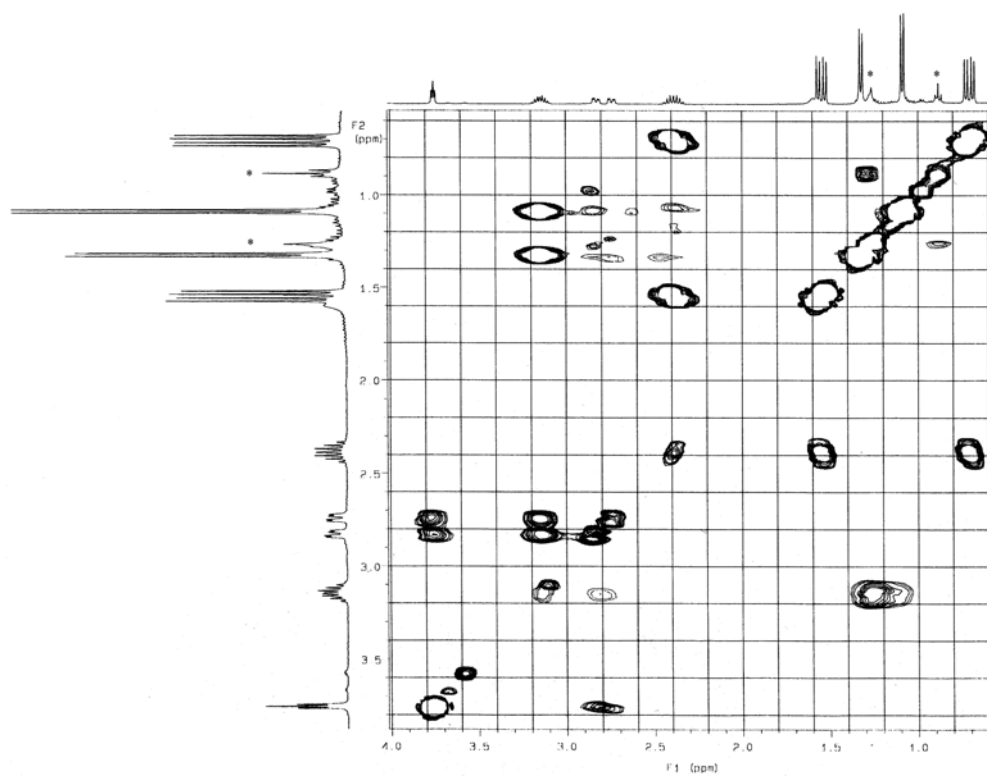


**Figure 36.**  $^1\text{H}$ - $^1\text{H}$  COSY spectrum (400MHz,  $\text{CDCl}_3$ , 298K) of the aliphatic region in **L31**. \*: *n*-pentane.



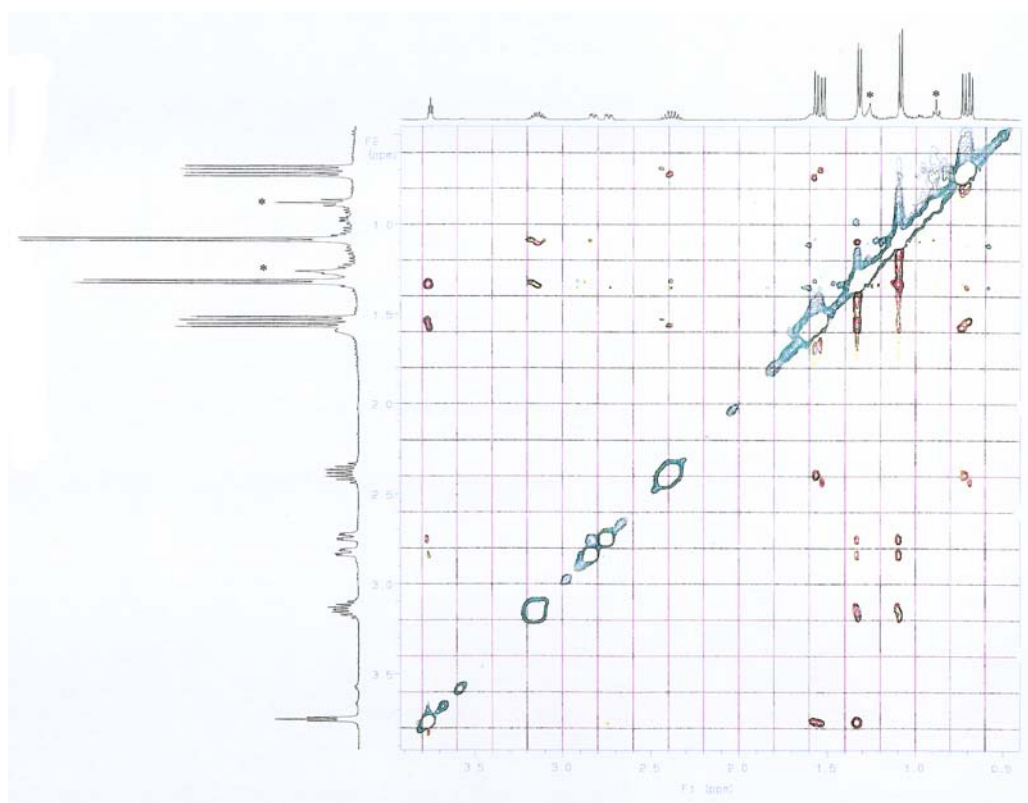


**Figure 37.**  $^1\text{H}$ - $^1\text{H}$  NOESY spectrum (400MHz,  $\text{CDCl}_3$ , 298K) of the aliphatic region in **L31**. \*: *n*-pentane.

Several data of this new compound **L31** is gathered in **Table 17**.

$^{11}\text{B NMR}^{\text{a,b}}$	$^{31}\text{P NMR}^{\text{a,b}}$	$^1\text{H NMR}^{\text{b}}$	$^{13}\text{C NMR}^{\text{a,b}}$
$\phi(\text{ppm})$	$\phi(\text{ppm})$	$\phi(\text{ppm})$	$\phi(\text{ppm})$
		0.71 ( <i>dd</i> , Me <sub>12</sub> , 15.6, 7.2)	16.4 ( <i>s</i> , C <sub>12</sub> )
		1.09 ( <i>d</i> , Me <sub>15</sub> , 6.4)	23.5 ( <i>s</i> , C <sub>15</sub> )
		1.32 ( <i>d</i> , Me <sub>16</sub> , 6.4)	22.2 ( <i>s</i> , C <sub>16</sub> )
		1.55 ( <i>dd</i> , Me <sub>13</sub> , 15.2, 6.8)	17.3 ( <i>d</i> , C <sub>13</sub> , 2.3)
-42.8 ( <i>d</i> , 38.0)	26.6 ( <i>d</i> , 44)	2.35-2.40 ( <i>m</i> , H <sub>11</sub> )	21.6 ( <i>d</i> , C <sub>11</sub> , 36.6)
		2.78 ( <i>ddd</i> , H <sub>10</sub> , 34.8, 10.8, 3.2)	50.1 ( <i>d</i> , C <sub>10</sub> , 3.1)
		3.12-3.18 ( <i>m</i> , H <sub>14</sub> )	25.8 ( <i>d</i> , C <sub>14</sub> )
		3.75 ( <i>t</i> , H <sub>9</sub> , 4.0)	37.8 ( <i>d</i> , C <sub>9</sub> , 19.8)

<sup>a</sup>: Proton decoupled.

<sup>b</sup>: Multiplicities and coupling constants (in Hertz) given in brackets. Acquisition conditions given in experimental part (Chapter VII, § 3.5).

**Table 17.** Characterization data for **L31**.

**Table 18** lists the observed NOE and COSY contacts in **L31**.

<i>NOE and COSY contacts between H in L31<sup>a</sup></i>							
$9 \leftrightarrow$		$10 \leftrightarrow$		$11 \leftrightarrow$		$14 \leftrightarrow$	
<i>NOE</i>	<i>COSY</i>	<i>NOE</i>	<i>COSY</i>	<i>NOE</i>	<i>COSY</i>	<i>NOE</i>	<i>COSY</i>
$9 \leftrightarrow 10^{\text{b}}$	$9 \leftrightarrow 10$	$10 \leftrightarrow 15$	$10 \leftrightarrow 14$	$11 \leftrightarrow 12$	$11 \leftrightarrow 12$	$14 \leftrightarrow 15$	$14 \leftrightarrow 15$
$9 \leftrightarrow 13$		$10 \leftrightarrow 16$		$11 \leftrightarrow 13$	$11 \leftrightarrow 13$	$14 \leftrightarrow 16$	$14 \leftrightarrow 16$
$9 \leftrightarrow 15$							

<sup>a</sup>: 400 MHz, CDCl<sub>3</sub>, 298 K. Contacts involving aromatic protons and/or carbons are not listed.

<sup>b</sup>: Very weak.

**Table 18.** Detected NOE and COSY contacts for **L31**.

Inspection of **Table 17** reveals a surprisingly large coupling constant between H<sub>10</sub> and the phosphorus atom: of  $^3J_{\text{H}_{10}\text{-P}} = 34.8$  Hz. This coupling constant is much larger than any other  $J_{\text{PH}}$  in the molecule, including the protons bound to carbons in  $\phi$  to the phosphorus atom.

To corroborate this large coupling constant, a  $^1\text{H}\{^{31}\text{P}\}$  experiment was performed. The resulting spectrum of this experiment is shown in **Figure 38**.

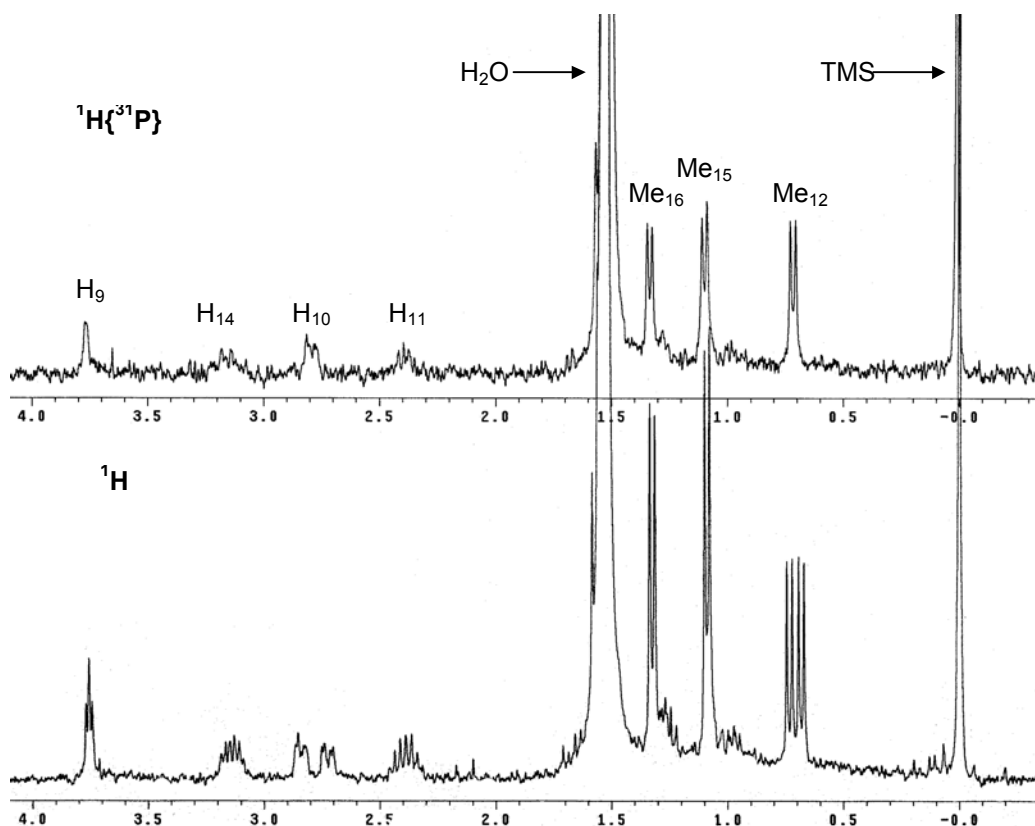


**Figure 38.** Comparison between the  $^1\text{H}$  and the  $^1\text{H}\{^{31}\text{P}\}$  NMR spectra of **L31**, in the aliphatic region. Both spectra were recorded at a field of 300 MHz, in  $\text{CDCl}_3$  and at 298 K.

Although the resolution is rather low, it can be clearly seen that the large coupling in *ddd* of  $\text{H}_{10}$  disappears confirming that the largest coupling constant was due to the phosphorus atom. At the same time, it can be seen how the triplet at  $\phi = 3.75$  ppm ( $\text{H}_9$ ) and the doublet of doublets at  $\phi = 0.71$  ppm ( $\text{H}_{12}$ ) are also simplified.

In order to gain further insight into the mechanism of the formation of **L31**, the preparation of this compound was repeated, but quenching with  $\text{D}_2\text{O}$ . After the usual workup, the expected white solid was obtained and characterized.

The aliphatic region of the  $^1\text{H}$  NMR spectrum is shown in **Figure 39**. It can be compared with the one in **Figure 32**, corresponding to the non-deuterated **L31**.

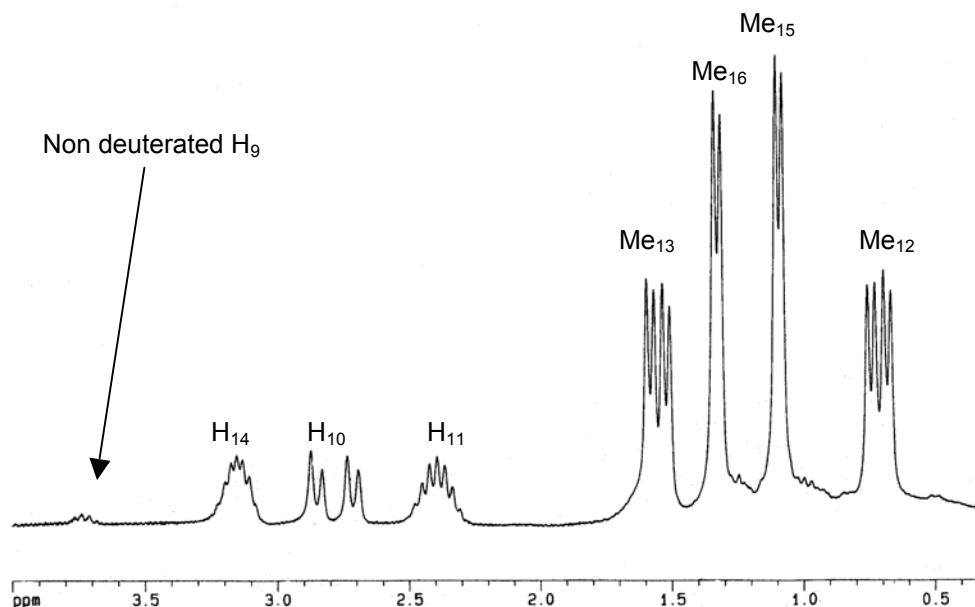


**Figure 39.** Aliphatic region of the  $^1\text{H}$  NMR spectrum (250 MHz,  $\text{CDCl}_3$ , 298K) of **L31-d**.

Comparing the two spectra, only two differences can be detected. **Figure 39** witnesses, firstly, the disappearing of the peak of  $\text{H}_9$ , at  $\phi = 3.75$  ppm (a small peak of  $\text{H}_9$  is visible, due to the small amount of  $\text{H}_2\text{O}$  contained in the  $\text{D}_2\text{O}$ ), and secondly a simplification of the *ddd* at  $\phi = 2.78$  ppm, corresponding to  $\text{H}_{10}$ . In the latter case, just the smallest coupling constant –of 3.2 Hz, *viz.* **Table 17**– vanishes. These results are consistent with the structure resulting from a deuteration at 9-position (numbering in **Figure 34**), giving the **L31-d** product, shown in **Figure 40**.

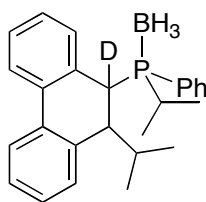
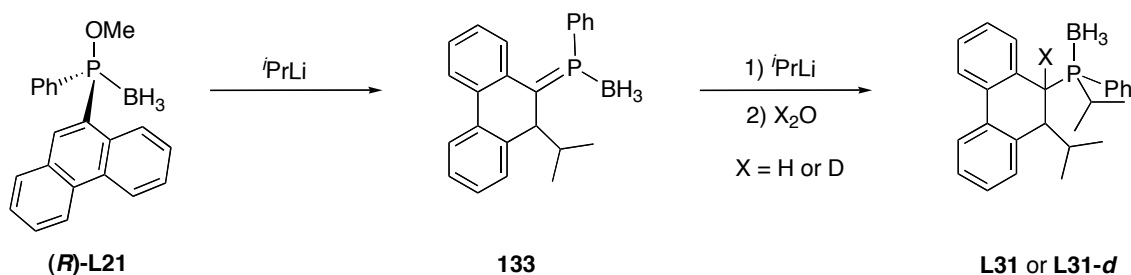


**Figure 40.** Proposed structure for **L31-d**.

The isolation of **L31-d** indicates that after the attack of the two equivalents of isopropylolithium, an anion remains in the –former– 9 position of phenanthrene. This anion captures the necessary hydrogen (or deuterium) atom from the quenching with water or deuterium oxide.

Based on that fact, a mechanism for the formation of **L31** and **L31-d** was suggested, illustrated in **Scheme 46** and compatible with the experimental data.



**Scheme 46.** Suggested mechanism for the formation of **L31** and **L31-d**.

Isopropyllithium initially attacks the 10 position of the phenanthrene moiety –because, presumably, the phosphorus atom is too sterically hindered– yielding the intermediate **133** with a C-P double bond. In this intermediate, which has not been detected, the phosphorus atom has been released of steric hindrance and is readily attacked by isopropyllithium, producing an anion at the 9 position. This anion is then quenched with H<sub>2</sub>O or D<sub>2</sub>O to furnish **L31** or **L31-d** respectively.

This section has given full account of the characterization of **L31**, but the stereochemical aspects of the reaction of formation of this compound remain to be described. The structure of **L31** includes 3 stereogenic centres, that can originate up to 8 different isomers of the compound. From NMR data, however, it seemed clear that no mixtures of diastereomers were formed because these would have given rise to more complicated patterns, at least in <sup>1</sup>H NMR spectrum. It was considered, hence, that **L31** was either enantiomerically pure or a mixture between two enantiomers.

Optical rotation measurements of solutions of **L31** gave values of  $[\phi]_D$  close to zero, pointing out that **L31** was a racemic mixture, named *rac*-**L31**. Final proof of that was given by HPLC analysis on a chiral column, which clearly separated the two enantiomers as can be seen in **Figure 41**.

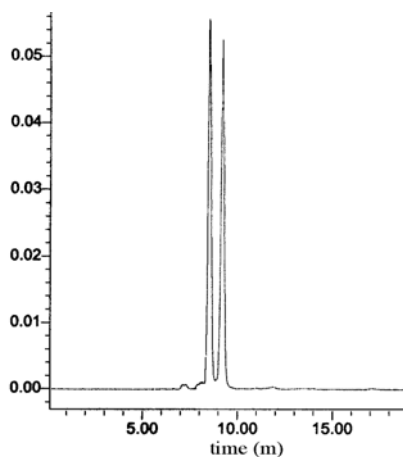


**Figure 41.** HPLC chromatogram showing the two enantiomers of *rac*-**L31**.

It is feasible that the phosphorus racemization is produced in the second nucleophilic attack, assuming a P-C double bond as proposed in **Scheme 46**. The identity of the two enantiomers came after X-ray structure determination, as will be described in the next section.

### 9.3.3.3. Crystalline structure of *rac*-L31

In order to confirm the structure proposed for *rac*-L31, colorless crystals of enough quality for X-ray analysis were grown from dichloromethane/hexane mixtures, at 4 °C.

The unit cell contains one molecule of (*R<sub>p</sub>,S,S*)-L31 and another of (*S<sub>p</sub>,R,R*)-L31, confirming, therefore, that L31 is a racemic mixture. The two molecules have similar structural parameters and only the parameters of (*R<sub>p</sub>,S,S*)-L31 will be discussed here. The molecular structure of (*R<sub>p</sub>,S,S*)-L31 is shown in **Figure 42**. Some hydrogen atoms have been omitted for clarity.

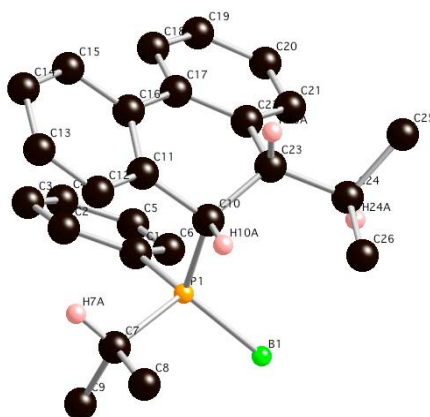


**Figure 42.** Molecular structure of (*R<sub>p</sub>,S,S*)-L31. Arbitrary numbering of the atoms.

The geometry around the phosphorus atom is approximately tetrahedral, with normal P-B and P-C distances. Selected bond distances and angles of this structure, are reported in **Table 19**, following the numbering of **Figure 42**.

<i>Bond</i>	<i>Length (Å)<sup>a</sup></i>	<i>Angle</i>	<i>Value (°)<sup>a</sup></i>
P-B	1.939(5)	C(1)-P(1)-C(7)	103.89(16)
P-C(1)	1.815(3)	C(1)-P(1)-C(10)	109.00(14)
P-C(7)	1.835(3)	C(1)-P(1)-B	111.0(2)
P-C(10)	1.867(3)	C(7)-P(1)-C(10)	103.95(16)
C(10)-C(11)	1.520(4)	C(7)-B-P(1)	110.4(2)
C(10)-C(23)	1.553(4)	C(10)-B-P(1)	117.5(2)
C(23)-C(24)	1.538(4)	C(8)-C(7)-P(1)	112.6(2)
C(16)-C(17)	1.474(5)	C(9)-C(7)-P(1)	110.8(3)
C(7)-C(8)	1.532(4)	C(8)-C(7)-C(9)	110.5(3)
C(7)-C(9)	1.538(5)	C(23)-C(24)-C(25)	109.5(3)
C(24)-C(25)	1.547(4)	C(23)-C(24)-C(26)	112.8(3)
C(24)-C(26)	1.521(4)	C(24)-C(25)-C(26)	108.3(3)
		C(11)-C(10)-C(23)	107.4(3)

<sup>a</sup>: Standard deviations in parentheses.

**Table 19.** Selected bond distances and angles of (*R<sub>p</sub>,S,S*)-**L31**.

The distortion from planarity suffered by the central ring of the phenanthrene, due to the loss of aromaticity and consequent rehybridation, to sp<sup>3</sup>, of the carbons C10 and C23 is easily appreciable in the structure. This fact also causes a twist between the two remaining aromatic rings in the dihydrophenanthrene group. This twist is evidenced by the non negligible dihedral angle (21.69°) defined by the bonds C(22)-C(17) and C(16)-C(11) with respect to the C(16)-C(17) bond. It is also noteworthy the *quasi* eclipsed relative position between the phenyl group at the phosphorus atom and the aromatic ring C(17)-C(22) of the dihydrophenanthrene moiety.

Before finishing this section, an interesting comparison between <sup>1</sup>H NMR data (*viz.* **Table 17**, § 9.3.3.2) and data from the crystalline structure of **L31** can be made.

The crystalline structure of **L31** gives the values of the dihedral angles between H(23A) and H(10A) and between H(23A) and H(24A). With these angles ( $\phi$ ), the well-known Karplus equation<sup>134</sup>, shown in **Equation 44**, allows the estimation of the coupling constant of vicinal protons, provided that the values of A, B and C are known. These values are empirical and close to +7 Hz, -1 Hz and +5 Hz respectively<sup>135</sup>.

$$J_{HH}^3 = A + B \cos \phi + C \cos 2\phi$$

**Equation 44.** Karplus relationship between the vicinal coupling constant and the dihedral angle.

In summary, hence, the coupling constants can be calculated from Karplus equation and compared with those calculated from NMR. With this aim, **Table 20** has been prepared.

<i>Atoms</i> <sup>a</sup>	$\phi$	$J^3$ ( <i>Karplus</i> ) <sup>b</sup>	$J^3$ ( <i>experimental</i> ) <sup>c</sup>
H(10A)-H(23A)	63.534°	3.5 Hz	3.2 Hz
H(23A)-H(24A)	160.877°	11.9 Hz	10.8 Hz

<sup>a</sup>: Numbering scheme shown in **Figure 42**.  
<sup>b</sup>: Calculated from **Equation 44**, taking A = 7 Hz, B = -1 Hz, C = 5 Hz.  
<sup>c</sup>: *viz.* **Table 17**.

**Table 20.** Comparison between calculated and experimental coupling constants in **L31**.

From this table a good degree of agreement can be seen between the calculated and experimental coupling constants, specially in the one between H(10A) and H(23A). This fact can be rationalized because these two protons are in a rigid 6-membered ring, whose structure in solution should not differ substantially from the one in the solid state. The same arguments probably account for the lower than expected coupling constant found between H(23A) and H(24A). The C(23)-C(24) bond of the isopropyl group bearing H(24A) probably rotates freely in solution, making the average dihedral angle between H(23A) and H(24A) inferior to the one listed in **Table 20** and hence producing a lower coupling constant.

## 9.4. Phosphine-boranes bearing a 1-pyrenyl group

After the study of the preparation of phosphine-boranes with 1-naphthyl and 9-phenanthryl groups, the efforts were focused to the phosphine-boranes containing a 1-pyrenyl group. The three aromatic groups are rendered in **Figure 43**.

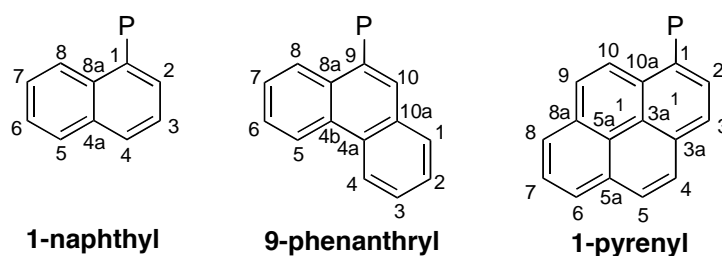
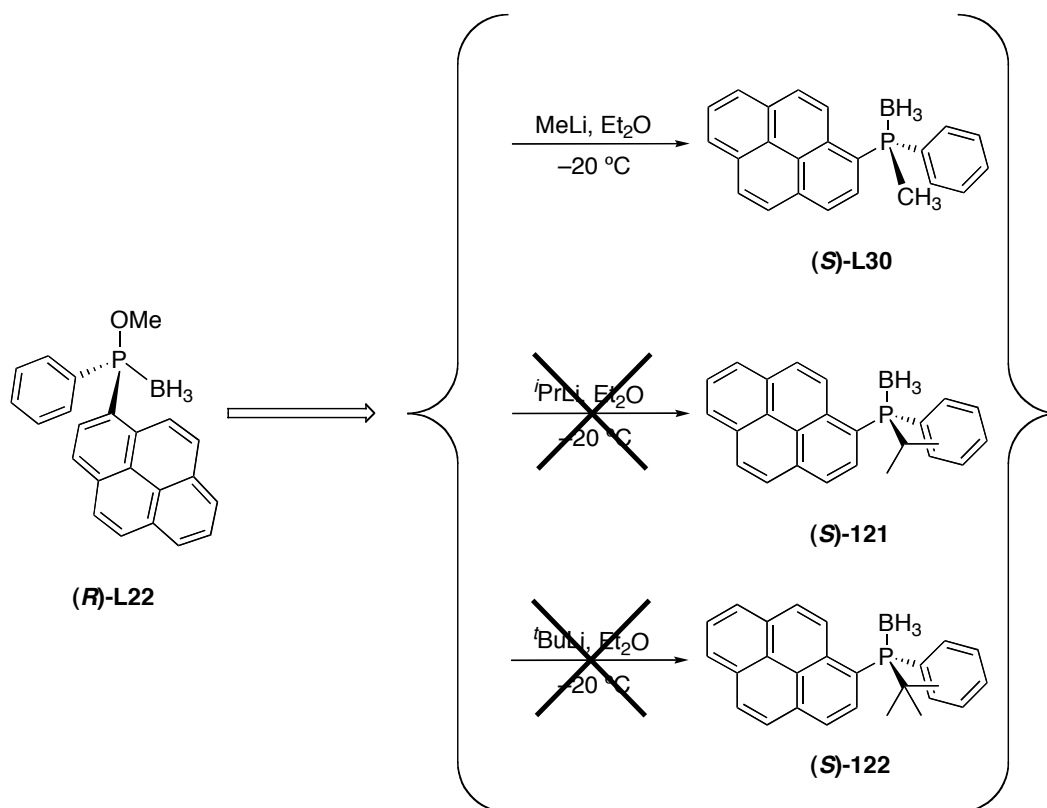


**Figure 43.** Molecular structures and numbering for 1-naphthyl, 9-phenanthryl and 1-pyrenyl groups.

With the introduction of this group, the basic study of a family of *P*-stereogenic phosphines bearing one polycyclic, fused aryl substituent at the phosphorus atom was concluded.



The planned phosphine-boranes to be prepared and the results obtained are summarized in **Scheme 47**.



**Scheme 47.** Preparation of phosphine-boranes bearing a 1-pyrenyl group.

A literature survey revealed that, to the best of our knowledge, none of the phosphine-boranes of **Scheme 47** had been reported, neither their free phosphines.

From the phosphinite-borane **(R)-L22** it was only possible to prepare **(S)-L30** as a bright yellow solid with a 37% of yield after recrystallization. In the other two attempts,  $^{31}\text{P}\{^1\text{H}\}$  NMR spectra only showed the presence of the starting phosphinite-borane **(R)-L22**.

Apparently, hence, the presence of the 1-pyrenyl group at the phosphorus atom in **(R)-L22** seriously hinders the nucleophilic substitution of the methoxy group.

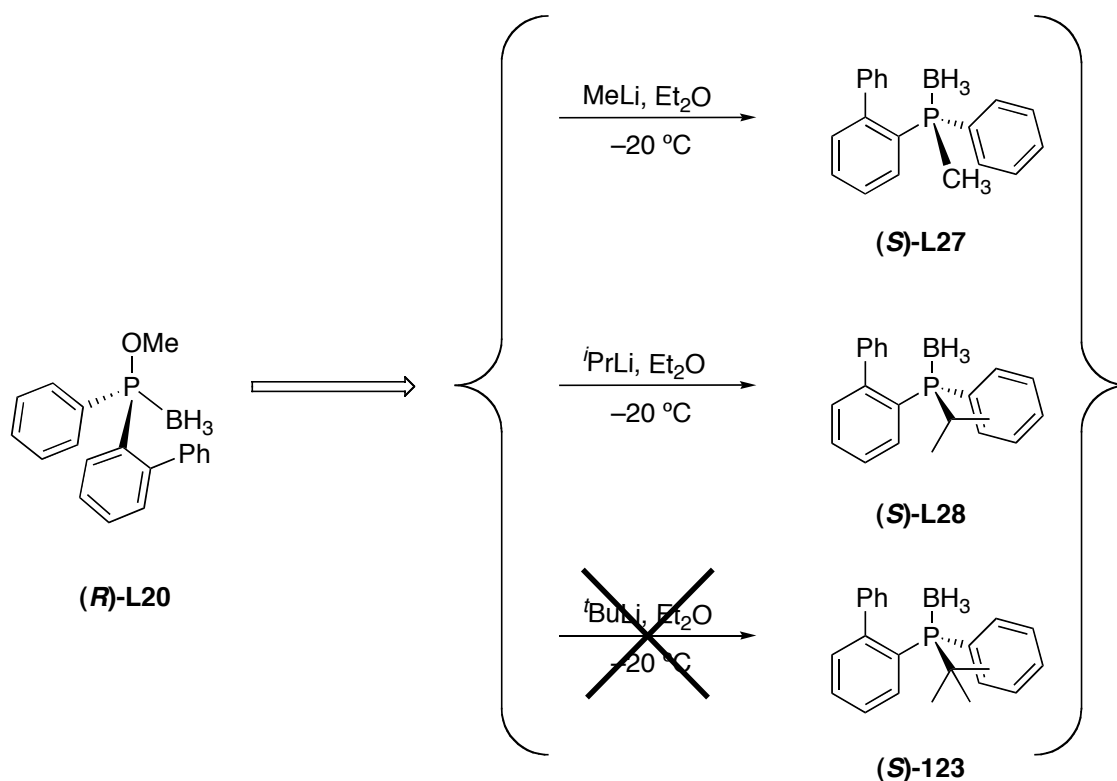
This result brings into line with an increasing bulkiness going from 1-naphthyl to 9-phenanthryl and then to 1-pyrenyl. As reasonable, it has been observed that the bulkier the aryl group, the more difficult the nucleophilic substitution at the phosphorus atom. It has to be noted, however, that other factors –such as the specific degree of aromaticity in each group– may play their role.

## 9.5. Phosphine-boranes bearing a 2-biphenyl group

### 9.5.1. Synthesis of (S)-L27 and (S)-L28

In order to broaden the range of phosphine-boranes available, a family of phosphines bearing a 2-biphenyl group was designed. The choice of this group was made because a literature screening showed that monodentate phosphines possessing a 2-biphenyl group had been employed as effective ligands in asymmetrically catalyzed reactions<sup>136</sup>, such as Pd-catalyzed carbon-carbon bond forming processes. Moreover, Imamoto's group had synthesized *via* menthylphosphinite-boranes— some *P*-stereogenic, biphenyl-containing phosphines, which were found to be good ligands for palladium-catalyzed asymmetric allylic alkylation<sup>136</sup>.

Consequently, the synthesis of the phosphine-boranes shown in **Scheme 48** was undertaken.



**Scheme 48.** Preparation of phosphine-boranes bearing a 2-biphenyl group.

Upon inspection of literature, it was found that phosphine-boranes **(S)-L27** and **(S)-123**; and their derived free phosphines, had already been prepared in enantiomerically pure form by Imamoto<sup>136</sup>. Phosphine-borane **(S)-L28**, and its derived free phosphine, have been, to the best of our knowledge, not reported.

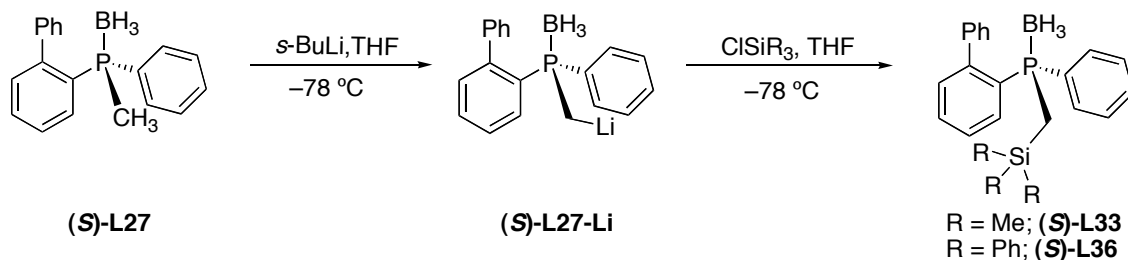
The reactions depicted in **Scheme 48** went smoothly for (*S*)-**L27** and (*S*)-**L28** and these products were isolated as white and crystalline solids with 55% and 31% yields respectively, after recrystallization. Their characterization, including their X-ray structures, is developed in section 9.7.

The introduction of *t*Bu group was again troublesome. In standard conditions, reaction of (*R*)-**L20** with *tert*-butyllithium was sluggish and when a large excess of organolithium reagent was used many products were formed according to the  $^{31}\text{P}\{^1\text{H}\}$  NMR spectrum.

The disappointing experiences encountered before when introducing the *tert*-butyl substituent (§ 9.2.2, 9.3.1 and 9.4) made us abandon the synthesis of (*S*)-**123**. Imamoto, however, succeeded in the synthesis of such a compound, albeit with another totally different procedure<sup>136</sup>.

### 9.5.2. $\phi$ -silylation of (*S*)-**L27**

In parallel to sections 9.2.3.2 and 9.3.2, the  $\phi$ -functionalization of the methylphosphine-borane (*S*)-**L27** was carried out and it is described in **Scheme 49**. The deprotonation of the methyl group in (*S*)-**L27** by *sec*-butyllithium was straightforward and the violet (*S*)-**L27-Li** was detected by  $^{31}\text{P}\{^1\text{H}\}$  NMR spectroscopy.

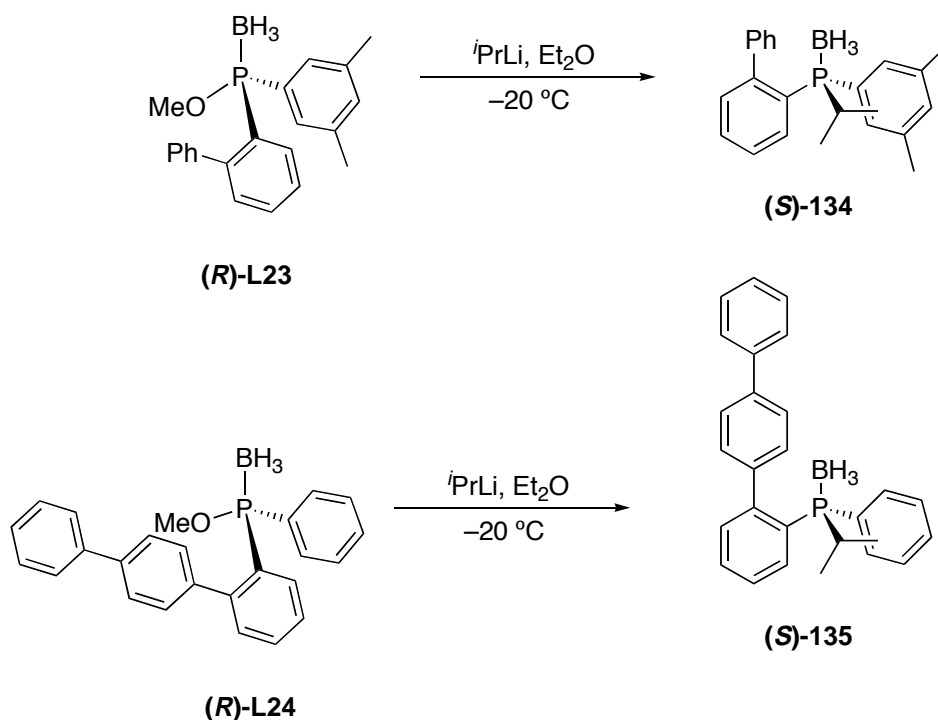


**Scheme 49.**  $\phi$ -silylation of (*S*)-**L27** to furnish (*S*)-**L33** and (*S*)-**L36**.

After quenching this organolithium reagent with a chlorosilane and the usual work-up, the products (*S*)-**L33** and (*S*)-**L36** were isolated as white solids, with 63% and 55% yields respectively, after recrystallization. Their characterization is developed in section 9.7 and in the chapter VII, section 3.6.

## 9.6. Phosphine-boranes bearing other groups

After having prepared the *basic* families of phosphine-boranes presented in **Figure 30** (§ 9.1), it seemed worthwhile the use of the phosphinite-boranes (**R**)-**L23** and (**R**)-**L24** to prepare their derived phosphine-boranes with the isopropyl group, which is –according to what has been described in previous sections– the largest group that can be introduced easily into the phosphorus atom. As a result, the phosphine-boranes (**S**)-**134** and (**S**)-**135**, shown in **Scheme 50**, were prepared.



**Scheme 50.** Synthesis of phosphine-boranes (**S**)-**134** and (**S**)-**135**.

Their synthesis was carried out as usual and, according to  $^{31}\text{P}\{^1\text{H}\}$  NMR spectroscopy, the expected phosphine-boranes were formed with no significant side-products. After work-up, however, the pure solid products could not be precipitated, but yellowish pasty substances were obtained instead. These substances were repeatedly washed with pentane until the  $^{31}\text{P}\{^1\text{H}\}$  and  $^1\text{H}$  NMR spectra showed that the chemical purity was high enough for synthetic purposes. The impurities detected in the  $^1\text{H}$  NMR spectrum are of alkylic type and are probably due to side products formed by isopropyllithium and from other previous steps in the synthesis.

## 9.7. Characterization of phosphine-boranes

### 9.7.1. Introduction

The obtained phosphine-boranes were thoroughly characterized by the usual techniques. These included the usual spectroscopic characterization as well as the determination of the optical purity of the phosphine-boranes, which is key issue to any ligand designed for asymmetric catalysis. Finally, some crystalline structures of these phosphine-boranes were obtained, in order to compare the structures and to check the expected *S* absolute configuration of the phosphorus atom. This section summarizes all this characterization data. The characterization of *rac*-L31 has already been described in sections 9.3.3.2 and 9.3.3.3.

### 9.7.2. Spectroscopic characterization of phosphine-boranes

#### 9.7.2.1. Phosphine-boranes bearing a methyl group

This paragraph is devoted to the spectroscopical characterization of the phosphine-boranes bearing a methyl group, *i.e.* the phosphine-boranes (*S*)-L25, (*S*)-L29, (*S*)-L27 and (*S*)-L30, shown in Figure 44.

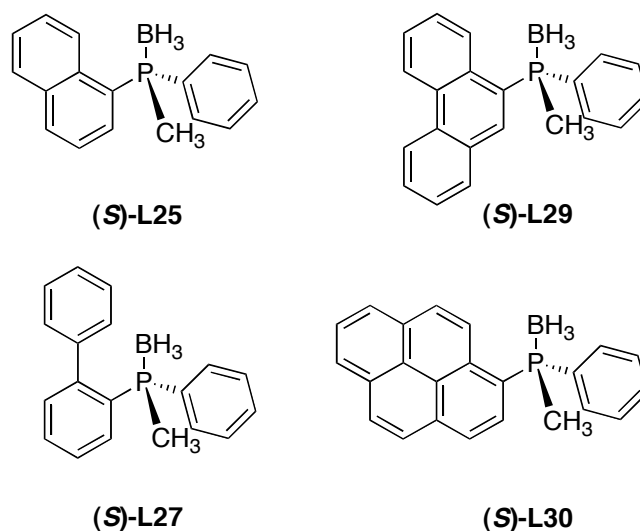


Figure 44. Methylphosphine-boranes prepared.

The IR spectrum of these compounds showed characteristic B-H stretching bands between 2300 cm<sup>-1</sup> and 2400 cm<sup>-1</sup>, along with C-H stretching bands of aryl and alkyl C-H groups.

Regarding to NMR data, the most relevant of it –along with yield and rotatory power– are gathered in **Table 21**.

<i>Compound</i>	<i>Yield</i> (%)	<i><sup>11</sup>B NMR</i>	<i><sup>31</sup>P NMR</i>	<i><sup>1</sup>H NMR</i>	<i><sup>13</sup>C NMR</i>	<i>[φ]<sub>D</sub></i>
		<i>φ(ppm)<sup>a, b</sup></i>	<i>φ(ppm)<sup>a, b</sup></i>	<i>φ(ppm)<sup>b</sup></i> <i>P-CH<sub>3</sub></i>	<i>φ(ppm)<sup>a, b</sup></i> <i>P-CH<sub>3</sub></i>	<i>[φ]<sub>D</sub></i>
<b>(S)-L25</b>	63	-36.3	11.5	2.01	13.0	+46.4°
		( <i>d</i> , 52.5)	( <i>q</i> , 63)	( <i>d</i> , 9.8)	( <i>d</i> , 40.5)	+43.6°
<b>(S)-L29</b>	44	-35.6	10.8	2.12	12.9	+50.2°
		( <i>d</i> , 40.0)	( <i>d</i> , 63)	( <i>d</i> , 9.8)	( <i>d</i> , 40.9)	— <sup>d</sup>
<b>(S)-L27</b>	55	-35.8	13.1	1.43	11.9	+56.6°
		( <i>d</i> , 56.7)	( <i>d</i> , 70)	( <i>d</i> , 10.1)	( <i>d</i> , 41.0)	+54.8°
<b>(S)-L30</b>	37	-35.6	10.6	2.17	13.6	-2.7°
		( <i>d</i> , 40.0)	( <i>d</i> , 65)	( <i>d</i> , 9.9)	( <i>d</i> , 40.9)	— <sup>e</sup>

<sup>a</sup>: Proton decoupled.  
<sup>b</sup>: Multiplicities and coupling constants (in Hertz) given in brackets. Acquisition conditions given in experimental part (chapter **VII**), section **3.5**.  
<sup>c</sup>: Literature value.  
<sup>d</sup>: Value not reported.  
<sup>e</sup>: Compound not reported.

**Table 21.** Relevant characterization data for methylphosphine-boranes.

From the table, it is clear that  $^{11}\text{B}\{^1\text{H}\}$  and  $^{31}\text{P}\{^1\text{H}\}$  NMR spectra do not change considerably from one compound to another. The former shows a doublet near  $\phi = -36$  ppm while the latter constitutes a doublet or a quartet centred near  $\phi = 11$  ppm. Similarly, the methyl group appears as a sharp doublet (coupled to the phosphorus atom) in the  $^1\text{H}$  and  $^{13}\text{C}\{^1\text{H}\}$  NMR spectra, as listed in the table.

Just to illustrate an example, the  $^1\text{H}$  NMR spectrum of (*S*)-**L27** is shown in **Figure 45**.

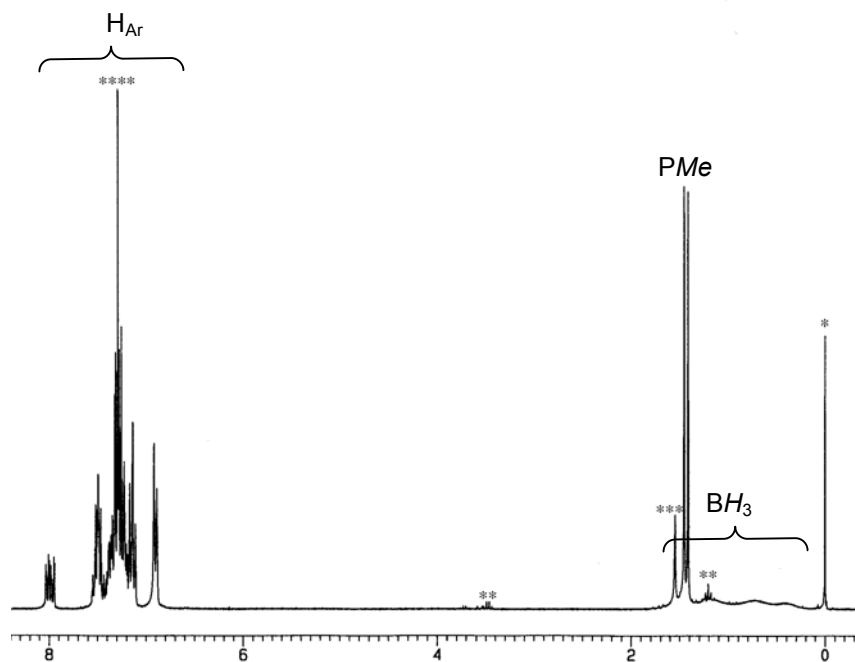


**Figure 45.**  $^1\text{H}$  NMR spectrum (250 MHz,  $\text{CDCl}_3$ , 298K) of (*S*)-**L27**. \*: TMS, \*\*:  $\text{Et}_2\text{O}$ , \*\*\*:  $\text{H}_2\text{O}$ , \*\*\*\*:  $\text{CHCl}_3$ .

### 9.7.2.2. Phosphine-boranes bearing an isopropyl group

This paragraph summarizes the spectroscopic characterization of the isopropyl-containing phosphine-boranes prepared, listed in **Figure 46**.

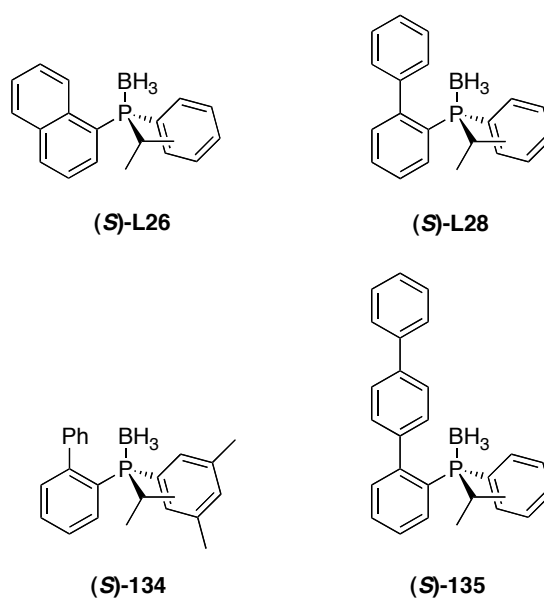


**Figure 46.** Prepared isopropylphosphine-boranes.

Similarly to what has been said in section 9.7.2.1, the IR spectrum of these compounds showed the characteristic B-H stretching bands between 2300 cm<sup>-1</sup> and 2400 cm<sup>-1</sup> along with C-H stretching bands of aryl and alkyl groups. In this case, accordingly to the structure, more C-H stretching bands corresponding to alkyl C-H groups were observed.

A summary of relevant NMR data is listed in **Table 22**. This table is not complete because the compounds (S)-**134** and (S)-**135** were not fully characterized, owing to the fact that they were not obtained as pure products, as described in section 9.6. The alkyl impurities made <sup>13</sup>C{<sup>1</sup>H} NMR spectrum of these two compounds difficult to assign and it was finally not attempted.

Compound	<sup>11</sup> B NMR	<sup>31</sup> P NMR	<sup>1</sup> H NMR			<sup>13</sup> C NMR		
	ϕ(ppm) <sup>a, b</sup>	ϕ(ppm) <sup>a, b</sup>	ϕ(ppm) <sup>b</sup>		ϕ(ppm) <sup>a, b</sup>			
			P- <u>CH</u> (CH <sub>3</sub> ) <sub>2</sub>	P-CH( <u>CH</u> <sub>3</sub> ) <sub>2</sub>	P- <u>CH</u> (CH <sub>3</sub> ) <sub>2</sub>	P-CH( <u>CH</u> <sub>3</sub> ) <sub>2</sub>		
(S)- <b>L26</b>	-39.7 (d, 53.4)	25.6 (d, 66)	2.98 (m, 6.9, 13.8)	1.22 (dd, 7.0, 16.4)	1.26 (dd, 7.0, 16.4)	23.8 (d, 57.4)	17.6 (d, 3.5)	17.7 (s)
(S)- <b>L28</b>	-40.2 (d, 56.2)	26.4 (d, 72)	2.42 (m, 7.0, 13.8)	1.05 (dd, 6.9, 14.2)	1.12 (dd, 6.9, 14.2)	22.3 (d, 35.5)	17.2 (d, 2.7)	17.8 (s)
(S)- <b>134</b>	- <sup>c</sup>	29.8 (d, 85)	2.36-2.45 <sup>d</sup> (m)	1.06 (dd, 7.0, 16.7)	1.13 (dd, 6.9, 13.5)	- <sup>c</sup>	- <sup>c</sup>	- <sup>c</sup>
(S)- <b>135</b>	- <sup>c</sup>	30.2 (s, broad)	2.51-2.70 <sup>d</sup> (m)	1.13 (dd, 6.8, 16.7)	1.17 <sup>d</sup> (dd, 6.6, 15.5)	- <sup>c</sup>	- <sup>c</sup>	- <sup>c</sup>

<sup>a</sup>: Proton decoupled.

<sup>b</sup>: Multiplicities and coupling constants (in Hertz) given in brackets. Acquisition conditions, for (S)-**L26** and (S)-**L28** given in experimental part (Chapter VII), section 3.5.

<sup>c</sup>: Not determined.

<sup>d</sup>: Peaks partially overlapped with others from alkyl impurities.

**Table 22.** Relevant NMR data for isopropylphosphine-boranes.

The data from the table reflects close similarity between the compounds. <sup>11</sup>B{<sup>1</sup>H} and <sup>31</sup>P{<sup>1</sup>H} NMR spectra show a doublet at near ϕ = -40 ppm for the former and at ϕ = 25-30 ppm for the latter. A common feature in all the compounds is that the two methyl substituents of the isopropyl group –which are diastereotopic– appear as distinguishable both in <sup>1</sup>H and <sup>13</sup>C{<sup>1</sup>H} NMR spectra. Interestingly, only the methyl group whose peak appears at higher field was found to be coupled to the phosphorus atom.



Just to show an example, the  $^1\text{H}$  NMR spectrum of (*S*)-**L28** is shown in **Figure 47**.

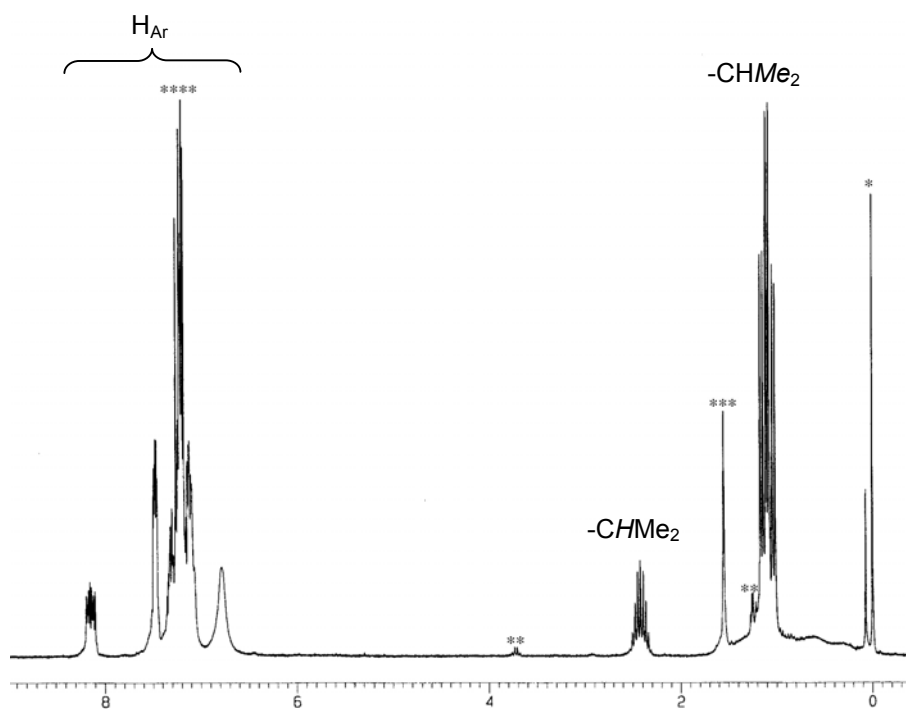


**Figure 47.**  $^1\text{H}$  spectrum (250 MHz,  $\text{CDCl}_3$ , 298K) of (*S*)-**L28**. \*: TMS, \*\*:  $\text{Et}_2\text{O}$ , \*\*\*:  $\text{H}_2\text{O}$ , \*\*\*\*:  $\text{CHCl}_3$ .

### 9.7.2.3. Phosphine-boranes bearing an $\phi$ -silyl group

This paragraph deals with the spectroscopic characterization of the phosphine-boranes bearing a  $-\text{CH}_2\text{SiMe}_3$  or a  $-\text{CH}_2\text{SiPh}_3$  group attached to the phosphorus atom. These compounds are rendered in **Figure 48**.

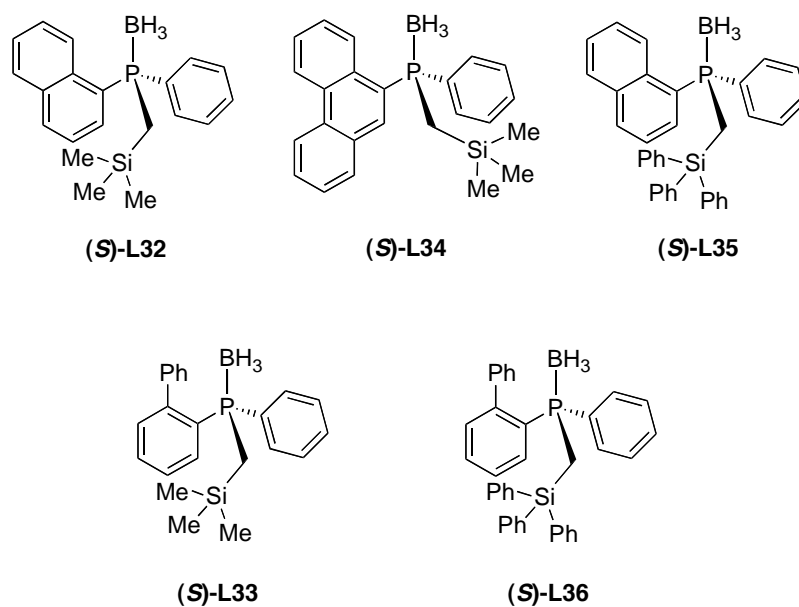


**Figure 48.** Prepared phosphine boranes with an  $\phi$ -silyl group.

The IR spectrum of these compounds confirms the presence of a BH<sub>3</sub> group, which gives stretching bands between 2300 cm<sup>-1</sup> and 2400 cm<sup>-1</sup>.

Regarding the NMR data, apart from <sup>11</sup>B{<sup>1</sup>H} and <sup>31</sup>P{<sup>1</sup>H} NMR  $\phi$  values, the most characteristic of these compounds is the <sup>1</sup>H and <sup>13</sup>C{<sup>1</sup>H} NMR spectrum of the -CH<sub>2</sub>- group.

**Table 23** lists some of the data for the  $\phi$ -silylated phosphine-boranes.

Compound	Yield (%)	<sup>11</sup> B NMR $\phi$ (ppm) <sup>a, b</sup>	<sup>31</sup> P NMR $\phi$ (ppm) <sup>a, b</sup>	<sup>1</sup> H NMR $\phi$ (ppm) <sup>b</sup>		<sup>13</sup> C NMR $\phi$ (ppm) <sup>a, b</sup>
				P-CH <sub>2</sub> -Si		P-CH <sub>2</sub> -Si
(S)-L32	45	-35.5 (d, 57.1)	15.4 (q, 63)	1.72 (pt, 13.7)	1.95	12.4 (d, 25.1)
(S)-L35	19	-34.6 (s, br)	15.2 (d, br)	2.68 (pt, 13.8)	2.87 (pt, 15.8)	9.7 (d, 25.1)
(S)-L34	50	-35.0 (d, br)	15.5 (d, br)	1.80 (pt, 13.5)	2.03 (pt, 16.2)	12.8 (d, 25.0)
(S)-L33	63	-35.3 (d, 54.3)	18.5 (q, 68)	0.90-1.18 (m)		10.0 (d, 24.6)
(S)-L36	55	-34.6 (s, br)	18.0 (s, br)	1.95-2.15 (m)		7.8 (d, 25.4)

<sup>a</sup>: Proton decoupled.  
<sup>b</sup>: Multiplicities and coupling constants (in Hertz) given in brackets. Acquisition conditions given in experimental part (Chapter VII), section 3.6.

**Table 23.** Selected characterization data for the prepared  $\phi$ -silylated phosphine-boranes.

As usual, <sup>11</sup>B{<sup>1</sup>H} <sup>31</sup>P{<sup>1</sup>H} and <sup>13</sup>C{<sup>1</sup>H} NMR  $\phi$  values do not show significant differences among the compounds, only a slight higher value for  $\phi_p$  is found in biphenyl phosphine-boranes (S)-L33 and (S)-L36. The protons in the -CH<sub>2</sub>- group are diastereotopic and hence they are theoretically discernible in <sup>1</sup>H NMR spectrum (anisochrony). This fact is certainly observed in the phosphine-boranes (S)-L32, (S)-L34 and (S)-L35, bearing 1-naphthyl or 9-phenanthryl groups. The coupling constants between the two geminal protons and with the phosphorus atom is in fact similar and as a result, the two H appear as *pseudotriplets*. The diastereotopic nature of the two protons is also manifested by the different coupling constants (anisogamy) to the phosphorus atom they present, except in (S)-L32. Regarding the phosphine-boranes (S)-L33 and (S)-L36, bearing a 2-biphenyl group, the <sup>1</sup>H NMR spectrum in the region of the -CH<sub>2</sub>-Si group presents a complex pattern, attributable to second order effects,

The  $^1\text{H}$  NMR spectrum of (*S*)-L32 and (*S*)-L35 are shown in **Figure 49** and **Figure 50** respectively.

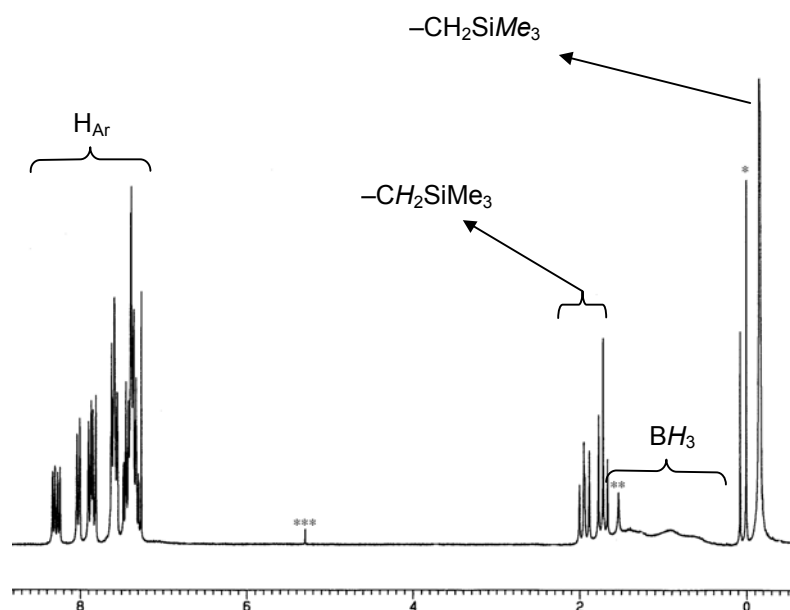


**Figure 49.**  $^1\text{H}$  NMR spectrum (250 MHz,  $\text{CDCl}_3$ , 298 K) of (*S*)-L32. \*: TMS, \*\*:  $\text{H}_2\text{O}$ , \*\*\*:  $\text{CH}_2\text{Cl}_2$ .

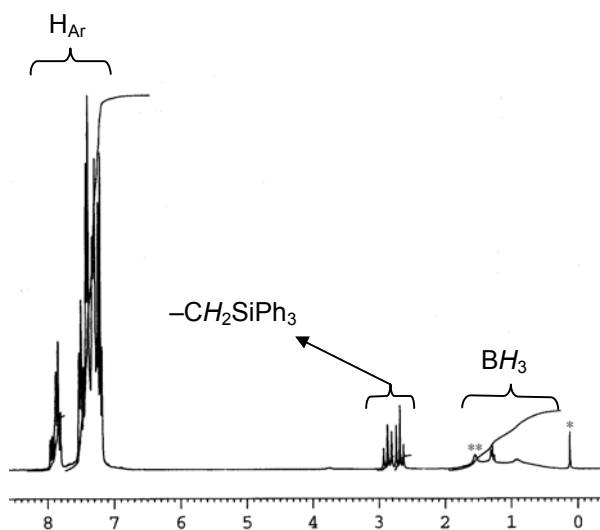


**Figure 50.**  $^1\text{H}$  NMR spectrum (250 MHz,  $\text{CDCl}_3$ , 298 K) of (*S*)-L35. \*: TMS, \*\*:  $\text{H}_2\text{O}$ .

### 9.7.3. Determination of the optical purity of phosphine-boranes

The last sections have been devoted to the spectroscopic characterization of the obtained monophosphine-boranes, confirming the molecular identity of these compounds. This section is devoted to an equally important issue: the assessment of their optical purity.

These *P*-stereogenic phosphine-boranes are the precursors of the *P*-stereogenic phosphines that will be used as ligands in asymmetric catalysis. For this reason, it is crucial to assure that the phosphine-boranes are enantiomerically pure. The method used for the preparation of the ligands, based on the use of (–)-ephedrine as a chiral auxiliary, is known to yield the final phosphine-boranes in very high optical purity. Moreover, the majority of the obtained phosphine-boranes have been recrystallized and hence, presumably, the final products should be enantiomerically pure.

To assess this question, all the obtained phosphine-boranes were subjected to HPLC analysis on a chiral column (except (*S*)-**134** and (*S*)-**135**, which were not obtained pure, *viz.* § 9.6).

In all the cases, the HPLC chromatogram showed only one peak, indicating, in principle, an e.e. greater than 95%. This result demonstrated that the final phosphine-boranes were obtained as enantiomerically pure products, except for *rac*-**L31**, whose special characteristics have been described in detail in section 9.3.3.

A screening in the literature reveals that HPLC analysis is the method of choice to determine the optical purity of phosphine-boranes<sup>54,58,59</sup> (except when the phosphine-borane is not soluble enough in the mobile phase, then alternative approaches are used<sup>58,137,138</sup>).

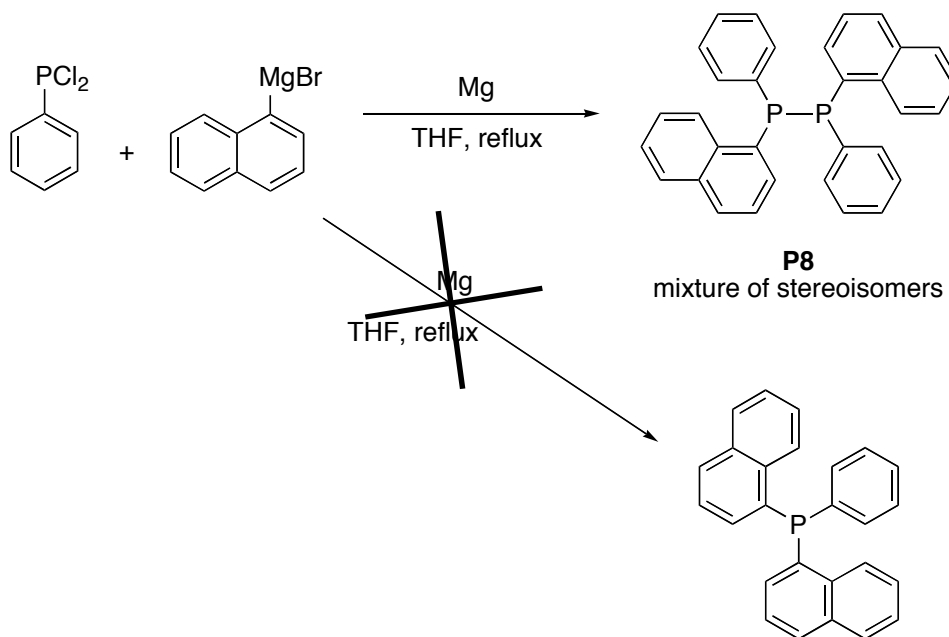
Therefore, it was considered that the optical purity of the prepared phosphine-boranes should be very high.

Notwithstanding, the preparation of one of the phosphine-boranes in racemic form was undertaken, in order to check the correct separation and quantification of the two enantiomers by HPLC.

The efforts were directed towards the preparation of **L26** in racemic form (called *rac*-**L26**) and its analysis by HPLC.

Among the different conceivable ways to prepare *rac*-**L26**, one possibility was the synthesis *via* a P-P diphosphine, a route in which our group had previous experience<sup>35</sup>.

This route comprises two steps. The first of them is the synthesis of *P,P'*-bis(1-naphthyl)-*P,P'*-diphenyldiphosphine, **P8**, as rendered in **Scheme 51**.



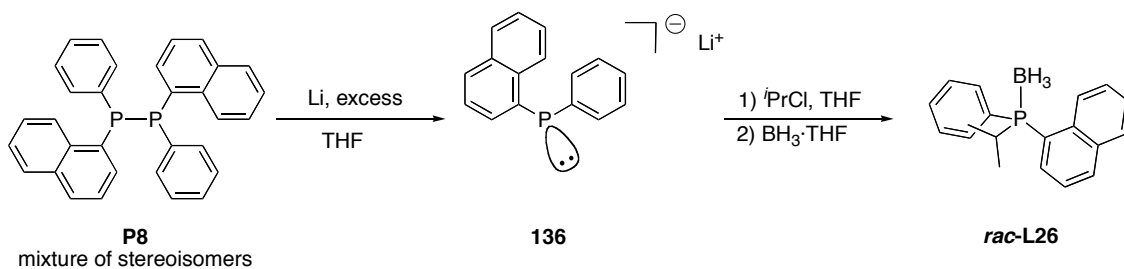
**Scheme 51.** Preparation of **P8**.

The reaction between dichlorophenylphosphine and 1-naphthylmagnesium bromide, in presence of an excess of magnesium, produces the compound **P8** as the only phosphorus product.

The bulky 1-naphthyl group precludes the formation of the expected tertiary phosphine and prevents the cleavage of the P-P bond in **P8** by further organometallic species, stabilizing the diphosphine. This type of reaction had been observed and reported by our group<sup>35</sup> and others<sup>139</sup> when trying to prepare highly crowded phosphines by nucleophilic substitutions at the phosphorus atom.

Compound **P8** is obtained, after recrystallization, as an off-white powder, in a 28% yield. It is moderately stable at air, and was characterized by NMR, EA and IR (chapter **VII**, § 3.1.2).

The second step in the synthesis of *rac*-**L26** is the cleavage of the P-P bond and an electrophilic substitution to yield the phosphine, which is protected with borane. These reactions are shown in **Scheme 52**.



**Scheme 52.** Preparation of (*rac*)-**L26** from **P8**.

Lithium effectively cleaves the P-P bond<sup>35</sup> yielding the strongly coloured phosphide anion **136**. The reaction was monitored by <sup>31</sup>P{<sup>1</sup>H} NMR spectroscopy ( $\phi_{136} \approx -34$  ppm, it appeared as a very broad peak due to the fluxional character of **136**) and was complete after one hour at rt.

This anion smoothly reacted with isopropyl chloride to yield the tertiary phosphine, which was protected with BH<sub>3</sub> to furnish the desired phosphine-borane *rac*-**L26**.

With *rac*-**L26** and (*S*)-**L26** in hand, their HPLC chromatogram were recorded and compared. The two chromatograms are shown in **Figure 51** and **Figure 52** respectively.

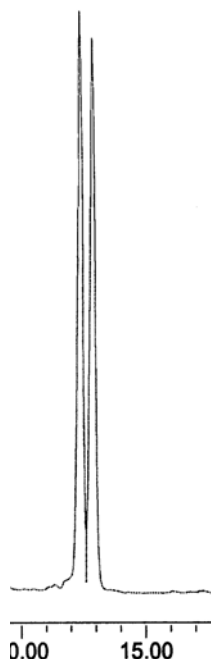


**Figure 51.** HPLC chromatogram of *rac*-**L26**.

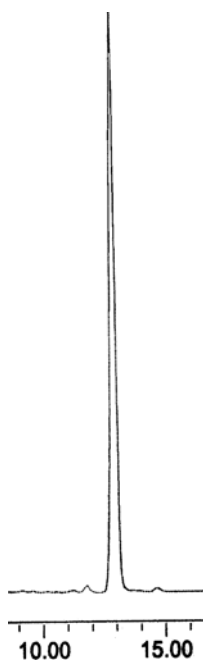


**Figure 52.** HPLC chromatogram of (*S*)-**L26**.

It was clear, hence, that HPLC effectively separated the enantiomers of **L26**. The integration of the chromatogram of *rac*-**L26** implied less than 5% of e.e.

It was assumed that this good separation and quantification was general to all the phosphine-boranes and consequently it was taken for granted that the uncertainty in the quantification by HPLC was  $\pm 5\%$  of e.e. For the same reason, when the HPLC chromatogram showed only one peak, an e.e. greater than 95% was supposed.

#### 9.7.4. Crystalline structures of phosphine-boranes

In order to complete the characterization of the phosphine-boranes, the crystalline structure of some of them was determined by X-ray analysis. The purposes of such determinations were to confirm the expected *S* absolute configuration at the phosphorus atom and to compare the structural parameters of the different phosphine-boranes. This section is devoted to the description of these structures.

### 9.7.4.1. Phosphine-boranes bearing a 1-naphthyl group

Among the phosphine-boranes that bear a 1-naphthyl group, the structure of the silylated phosphine-borane (*S*)-**L32** was determined. Mezzetti<sup>58</sup> had already determined the structure of the parent methylphosphine-borane (*S*)-**L25**. A view of the molecular structure of (*S*)-**L32** is shown in **Figure 53**. The crystals of (*S*)-**L32** were slowly grown from CH<sub>2</sub>Cl<sub>2</sub>/hexane mixtures, at 4 °C.

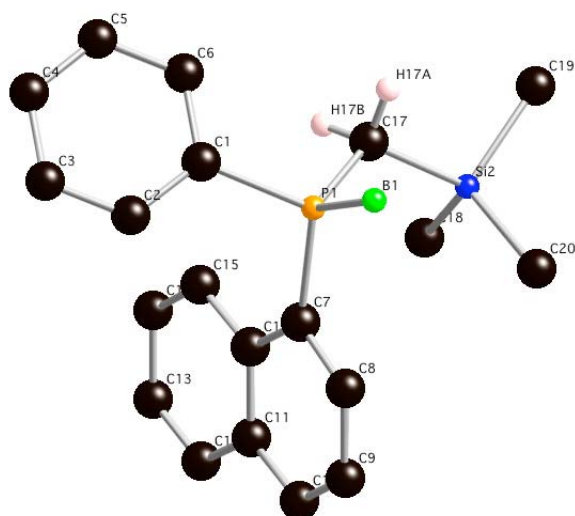


**Figure 53.** Molecular structure of (*S*)-**L32**. Most of the H atoms have been omitted for clarity.

The crystal contains discrete molecules of the phosphine-borane with nonbonded interactions between molecules. The structure confirms the *S* absolute configuration at the phosphorus atom. The distances and angles are normal in comparison with other similar phosphine-borane adducts<sup>52,58,60,140-142</sup>.



**Table 24** lists some selected distances and angles for the phosphine-boranes (**S**)-**L25** and (**S**)-**L32**. The data for (**S**)-**L25** comes from the results reported by Mezzetti.

<b>(S)-L25<sup>b</sup></b>			
<b>Bond</b>	<b>Length (Å)<sup>a</sup></b>	<b>Angle</b>	<b>Value (°)<sup>a</sup></b>
P-B	1.920(4)	C(1)-P-C(7)	104.9(1)
P-C(1)	1.807(3)	C(1)-P-C(17)	103.2(2)
P-C(7)	1.823(3)	C(1)-P-B	115.8(2)
P-C(17)	1.810(4)	C(7)-P-C(17)	106.0(2)
		C(7)-P-B	116.9(2)
		C(17)-P-B	108.9(2)
<b>(S)-L32</b>			
<b>Bond</b>	<b>Length (Å)<sup>a</sup></b>	<b>Angle</b>	<b>Value (°)<sup>a</sup></b>
P-B	1.937(3)	C(1)-P-C(7)	106.25(9)
P-C(1)	1.8285(18)	C(1)-P-C(17)	105.62(9)
P-C(7)	1.831(2)	C(1)-P-B	109.88(11)
P-C(17)	1.814(2)	C(7)-P-C(17)	108.85(10)
C(17)-Si	1.912(2)	C(7)-P-B	113.76(14)
C(18)-Si	1.853(3)	C(17)-P-B	112.01(14)
C(19)-Si	1.855(3)	P-C(17)-Si	122.43(11)
C(20)-Si	1.856(3)		

<sup>a</sup>: Standard deviations in parentheses.  
<sup>b</sup>: The numbering for this phosphine-borane is analogous to the one used in (**S**)-**L32**.

**Table 24.** Selected bond lengths and angles in (**S**)-**L25** and (**S**)-**L32**.

The table shows longer bond distances for (**S**)-**L32** compared to (**S**)-**L25** for the atoms bonded directly to the phosphorus atom, probably due to the increased steric factors in (**S**)-**L32**. For the same reason, the angles C-P-C are greater in (**S**)-**L32** than those in (**S**)-**L25**, whereas the angles C-P-B are smaller. Regarding the length of the Si-C bonds, the Si-C(17) bond is much larger than the other three, due to the bulkiness of the group attached to C(17).

Comparison between the P-B distance of the phosphinite-borane (**R**)-**L22** (**Table 16**, § 8.3) and the P-B distance in either (**S**)-**L25** or (**S**)-**L32** reveals a significantly longer distance in the latter cases. This agrees with the general observation that P-B bond lengths appear to decrease on increasing the electronegativity of the substituents at the phosphorus atom<sup>143-145</sup>.

### 9.7.4.2. Phosphine-boranes bearing a 9-phenanthryl group

This paragraph describes the crystalline structures of (*S*)-**L29** and (*S*)-**L34**, the two phosphine-boranes that bear a 9-phenanthryl group, whose structure has been determined. Colourless crystals of both products were slowly grown from CH<sub>2</sub>Cl<sub>2</sub>/hexane mixtures, at 4 °C. In section 9.3.3.3 the structure of *rac*-**L31**, a phosphine-borane bearing a 9,10-dihydrophenanthryl group has already been described.

**Figure 54** shows the molecular structure for (*S*)-**L29**, whereas **Figure 55** does the same for (*S*)-**L34**. In both structures, the numbering is arbitrary.

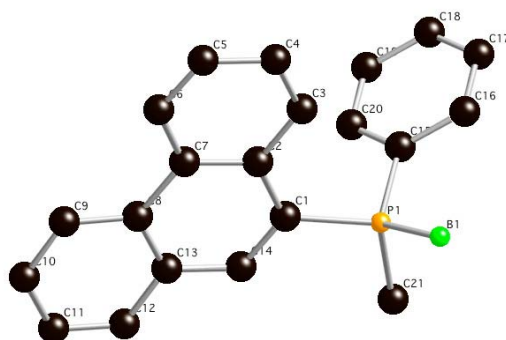


**Figure 54.** Molecular structure for (*S*)-**L29**. Hydrogen atoms have been omitted for clarity.

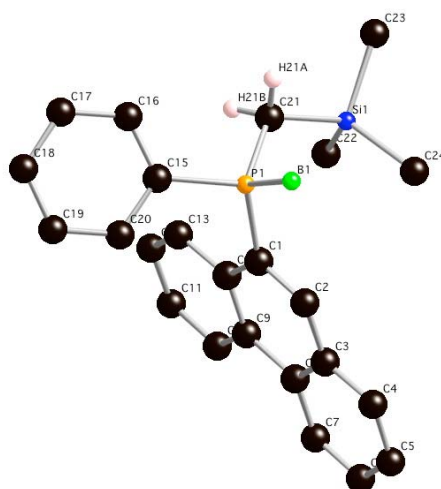


**Figure 55.** Molecular structure for (*S*)-**L34**. Most hydrogen atoms have been omitted for clarity.

In both structures, the expected *S* absolute configuration at the phosphorus atom is confirmed. Both phosphine-boranes show normal bond distances and angles, some of which are listed in **Table 25**.

<i>(S)</i> -L29			
<i>Bond</i>	<i>Length (Å)<sup>a</sup></i>	<i>Angle</i>	<i>Value (°)<sup>a</sup></i>
P-B	1.934(2)	C(1)-P-C(15)	104.66(7)
P-C(1)	1.8139(15)	C(1)-P-C(21)	106.43(8)
P-C(15)	1.8164(17)	C(1)-P-B	115.18(10)
P-C(21)	1.7958(17)	C(15)-P-C(21)	104.61(8)
		C(15)-P-B	117.74(12)
		C(21)-P-B	107.23(11)
<i>(S)</i> -L34			
<i>Bond</i>	<i>Length (Å)<sup>a</sup></i>	<i>Angle</i>	<i>Value (°)<sup>a</sup></i>
P-B	1.915(3)	C(1)-P-C(15)	106.70(9)
P-C(1)	1.813(2)	C(1)-P-C(21)	107.89(10)
P-C(15)	1.813(2)	C(1)-P-B	114.53(11)
P-C(21)	1.801(2)	C(15)-P-C(21)	107.32(9)
C(21)-Si	1.898(2)	C(15)-P-B	108.62(11)
C(22)-Si	1.854(3)	C(21)-P-B	111.44(11)
C(23)-Si	1.850(3)	P-C(21)-Si	121.26(12)
C(24)-Si	1.861(3)		

<sup>a</sup>: Standard deviations in parentheses.

**Table 25.** Selected crystallographic data for *(S)*-L29 and *(S)*-L34.

The comparison between the two structures reveals the same results than the comparison done in section 9.7.4.1 between the structures of *(S)*-L25 and *(S)*-L32. These results show the increased bulkiness of *(S)*-L34 compared to *(S)*-L29.

### 9.7.4.3. Phosphine-boranes bearing a 2-biphenyl group

Suitable crystals for X-ray analysis of (*S*)-**L27** and (*S*)-**L28** were grown from CH<sub>2</sub>Cl<sub>2</sub>/hexane solutions, at 4 °C. The molecular plot of (*S*)-**L27** is given in **Figure 56**, while **Figure 57** renders the molecular plot for (*S*)-**L28**. For both structures, the numbering is arbitrary.

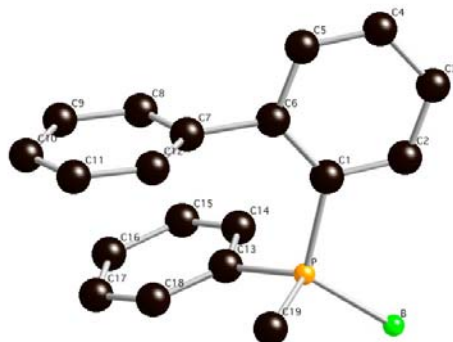


**Figure 56.** Molecular plot of (*S*)-**L27**. Hydrogen atoms have been omitted for clarity.

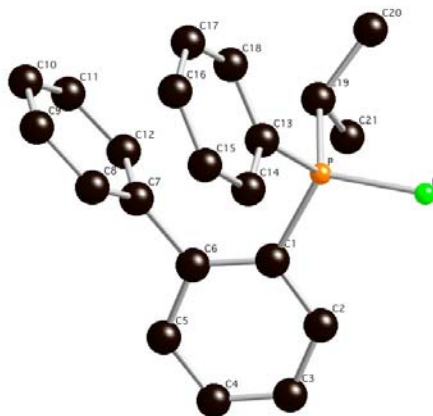


**Figure 57.** Molecular plot of (*S*)-**L28**. Hydrogen atoms have been omitted for clarity.

Both crystals contain the molecules of phosphine-boranes with standard, non-bonded interactions between them. The most relevant distances and angles are listed in **Table 26**.

<i>(S)</i> -L27			
<i>Bond</i>	<i>Length (Å)<sup>a</sup></i>	<i>Angle</i>	<i>Value (°)<sup>a</sup></i>
P-B	1.919(8)	C(1)-P-C(13)	107.1(2)
P-C(1)	1.822(5)	C(1)-P-C(19)	107.5(2)
P-C(13)	1.801(5)	C(1)-P-B	112.5(3)
P-C(19)	1.806(4)	C(13)-P-C(19)	108.2(3)
C(6)-C(7)	1.496(7)	C(13)-P-B	111.8(3)
		C(19)-P-B	109.7(3)
<i>(S)</i> -L28			
<i>Bond</i>	<i>Length (Å)<sup>a</sup></i>	<i>Angle</i>	<i>Value (°)<sup>a</sup></i>
P-B	1.910(3)	C(1)-P-C(13)	106.46(10)
P-C(1)	1.816(2)	C(1)-P-C(19)	107.51(10)
P-C(13)	1.788(2)	C(1)-P-B	112.94(12)
P-C(19)	1.829(2)	C(13)-P-C(19)	108.48(12)
C(6)-C(7)	1.492(3)	C(13)-P-B	109.75(11)
C(19)-C(20)	1.532(3)	C(19)-P-B	111.48(13)
C(19)-C(21)	1.522(4)	C(20)-C(19)-C(21)	109.7(2)
		C(20)-C(19)-P	111.79(17)
		C(21)-C(19)-P	108.42(16)

<sup>a</sup>: Standard deviations in parentheses.

**Table 26.** Selected crystallographic data for *(S)*-L27 and *(S)*-L28.

Both structures present similar structural parameters, with a *quasi* eclipsed disposition of the phenyl group bonded to the phosphorus atom and the phenyl group C(7)-C(12) of the biphenyl fragment. The two phenyl fragments of the biphenyl group are almost perpendicular, as it is deduced from the dihedral angle between the C(5)-C(6) and the C(7)-C(8) bonds. The value of this angle is 96.4° for *(S)*-L27 and 88.8° for *(S)*-L28.

The expected *S* absolute configuration at the phosphorus atom is confirmed by these two structures.

#### 9.7.4.4. Evaluation of the relative steric hindrance of phosphine-boranes

From the crystalline structures, discussed in the preceding paragraphs, it is possible to estimate the relative steric crowding of the phosphine-boranes. This estimation can be done from the mean value among the three values of the BPC angles. In this discussion, it is assumed that, in general, the smaller this mean value is, the higher the steric congestion around the phosphorus atom. From the crystallographic data given in the previous paragraphs, the values of the BPC angles are listed in **Table 27**. This table also gathers the values of the sum of these angles and their arithmetic mean.

<i>Compound</i>	<i>B-P-Ar<sup>a</sup></i>	<i>B-P-Ph</i>	<i>B-P-R<sup>b</sup></i>	<i>Sum</i>	<i>Mean<sup>c</sup></i>
<b>(R)-L22</b>	113.04	110.06	115.54 <sup>d</sup>	338.64	112.88
<b>(S)-L25</b>	116.90	115.80	108.90	341.60	113.87
<b>(S)-L27</b>	112.50	111.80	109.70	334.00	111.33
<b>(S)-L28</b>	112.94	109.75	111.48	334.17	111.39
<b>(S)-L29</b>	115.18	117.74	107.23	340.14	113.38
<b>rac-L31</b>	117.5	111.00	110.40	338.90	112.97
<b>(S)-L32</b>	113.76	109.88	112.01	335.65	111.88
<b>(S)-L34</b>	114.53	108.62	111.44	334.59	111.53

<sup>a</sup>: Ar = 1-naphthyl, 9-phenanthryl, 2-biphenyl or 9-(9,10)-dihydrophenanthryl.

<sup>b</sup>: R = methyl, isopropyl or -CH<sub>2</sub>SiMe<sub>3</sub>.

<sup>c</sup>: Mean = Sum/3.

<sup>d</sup>: B-P-O angle.

**Table 27.** Values of the BPC angles, their sum and their arithmetic mean.

From the table it is possible to order approximately the prepared phosphine-boranes –those whose crystalline structure has been determined– following their relative steric hindrance: **(S)-L27**  $\approx$  **(S)-L28** > **(S)-L34** > **(S)-L32** > **(R)-L22**  $\approx$  **rac-L31** > **(S)-L29** > **(S)-L25**. This order implies that the 2-biphenyl group is, in some sense, bulkier than the other aryl groups, probably due to the high hindrance produced by the phenyl group in the *ortho* position.

## 10. *P*-chirogenic diphosphine-boranes.

### Preparation and characterization

#### 10.1. *Introduction*

The previous section, 9, has dealt with the preparation and characterization of *P*-stereogenic monophosphine-boranes. The derived free monophosphines were used, among other applications, in palladium-catalyzed hydrovinylation of styrene, as it will be described in detail in chapter III. In hydrovinylation, it is mandatory to have a monodentate ligand. In many other catalyzed reactions, however, it has been proved that bidentate phosphines are much better than the corresponding monodentate counterparts, in terms of activity and stereoselectivity. This is the reason of the much larger quantity of diphosphines compared to monophosphines that have been reported over the last decades. Focusing on *P*-stereogenic phosphines, the most prominent member, DIPAMP, was prepared long time ago as it was pointed out in Part I. The last decades have witnessed the outburst of many other *P*-chirogenic diphosphines, whose synthesis have been accomplished mainly by the use of phosphine-boranes as intermediates.

After having prepared several *P*-stereogenic monophosphine-boranes, it was also found interesting the preparation of some *P*-stereogenic diphosphine-boranes with similar groups at the phosphorus atom but with variation of the bridge between the two P atoms. These diphosphine-boranes, once deboronated, were used in palladium-catalyzed allylic alkylation and compared with the analogous monophosphines.

A literature survey revealed that several groups have been developing new methods for the asymmetric synthesis of *P*-stereogenic diphosphines that fulfil the requirements of easy and large-scale preparation. These new methods rely on phosphine-boranes as synthetic intermediates. They are crystalline, chemically and configurationally stable even under vigorous reaction conditions, and easily converted into the free diphosphines by reaction with an amine. For these reasons, borane adducts appear to be particularly versatile intermediates and were used to prepare *P*-stereogenic diphosphines as it is detailed in this section.

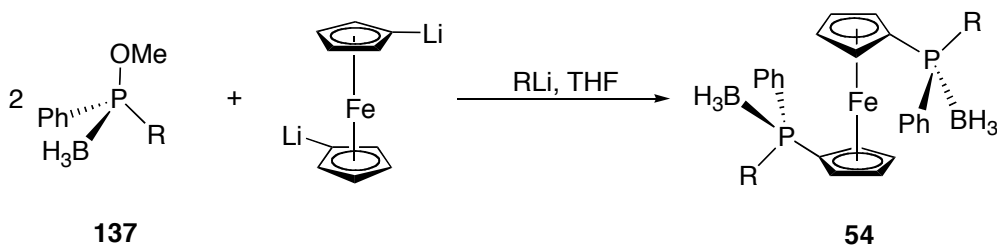
Pursuing in the development of the method of Jugé, two different strategies to prepare *P*-chirogenic diphosphine-boranes were envisaged.

The first conceived strategy was the use of diorganolithium reagents in the method of Jugé, either in the oxazaphospholidine-borane stage or either in the last nucleophilic stage.

The second strategy was the use of the lithiated methylphosphine-boranes already prepared as nucleophilic synthons, whose coupling or quenching with a suitable electrophile would lead to diphosphine-boranes.

## 10.2. Use of dilithium reagents to prepare diphosphine-boranes

The first approach was the use of diorganolithium compounds in the Jugé method to prepare *P*-stereogenic diphosphine-boranes. This idea had already been exploited by Jugé<sup>65</sup>, Mezzetti<sup>75</sup> and van Leeuwen<sup>59,77</sup>, with 1,1'-dilithioferrocene. The dilithium reagent can be reacted with the starting oxazaphospholidine (**R<sub>P</sub>**)-**L1**, but as it was explained in Part I (§ 3.3.4.3) the reaction led to the formation of a mixture of monosubstituted products along with mixtures of diastereomers. Success came with the introduction of 1,1'-dilithioferrocene later in the synthesis, as it was pointed out in Part I, section 3.3.4.4. Equation 45 renders the synthesis of *P*-stereogenic dppf analogues<sup>59</sup>.



R = 1-naphthyl, 2-naphthyl, 2-anisyl, 2-biphenyl, 9-phenanthryl

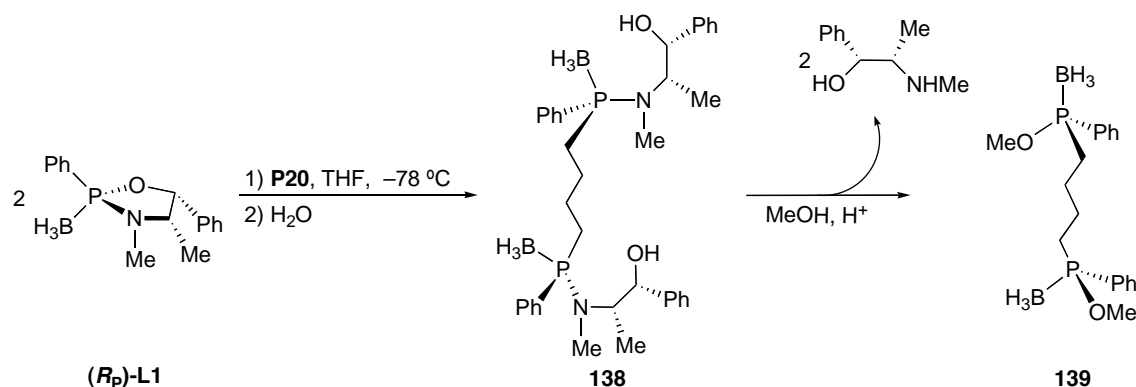
**Equation 45.** Preparation of *P*-stereogenic dppf analogues.

The final diphosphine-boranes **54** were obtained as chemically and optically pure products after column chromatography and recrystallization.

A literature survey revealed that, surprisingly, to the best of our knowledge, no other dilithium reagent has ever been used in conjunction with the method of Jugé to prepare *P*-stereogenic diphosphine-boranes. Consequently, it was found interesting to test whether dilithium compounds **P20** and **P21** (§ 7.2) could be useful in the preparation of diphosphine-boranes bearing a 4 membered bridge between the P atoms.



The starting point was 1,2-dilithiobutane, **P20**. The planned strategy is shown in **Scheme 53**.



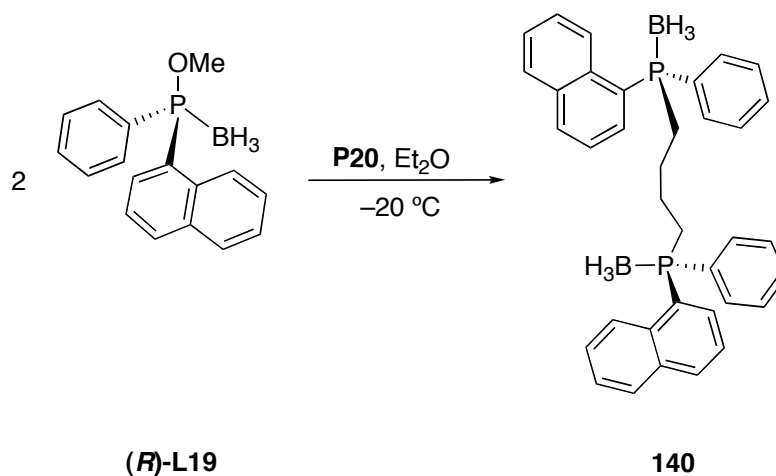
**Scheme 53.** Use of **P20** to prepare diphosphine-boranes.

The reaction of **P20** with **(R<sub>p</sub>)-L1** produced a sticky yellowish substance, showing solely one signal at  $\delta = 69.5$  ppm in the  $^{31}\text{P}\{^1\text{H}\}$  NMR spectrum. The  $^1\text{H}$  NMR spectrum was consistent with the structure of **138** and hence it was subjected to the usual acidic methanolysis. The  $^{31}\text{P}\{^1\text{H}\}$  NMR spectrum of the obtained pasty solid showed the expected quartet at  $\delta = 116.2$  ppm (61%) along with another peak at  $\delta = 96.7$  ppm (39%), of an unidentified product. The  $^1\text{H}$  NMR spectrum showed a complicated pattern (up to six peaks) at  $\delta = 3.50$ - $3.60$  ppm, where the doublet of the Me of the methoxy group was expected.

These results account for the formation of a mixture of products. This mixture is probably composed of the expected diphosphinite-borane **139** along with minor amounts of the monophosphite-borane bearing an *n*-butyl group. This supposed mixture does not account for the complex  $^1\text{H}$  NMR pattern of the methoxy group. Consequently, it was supposed that other species with an OMe group could be present. Among them, it is possible that a mixture of diastereomers of **139** may have formed. The *u* (*meso*) isomer of **139** could, in principle, lead to different  $^1\text{H}$  NMR shift of the OMe groups compared to the *l* isomer.

These results agree with the inconvenience –in terms of stereoselectivity– of reacting the oxazaphospholidine-borane **(R<sub>p</sub>)-L1** with 1,1'-dilithioferrocene encountered by Jugé and van Leeuwen. Due to the uncertainty about the optical purity of **139**, this strategy was abandoned.

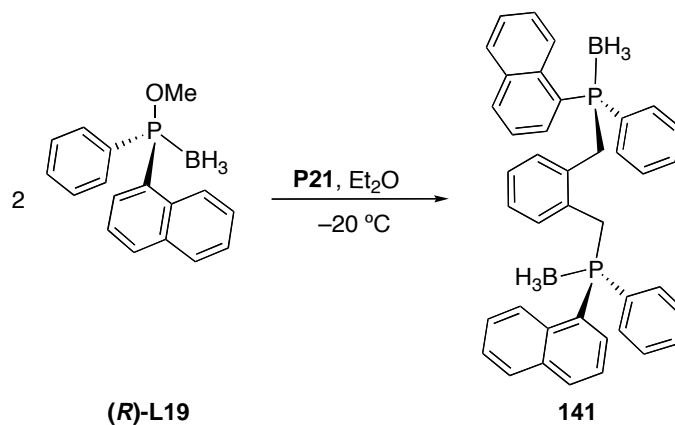
The next attempt was the reaction of **P20** with a phosphinite-borane to render directly the desired diphosphine-borane. Consequently, the reaction depicted in **Equation 46** was attempted.



**Equation 46.** Attempted preparation of **140**.

After stirring overnight, the  $^{31}\text{P}\{^1\text{H}\}$  NMR spectrum of the mixture consisted in starting **(R)-L19** ( $\delta = 112.4$  ppm) and three additional peaks at  $\delta = 16.9$  ppm,  $\delta = 21.0$  ppm and  $\delta = 31.1$  ppm. This mixture of products is probably composed of the desired diphosphine-borane **140** and the product of monosubstitution, along with another unidentified product. All attempts to separate the three products (recrystallization, column chromatography) failed and the strategy was discarded. At this point, it has to be said that Imamoto's team prepared<sup>49</sup> a diphosphine-borane very similar to **140**, with a 4 membered bridge, but with *o*-anisyl instead of 1-naphthyl groups. Their synthetic method, however, was very different to the one in **Equation 46**, and was based, in the key step, in an Ullmann-type coupling.

After this unsuccessful attempt, the reaction was repeated but using the more rigid  $\phi,\phi'$ -dilithio-*o*-xylene, **P21**. The reaction was attempted with the aim of obtaining the diphosphine-borane **141**, as it is rendered in **Equation 47**.



**Equation 47.** Attempted preparation of **141**.

Again, the  $^{31}\text{P}\{^1\text{H}\}$  NMR spectrum showed the formation of a mixture of products. The reaction was very sluggish, and a large quantity of the starting product, **L19** ( $\phi = 112.4$  ppm) was present. Moreover, three additional peaks at  $\phi = 10.4$  ppm,  $\phi = 19.0$  ppm and  $\phi = 27.7$  ppm had appeared as well. In analogy to what has been encountered before, the three products could not be separated and the preparation of **141** was not further pursued.

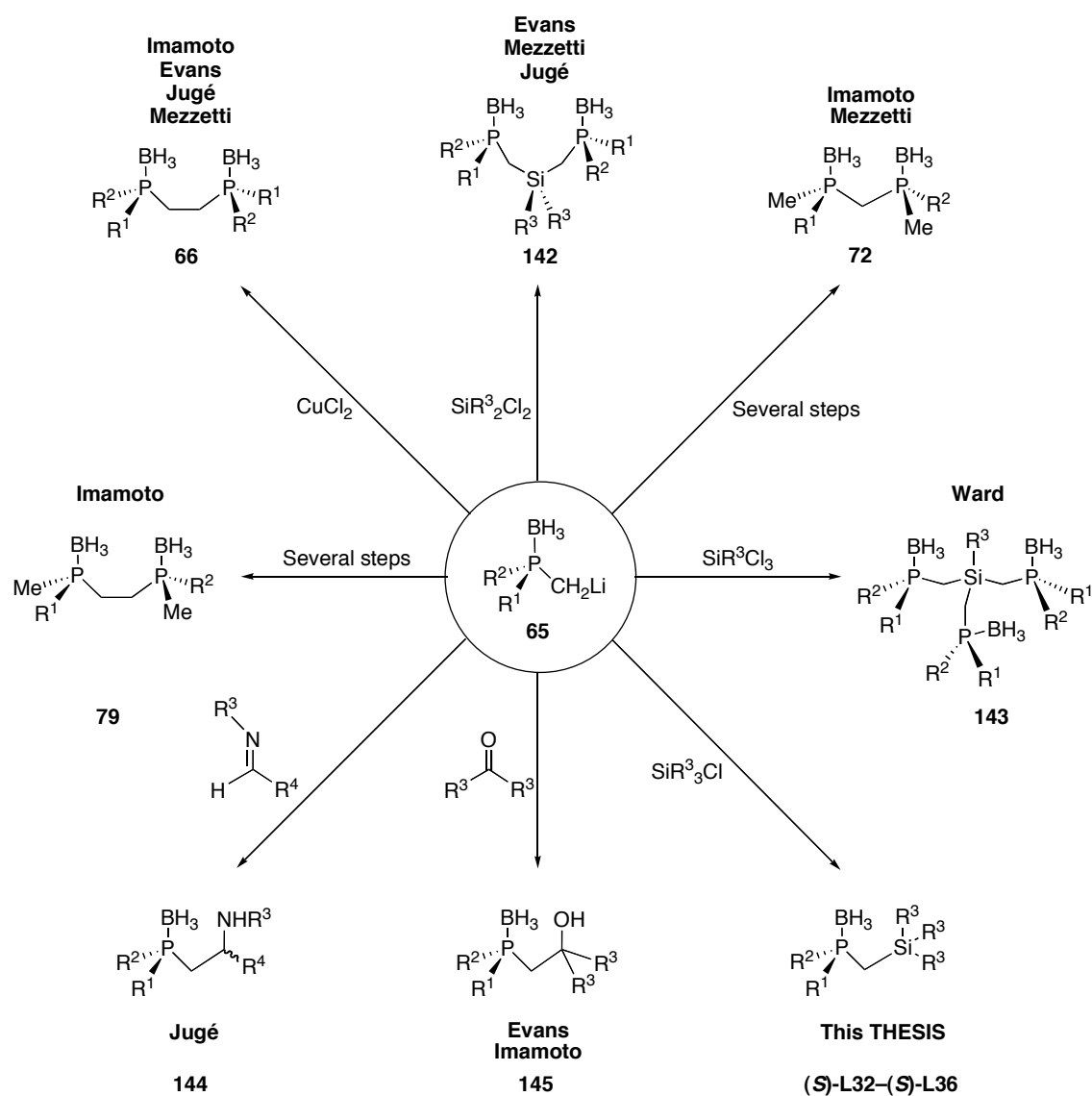
The special structure of 1,1'-dilithioferrocene probably explains its success compared to the unsuccessful performance of **P20** and **P21**.

## 10.3. Use of $\phi$ -deprotonated methylphosphine-boranes

### 10.3.1. Introduction

As it has been stated in Part I (§ 3.3.5.1) and later (§ 9.2.1), the methylphosphine-boranes are readily  $\phi$ -deprotonated by strong bases such as organolithium reagents. The derived carbanions, **65**, are valuable synthons, which have been used in a variety of synthetic transformations, some of them schematized in **Scheme 54**. It has been described in Part I that the optically pure carbanions **65** can be prepared either by deprotonation of *P*-resolved phosphine-boranes or by enantioselective deprotonation of dimethylphosphine-boranes, using (-)-sparteine.

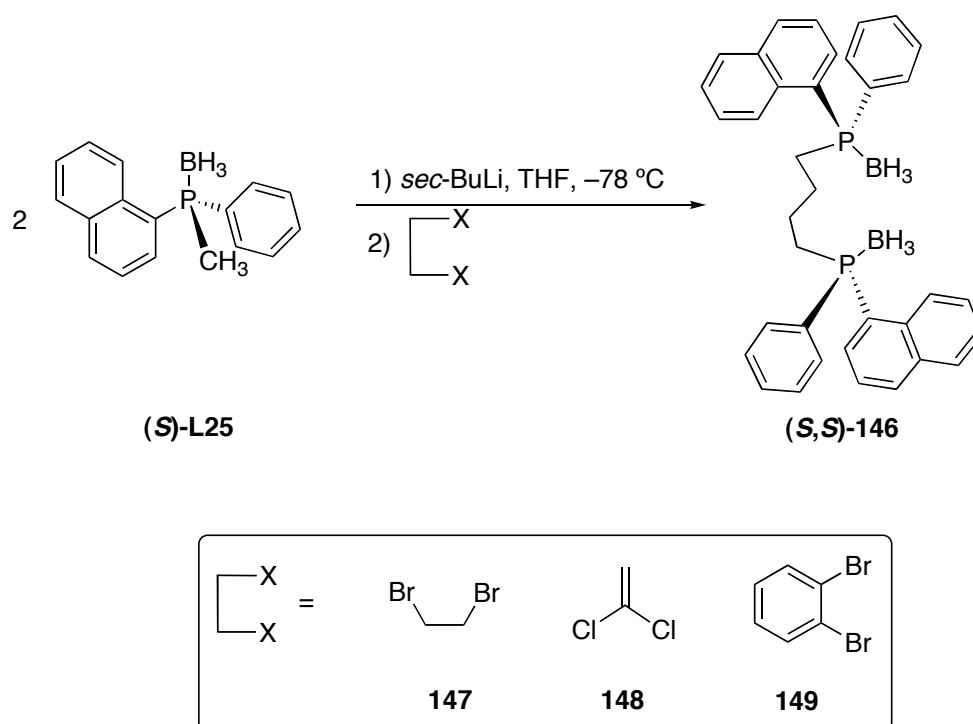
These carbanions have been applied to the preparation of several types of diphosphine-boranes. The synthesis of **66**, **72** and **79** had already been described in Part I, section 3.3.5. Other applications of carbanions **65** are the preparation of the silylated diphosphine-boranes **142**<sup>58,80,86</sup> and a silylated triphosphine-borane **143**<sup>24</sup>. Finally, taking advantage of the nucleophilicity of the anions **65**, the synthesis of the  $\phi$ -functionalized phosphine-boranes **144**<sup>146</sup> and **145**<sup>86,92,93</sup> has been as well reported. Previously (§ 9.2.3.2, 9.3.2 and 9.5.2), the synthesis of the  $\phi$ -silylated phosphine-boranes (*S*)-**L32**–(*S*)-**L36** has already been described.



**Scheme 54.** Various synthetic transformations starting from the *P*-chirogenic carbanions, **65**.

### 10.3.2. Preparation of diphosphine-boranes by nucleophilic attack of carbanions **65**

As a model substrate to perform the first attempts with the carbanions **65**, the phosphine-borane (*S*)-**L25** was selected. As bridges, a variety of dihalogenated substrates, as shown in **Equation 48**, were also chosen.



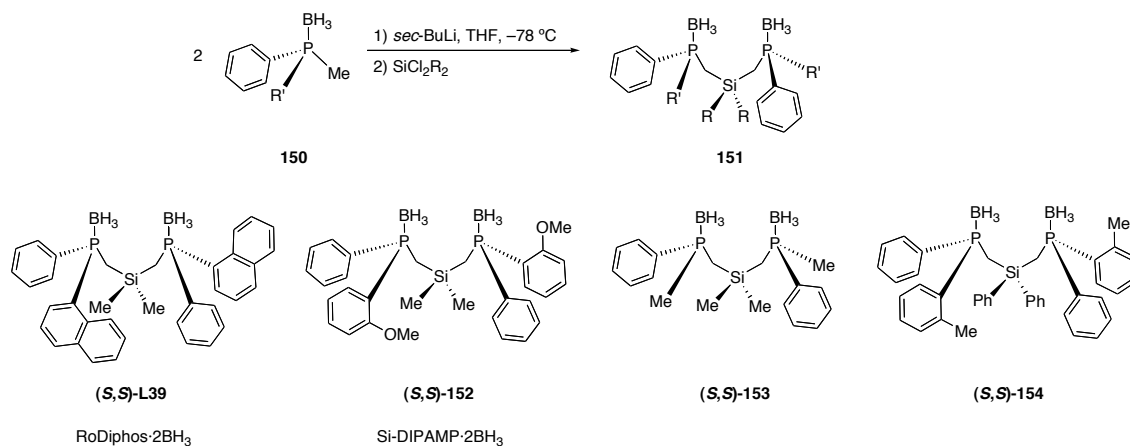
**Equation 48.** Attempt to obtain the diphosphine-boranes, **146**.

The  $^{31}\text{P}\{^1\text{H}\}$  NMR spectrum of the mixtures, after stirring overnight, showed only the peak corresponding to the starting phosphine-borane (*S*)-**L25** for the essays with **147** and **148** and peaks corresponding to a mixture of (*S*)-**L25** and other unidentified products for the essay with **149**. Although one of the unidentified peaks could correspond to the desired diphosphine-borane (*S,S*)-**146**, it would definitely be in a scarce amount and hence no further attempts to prepare diphosphine-boranes of the type (*S,S*)-**146** were carried out.

The reasons for this failure can be attributed to the steric hindrance of the anions derived from (*S*)-**L25** and their high basicity. These two factors can preclude the expected double nucleophilic substitution and cause elimination reactions, restoring the initial phosphine-borane (*S*)-**L25**.

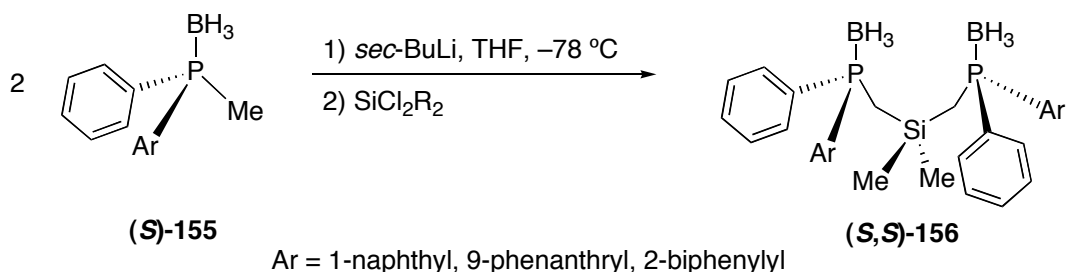
The next set of essays was devoted to the use of dichlorosilanes as electrophiles to prepare diphosphine-boranes bearing a  $-\text{CH}_2\text{Si}(\text{R}_2)\text{CH}_2-$  spacer between the two phosphorus atoms, these are the compounds **142** of Scheme 54.

Equation 49 shows the reaction conditions used as well as the diphosphine-boranes already prepared by other authors<sup>58,80,86</sup>.



Equation 49. Preparation of the silylated diphosphines **151**.

Following this approach, the use of some of the methylphosphine-boranes already prepared ((*S*)-**155**, Equation 50) was envisaged, in order to synthesize similar diphosphine-boranes (*S,S*)-**156**.



Equation 50. Preparation of diphosphine-boranes (*S,S*)-**156**.

Particularly, the preparation of the diphosphine-boranes listed in **Figure 58** was attempted.

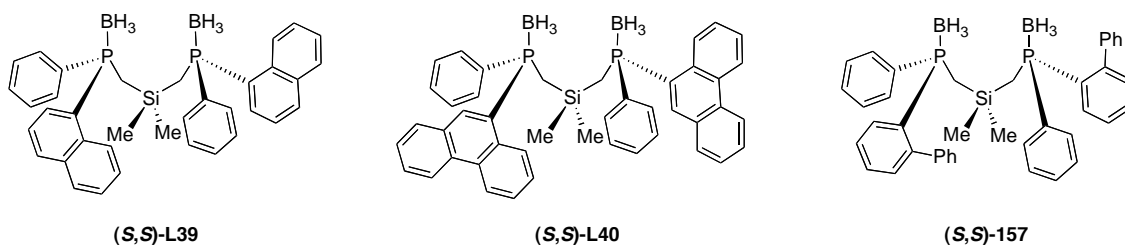


**Figure 58.** Silylated diphosphine-boranes planned to be prepared.

Among the diphosphine-boranes depicted in the figure, to the best of our knowledge, only (S,S)-L39 –known as RoDiphos·BH<sub>3</sub>–, had already been prepared in Mezzetti's laboratories<sup>58</sup>; and used in rhodium-catalyzed hydrogenation and in palladium-catalyzed allylic alkylation.

Success was found in the preparation of (S,S)-L39 and (S,S)-L40, although these diphosphine-boranes were impurified with the starting monophosphine-borane (S)-155. The two compounds were obtained as white foams after work-up. The impurity of the monophosphines was separated later, upon complexation with palladium. The characterization of these phosphine-boranes is given in section 10.4.

The preparation of (S,S)-157 was not successful, as many unidentified signals were observed in the <sup>31</sup>P{<sup>1</sup>H} NMR spectrum, along with an important quantity of the starting methylphosphine-borane (S)-L27. After deboronation and complexation to palladium (chapter III) a large number of signals were still observed and the pure product containing the diphosphine derived from (S,S)-157 could not be obtained.

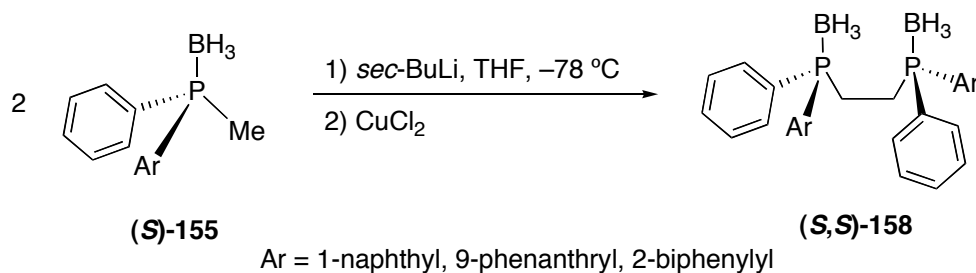
The steric hindrance caused by the *o*-biphenyl group is probably responsible for the failure in the formation of (S,S)-157.

### 10.3.3. Preparation of diphosphine-boranes by oxidative coupling of carbanions **65**

In **Scheme 54**, one of the most widely used methods to prepare diphosphine-boranes is the Cu(II)-promoted coupling of the carbanions **65**, to yield the diphosphine-boranes **66**. The deboronation of these diphosphine-boranes constitute a family of diphosphines whose more representative member, DIPAMP, has been known for 30 years and is, surely, the most well-known *P*-stereogenic ligand.

The Cu(II)-promoted oxidative coupling has been used for many authors<sup>54,57,86,147</sup> to prepare DIPAMP analogues. Among them, Imamoto has prepared a large quantity of diphosphine-boranes by enantioselective deprotonation of dimethylphosphine-boranes as has been explained in section 3.3.5.3.

Following **Equation 51**, some of the methylphosphine-boranes (*S*)-**155** were used to obtain their corresponding ethylene-bridged diphosphine-boranes.



**Equation 51.** Preparation of diphosphine-boranes (*S,S*)-**158** by oxidative coupling.

In analogy to the ligands in **Figure 58**, the synthesis of the diphosphine-boranes shown in **Figure 59** was attempted.

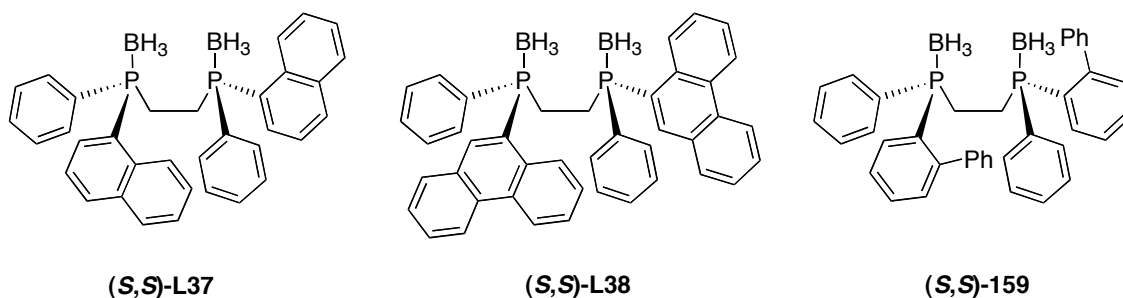


**Figure 59.** DIPAMP-analogues planned to be prepared.

To the best of our knowledge, only the compound (*S,S*)-**L37**, whose derived free diphosphine is known as BNPE, had already been prepared in optically pure form, by Jugé<sup>54</sup> and Mezzetti<sup>147</sup>.



The preparation of (*S,S*)-**L37** and (*S,S*)-**L38** was successful, although in analogy to the silylated diphosphine-boranes (*S,S*)-**156**, these diphosphine-boranes were impurified with the starting monophosphine-borane (*S*)-**155**. This impurity was separated later, upon complexation to palladium. The two compounds were obtained as white foams after work-up. Characterization of these phosphine-boranes is given in section **10.4**.

In analogy to the preparation of the silylated diphosphine-borane (*S,S*)-**157**, the analogous product (*S,S*)-**159** could not be isolated. The  $^{31}\text{P}\{^1\text{H}\}$  NMR spectrum showed a complex mixture of products, although no remaining monophosphine-borane (*S*)-**L27** was detected. The peaks were spread between  $\phi = -27$  ppm and  $\phi = 35$  ppm, indicating that decomposition of (*S*)-**L27** had occurred. It seems clear, hence, that the *o*-biphenyl group prevents the facile preparation of diphosphine-boranes, at least by the methods outlined in this section.

## 10.4. Characterization of diphosphine-boranes

### 10.4.1. Spectroscopic characterization

As it was done for the monophosphine-boranes, (§ 9.7.2), this paragraph gives some NMR data of the prepared diphosphine-boranes. This information is gathered in **Table 28**.

<i>Diphosphine-boranes with <math>-\text{CH}_2\text{CH}_2-</math> bridge between the P atoms (158)</i>				
<i>Compound</i>	<i>Combined Yield<sup>a</sup></i> (%)	<i>MonoP-borane<sup>b</sup></i> (%)	<i><math>^{31}\text{P}</math> NMR</i> $\phi(\text{ppm})^{\text{c, d}}$	<i><math>^1\text{H}</math> NMR</i> $\phi(\text{ppm})^{\text{d}}$ <i>P-<math>\underline{\text{CH}_2\text{CH}_2}</math>-P</i>
( <i>S,S</i> )- <b>L37</b>	99	11	18.6 ( <i>s, br</i> )	2.60 ( <i>m, br</i> )
( <i>S,S</i> )- <b>L38</b>	79	22	21.0 ( <i>s, br</i> )	2.65 ( <i>m, br</i> )

*Diphosphine-boranes with –CH<sub>2</sub>Si(Me<sub>2</sub>)CH<sub>2</sub>– bridge between the P atoms (156)*

Compound	Combined Yield <sup>a</sup> (%)	MonoP-borane <sup>b</sup> (%)	<sup>31</sup> P NMR ϕ(ppm) <sup>c, d</sup>	<sup>1</sup> H NMR ϕ(ppm) <sup>d</sup>	
				P–CH <sub>2</sub> Si(Me <sub>2</sub> )CH <sub>2</sub> –P	P–CH <sub>2</sub> Si(Me <sub>2</sub> )CH <sub>2</sub> –P
(S,S)-L39	78	19	13.3 (s, br)	1.60-2.15 (m, br)	–0.31 (s)
(S,S)-L40	95	12	14.3 (s, br)	1.60-2.15 (m, br)	–0.31 (s)

<sup>a</sup>: Total yield of diphosphine-borane + remaining monophosphine-borane.  
<sup>b</sup>: % of starting monophosphine-borane after work-up.  
<sup>c</sup>: Proton decoupled.  
<sup>d</sup>: Multiplicities given in brackets. Acquisition conditions given in experimental part (Chapter VII), section 3.7.

**Table 28.** Characterization data for the prepared diphosphine-boranes.

The table shows the close similarity between the compounds (S,S)-L37 and (S,S)-L38, and between (S,S)-L39 and (S,S)-L40. The reported data for diphosphine-boranes (S,S)-L37 and (S,S)-L39 agrees with those in **Table 28**.

### 10.4.2. Verification of the optical purity of diphosphine-boranes

After having synthesized and characterized the diphosphine-boranes (S,S)-L37–(S,S)-L40, their optical purity had to be checked. These phosphine-boranes have been prepared starting from the enantiomerically pure methylphosphine-boranes (S)-155, involving processes that do not modify the phosphorus atom. Hence, the stereoselectivity in the formation of the diphosphine-boranes ((S,S)-156 or (S,S)-158) should be complete, yielding optically active diphosphine-boranes.

Nevertheless, either racemization of the monophosphine-borane (S)-155 before coupling or epimerization of the obtained diphosphine-borane thereafter would lead to the formation of observable amounts of (u)-155 (the *meso* form). Consequently, it was found necessary to estimate the optical purity of the products.

The normal method to determine the optical purity of these compounds, applied in the monophosphine-boranes (§ 9.7.3), is HPLC analysis. This method, however, has not been applied with the diphosphine-boranes prepared here, because it was not possible to recrystallize them –foams or oils were invariably obtained– and small impurities could give misleading results when determining the optical purity. Moreover, these diphosphine-boranes are scarcely

soluble in the hexane/isopropanol mixtures, preventing a reliable determination of the enantiomeric purity by HPLC in the available chiral columns.

To overcome this problem, it was found that NMR was a useful tool to check that the diastereomeric ratio (*l*):(*u*) was, at least, 99:1.

#### 10.4.2.1. Verification of the optical purity of (S,S)-156

The (*l*)-isomers –(*S,S*) or (*R,R*)– of the two silylated diphosphine-boranes **156**–**L39** and **L40**– bear a  $C_2$  symmetry axis. This axis implies that the two methyl groups at the silicon atom are homotopic. In the (*u*)-isomer (the *meso* form) this axial symmetry is destroyed and replaced by a plane of symmetry that makes the two methyl groups diastereotopic and hence potentially discernible in  $^1\text{H}$  NMR.

Studying the diphosphine-borane **L39**, Mezzetti<sup>58,138</sup> was able to estimate the diastereomeric ratio of this compound by NMR. In the (*l*)-isomers of **L39** the homotopic methyl groups on the silicon appear as a sharp singlet in the  $^1\text{H}$  NMR spectrum, at  $\phi = -0.31$  ppm. It was found that in contrast, the (*u*)-isomer gives two resolved singlets at  $\phi = -0.23$  ppm and  $\phi = -0.40$  ppm. No sign of these latter two peaks could be detected in the  $^1\text{H}$  NMR spectrum of **L39** and hence a d.e. greater than 98% was assumed. Similar results were found for **L40**. Provided that the starting point were enantiopure phosphine-boranes and no diastereomers are found, it was also assumed that also the e.e. is greater than 98%.

No information can be obtained from the  $^{31}\text{P}\{^1\text{H}\}$  NMR spectrum, because it has been reported that the diastereomers are not resolved.

#### 10.4.2.2. Verification of the optical purity of (S,S)-158

The analysis carried out in section 10.4.2.1 can be done for diphosphine-boranes **158** (**L37** and **L38**) too. Similar to what has been seen in paragraph 10.4.2.1, the diastereomeric ratio of the diphosphine-boranes has to be determined by  $^1\text{H}$  NMR, since in the  $^{31}\text{P}\{^1\text{H}\}$  NMR spectrum the diastereomers are not resolved.

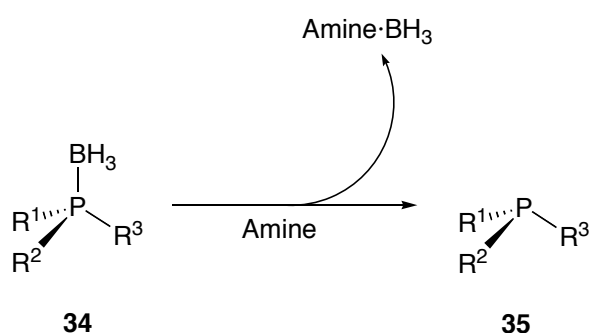
Mezzetti<sup>138,147</sup> carried out this analysis for **L37**, although it should be applicable as well to **L38** given the close similarity between the two compounds. He found that in the (*l*)-isomers of **L37** –(*S,S*) or (*R,R*)– there is a  $C_2$  symmetry axis, which means that the 4 H atoms of the bridge constitute two pairs of homotopic protons (AA'BB' spin system). These 4 H appear as a broad singlet at  $\phi = 2.60$  ppm. He also prepared the (*u*)-isomer (the *meso* form), and found that in the  $^1\text{H}$  spectrum two distinct doublets appeared, at  $\phi = 2.76$  ppm and  $\phi = 2.42$  ppm, corresponding to the two pairs of enantiotopic protons. Mezzetti also used HPLC to evaluate the e.e. of the of **L37**, which was found to be greater than 99%.

In our case, in the  $^1\text{H}$  NMR spectra of either **L37** or **L38**, only broad singlets at  $\delta = 2.60$  ppm and  $\delta = 2.65$  ppm, respectively, were found. No signs of other peaks in this region were detected, indicating a diastereomeric ratio better than 99:1. A high optical purity of the diphosphine-boranes **L37** or **L38** was taken for granted and consequently their deprotection and use as ligands was resumed.

## 11. Deboronation of phosphine-boranes

### 11.1. Introduction

From phosphine-boranes prepared in the preceding sections, the next step was their deboronation in order to obtain the free phosphines, ready to be complexed to palladium or ruthenium. In Part I (§ 3.3.4.6), the main methods of deboronation have been summarized. The method of choice is the treatment of the phosphine-borane **34** with a large excess of amines, as it is reminded in **Equation 52**.



**Equation 52.** Deprotection of phosphine-boranes by means of amines.

The amines used are given in **Figure 60**, along with their boiling points at atmospheric pressure.

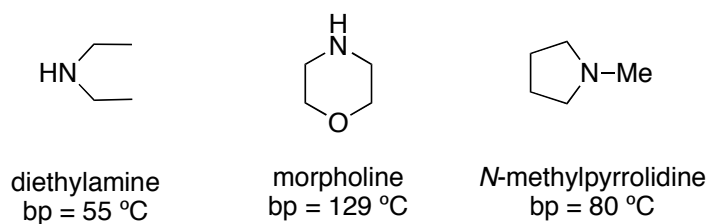
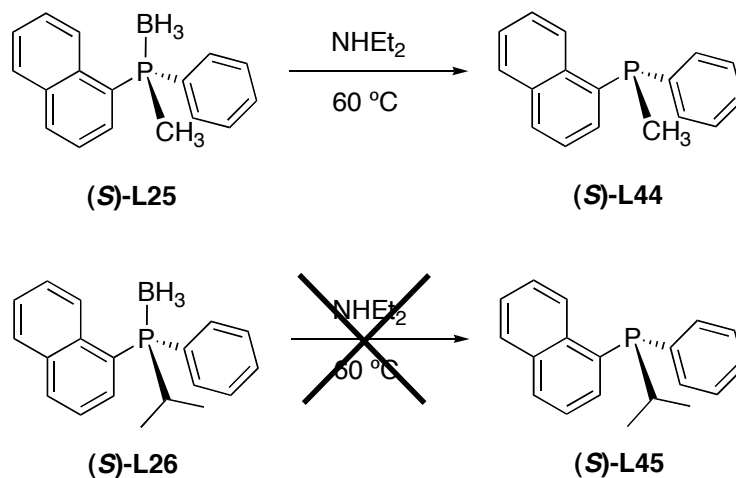


**Figure 60.** Amines used to deprotect phosphine-boranes.

The first essays of deboration were done by dissolving the phosphine-borane in refluxing diethylamine, as illustrated in **Scheme 55**.

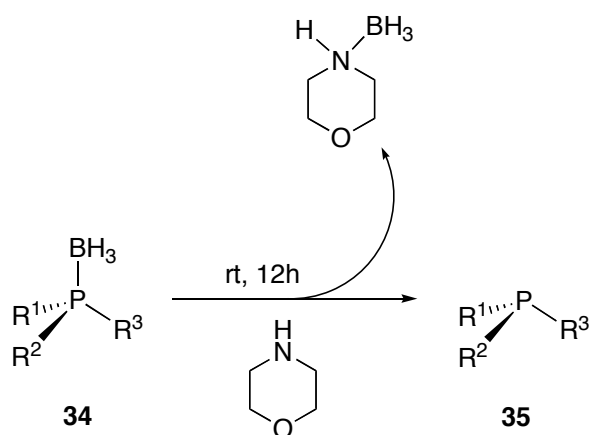


**Scheme 55.** Deboronation of phosphine-boranes using diethylamine.

The  $^{31}\text{P}\{^1\text{H}\}$  NMR spectrum showed that the deboration of **(S)-L25** proceeded smoothly, as had already been reported by Juge<sup>54</sup>. In contrast, the same reaction with **(S)-L26** produced a  $^{31}\text{P}\{^1\text{H}\}$  NMR spectrum with a large quantity of peaks, indicating decomposition of the phosphine-borane. This fact evidences again that subtle steric variations in the phosphine-boranes produce pronounced changes in reactivity.

A literature survey revealed that deboration with morpholine<sup>49,57,58,64,147</sup> (**Figure 60**) at room temperature is a milder procedure and was applied successfully to obtain the free phosphine **(S)-L46**. Mezzetti<sup>58</sup> also reported that the stereoselectivity was better with this amine at rt than with diethylamine at reflux. The only drawback of this amine is the high boiling point, which makes difficult the elimination of the excess of amine. *N*-methylpyrrolidine was also used with equal success with those phosphine-boranes containing a 2-biphenyl group, following the work of Imamoto<sup>136</sup>. However, for the sake of simplicity, morpholine was the amine used in all the deborations except for **(S)-L25**.

The reaction conditions are illustrated in **Equation 53**.



**Equation 53.** Standard deboronation reaction conditions.

The final point of the reaction was easily monitored by  $^{31}\text{P}\{^1\text{H}\}$  NMR and  $^{11}\text{B}\{^1\text{H}\}$  NMR spectroscopies. When the reaction was complete, the former showed the sharp signal of the free phosphine or phosphinite, while the latter showed only the peak corresponding to the Lewis adduct morpholine- $\text{BH}_3$ , at  $\delta = -15.1$  ppm.

After checking the completeness of the reaction, the excess of morpholine was removed *in vacuo*, yielding a pasty substance containing the desired free phosphine and the Lewis adduct morpholine- $\text{BH}_3$ . In some cases ((*S*)-**L44**, (*S*)-**L45**, (*S*)-**L47**, (*S*)-**L48**), the desired free phosphine was obtained pure by recrystallization in  $\text{CH}_2\text{Cl}_2$ /ethanol. In the other cases, the amine-borane adduct was effectively separated by filtration of the crude mixture through a column of alumina with degassed toluene as eluent. Evaporation of this toluene furnished the pure phosphines. This method had been used successfully in the literature<sup>58</sup>. Details of these processes can be found in chapter **VII**, sections **3.8-3.11**.

The deboronation is assumed to occur with clean retention of configuration at the phosphorus atom<sup>49</sup>. A literature survey revealed that only small losses of optical purity are observed in some cases<sup>58</sup>, especially when heating is needed. These losses were checked by reprotection of the free phosphine with borane and comparison between the optical purity between the phosphine-boranes before and after the deprotection. The stereoselectivity of the deprotection of some of the prepared phosphine-boranes and other similar ones has been checked by this method in the literature<sup>147</sup>, demonstrating that no significant losses of stereochemical integrity occur.

## 11.2. Characterization of free P-stereogenic compounds

### 11.2.1. Free phosphinites

This THESIS is devoted to the synthesis and coordination chemistry of *P*-stereogenic phosphines. Notwithstanding, some of the precursor phosphinite-boranes were also deboronated and used as ligands, to compare their properties with those from phosphines. The deboronations were performed under the usual conditions: excess of morpholine at rt.

The free phosphinites obtained are shown in **Figure 61**. They were obtained as viscous, colourless oils.

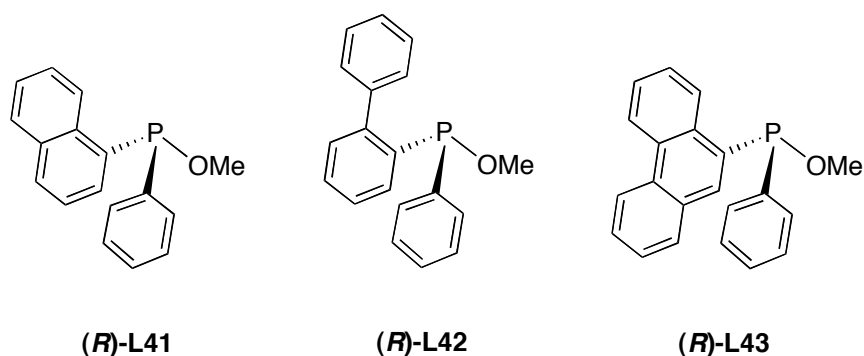


**Figure 61.** Free phosphinites prepared.

These phosphinites were characterized by multinuclear NMR. **Table 29** lists a summary of the characterization data for these compounds. The table also lists the coordination chemical shift (CCS)<sup>52,148,149</sup>, which is the difference between the chemical shift of the borane adduct of a tricoordinated phosphorus compound and the chemical shift of the free compound.



<i>Compound</i>	<i>Yield</i> (%)	<sup>31</sup> P NMR $\phi$ (ppm) <sup>a, b</sup>	CCS (ppm)	<sup>1</sup> H NMR	<sup>13</sup> C NMR
				$\phi$ (ppm) <sup>b</sup> <i>P-OCH<sub>3</sub></i>	$\phi$ (ppm) <sup>a, b</sup> <i>P-OCH<sub>3</sub></i>
<b>(R)-L41</b>	90	113.4 (s)	-1.0	3.78 (d, 14.1)	57.3 (d, 20.7)
<b>(R)-L42</b>	60	109.4 (s)	-0.3	3.57 (d, 14.1)	56.7 (d, 21.9)
<b>(R)-L43</b>	37	114.4 (s)	-2.9	3.79 (d, 14.2)	57.6 (d, 21.4)

<sup>a</sup>: Proton decoupled.  
<sup>b</sup>: Multiplicities and coupling constants (in Hertz) given in brackets. Acquisition conditions given in experimental part (Chapter VII, § 3.8).

**Table 29.** Relevant data for the prepared phosphinites.

As can be inferred from the table, the phosphinites are obtained in variable yields. Their <sup>31</sup>P{<sup>1</sup>H} NMR spectra show very little variation, in analogy to the parent phosphiniteboranes. In the <sup>13</sup>C{<sup>1</sup>H} and <sup>1</sup>H NMR spectra the peak of the methyl substituent of the methoxy group is very characteristic. In the <sup>1</sup>H NMR spectrum, it appears as a sharp doublet, around  $\phi = 3.7$  ppm, with a large coupling constant (> 10 Hz) with the phosphorus atom. In the <sup>13</sup>C{<sup>1</sup>H} NMR spectrum it also appears as a doublet very close to  $\phi = 57$  ppm, with a coupling constant around 21 Hz.

The CCS is negative but very close to zero. This points out that phosphinites, upon complexation with borane, suffer a slight shielding, in analogy to aminophosphines and phosphites. This is in sharp contrast to phosphines, as it will be described in the next sections.

An example of  $^1\text{H}$  NMR spectrum is the one of (**R**)-**L42**, depicted in **Figure 62**.

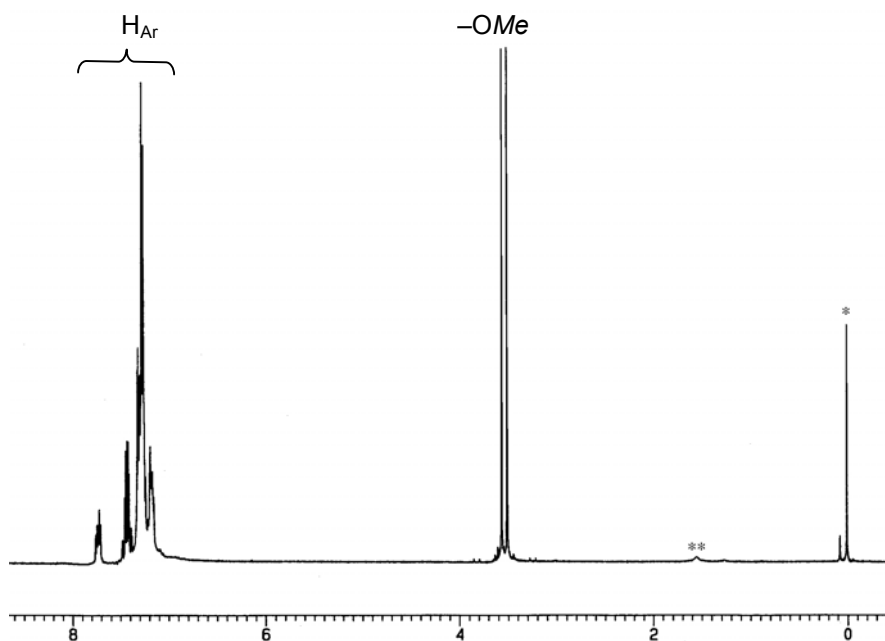


**Figure 62.**  $^1\text{H}$  NMR spectrum (250 MHz,  $\text{CDCl}_3$ , 298K) of (**R**)-**L42**. \*: TMS, \*\*:  $\text{H}_2\text{O}$ .

### 11.2.2. Free phosphines containing a methyl group

The obtained phosphines bearing a methyl group are shown in **Figure 63**.

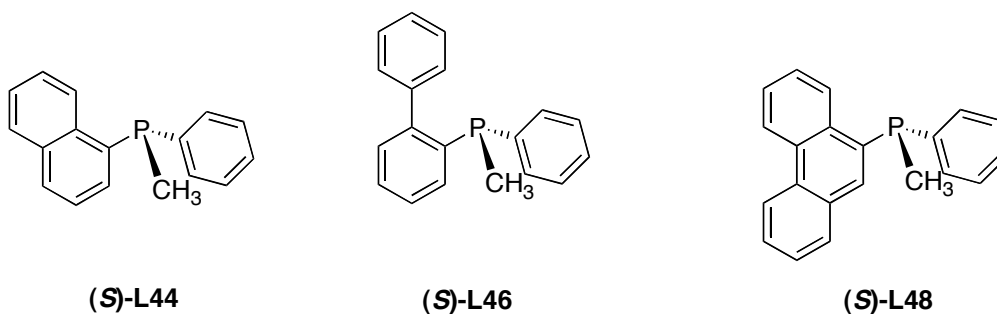


**Figure 63.** Obtained free phosphines bearing a methyl group.

The decomplexation reaction was carried out in diethylamine at reflux for (**S**)-**L44** and with morpholine at rt for the rest. (**S**)-**L46** was isolated as viscous oil whereas the other phosphines were isolated as white solids.

A summary of the spectroscopic data for these phosphines is gathered in **Table 30**.

Compound	Yield (%)	$^{31}\text{P}$ NMR $\phi(\text{ppm})^{a,b}$	CCS (ppm)	$^1\text{H}$ NMR	$^{13}\text{C}$ NMR
				$\phi(\text{ppm})^b$ $P-\underline{\text{C}}\text{H}_3$	$\phi(\text{ppm})^{a,b}$ $P-\underline{\text{C}}\text{H}_3$
(S)-L44	65	-35.7 (s)	49.4	1.71 (d, 4.0)	13.9 (d, 13.7)
(S)-L46	69	-36.4 (s)	49.5	1.50 (d, 4.8)	13.3 (d, 15.0)
(S)-L48	95	-35.4 (s)	46.2	1.79 (d, 3.9)	12.5 (d, 13.8)

<sup>a</sup>: Proton decoupled.  
<sup>b</sup>: Multiplicities and coupling constants (in Hertz) given in brackets. Acquisition conditions given in experimental part (Chapter VII, § 3.9).

**Table 30.** Selected data for the prepared free phosphines bearing a methyl group.

From the table, it is clear that the  $^{31}\text{P}\{^1\text{H}\}$  NMR spectrum do not change considerably from one compound to another, showing a singlet near  $\phi = -36$  ppm. Similarly, the methyl group appears as a sharp doublet (coupled to the phosphorus atom) in  $^1\text{H}$  and  $^{13}\text{C}\{^1\text{H}\}$  NMR spectra, as listed in the table. Complexation with borane of these free phosphines results in a strong deshielding (CCS close to 50 ppm), in analogy to other trialkyl- or triarylphosphines. This fact is in sharp contrast with the phosphinites discussed in section 11.2.1.

The  $^1\text{H}$  NMR spectrum of (S)-L48 is shown as example in **Figure 64**.

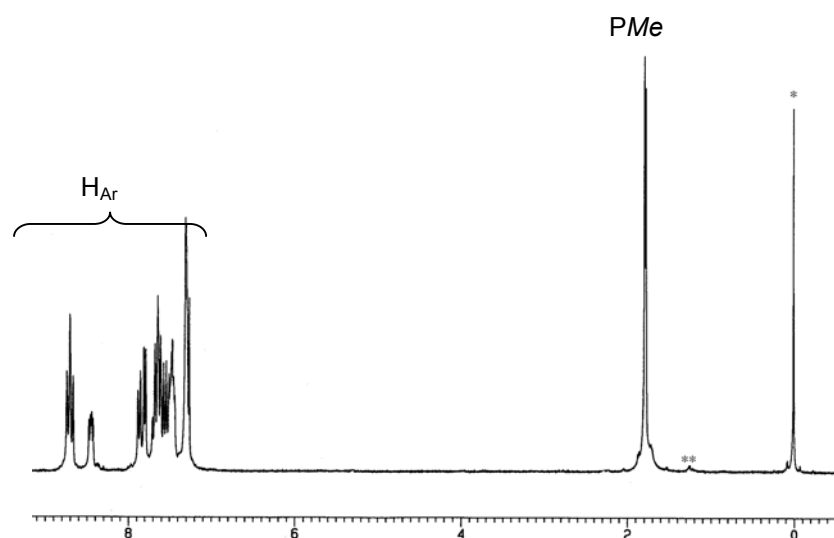


**Figure 64.**  $^1\text{H}$  NMR spectrum (250 MHz,  $\text{CDCl}_3$ , 298K) of (S)-L48. \*: TMS, \*\*:  $\text{H}_2\text{O}$ .

### 11.2.3. Free phosphines containing an isopropyl group

The phosphines bearing an isopropyl group are shown in **Figure 65**. The deboronation was carried out with morpholine in all the cases. Phosphines (*S*)-**L45** and (*S*)-**L47** were obtained as pure white solids, whereas a small amount of (*S*)-**160** and (*S*)-**161** were isolated as impure, oily products.

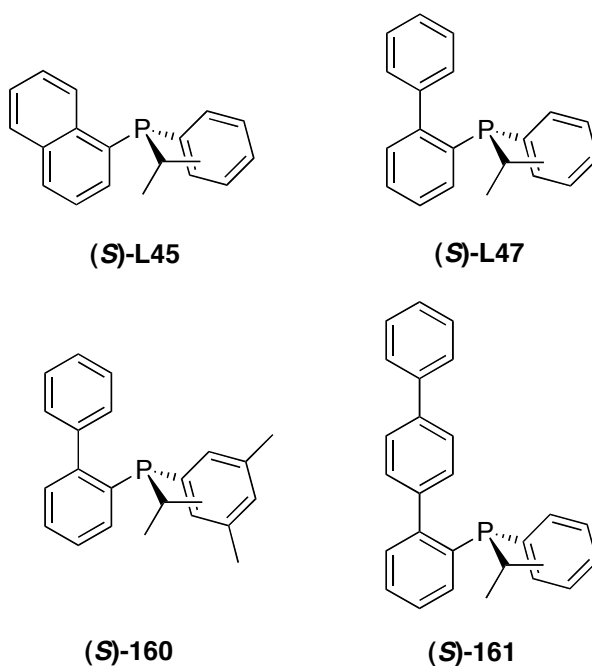


**Figure 65.** Free phosphines bearing an isopropyl group.

A summary of the spectroscopic properties of those products is given in **Table 31**.

Compound	$^{31}\text{P}$ NMR $\phi(\text{ppm})^{a, b}$	CCS (ppm)	$^1\text{H}$ NMR $\phi(\text{ppm})^b$		$^{13}\text{C}$ NMR $\phi(\text{ppm})^{a, b}$			
			$P-\underline{\text{C}}\text{H}(\text{CH}_3)_2$	$P-\text{C}\underline{\text{H}}(\text{CH}_3)_2$	$P-\underline{\text{C}}\text{H}(\text{CH}_3)_2$	$P-\text{C}\underline{\text{H}}(\text{CH}_3)_2$	$P-\text{C}\underline{\text{H}}(\text{CH}_3)_2$	
(S)-L45	-12.3 (s)	37.9	2.56 (m, 6.9, 13.8)	1.11 (dd, 6.9, 15.9)		25.1 (d, 7.3)	19.8 (d, 9.6)	20.2 (d, 9.1)
(S)-L47	-10.5 (s)	36.9	2.50 (m, 6.8, 13.7)	0.92 (dd, 6.9, 15.9)	1.04 (dd, 6.8, 15.7)	25.5 (d, 9.6)	19.5 (d, 19.7)	19.9 (d, 19.7)
(S)-160	-9.3 (s)	39.1	2.39 <sup>d</sup> (m)	0.93 (dd, 6.9, 15.5)	1.01 (dd, 6.9, 15.4)	25.7 (br)	19.9 (d, 21.5)	20.3 (d, 19.4)
(S)-161	-8.5 (s)	38.7	2.30-2.49 <sup>d</sup> (m)	0.95 (dd, 6.8, 15.3)	1.09 (dd, 6.7, 15.7)	— <sup>c</sup>		— <sup>c</sup>

<sup>a</sup>: Proton decoupled.

<sup>b</sup>: Multiplicities and coupling constants (in Hertz) given in brackets. Acquisition conditions, for (S)-L26 and (S)-L28 given in experimental part (Chapter VII, § 3.9).

<sup>c</sup>: Not determined.

<sup>d</sup>: Peaks partially overlapped with others from alkyl impurities.

**Table 31.** Selected data for the free obtained phosphines bearing an isopropyl group.

Inspection of the data in the table shows that  $^{31}\text{P}\{^1\text{H}\}$  NMR values do not change considerably from one compound to another, showing a singlet near  $\phi = -10$  ppm. From the table it can be also deduced that in all cases –except for (S)-L45– the two diastereotopic methyl groups of the isopropyl moiety appear as distinct (anisochronous) in the  $^1\text{H}$  NMR spectrum. In (S)-L45, however, the two methyl groups appear as indistinguishable, as a *dd* by coupling to the  $-\text{CH}-$  proton and to the *P* atom. This non-equivalence between the diastereotopic methyl groups has already been found in the phosphine-boranes (§ 9.7.2.2). Complexation with borane of these free phosphines results in a strong deshielding (CCS close to 40 ppm), in analogy to the methylphosphines. In the isopropylphosphines, however, this deshielding is more moderate.

The  $^1\text{H}$  NMR spectrum of (*S*)-**L45** is shown in **Figure 66**, whereas **Figure 67** does the same for (*S*)-**L47**.

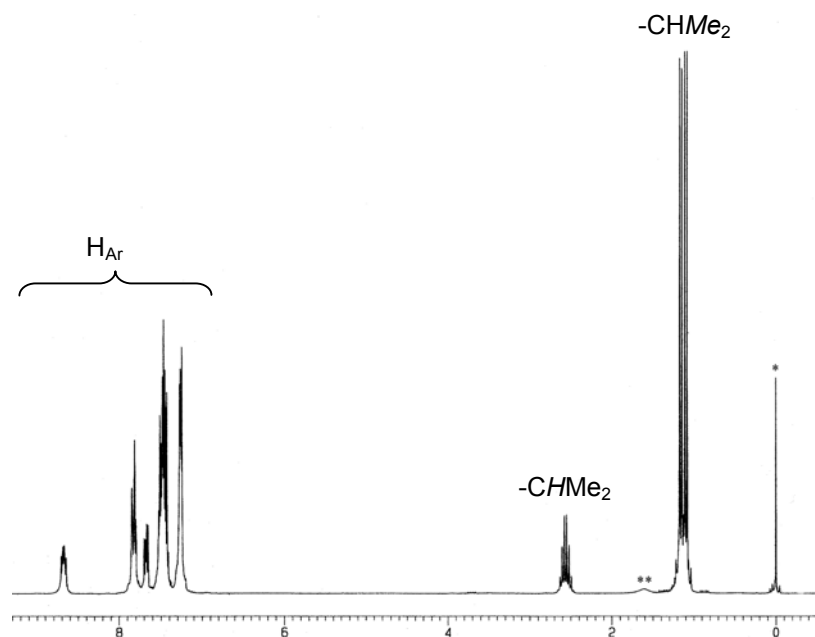


**Figure 66.**  $^1\text{H}$  NMR spectrum (250 MHz,  $\text{CDCl}_3$ , 298K) of (*S*)-**L45**. \*: TMS, \*\*:  $\text{H}_2\text{O}$ .

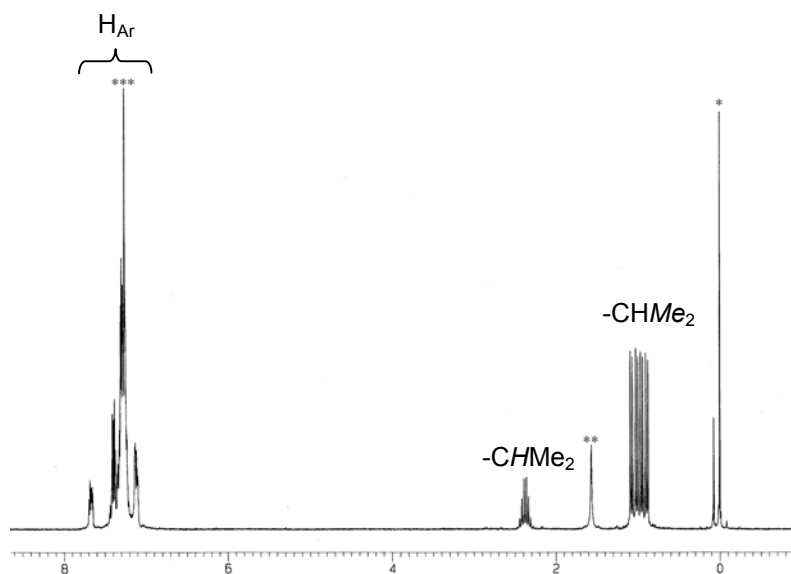


**Figure 67.**  $^1\text{H}$  NMR spectrum (250 MHz,  $\text{CDCl}_3$ , 298K) of (*S*)-**L47**. \*: TMS, \*\*:  $\text{H}_2\text{O}$ , \*\*\*:  $\text{CHCl}_3$ .

### 11.2.4. Free phosphines containing an $\phi$ -silyl group

Among the prepared phosphine-boranes bearing an  $\phi$ -silyl group, (*S*)-L33 and (*S*)-L36 were deboronated in morpholine to yield the free phosphines shown in **Figure 68**.

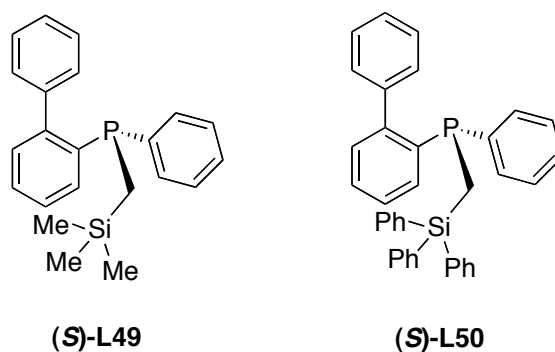


**Figure 68.** Free phosphines with an  $\phi$ -silyl group.

The pure phosphines were obtained as viscous oils. Their characterization is summarized in **Table 32**.

Compound	Yield (%)	$^{31}\text{P}$ NMR $\phi(\text{ppm})^{a, b}$	CCS (ppm)	$^1\text{H}$ NMR $\phi(\text{ppm})^b$		$^{13}\text{C}$ NMR
				<i>P-CH<sub>2</sub>-Si</i>	<i>P-CH<sub>2</sub>-Si</i>	$\phi(\text{ppm})^{a, b}$
( <i>S</i> )-L49	43	-29.1 (s)	47.6	1.23 (d, 17.0)	1.33 (d, 17.0)	15.1 (d, 28.4)
( <i>S</i> )-L50	82	-31.8 (s)	49.8	2.03 (d, 11.3)	2.13 (d, 11.3)	12.1 (d, 33.5)

<sup>a</sup>: Proton decoupled.  
<sup>b</sup>: Multiplicities and coupling constants (in Hertz) given in brackets. Acquisition conditions given in experimental part (Chapter VII), section 3.10.

**Table 32.** Selected data for the obtained free phosphines bearing an  $\phi$ -silylated group.

The table shows similar spectroscopic data for the two compounds. In both of them, the diastereotopic protons of the  $-\text{CH}_2-$  appear as a pseudoquartet. The high CCS value shows a strong deshielding when complexing these phosphines, in analogy to the methylphosphines of section 11.2.2.

The  $^1\text{H}$  NMR spectrum of (*S*)-**L50** is shown as example in **Figure 69**.

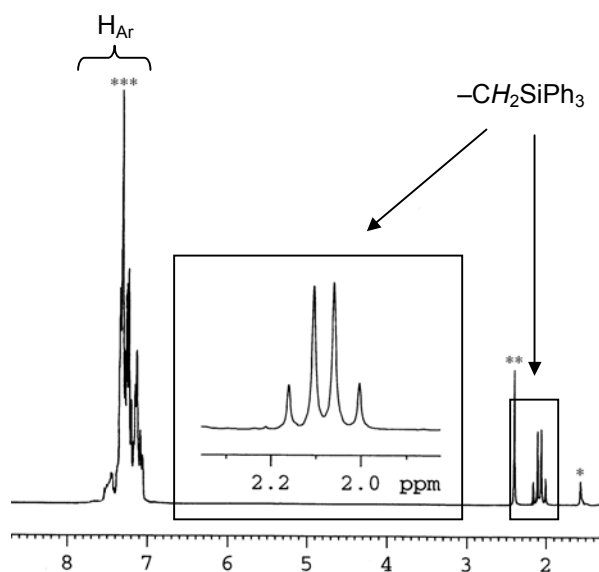


**Figure 69.**  $^1\text{H}$  NMR spectrum (250 MHz,  $\text{CDCl}_3$ , 298K) of (*S*)-**L50**. \*:  $\text{H}_2\text{O}$ , \*\*: toluene, \*\*\*:  $\text{CHCl}_3$ .

### 11.2.5. Free diphosphines

The obtained free diphosphines are depicted in **Figure 70**.

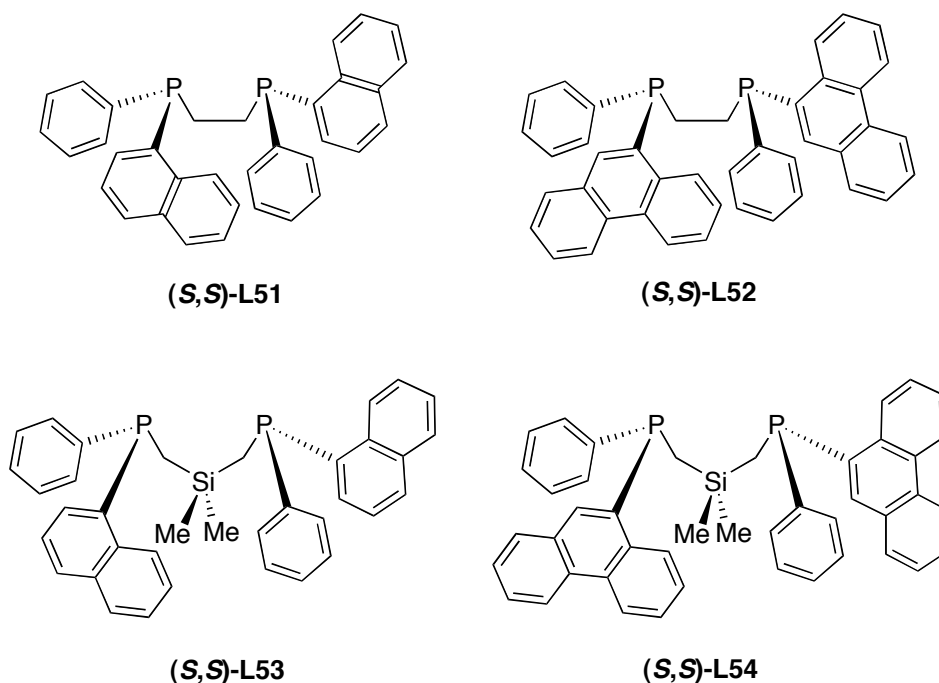


**Figure 70.** Prepared free diphosphines.

These diphosphines were obtained, as viscous oils, by deprotection of the corresponding diphosphine-boranes with morpholine at rt. At this point, it has to be reminded that the



diphosphine-boranes were impurified by the monophosphine-boranes. Consequently, the free diphosphines were not isolated pure, but impurified with the free monophosphines.

The spectroscopic data from the free diphosphines is gathered in **Table 33**.

<i>Diphosphine-boranes with <math>-\text{CH}_2\text{CH}_2-</math> bridge between the P atoms</i>						
<i>Compound</i>	<i>Combined Yield<sup>a</sup></i> (%)	<i>MonoP<sup>b</sup></i> (%)	<i>CCS</i>	<i><sup>31</sup>P NMR</i> $\phi(\text{ppm})^{c, d}$	<i><sup>1</sup>H NMR</i> $\phi(\text{ppm})^d$ <i>P-CH<sub>2</sub>CH<sub>2</sub>-P</i>	
<i>(S,S)</i> -L51	48	–	42.0	–23.4 (s)	2.06-2.36 (m, br)	
<i>(S,S)</i> -L52	47	15	47.9	–26.9 (s)	2.10-2.78 (m, br)	
<i>Diphosphine-boranes with <math>-\text{CH}_2\text{Si}(\text{Me}_2)\text{CH}_2-</math> bridge between the P atoms</i>						
<i>Compound</i>	<i>Combined Yield<sup>a</sup></i> (%)	<i>MonoP<sup>b</sup></i> (%)	<i>CCS</i>	<i><sup>31</sup>P NMR</i> $\phi(\text{ppm})^{c, d}$	<i>P-CH<sub>2</sub>Si(Me<sub>2</sub>)CH<sub>2</sub>-P</i>	<i>P-CH<sub>2</sub>Si(Me<sub>2</sub>)CH<sub>2</sub>-P</i>
<i>(S,S)</i> -L53	59	21	48.5	–35.2 (s)	0.88-0.95 (m, br)	–0.19 (s)
<i>(S,S)</i> -L54	38	19	47.2	–32.9 (s)	0.90-0.95 (m, br)	–0.05 (s)

<sup>a</sup>: Total yield of diphosphine + monophosphine  
<sup>b</sup>: % of monophosphine after work-up.  
<sup>c</sup>: Proton decoupled.  
<sup>d</sup>: Multiplicities given in brackets. Acquisition conditions given in experimental part (Chapter VII), section 3.11.

**Table 33.** Selected data for the prepared free diphosphines.

The table shows similar spectroscopic values for the each pair of compounds, with a high CCS value, indicating a considerable deshielding of the phosphines when they coordinated to borane.

Mezzetti<sup>58</sup> prepared the diphosphine **L53** as a mixture of the (*l*) and (*u*) isomers. The (*u*)-isomer, which is in fact the *meso* form, presents a different  $^{31}\text{P}\{^1\text{H}\}$  NMR shift than the

(*l*)-isomers. In the (*u*)-isomer, moreover, the diastereotopic methyl groups on the silicon atom appear as two resolved singlets.

None of these peaks of the (*u*)-isomer has been found in the preparation of (*S,S*)-**L53**, indicating, hence, a high diastereomeric ratio towards the (*l*)-isomers, in our case the (*S,S*). This analysis was already done in the diphosphine-boranes (**6.4.2.1**), but in that case the  $^{31}\text{P}\{^1\text{H}\}$  NMR peaks of the (*l*) and (*u*) isomers were not distinguishable.

## 12. Conclusion

This long chapter has given, in Part I, a brief account of the methods existing in the literature to prepare *P*-stereogenic compounds. In part II, the preparation and characterization of the *P*-stereogenic compounds that will serve as ligands in this THESIS has been described in detail.

After the description of the synthesis and characterization of the required *bis*(diethylamino)phosphines, the preparation and characterization of the starting, *P*-resolved, oxazaphospholidine-boranes has been illustrated. The obtained results agree with the previous reports existing in the literature. Loss of stereoselectivity in the (–)-ephedrine cyclization was found when using an isopropyl substituent, smaller than the phenyl group. The first attempt to obtain a diphosphine precursor failed, at this stage, due to the polymerization between the (–)-ephedrine and **P10**.

With the oxazaphospholidine-boranes obtained, their stereo- and regioselective ring opening has been described. The reaction was found to be facile, except in when *o,o'*-disubstituted aryllithium reagents were employed. In this case, the reaction failed, in concordance with published results. Full characterization of the obtained aminophosphine-boranes has been given.

The next section has been the description of the acidic methanolysis of the aminophosphine-boranes. The reaction was found to be general, except with the *tert*-butyl group, which did not react, as reported. The characterization of the obtained phosphinite-boranes has been described in detail, including the crystalline structure of (**R**)-**L22**.

With these phosphinite-boranes, the synthesis of the phosphine-boranes has been depicted, pointing out the unsuccessful essays –introduction of a *tert*-butyl and neopentyl groups– and the serendipitous preparation of *rac*-**L31**. The spectroscopic characterization of all the obtained phosphine-boranes has been described in detail and completed with the description of several crystalline structures of the phosphine-boranes.

From the preparation of the phosphine-boranes, it has been learned that nucleophilic substitutions in phosphinite-boranes having a bulky aryl group at the phosphorus atom are severely restricted by steric reasons, which preclude the introduction of other bulky fragments. The serendipitous preparation of **L31** has revealed subtle aspects of the nucleophilic substitutions in crowded phosphinite-boranes, demonstrating again that steric bulkiness is a crucial factor for both the starting phosphinite-borane and the incoming group in the organolithium compound.

The utility of the carbanions derived from methylphosphine-boranes, as interesting synthons in the preparation of further phosphine-boranes, has been also demonstrated in this chapter, with the synthesis and characterization of several  $\phi$ -silylated phosphine-boranes.

After the thorough characterization of all the phosphine-boranes, the preparation of some diphosphine-boranes has been also explained. After some unsuccessful attempts using diorganolithium reagents, success was met with known methods. Two pairs of phosphine-boranes bearing two and three membered bridges between the phosphorus atoms were prepared. The 2-biphenyl group appears to be not suitable for the preparation of these kind of diphosphines.

A final section devoted to the deboration of the phosphine-boranes described the obtention and characterization of the free mono- and diphosphines.

With these obtained free mono- and diphosphines, their coordinating capacity towards palladium and ruthenium was exploited. Eventually, the catalytic applications of the obtained complexes were also explored. These topics will be described in detail in the next chapters of this THESIS.

## 13. Literature

- (1) Osborn, J. A.; Jardine, F. H.; Young, J. F.; Wilkinson, G. J. *J. Chem. Soc. (A)* **1966**, 1711-1732.
- (2) Knowles, W. S.; Sabacky, M. J. *Chem. Commun.* **1968**, 1445-1446.
- (3) Horner, L.; Siegel, H.; Büthe, H. *Angew. Chem. Int. Ed.* **1968**, 7, 942.
- (4) Nozaki, H.; Moriuti, S.; Takaya, H.; Noyori, R. *Tetrahedron Lett.* **1966**, 43, 5239-5244.
- (5) For their pioneering work in asymmetric catalysis, W. S. Knowles, R. Noyori and K. B. Sharpless were awarded with the Nobel Prize in chemistry of the year 2001.
- (6) Kagan, H. B.; Dang, T. *J. Am. Chem. Soc.* **1972**, 94, 6429-6433.
- (7) Fryzuk, M. D.; Bosnich, B. *J. Am. Chem. Soc.* **1977**, 99, 6262-6267.
- (8) Fryzuk, M. D.; Bosnich, B. *J. Am. Chem. Soc.* **1978**, 100, 5491-5494.
- (9) Hayashi, T.; Mise, T.; Mitachi, S.; Yamamoto, K.; Kumada, M. *Tetrahedron Lett.* **1976**, 17, 1133-1134.
- (10) Hayashi, T.; Mise, T.; Kumada, M. *Tetrahedron Lett.* **1976**, 17, 4351-4354.
- (11) Miyashita, A.; Yasuda, A.; Takaya, H.; Toriumi, K.; Ito, T.; Souchi, T.; Noyori, R. *J. Am. Chem. Soc.* **1980**, 102, 7932-7934.
- (12) Schmid, R.; Cereghetti, M.; Heiser, B.; Schönholzer, P.; Hansen, H. *Helv. Chim. Acta* **1988**, 71, 897-929.
- (13) Miyashita, A.; Karino, H.; Shimamura, J.; Chiba, T.; Nagano, K.; Nohira, H.; Takaya, H. *Chem. Lett.* **1989**, 1007.
- (14) Burk, M. J.; Feaster, J. E.; Harlow, R. L. *Organometallics* **1990**, 9, 2653-2655.
- (15) Burk, M. J. *J. Am. Chem. Soc.* **1991**, 113, 8518-8519.
- (16) Togni, A.; Breutel, C.; Schnyder, A.; Spindler, F.; Landert, H.; Tijani, A. *J. Am. Chem. Soc.* **1994**, 116, 4062-4066.
- (17) Pye, J. P.; Rossen, K.; Reamer, R. A.; Tsou, N. N.; Volante, R. P.; Reider, P. J. *J. Am. Chem. Soc.* **1997**, 119, 6207-6208.
- (18) Kromm, K.; Osburn, P. L.; Gladysz, J. A. *Organometallics* **2002**, 21, 4275-4280.
- (19) Meisenheimer, J.; Lichtenstadt, L. *Chem. Ber.* **1911**, 44, 456.
- (20) Knowles, W. S. *Adv. Synth. Catal.* **2003**, 345, 3-13.
- (21) Whitesell, J. K. *Chem. Rev.* **1989**, 89, 1581-1590.
- (22) Pietrusiewicz, K. M.; Zablocka, M. *Chem. Rev.* **1994**, 94, 1375-1411.
- (23) Imamoto, T.; Crépy, K. V. L.; Katagiri, K. *Tetrahedron: Asymmetry* **2004**, 15, 2213-2218.

- (24) Ward, T. R.; Venanzi, L. M.; Albinati, A.; Lianza, F.; Gerfin, T.; Gramlich, V.; Ramos Tombo, G. *Helv. Chim. Acta* **1991**, *74*.
- (25) Imamoto, T.; Tsuruta, H.; Wada, Y.; Masuda, H.; Yamaguchi, K. *Tetrahedron Lett.* **1995**, *36*, 8271-8274.
- (26) Otsuka, S.; Nakamura, A.; Kano, T.; Tani, K. *J. Am. Chem. Soc.* **1971**, *93*, 4301-4303.
- (27) Tani, K.; Brown, L. D.; Ahmed, J.; Ibers, J. A.; Yokota, M.; Nakamura, A.; Otsuka, S. *J. Am. Chem. Soc.* **1977**, *99*, 7876-7886.
- (28) Wild, S. B. *Coord. Chem. Rev.* **1997**, *166*, 291-311.
- (29) Albert, J.; Cadena, J. M.; Granell, J. R.; Muller, G.; Ordinas, J. I.; Panyella, D.; Puerta, C.; Sañudo, C.; Valerga, P. *Organometallics* **1999**, *18*, 3511-3518.
- (30) Albert, J.; Bosque, R.; Magali Cadena, J.; Granell, J. R.; Muller, G.; Ordinas, J. I. *Tetrahedron: Asymmetry* **2000**, *11*, 3335-3343.
- (31) Albert, J.; Magali Cadena, J.; Granell, J. R.; Muller, G.; Panyella, D.; Sañudo, C. *Eur. J. Inorg. Chem.* **2000**, 1283-1286.
- (32) Albert, J.; Cadena, J. M.; Granell, J. R.; Solans, X.; Font Bardia, M. *Tetrahedron: Asymmetry* **2000**, *11*, 1943-1955.
- (33) Albert, J.; Cadena, J. M.; Delgado, S.; Granell, J. R. *J. Organomet. Chem.* **2000**, *603*, 235-239.
- (34) Albert, J.; Bosque, R.; Cadena, J. M.; Delgado, S.; Granell, J. R. *J. Organomet. Chem.* **2001**, *634*, 83-89.
- (35) Albert, J.; Bosque, R.; Magali Cadena, J.; Delgado, S.; Granell, J. R.; Muller, G.; Ordinas, J. I.; Font Bardia, M.; Solans, X. *Chem. Eur. J.* **2002**, *8*, 2279-2287.
- (36) Nudelman, A.; Cram, D. J. *J. Am. Chem. Soc.* **1968**, *90*, 3869-3870.
- (37) Korpium, O.; Mislow, K. *J. Am. Chem. Soc.* **1967**, *89*, 4784-4786.
- (38) Korpium, O.; Lewis, R. A.; Chickos, J.; Mislow, K. *J. Am. Chem. Soc.* **1968**, *90*, 4842-4846.
- (39) Horner, L.; Schlotthauer, B. *Phosphorus, Sulphur* **1978**, *4*, 155.
- (40) Vineyard, B. D.; Knowles, W. S.; Sabacky, M. J.; Bachman, G. L.; Weinkauff, D. J. *J. Am. Chem. Soc.* **1977**, *99*, 5946-5952.
- (41) Oshiki, T.; Imamoto, T. *J. Am. Chem. Soc.* **1992**, *114*, 3975.
- (42) Oshiki, T.; Hikosaka, T.; Imamoto, T. *Tetrahedron Lett.* **1991**, *32*, 3371-3374.
- (43) Koide, Y.; Sakamoto, A.; Imamoto, T. *Tetrahedron Lett.* **1991**, *32*, 3375-3376.
- (44) Horner, L.; Balzer, W. D. *Tetrahedron Lett.* **1965**, *6*, 1157-1162.
- (45) Marsi, K. L. *J. Org. Chem.* **1974**, *39*, 265-267.
- (46) Naumann, K.; Zon, G.; Mislow, K. *J. Am. Chem. Soc.* **1969**, *91*, 7012-7023.
- (47) Valentine, D.; Blount, J. F.; Toth, K. *J. Org. Chem.* **1980**, *45*, 3691-3698.

- (48) Henson, P. D.; Naumann, K.; Mislow, K. *J. Am. Chem. Soc.* **1969**, *91*, 5645-5646.
- (49) Imamoto, T.; Hoshiki, T.; Onozawa, T.; Kusumoto, T.; Sato, K. *J. Am. Chem. Soc.* **1990**, *112*, 5244-5252.
- (50) Imamoto, T. *Pure Appl. Chem.* **1993**, 655-660.
- (51) Ohff, M.; Holz, J.; Quirnbach, M.; Börner, A. *Synthesis* **1998**, 1391-1415.
- (52) Brunel, J. M.; Faure, B.; Maffei, M. *Coord. Chem. Rev.* **1998**, *178-180*, 665-698.
- (53) Carboni, B.; Monnier, L. *Tetrahedron* **1999**, *55*, 1197-1248.
- (54) Jugé, S.; Stephan, M.; Laffitte, J. A.; Genet, J. P. *Tetrahedron Lett.* **1990**, *31*, 6357-6360.
- (55) Carey, J. V.; Barker, M. D.; Brown, J. M.; Russell, M. J. H. *J. Chem. Soc. Perkin Trans. I* **1993**, *7*, 831-839.
- (56) Corey, E. J.; Chen, Z.; Tanoury, G. J. *J. Am. Chem. Soc.* **1993**, *115*, 11000-11001.
- (57) Maienza, F.; Spindler, F.; Thommen, M.; Pugin, B.; Malan, C.; Mezzetti, A. *J. Org. Chem.* **2002**, *67*, 5239-5249.
- (58) Stoop, R. M.; Mezzetti, A. *Organometallics* **1998**, *17*, 668-675.
- (59) Nettekoven, U.; Kamer, P. C. J.; van Leeuwen, P. W. N. M.; Widhalm, M.; Spek, A. L.; Lutz, M. *J. Org. Chem.* **1999**, *64*, 3996-4004.
- (60) Rippert, A. J.; Linden, A.; Hansen, H. *Helv. Chim. Acta* **2000**, *83*, 311-321.
- (61) Moulin, D.; Bago, S.; Bauduin, C.; Darcel, C.; Jugé, S. *Tetrahedron: Asymmetry* **2000**, *11*, 3939-3956.
- (62) Jugé, S.; Stephan, M.; Merdès, R.; Genet, J. P.; Halut-Desportes, S. *J. Chem. Soc., Chem. Commun.* **1993**, 531-533.
- (63) Moulin, D.; Darcel, C.; Jugé, S. *Tetrahedron: Asymmetry* **1999**, *10*, 4729-4743.
- (64) Yang, H.; Lugan, N.; Mathieu, R. *Organometallics* **1997**, *16*, 2089-2095.
- (65) Kaloun, E. B.; Merdès, R.; Genêt, J. P.; Uziel, J.; Jugé, S. *J. Organomet. Chem.* **1997**, *529*, 455-463.
- (66) Ewalds, R.; Eggeling, E. B.; Hewat, A. C.; Kamer, P. C. J.; van Leeuwen, P. W. N. M.; Vogt, D. *Chem. Eur. J.* **2000**, *6*, 1496-1504.
- (67) Colby, E. A.; Jamison, T. F. *J. Org. Chem.* **2003**, *68*, 156-166.
- (68) Nettekoven, U.; Widhalm, M.; Kalchhauser, H.; Kamer, P. C. J.; van Leeuwen, P. W. N. M.; Lutz, M.; Spek, A. L. *J. Org. Chem.* **2001**, *66*, 759-770.
- (69) Nettekoven, U.; Kamer, P. C. J.; van Leeuwen, P. W. N. M. *Organometallics* **2000**, *19*, 4596-4607.
- (70) Richter, W. J. *Chem. Ber.* **1985**, *117*, 2328-2336.
- (71) Jugé, S.; Stephan, M.; Genet, J. P.; Halut-Desportes, S.; Jeannin, S. *Acta Cryst. Sect. C* **1990**, *46*, 1869.

- (72) Johansson, M. J.; Kann, N.; Larsson, K. *Acta Cryst. A* **2004**, *E60*, o287-o288.
- (73) Hall, C. R.; Inch, T. D. *Tetrahedron* **1980**, *36*, 2059-2095.
- (74) Li, J.; Beak, P. *J. Am. Chem. Soc.* **1992**, *114*, 9206-9207.
- (75) Maienza, F.; Wörle, M.; Steffanut, P.; Mezzetti, A. *Organometallics* **1999**, *18*, 1041-1049.
- (76) Nettekoven, U.; Widhalm, M.; Kamer, P. C. J.; van Leeuwen, P. W. N. M.; Mereiter, K.; Lutz, M.; Spek, A. L. *Organometallics* **2000**, *19*, 2299-2309.
- (77) Nettekoven, U.; Widhalm, M.; Kamer, P. C. J.; van Leeuwen, P. W. N. M. *Tetrahedron: Asymmetry* **1997**, *8*, 3185-3188.
- (78) Brisset, H.; Gourdel, Y.; Pellon, P.; Le Corre, M. *Tetrahedron Lett.* **1993**, *34*, 4523-4526.
- (79) Haag, D.; Runsink, J.; Scharf, H. D. *Organometallics* **1998**, *17*, 398-409.
- (80) Darcel, C.; Kaloun, E. B.; Merdès, R.; Moulin, D.; Riegel, N.; Thorimbert, S.; Genêt, J. P.; Jugé, S. *J. Organomet. Chem.* **2001**, *662*, 333-343.
- (81) McKinsty, L.; Livinghouse, T. *Tetrahedron Lett.* **1994**, *35*, 9319-9322.
- (82) Humbel, S.; Bertrand, C.; Darcel, C.; Bauduin, C.; Jugé, S. *Inorg. Chem.* **2003**, *42*, 420-427.
- (83) Bauduin, C.; Moulin, D.; Kaloun, E. B.; Darcel, C.; Jugé, S. *J. Org. Chem.* **2003**, *68*, 4293-4301.
- (84) Maryanoff, C. A.; Maryanoff, B. E.; Tang, R.; Mislow, K. *J. Am. Chem. Soc.* **1973**, *95*, 5839.
- (85) Imamoto, T.; Kusumoto, T.; Suzuki, N.; Sato, K. *J. Am. Chem. Soc.* **1985**, *107*, 5301-5303.
- (86) Muci, A. R.; Campos, K. R.; Evans, D. A. *J. Am. Chem. Soc.* **1995**, *117*, 9075-9076.
- (87) Byrne, L. T.; Engelhardt, L. M.; Jacobsen, G. E.; Leung, W.; Papasergio, R. I.; Raston, C. L.; Skelton, B. W.; Twiss, P.; White, A. H. *J. Chem. Soc. Dalton Trans.* **1989**, 105-113.
- (88) Strohmman, C.; Strohfeldt, K.; Schildbach, D.; McGrath, M. J.; O'Brien, P. *Organometallics* **2004**, *23*, 5389-5391.
- (89) Imamoto, T.; Watanabe, J.; Wada, Y.; Masuda, H.; Yamada, H.; Tsuruta, H.; Matsukawa, S.; Yamaguchi, K. *J. Am. Chem. Soc.* **1998**, *120*, 1635-1636.
- (90) Tsuruta, H.; Imamoto, T. *Tetrahedron: Asymmetry* **1999**, *10*, 877-882.
- (91) Imamoto, T.; Yamamoi, Y. *J. Org. Chem.* **1999**, *64*, 2988-2989.
- (92) Ohashi, A.; Imamoto, T. *Tetrahedron Lett.* **2001**, *42*, 1099-1101.
- (93) Ohashi, A.; Kikuchi, S.; Yasutake, M.; Imamoto, T. *Eur. J. Org. Chem.* **2002**, 2535-2546.



- (94) Nagata, K.; Matsukawa, S.; Imamoto, T. *J. Org. Chem.* **2000**, *65*, 4185-4188.
- (95) Wolfe, B.; Livinghouse, T. *J. Am. Chem. Soc.* **1998**, *120*, 5116-5117.
- (96) Kovacic, I.; Wicht, D. K.; Grewal, N. S.; Glueck, D. S. *Organometallics* **2000**, *19*, 950-953.
- (97) Moncarz, J. R.; Laritcheva, N. F.; Glueck, D. S. *J. Am. Chem. Soc.* **2002**, *124*, 13356-13357.
- (98) Moncarz, J. R.; Brunker, T. J.; Glueck, D. S.; Sommer, R. D.; Rheingold, A. L. *J. Am. Chem. Soc.* **2003**, *125*, 1180-1181.
- (99) Moncarz, J. R.; Brunker, T. J.; Jewett, J. C.; Orchowski, M.; Glueck, D. S. *Organometallics* **2003**, *22*, 3205-3221.
- (100) Xu, Y.; Zhang, J. *J. Chem. Soc. Chem. Commun.* **1986**, 1606.
- (101) Imamoto, T.; Oshiki, T.; Onozawa, T.; Matsuo, M.; Hikosaka, T.; Yanagawa, M. *Heteroat. Chem.* **1992**, *3*, 563-575.
- (102) Al-Masum, M.; Kumaraswamy, G.; Livinghouse, T. *J. Org. Chem.* **2000**, *65*, 4776-4778.
- (103) Korff, C.; Helmchen, G. *Chem. Commun.* **2004**, 530-531.
- (104) Miura, T.; Yamada, H.; Kikuchi, S.; Imamoto, T. *J. Org. Chem.* **2000**, *65*, 1877-1880.
- (105) Ceder, R.; Muller, G.; Sales, J.; Vidal, J.; Neibecker, D.; Tkatchenko, I. *J. Mol. Catal. A* **1991**, *68*, 23-31.
- (106) Ceder, R.; Cubillo, J.; Muller, G.; Rocamora, M.; Sales, J. *J. Organomet. Chem.* **1992**, *429*, 391-401.
- (107) Ceder, R.; Muller, G.; Ordinas, J. I. *J. Mol. Catal. A* **1994**, *92*, 127-139.
- (108) Hayakawa, Y.; Hirose, M.; Hayakawa, M.; Noyori, R. *J. Org. Chem.* **1995**, *60*, 925-930.
- (109) King, R. B.; Sundaram, P. M. *J. Org. Chem.* **1984**, *49*, 1784-1789.
- (110) van der Knaap, T. A.; Klebach, T. C.; Visser, F.; Bickelhaupt, F.; Ros, P.; Baerends, E. J.; Stam, C. H.; Konijn, M. *Tetrahedron* **1984**, *40*, 765-776.
- (111) Burg, A. B.; Slota, P. J. *J. Am. Chem. Soc.* **1958**, *80*, 1107-1109.
- (112) van Linthoudt, J. P.; van den Berghe, E. V.; van der Kelen, G. P. *Spectrochimica Acta* **1979**, *36A*, 315-319.
- (113) Mallan, J.; Bebb, R. L. *Chem. Rev.* **1969**, *69*, 693-755.
- (114) Gilman, H.; Gorsich, R. D. *J. Am. Chem. Soc.* **1955**, *77*, 3134-3135.
- (115) Gilman, H.; Gaj, B. J. *J. Org. Chem.* **1963**, *28*, 1725-1727.
- (116) Wakefield, B. J. *Organolithium Methods*; Academic Press: London, 1990.
- (117) Eberhardt, G. G.; Butte, W. A. *J. Org. Chem.* **1964**, *29*, 2928-2932.
- (118) West, R.; Rochow, E. G. *J. Org. Chem.* **1953**, *18*, 1739-1742.
- (119) Schrock, R. R.; Fellmann, J. D. *J. Am. Chem. Soc.* **1978**, *100*, 3359-3370.

- (120) Bailey, W. F.; Punzalan, E. R. *J. Org. Chem.* **1990**, *55*, 5404-5406.
- (121) Negishi, E.; Swanson, D. R.; Rousset, C. J. *J. Org. Chem.* **1990**, *55*, 5406-5409.
- (122) Wittig, G.; Pockels, U.; Droge, H. *Chem. Ber.* **1938**, *71*, 1903-1912.
- (123) Gilman, H.; Langham, W.; Jacoby, A. L. *J. Am. Chem. Soc.* **1939**, *61*, 106-109.
- (124) Mitchell, R. H.; Lai, Y.; Williams, R. V. *J. Org. Chem.* **1979**, *44*, 4733-4735.
- (125) Dingemans, T. J.; Murthy, N. S.; Samulski, E. T. *J. Phys. Chem. B* **2001**, *105*, 8845-8860.
- (126) Klein, J.; Medlik, A.; Meyer, A. Y. *Tetrahedron* **1976**, *32*, 51-56.
- (127) Eisch, J. J.; Kotowicz, W. *Eur. J. Inorg. Chem.* **1998**, 761-769.
- (128) Chottard, J. C.; Julia, M. *Tetrahedron* **1972**, *28*, 5615-5633.
- (129) Cortfield, J. R.; De'ath, N. J.; Trippett, S. *J. Chem. Soc.* **1971**, 1930-1933.
- (130) Brown, J. M.; Laing, J. C. P. *J. Organomet. Chem.* **1997**, *529*, 435-444.
- (131) Gourdel, Y.; Ghanimi, A.; Pellon, P.; Le Corre, M. *Tetrahedron Lett.* **1993**, *34*, 1011-1012.
- (132) Pescher, P.; Caude, M.; Rosset, J. M.; Tambuté, A.; Oliveros, L. *Nouv. J. Chim.* **1985**, *9*, 621-627.
- (133) Streitwieser, A.; Heathcock, C. H. *Química Orgánica*; 3 ed.; McGraw-Hill: Fuenlabrada (Madrid), 1987.
- (134) Friebolin, H. *Basic one- and two-dimensional NMR spectroscopy*; 1 ed.; VCH Publishers: New York, 1993.
- (135) Atkins, P. W. *Química Física*; 6 ed.; Ediciones Omega: Barcelona, 1999.
- (136) Tsuruta, H.; Imamoto, T. *Synlett* **2001**, 999-1002.
- (137) Maienza, F.; Swiss Federal Institute of Technology: Zürich, 2001, p 167.
- (138) Stoop, R. M.; Swiss Federal Institute of Technology: Zürich, 1999, p 173.
- (139) Brady, F. J.; Cardin, C. J.; Cardin, D. J.; Wilcock, D. J. *Inorganica Chimica Acta* **2000**, *298*, 1-8.
- (140) Huffmann, J. C.; Skupinski, W. A.; Caulton, K. G. *Cryst. Struct. Commun.* **1982**, *11*, 1435.
- (141) Schmidbaur, H.; Wimmer, T.; Lachmann, J.; Müller, G. *Chem. Ber.* **1991**, *124*, 275-278.
- (142) Schmidbaur, H.; Stützer, A.; Bissinger, P.; Schier, A. *Anorg. Allg. Chem.* **1993**, *619*, 1519.
- (143) Verkade, J. G. *Coord. Chem. Rev.* **1972**, *9*, 1-106.
- (144) Bryan, P. S.; Kuczkowski, R. L. *Inorg. Chem.* **1972**, *11*, 553-559.
- (145) Rodgers, J.; White, D. W.; Verkade, J. G. *J. Chem. Soc. A* **1971**, 77-80.

- 
- (146) Camus, J. M.; Andrieu, J.; Richard, P.; Poli, R.; Darcel, C.; Jugé, S. *Tetrahedron: Asymmetry* **2004**, *15*, 2061-2065.
- (147) Stoop, R. M.; Bauer, C.; Setz, P.; Wörle, M.; Wong, T. Y. H.; Mezzetti, A. *Organometallics* **1999**, *18*, 5691-5700.
- (148) Cowley, A. H.; Damasco, M. C. *J. Am. Chem. Soc.* **1971**, *93*, 6815-6821.
- (149) Klanberg, F.; Muetterties, E. L. *J. Am. Chem. Soc.* **1968**, *90*, 3296-3297.

